# IDENTIFICATION OF IMMUNE PATHWAYS INVOLVED IN EQUINE HERPESVIRUS 1 PATHOGENESIS AND PROTECTION FROM DISEASE IN HORSES

By

Lila Marek Zarski

# A DISSERTATION

Submitted to
Michigan State University
in partial fulfillment of the requirements
for the degree of

Comparative Medicine and Integrative Biology – Doctor of Philosophy

2020

#### ABSTRACT

# IDENTIFICATION OF IMMUNE PATHWAYS INVOLVED IN EQUINE HERPESVIRUS 1 PATHOGENESIS AND PROTECTION FROM DISEASE IN HORSES

By

# Lila Marek Zarski

Equine herpesvirus 1 (EHV-1) is an alpha herpesvirus ubiquitous in horses worldwide. It initially infects the epithelium of the upper respiratory tract from where peripheral blood lymphocytes are infected that transport the virus to secondary sites of infection, including the spinal cord which results in crippling neurologic disease equine herpesvirus myeloencephalopathy (EHM). Immunity following vaccination or primary infection is incomplete and unable to protect against reinfection and development of disease. The long term objective of the described work is to identify and target pathways involved in EHM pathogenesis in order to prevent disease. Due to the complex interplay between viral immune-modulating features as well as host immunity, understanding protection from EHM following EHV-1 infections remains elusive. This dissertation is aimed at providing clarity to ultimately understand how EHV-1 immunity can be altered in order to offer more complete protection. We conducted an evolving assortment of in vitro and in vivo experiments investigating differing aspects of EHV-1 infection and immunity at key sites of infection including the respiratory epithelium and peripheral blood lymphocytes. As the site of first contact and viral replication, the respiratory epithelium is the site where the first innate immune responses occur which dictates the phenotype and success of downstream adaptive immunity. As such, in Chapters 2 and 3 I describe experiments to interfere with viral replication and boost host immunity in the respiratory epithelium. Chapters 4 and 5 discuss in-depth transcriptomic analyses to investigate

the systemic host immune response as well as viral and host gene expression in peripheral blood cells during peak EHV-1 viremia and EHM disease.

To my husband, Stephen.

# TABLE OF CONTENTS

LIST OF TABLES	ix
LIST OF FIGURES	ix
CHAPTER 1	1
INTRODUCTION	
BACKGROUND AND SIGNIFICANCE	
VIRAL AND HOST FACTORS INVOLVED IN EHM PATHOGENESIS	
OVERVIEW OF EHV-1 IMMUNITY	
Mucosal innate immunity	
Humoral immunity	
Cell-mediated immunity	
EHV-1 immune modulation	
PURPOSE AND HYPOTHESES	9
CHAPTER 2	11
ADMINISTRATION OF RECOMBINANT ADENOVIRUS EXPRESSING	
INHIBITORY IR2 PROTEIN FOR CONTROL OF EQUINE HERPESVIRUS 1	
INFECTION AND DISEASE	11
ABSTRACT	12
KEYWORDS	13
INTRODUCTION	13
MATERIAL AND METHODS	
Viruses, plasmids, and vectors	
EHV-1 viruses	
Plasmids	
Recombinant adenoviruses	
In vitro experiments	
Culture of cell lines NBL-6 and ARPE-19	
Culture of primary equine respiratory epithelial cells (ERECs	,
Detecting IR2P in Ad-IR2 transduced NBL-6 cells	
Determining effect of Ad-IR2 transduction on EHV-1 replica	
in NBL-6 and ARPE-19 cells	
Determining Ad vector transduction efficiency in ERECs	
Determining effect of IR2 transduction on EHV-1 replication	
ERECs	
In vivo experiments	
Animals	
Experimental design	
Evaluating clinical disease and body temperatures	
Analysis of nasal viral shedding	
Detection of cell-associated viremia	
qPCR for EHV-1 quantification	23

Analysis of virus neutralizing antibody response in blood seri	
Analysis of nasal cytokine expression	
Detection of IR2P in nasal secretions of horses	24
Statistical Analysis	
RESULTS	
Ad vector generation	
Ad-IR2 transduction reduces EHV-1 replication in NBL-6 and ARPE	
cells	
IR2 transduction efficiency in ERECs	
· ·	
Ad-IR2-GFP or Ad-IR2 transduction does not reduce EHV-1 replicate	
in ERECs	
Effect of Ad-IR2 or null Ad on EHV-1 infection and disease in horse	
Ad-IR2 and null Ad treatments reduced body temperatures an	
clinical disease	
Ad vector treatment did not affect nasal viral shedding	
Ad-IR2 and null Ad treatments reduced viremia	28
EHV-1 infection induces interferon expression in all horses as	nd
null Ad alters nasal cytokine response following EHV-1 chall	enge
	28
Ad-IR2 and null Ad have no effect on VN titers	29
IR2 protein is not detectable in nasal secretions following Ad-	-IR2
administration	
DISCUSSION	
CONFLICT OF INTEREST	
AUTHOR CONTRIBUTIONS	
FUNDING	
ACKNOWLEDGMENTS	
ACKINO WLEDOWIEN 13	30
CHAPTER 3	37
A LIVE-ATTENUATED EQUINE INFLUENZA VACCINE STIMULATES	31
IMMUNITY TO EQUINE HERPESVIRUS 1 IN EQUINE RESPIRATORY	
EPITHELIAL CELLS	27
ABSTRACT	
KEYWORDS	
INTRODUCTION	
MATERIALS AND METHODS	
Experimental design	
Viruses	
Animals and equine respiratory epithelial (EREC) cell cultures	
Toxicity of Flu Avert in ERECs	
Cell culture and inoculation	45
Microscopic evaluation	46
Cell viability analysis	46
Effects of Flu Avert treatment on immune response in ERECs	
Effects of Flu Avert treatment and EHV-1 inoculation in ERECs	
EHV-1 intracellular and extracellular growth curves	
Cytokine protein expression in EREC supernatants	
Cytomic protein empression in Ditte superintums	

mRNA isolation	. 48
RT-qPCR for mRNA expression analysis	. 49
Statistical Analysis	. 49
RESULTS	
Flu Avert is non-toxic in ERECs	. 50
Flu Avert induces cytokine responses in ERECs between days 5 and 10	,
post inoculation	. 50
Flu Avert treatment reduces EHV-1 replication in ERECs	. 51
Flu Avert treatment enhances cytokine response to EHV-1 infection in	
ERECs	. 52
DISCUSSION	. 54
AUTHORSHIP	. 61
FUNDING	. 61
COMPETING INTERESTS	. 61
ETHICAL ANIMAL RESEARCH	. 61
OWNER INFORMED CONSENT	. 61
ACKNOWLEDGEMENTS	. 62
MANUFACTURERS' DETAILS	. 62
CHAPTER 4	. 63
TRANSCRIPTOMIC PROFILING OF EQUINE AND VIRAL GENES IN	
PERIPHERAL BLOOD MONONUCLEAR CELLS IN HORSES DURING EQUINE	
HERPESVIRUS 1 INFECTION	
ABSTRACT	
KEYWORDS	
INTRODUCTION	
RESULTS	
Clinical disease and viremia	
Horse mRNA sequencing and differential gene expression	
Gene ontology (GO) overrepresentation	
in silico cell sorting	
Viral mRNA sequencing	
Identification of miRNAs	
Differential expression of miRNAs	
DISCUSSION	
MATERIALS AND METHODS	
Viruses	
Animals	
Experiment design	
Sample collection	
RNA isolation, library preparation, and sequencing	
Genome guided mRNA alignment	
Host and viral miRNA identification and quantification	
Differential gene expression	
Gene enrichment analysis	
Viral gene identification and counting	
in silico cell sorting	. 89

SU	JPPLEMENTARY MATERIALS	89
AU	UTHOR CONTRIBUTIONS	89
FU	JNDING	90
A	CKNOWLEDGEMENTS	90
CO	ONFLICTS OF INTEREST	90
CHAPTER 5		91
	ICATION OF HOST FACTORS ASSOCIATED WITH THE	
	PMENT OF EQUINE HERPESVIRUS MYELOENCEPHALOPATI	HY IN
	BY TRANSCRIPTOMIC ANALYSIS OF PERIPHERAL BLOOD	
	UCLEAR CELLS	91
	BSTRACT	
	EYWORDS	
	TRODUCTION	
M	ATERIALS AND METHODS	96
	Animals	
	Viruses	
	Experimental design and sample collection	
	RNA isolation, library preparation, and sequencing	
	Genome guided mRNA alignment	
	Host and viral miRNA identification and quantification	
	Differential gene expression analysis	
	Gene ontology (GO) enrichment analysis	
	In silico cell sorting	
	Whole blood cytokine RT-qPCR	
RI	ESULTS	
	Clinical disease and viremia	
	Horse mRNA sequencing and differential gene expression	
	Gene ontology overrepresentation	
	In silico cell sorting	
	Whole blood cytokine RT-qPCR	
	Viral mRNA sequencing	
	Identification of miRNAs	
	Differential expression of miRNAs	
DI	SCUSSION	
SU	JPPLEMENTARY MATERIALS	123
	UTHOR CONTRIBUTIONS	
	JNDING	
	CKNOWLEDGEMENTS	
	ONFLICTS OF INTEREST	
CHAPTER 6		124
	SIONS AND FUTURE DIRECTIONS	
APPENDIX		130
REFERENCES		207

# LIST OF TABLES

Table 1. Experimental design
Table 2. Clinical score grading criteria
Table 3. Grading criteria for Flu Avert toxicity in EREC cultures140
Table 4. Primer and probe source list
Table 5. Intracellular and extracellular EHV-1 virus
Table 6. Mapping summary statistics of mRNA sequencing
Table 7. Differentially expressed genes
Table 8. Average fraction of cell population fractions
Table 9. Mapping summary statistics for miRNA
Table 10. Differentially expressed miRNAs
Table 11. Mapping summary statistics of mRNA sequencing
Table 12. Enriched GO terms for contrast comparison between group comparison between EHM and Non-EHM horses
Table 13. Enriched GO terms based on differentially expressed genes in EHM horses180
Table 14. Differentially expressed genes unique to non-EHM horses
Table 15. Average fractions of cell populations in PBMCs
Table 16. Mapping summary statistics of miRNA sequencing
Table 17. Differentially expressed miRNAs

# LIST OF FIGURES

Figure 1. Overview of adaptive immunity involved in protection from EHV-1131
Figure 2. Detection of IR2P in NBL-6 cells by western blot analysis
Figure 3. IR2P-expressing recombinant adenovirus (Ad-IR2) reduces EHV-1 yield135
Figure 4. Clinical disease following EHV-1 infection
Figure 5. Viral load following EHV-1 infection
Figure 6. Nasal cytokine protein expression
Figure 7. Virus neutralizing (VN) antibody titers in blood serum following EHV-1 infection
Figure 8. Cell viability and chemokine mRNA expression following Flu Avert treatment in ERECs
Figure 9. Difference in EHV-1 copy number between Flu Avert treated and media treated ERECs
Figure 10. Difference in EHV-1 copy number between Flu Avert treated and media treated ERECs
Figure 11. Effect of Flu Avert treatment on chemokine mRNA expression in ERECs 24 hours following EHV-1 inoculation
Figure 12. Effect of Flu Avert treatment on chemokine mRNA expression in ERECs 48 hours following EHV-1 inoculation
Figure 13. Effect of Flu Avert treatment on chemokine mRNA expression in ERECs 72 hours following EHV-1 inoculation
Figure 14. IL-10 protein expression in EREC supernatants 72 hours post EHV-1 infection
Figure 15. Clinical and virological disease post EHV-1 challenge
Figure 16. Principal component analysis and differentially expressed genes
Figure 17. Gene ontology enrichment results

Figure 19. Read coverage plot of the EHV-1 genome1	172
Figure 20. Normalized counts of viral genes	173
Figure 21. miRNA expression analyses	174
Figure 22. Summary of data analysis	176
Figure 23. Summary of mRNA sequencing data analysis	189
Figure 24. Summary of miRNA sequencing data analysis	190
Figure 25. Clinical and virological disease between EHM and non-EHM horses	91
Figure 26. Principle component analysis (PCA) plot	192
Figure 27. Venn diagrams of up- and down- regulated genes in response to EHV-1 challenge	93
Figure 28. Volcano plots of differentially expressed genes	94
Figure 29. GO terms for biological processes overrepresented in EHM horses compared non-EHM horses	
Figure 30. Net plot of the most significantly enriched GO terms and associated genes1	98
Figure 31. Normalized read counts (cpm) of selected genes in PBMCs of horses	200
Figure 32. Gene expression as determined by RT-qPCR and RNA sequencing	201
Figure 33. Normalized counts of viral genes post EHV-1 challenge	203
Figure 34. Principle component analysis (PCA) plot for miRNA read counts2	204
Figure 35. Differentially expressed miRNAs	205

# **CHAPTER 1**

# INTRODUCTION

## BACKGROUND AND SIGNIFICANCE

Equine herpesvirus 1 (EHV-1) is a member of the family *Herpesviridae* and the subfamily Alphaherpesvirinae. It is ubiquitous in horses worldwide, and causes upper respiratory disease, abortion, and neurologic disease (equine herpesvirus myeloencephalopathy; EHM). It has been observed that many foals encounter the virus at a young age, likely from nasal contact with their dam [1–4]. After primary infection, the virus then establishes a latent lifelong infection in the neurons or peripheral blood mononuclear cells (PBMCs) [5–8]. Despite this early natural infection and/or vaccination, horses remain susceptible to disease following a repeat exposure or reactivation of latent virus. Acute primary infection or re-infection results in lytic viral replication in the epithelium of the upper respiratory tract and upper respiratory disease in younger horses [9]. In the period of 4-14 days following exposure, EHV-1 is detectable in the PBMCs and transported throughout the body during a period of cell-associated viremia [10]. Viremic circulating PBMCs in the vasculature of the pregnant uterus or the central nervous system are capable of transferring the virus to the vascular endothelial cells, where the virus begins to replicate [11,12]. The subsequent vasculitis results in thrombosis and tissue destruction, leading to abortion or EHM [13,14]. In response to recent multi-state outbreaks in the United States in which as much as 14% of EHV-1 infected horses died or were euthanized as a result of severe neurologic disease, EHM prevention has become of great importance to the equine and veterinary communities [15,16]. At this time, quarantine and strict biosecurity practices during outbreaks or high risk situations remain the most effective prevention strategies against EHM. According to the United States Animal Health Association, state animal health officials are advised to issue a quarantine on premises with EHV-1 confirmed cases for 21 days from the onset of disease in the latest case [17]. In addition to death of animals, quarantines and

event cancellations due to an EHV-1 outbreak bring tremendous economic losses to the equine industry [16]. With the economic implications of disease outbreak and movement restrictions, it is clear that alternative prophylactics and therapies are needed to prevent EHM.

# VIRAL AND HOST FACTORS INVOLVED IN EHM PATHOGENESIS

Viremia has been identified as a critical feature to the development of EHM. High profile outbreaks of EHM in association with EHV-1 infection have prompted investigation into virulence factors of different strains that may contribute to the neuropathogenicity of the virus [16,18]. It has been established that a single nucleotide polymorphism in the DNA polymerase gene of the virus, which encodes an aspartic acid residue at position 752 (genotype D<sub>752</sub>), has been associated with more neurologic disease during outbreaks than that which encodes an asparagine at this position (genotype N<sub>752</sub>) [18,19]. Many experiments have confirmed that infection with the neuropathogenic D<sub>752</sub> strain is associated with higher magnitude and longer duration of EHV-1 viremia during a challenge infection when compared to the lower neuropathogenic N<sub>752</sub> strain; and horses with higher magnitude of viremia are more likely to develop neurologic symptoms [20–23]. It is presumed that increased viral load in PBMCs increases the exposure of the vascular endothelium to EHV-1 and thereby increases the likelihood of endothelial infection, resulting in vasculitis and CNS damage.

In addition to viral factors, hosts factors undoubtably play a role in the propensity to develop CNS damage following EHV-1 infection. The coagulation cascade is known to be induced in horses during EHV-1 viremia, and it is thought that this is a major contributor to thrombosis, leading to endothelial damage and subsequent immunopathology causing secondary disease such as EHM [24–27]. However, perhaps the most critical, yet complex, host factor involved with EHM pathogenesis are shortcomings in immunity. EHV-1 employs methods of

avoiding immune detection while in PBMCs, which facilitates infection of these cells and persistence in the bloodstream. Infection in PBMCs is characterized by a restricted viral gene expression, which delays viral replication until the cell has made contact with the vascular endothelium [28,29]. Furthermore, it was found that viral antigens are absent from the surface of 98% of infected PBMCs, allowing the virus to remain undetected in circulation [30]. While it is evident that viremia is essential to the development of EHM, the ability of EHV-1 to "hide" in these cells has proven to be a challenge in the prevention of viremia and EHM, and increased viremia may indicate less proficient immune targeting of the host. While viremia is a central feature of EHV-1 pathogenesis and infection, EHM only develops in select numbers of horses. It is unclear what characterizes the host factors responsible for the progression of EHV-1 infection into EHM, however, age likely is one of the most reliable risk factors, with older animals being more likely to develop the disease [21,31]. This leads to the idea that factors generally associated with the "aged" immune system are likely also involved in EHM pathogenesis.

# **OVERVIEW OF EHV-1 IMMUNITY**

Establishing lasting protective immunity to EHV-1 disease, particularly EHM, has been an elusive endeavor. In order to better contextualize protective immunity to EHV-1, it is helpful to review the basic components of the anti-viral immune response. The immune response can be generally divided into two major divisions: *innate* immunity (or the immediate cellular response to non-specific molecular patterns) and *adaptive* immunity (pathogen specific response).

Adaptive immunity can also be further subdivided in to *humoral* or *cell-mediated* branches.

These components are all interrelated and serve various functions in the response to EHV-1 and are reviewed below.

# Mucosal innate immunity

Innate immune events are critical for establishing and shaping pathogen-specific adaptive immunity [32–34]. The type of pathogen dictates the polarization of dendritic cells, which determines the polarization of the Th cells upon activation. Viral stimulation typically elicits polarization of Th1 immunity, which further perpetuates CTL responses (Figure 1). Furthermore, the extra-cellular cytokine milieu during antigen presentation additionally shapes such polarizing events. While Th cells are responsible for many of these cytokines, the respiratory epithelium can also be a source. For example, cytokines such as IFNγ will encourage Th1 development, while IL-10 will encourage Th2 development (Figure 1).

As the first site of exposure, the respiratory epithelium provides a physical barrier against inhaled pathogens, such as EHV-1. Respiratory epithelial integrity and tight junctions form a physical barrier and are an important aspect of innate immune protection against EHV-1 infection [35]. In the respiratory epithelium, EHV-1 upregulates pattern recognition receptors such as TLR3 and TLR9, which signals downstream production of antiviral cytokines and chemokines known to promote Th1 and CTL cellular adaptive immunity [36–38].

Respiratory epithelial cells respond to EHV-1 infection by secreting type 1 interferons, which act as part of a cascade to produce a group of antiviral genes, known as interferon stimulated genes (ISGs) [37–41]. Induction of type 1 interferons has also been shown to be a potent antiviral against EHV-1 infection *in vitro* in respiratory epithelial cells [42]. Furthermore, evidence indicates that lower IFNα responses in nasal secretions of horses one day following EHV-1 infection may increase the likelihood of developing EHM, which indicates a role for early interferon production at the epithelium in EHM disease protection [22]. In addition, recruitment of leukocytes is pivotal in initiating adaptive immunity and is achieved by expressing

chemokines. EHV-1 infection of equine respiratory epithelial cells induces expression of chemokines, such as IL-8, CCL2, CCL5, CXCL9, and CXCL10 [37–39,43–45]. The specific population of leukocytes that are recruited is shaped by the specific profile of chemokines secreted and likely is important for protection against EHV-1 disease, such as EHM [32,34,46]. Furthermore, it is known that the profile of cytokine expression at the epithelium can also shape the phenotype of T-cells upon activation [47]. Equine respiratory epithelial cells express a variety of these cytokines in response to EHV-1, such as IL-12 and IL-10 [37,39].

# **Humoral immunity**

Humoral immunity (also known as antibody mediated immunity) is a component of the adaptive immune response. However, antibody mediated immunity does not offer complete protection to all manifestations of EHV-1 disease, particularly EHM. Antibodies are produced by plasma cells, which are activated B-cells. B-cells become activated when exposed to cognate antigen as well as T-helper cell type 2 (described below) cytokines, such as IL-4 (Figure 1) [48]. Currently available commercial vaccines can induce virus neutralizing (VN) antibodies in the serum and protect against clinical respiratory disease and nasal shedding. However, no available vaccine has been shown to be effective at reducing viremia or preventing EHM [31,49,50]. Furthermore, high titers of EHV-1 neutralizing antibodies in serum do not protect against viremia or the development of EHM following a challenge infection [21]. On the other hand, it has been shown that EHV-1 specific mucosal IgA antibodies in the nasal epithelium protects horses from EHV-1 shedding at this site, as well as clinical disease. However, these mucosal antibodies are short lived following infection and difficult to induce with vaccination [51].

# **Cell-mediated immunity**

Though humoral immunity is ineffective against viremia, it is likely that the cellmediated adaptive immune response is the most protective against EHV-1 viremia and likely EHM. T-cells are activated by stimulation with an antigen presenting cell expressing the specific cognate antigen uniquely identified by that T-cell. Cells expressing the CD8 co-receptor protein are destined to become cytotoxic lymphocytes (CTL), while cells expressing CD4 mature into Thelper (Th) cells [52]. Once stimulated with its cognate antigen, activated CTLs and Th cells express IL-2 cytokines that act in an autocrine matter to further proliferate the population. These clones then go on to serve their effector functions – for CTLs this includes killing of virally infected cells. The effector function of Th cells is to express cytokines to "help" induce designated immunity and lymphocyte activation. Depending on the cytokine signals during activation, CD4+ cells can be activated to become one of many phenotypes. The main dichotomy describes two primary phenotypes. Th1 cells are activated with IFNy or IL-12 and effector cells produce "type 1" pro-inflammatory cytokines, including IFNγ. These cytokines can then serve to perpetuate the Th1 and CTL effector T-cell population. Th2 cells, on the other hand, are activated with IL-10 and Th2 effectors produce "type 2" cytokines including IL-4 and IL-5. Type 2 cytokines perpetuate activation of B-cell, and are thus considered as helpers to facilitate the humoral, rather than the cell-mediated adaptive immune response (Figure 1) [47]. Horses with higher levels of EHV-1-specific CTLs prior to EHV-1 challenge tend to have lower levels or shorter duration of viremia and are less likely to abort or develop neurologic symptoms, regardless of pre-infection serum VN titers [21,53,54]. However, inducing EHV-1-specific CTLs with vaccination has proven to be difficult and inconsistent [53,54].

# EHV-1 immune modulation

The shortcomings of adaptive immunity are likely influenced by the ability of EHV-1 to downmodulate crucial aspects of the innate and adaptive immunity. It is known that effective and robust innate immune stimulation is critical for sufficient adaptive responses [33]. EHV-1 has been shown to downregulate expression of MHC-1, which interferes with antigen presentation and thus effective adaptive immune responses, specifically activation of CTLs [37,39,55–57]. EHV-1 establishes intracellular infection quickly, which can explain the ability of the virus to avoid detection by VN antibody, especially during viremia in the PBMCs [58–60]. Additionally, several immune modulating properties of EHV-1 are known to interfere with mucosal innate immunity at the respiratory epithelium. Importantly, EHV-1 is known to selectively interfere with leukocyte chemotaxis to the respiratory epithelium [61]. EHV-1 glycoprotein G (gG) is known to bind chemokines which interferes with IL-8 expression and chemotaxis of neutrophils in vitro [62,63]. In mice, EHV-1 gG interferes with chemotaxis of leukocytes to the lung, which resulted in increased viral replication [63,64]. Additionally, the EHV-1 protein, pUL56 is known to interfere with chemokine expression, as well as neutrophil and monocyte chemotaxis in epithelial cells in vitro [39]. In addition to chemotaxis, pUL56 also interferes with interferon production and can induce expression of the anti-inflammatory cytokine IL-10, which could potentially skew downstream Th cell activation towards a Th2, rather than a Th1 response [39]. Collectively, these immune evasive strategies of EHV-1 contribute to the inability of horses to develop lasting protective immunity to the virus following vaccination or previous infection.

#### PURPOSE AND HYPOTHESES

The long term objective of this work is to identify and target pathways involved in EHM pathogenesis in order to prevent disease. Due to the complex interplay between viral immunemodulating features as well as host immunity, understanding protection from EHM following EHV-1 infections remains elusive. This work is aimed at providing clarity to ultimately understand how EHV-1 immunity can be altered in order to offer more complete protection. We conducted an evolving assortment of *in vitro* and *in vivo* experiments investigating differing aspects of EHV-1 infection and immunity at key sites of infection including the respiratory epithelium and PBMCs. As the site of first contact and viral replication, the respiratory epithelium is the site where the first innate immune responses occur which dictates the phenotype of downstream adaptive immunity. As such, in Chapters 2 and 3 we describe experiments where we sought to interfere with viral replication and boost host immunity in the respiratory epithelium. In Chapters 3 and 4 take a closer look at the systemic host immune response and gene expression in PBMCs during peak EHV-1 viremia. In our first study (described in Chapter 2) we hypothesized that reducing EHV-1 replication in the nasal epithelium would ameliorate viral replication and all aspects of clinical disease, including respiratory disease and viremia. For this, we used a viral vector to deliver an EHV-1 replication inhibition gene (IR2) intranasally. In this experiment, we did not see an advantage to IR2 delivery, yet we found that horses that received either the IR2 delivery vector or the null vector had reduced levels of viremia compared to horses that did not receive any vector treatment prior to challenge. This lead to speculation on the protective effects of viral stimulation at the respiratory tract prior to EHV-1 challenge.

In the second study (described in Chapter 3) we further investigated the hypothesis that non-pathogenic viral stimulation would trigger protective anti-viral innate immune responses in respiratory epithelial cells. For this, we treated equine respiratory epithelial cells *in vitro* with a live-attenuated equine influenza virus (LAIV) vaccine at various timepoints prior to EHV-1 inoculation and measured interferon, chemokine, and EHV-1 viral load. After characterizing the epithelial immunity identifying timing of peak cytokine expression and EHV-1 inhibition *in vitro*, our goal was to use LAIV in horses *in vivo* prior to EHV-1 challenge. Unfortunately, we were unable to complete this study due to an unintended illness in the herd. More work remains to identify how LAIV treatment may alter host innate and adaptive responses to EHV-1 and clinical disease. However, our *in vitro* results strongly suggest that viral stimulation of the respiratory epithelium primes the innate immune system to better protect against EHV-1 infection.

The next chapters focus on systemic host immunity during EHV-1 infection and EHM disease. Chapter 3 and Chapter 4 describe discovery driven studies which investigate the host and viral transcriptome of PBMCs *in vivo* prior to EHV-1 challenge infection and during peak viremia. In Chapter 3 we hypothesized that we could use next generation RNA sequencing to identify key host biological processes that are differentially regulated in PBMCs of horses in response to EHV-1 infection. In Chapter 4, we aimed to identify host biomarkers or mechanisms involved in development of or protection from EHM. We hypothesized that differential expression in the PBMC transcriptome of horses with and without clinical EHM would provide key insights into the pathogenesis of the disease.

# **CHAPTER 2**

# ADMINISTRATION OF RECOMBINANT ADENOVIRUS EXPRESSING INHIBITORY IR2 PROTEIN FOR CONTROL OF EQUINE HERPESVIRUS 1 INFECTION AND DISEASE

Lila M. Zarski, Seong K. Kim, Yao Lee, Carine L. Holz, Rahul K. Nelli, Patty Sue D. Weber, Gisela Soboll Hussey

## **ABSTRACT**

Equine herpesvirus 1 (EHV-1) is an alpha herpesvirus of horses worldwide. It initially infects the epithelium of the upper respiratory tract from where peripheral blood lymphocytes are infected that transport the virus to secondary sites including the spinal cord and the pregnant uterus. This can result in crippling neurologic disease or abortion. Immunity following vaccination or primary infection is incomplete and unable to protect against reinfection and development of disease. The EHV-1 protein, IR2, negatively regulates viral gene expression and replication in cell lines using transient transfection protocols. In this study, we sought to investigate if adenovirus (Ad) vector mediated IR2 gene transfer would reduce replication in primary equine respiratory epithelial cells (ERECs) and reduce EHV-1 associated disease *in vivo* in horses.

EREC cultures were treated with of either a recombinant adenovirus vector containing the IR2 gene insert (Ad-IR2), an empty vector (null Ad), or no treatment (control) prior to EHV-1 inoculation. Horses were treated with intranasal instillation of Ad-IR2, null Ad, or no treatment (control) two days prior to intranasal inoculation with EHV-1.

Ad-IR2 had no effect on EHV-1 replication in EREC cultures. In horses, all groups developed respiratory disease, fever, and virus neutralizing antibodies consistent with EHV-1 infection following challenge infection. Clinical disease score, body temperature, and viremia were significantly greater in the control group compared to the Ad-IR2 and null Ad-treated horses. There were no differences in nasal viral load between groups. Levels of interferons in nasal secretions increased in all groups following EHV-1 challenge.

Our results suggest administration of Ad vector, independent of successful gene transfer, attenuates EHV-1 disease in horses, without reducing EHV-1 replication in the respiratory

epithelial cell cultures or the nasal epithelium of horses. More work is needed to determine what immune factors are involved with this protection against clinical disease and to develop a gene therapy system that can increase expression levels of the IR2 inhibitory protein in the respiratory epithelium of horses.

## **KEYWORDS**

Equine

Gene therapy

Adenovirus vector

EHV-1

Epithelial cell

IR2

# **INTRODUCTION**

Equine herpesvirus 1 (EHV-1), a member of the *Alphaherpesvirinae*, is a major pathogen affecting equines worldwide, and causes respiratory disease, abortion or the neurologic disease, equine herpesvirus myeloencephalopathy (EHM). Primary infection with this virus is via inhalation or nose to nose contact and begins with replication in the epithelium of the upper respiratory tract, causing rhinitis. The virus subsequently invades circulating lymphocytes and this cell-associated viremia can result in the spread of EHV-1 to the vascular endothelium of the pregnant uterus or the spinal cord, resulting in abortion or EHM [65].

A major challenge in preventing EHV-1 associated disease is that protective immunity following natural infection or vaccination is often incomplete. Humoral antibody levels do not correspond to protection from infection, viremia, abortion, or EHM [4,53,54]. Cellular immunity

13

via cytotoxic lymphocytes (CTLs) may protect against EHM development, but protective CTL levels are difficult to induce with current vaccination strategies [21,53,54]. In recent years, there has been evidence that induction of innate immune responses to viral infection of the respiratory tract are important for development of adequate adaptive immunity, by shaping the recruitment of leukocytes via expression of chemokines [32–34]. Furthermore, for EHV-1 infection, induction of interferons have been shown to be a powerful antiviral *in vitro*, and early interferon induction following EHV-1 infection has found to be higher in horses that do not develop EHM [22,42]. However, EHV-1 is known to possess many innate immune modulatory features that interfere with the induction of interferons and chemokines in addition to interfering with antigen presentation and induction of adaptive immunity [39,61–64,66]. These immune modulating features of EHV-1 are thought to be at the center of our difficulty in generating protective immunity to EHV-1.

It has become clear that alternative strategies to reduce EHV-1 replication other than conventional targeting of induction of adaptive immunity warrant further investigation.

Particularly, in order to protect horses from abortion and neurologic disease, EHV-1 spread via lymphocytes to the pregnant uterus and spinal cord must be stopped. Once in the lymphocytes, EHV-1 is a master of evading detection. It has been observed that as many as 98% of infected lymphocytes *in vivo* do not contain EHV-1 antigen on the surface [7,67]. Furthermore, EHV-1 employs a restricted gene expression pattern in PBMCs that is re-activated once contact with endothelium occurs, further "hiding" the virus while in circulation [28,29]. Thus, targeting EHV-1 infected lymphocytes in the periphery is a challenging endeavor. Instead, targeting EHV-1 replication in the upper respiratory tract during acute infection might be a more effective approach to reducing viremia and subsequent secondary disease.

The IR2 protein (IR2P) is unique to EHV-1 and is a truncated form (aa 323-1,487) of the virus's immediate early protein (IEP) [68,69]. IR2P acts a negative regulator of viral transcription, and though the exact role during the viral life-cycle is unknown, EHV-1 may use this protein to facilitate the switch from early to late protein expression. Furthermore, overexpression of IR2P has been shown to reduce EHV-1 IEP expression, and thus interfere with replication of the virus *in vitro* in an equine dermal cell line [70]. Cells engineered to stably express IR2P inhibit EHV-1 replication, allowing the cells to survive infection with 100 fold decrease in EHV-1 production compared to control cells [71].

Based on this information, we hypothesized that overexpression of IR2P in the nasal epithelium of horses at the time of EHV-1 intranasal challenge inoculation would protect horses, by reducing viral replication at the primary infection site and thus also reduce viremia and clinical disease. For delivery and expression, we used a recombinant human adenovirus vector system containing the IR2 gene and administered it to the nasal mucosa of the horses prior to EHV-1 challenge. Recombinant adenovirus vectors are commonly chosen for gene delivery, due to 1) the ability to package a large region of DNA, 2) capability of infecting a wide variety of cell types, and 3) the ability to grow the vectors to very large titers [72]. These vectors have an essential replication gene replaced with the gene of interest so that they are able to infect cells to deliver genetic material but cannot replicate to produce new virions. To test our hypothesis, we tested the value of administration of an adenovirus vector expressing IR2 *in vitro* and *in vivo* by measuring reduction of viral titers in cell lines and primary equine respiratory epithelial cells as well as effect on clinical disease and levels of EHV-1 in nasal secretions and PBMCs following EHV-1 challenge infection in horses.

## MATERIAL AND METHODS

# Viruses, plasmids, and vectors

EHV-1 viruses

For *in vitro* experiments, EHV-1 strains Ab4 (GenBank Accession No. AY665713.1) and RacL11 were used. EHV-1 strain Ab4 was propagated in rabbit kidney 13 (RK-13) cells with MEM-10 (Minimum Essential Medium Eagle (Sigma-Aldrich, St. Louis, MO USA)) supplemented with 100 IU / mL penicillin, 100 μg / mL streptomycin, 1% GlutaMAX (GIBCO, Life Technologies, Carlsbad, CA, USA), and 10% fetal bovine serum. EHV-1 strain RacL11 was grown in equine dermal cells (NBL-6) (ATCC® CCL-57<sup>TM</sup>) with MEM-10 with 1 mM sodium pyruvate and 1% non-essential amino acids (M7145, Sigma Aldrich).

For *in vivo* experiments, EHV-1 strain Ab4 was propagated in NBL-6 cells with MEM-10 with 1 mM sodium pyruvate and 1% non-essential amino acids (as for strain RacL11 above).

Prior to challenge infection, the virus stock was thawed and sonicated for three cycles of 30 sec at 50-1 amplification. The stock was stored on ice until inoculation.

EHV-1 virus stock titers were determined by plaque assay using NBL-6 or RK-13 cells as described previously [71]. Briefly, serial dilutions of virus stock from each passage were used to inoculate fresh cell monolayers. Infected monolayers were incubated in medium containing 1.5% methylcellulose. Plaques were quantitated after 4 days by fixing with 10% formalin solution (Fisher Scientific, Waltham, MA, USA) and staining with 0.5% crystal violet.

**Plasmids** 

Plasmids were constructed and maintained in *Escherichia coli* (*E. coli*) HB101 or JM109 by standard methods [73]. Plasmid pSVIR2 have been described previously [74].

## Recombinant adenoviruses

To generate recombinant shuttle vector containing IR2 gene pVQ-IR2, the 3.9-kb KpnI-HindIII fragment of plasmid pSV-IR2-H2 was cloned into the KpnI and HindIII sites of pVQAd5CMVK-NpA (ViralQuest Inc., North Liberty, IA) [71]. Recombinant adenovirus expressing IR2P (Ad-IR2) was generated at ViralQuest Inc. (North Liberty, IA). Null adenovirus (null Ad) was obtained from ViralQuest Inc. All viruses were purified by 3 rounds of CsCl banding, dialysis against 4% sucrose–50 mM Tris (pH 8.0)–2 mM MgCl2, and stored at –80 °C.

# *In vitro* experiments

Culture of cell lines NBL-6 and ARPE-19

For *in vitro* Ad vector transduction experiments, NBL-6 and human retinal epithelial (ARPE-19) cells were maintained at 37°C in complete Eagle's Minimum Essential Medium (EMEM) supplemented with 100 U/ml of penicillin, 100 µg/ml of streptomycin, nonessential amino acids, and 5% fetal bovine serum.

Culture of primary equine respiratory epithelial cells (ERECs)

Equine tracheal tissues were collected from horses euthanized for reasons unrelated to respiratory disease. All procedures were performed in compliance with the Institutional Animal Care and Use Committee of Michigan State University. ERECs were isolated from these tissues as previously described and cryopreserved in liquid nitrogen until culturing [38]. For experiments, the ERECs were thawed and re-suspended in DMEM/F12 (GIBCO) media supplemented with 5% non heat-inactivated FBS, 1 % MEM non-essential amino acid solution (GIBCO), 100 IU/mL penicillin, 100 μg/mL streptomycin, and 1.25 μg/mL amphotericin B. Two million cells were plated in an apical chamber with collagen-coated polyester membrane of a 12-well Corning ® Transwell ® plate with media added in the basolateral chamber. Cultures were

incubated at 37 °C with 5% CO<sub>2</sub>. The following day, the media was removed from both the apical and basolateral chambers. One mL of DMEM/F12 media supplemented with 2% Ultroser<sup>TM</sup> G (Pall, Port Washington, NY, USA), 100 IU/mL penicillin, 100 μg/mL streptomycin, and 1.25 μg/mL amphotericin B was added to the bottom chamber, such that the apical side of the cells was exposed to air, and replaced every 3-4 days. After 3 weeks the ERECs were well-differentiated and were ready to be used in the following experiments. *Detecting IR2P in Ad-IR2 transduced NBL-6 cells* 

To validate IR2 transduction by the newly generated recombinant Ad vector, NBL-6 cells were infected with Ad-IR2 or null Ad at an MOI of 5 and harvested 48 h later. As a positive control, cells were transfected with 1 pmol of pSVIR2. To determine presence of IR2, preparation of cytoplasmic and nuclear extracts of the cells and western blot analysis were performed as previously described [70]. Blots were incubated with a polyclonal antibody to EHV-1 IEP OC33, which also detects the IR2P, for 2 h [69]. Blots were washed three times for 10 min each in TBST and incubated with secondary antibody (anti-rabbit IgG [Fc]-alkaline phosphatase [AP] conjugate [Promega]) for 1 h. Proteins were visualized by incubating the membranes containing blotted protein in AP conjugate substrate (AP conjugate substrate kit, Bio-Rad) according to manufacturer's directions.

Determining effect of Ad-IR2 transduction on EHV-1 replication in NBL-6 and ARPE-19 cells

We previously determined that NBL-6 cells transiently transfected with pIR2 inhibited EHV-1 replication. [70] In order to see if Ad-IR2 transduction had an inhibitory effect on EHV-1 replication, NBL-6 and ARPE-19 cells were inoculated with the Ad-IR2 or null Ad at an MOI of 30. At 24 h following Ad vector administration, the cells were inoculated with EHV-1 RacL11 at an MOI of 0.02. After 2 h of incubation, the cells were washed with medium and cultured with

fresh medium. At 2, 24, 48, and 72 h post EHV-1 inoculation, the cell culture was harvested for use in a plaque assay. Intracellular virus was released by three freeze-thaw cycles. The EHV-1 titers (intracellular plus extracellular viruses) were determined by plaque assay on NBL-6 cells, as described above, and each sample assayed in triplicate.

Determining Ad vector transduction efficiency in ERECs

Primary ERECs cultured at the air-liquid-interface contain ciliated, fully differentiated, pseudostratified epithelial cells that mimic the morphology and immune system of the natural equine airway [38]. Because of this they are likely to represent an improved system to study respiratory pathogens and innate immunity compared to monolayer cell lines. To utilize this system to determine the optimal conditions for reduction of EHV-1 Ab4 prior to the *in vivo* study, we first wanted to determine transduction efficiency in ERECs. For this we used GFP tagged Ad vectors. Ad-IR2-GFP or null Ad-GFP were added to the apical chamber only or to both the apical and basolateral chambers of ERECs at an MOI of 40. After 6 h of incubation at 37 °C the vectors were removed from the apical chamber only, and the ERECs were washed twice with PBS. The cells remained incubated at 37 °C and were monitored via microscopy and the percent of GFP expressing cells were recorded at 24, 48, 36, and 65 h after removal of the vector from the apical chamber. A second transduction efficiency experiment was conducted in which GFP expression was recorded at 24, 48, 36, and 52 h following removal of the Ad vector. *Determining effect of IR2 transduction on EHV-1 replication in ERECs* 

After determining the conditions necessary for optimal transduction efficiency in the ERECs, our goal was to use this system to determine the optimal conditions for reduction of EHV-1 Ab4 prior to the *in vivo* study. The effect of IR2 transduction on EHV-1 titers were analyzed in three separate experiments. For all three experiments, ERECs from two horses were

treated with Ad vectors in the apical chambers. After 6 h incubation at 37 °C, the vectors were removed and the ERECs were washed twice with PBS. The ERECs were incubated for 52 h at 37 °C in order to achieve maximum transduction prior to inoculation with EHV-1 to the apical chamber and incubation for 2 h at 37 °C. After 2 h incubation, the EHV-1 inoculum was removed and ERECs were washed twice with PBS until sample collection.

For the first experiment, ERECs were transduced with Ad-IR2-GFP, null Ad-GFP, or media control at an MOI of 40, and then inoculated with EHV-1 Ab4 at an MOI of 1. Cells and supernatants were harvested at 24 and 48 h post EHV-1 inoculation to determine intracellular and extracellular EHV-1 load. To collect the ERECs, first, the top chamber was rinsed with 300 μL PBS, aspirated, and then incubated with 300 μL Accumax dissociation solution (Innovative Cell Technologies, Inc., San Diego, CA, USA) for 30 min at 37 °C. The dissociation solution was then collected on ice, and another 300 μL Accumax was added and further incubated for 20 m until all remaining cells were dissociated and this solution was added to the first aliquot. The top chamber was rinsed again with 300 μL PBS to collect any remaining cells and added to the Accumax/cell suspension. The cells were then pelleted by spinning at 300 x g for 10 m. Cell pellets collected from the transwell membrane and supernatants from the basolateral chamber were stored at -80 °C until further processing. Growth curves for EHV-1 Ab4 of the cell pellets or supernatants were determined by tissue culture infectious dose 50% (TCID<sub>50</sub>) assay using RK13 cells, as described previously [75].

Ultimately, *in vivo* experiments were to use Ad vectors without GFP. Therefore, the second EREC experiment repeated the first, but used Ad-IR2 or null Ad without GFP at an MOI of 100.

In order to determine if Ad-IR2 had different effects on replication of different EHV-1 strains in ERECs, the third experiment repeated the second, except it used the strain EHV-1 RacL11 at an MOI of 1 for inoculation and viral titers were determined by real-time PCR. Samples in this experiment were collected 24, 48, and 72 h post EHV-1 inoculation. DNA was then isolated using the QIAamp DNA Blood Mini Kit (Qiagen) according to the manufacturer's instructions from either 200  $\mu$ L of cell culture supernatant to measure extracellular viral titer, or frozen EREC cell pellet resuspended in 200  $\mu$ L PBS to measure intracellular viral titer. EHV-1 quantification for growth curves were determined via qPCR as described below, instead of TCID<sub>50</sub>.

# In vivo experiments

## Animals

Sixteen quarter horse or paint yearlings (9 males, 7 females) were part of this study. All animals were housed within a naturally ventilated building in large pens holding up to 5 horses each, and horses had contact with each other. Horses had access to free-choice grass hay and water for the entirety of the study. The animal maintenance and protocols were performed in compliance with Michigan State University's Institutional Animal Care and Use Committee. *Experimental design* 

Two sets of experiments were conducted at different times. Experiment 1 consisted of eight yearling quarter horses (3 males, 5 females) that were inoculated with EHV-1 Ab4 (without Ad vector administration) for use as a control group. Experiment 2 consisted of Ad-IR2 and null Ad groups and horses were randomly designated to receive either 3 x 10<sup>10</sup> plaque forming units (pfu) of Ad-IR2 (n=4, 3 males, 1 female) or 1.5 x 10<sup>10</sup> pfu of null Ad (n=4, 3 males, 1 female) by

intranasal instillation of the vectors in 5 mL of PBS two days prior to inoculation with 5 x  $10^7$  pfu of EHV-1 Ab4 via intranasal instillation. The experimental design is summarized in Table 1. Evaluating clinical disease and body temperatures

Physical examinations were performed at the timepoints described in Table 1. During the examination, rectal body temperature was taken. Furthermore, a total clinical score was determined by evaluating the presence and severity of cough, nasal discharge and ocular discharge. A grade was assigned to each of these three components and totaled for each horse on each sampling day, using the criteria described in Table 2. Neurologic disease was evaluated on a scale from 0-3 using the simplified version of the Mayhew scale, as described by Allen, 2008 [21].

Analysis of nasal viral shedding

For collection of nasal swabs, a polyester tipped swab was inserted into the ventral nasal meatus to collect secretions from the nasal mucosa. The tips were stored 1 mL of virus transport media (PBS with 0.5 % bovine serum albumin, 2,000 U/mL penicillin G, 4 mg/mL streptomycin, 0.016 mg/mL gentamicin, and 1,000 U/mL nystatin) at -80 °C until EHV-1 quantification. DNA was isolated from 200-400 µL of virus transport media to determine nasal viral shedding using the QIAamp DNA Blood Mini Kit (Qiagen) according to the manufacturer's instructions.

For detection of viremia, one hundred mL whole blood was collected via jugular venipuncture into heparinized syringes and immediately transported to the laboratory for PBMC isolation. PBMCs were separated by density gradient centrifugation over Histopaque-1077 (Sigma-Aldrich) as previously described. [76] The cell pellets of 1 x 10<sup>7</sup> were stored at -80 °C

for EHV-1 quantification. DNA was isolated using the QIAamp DNA Blood Mini Kit (Qiagen) according to the manufacturer's instructions.

qPCR for EHV-1 quantification

DNA concentration was determined for DNA isolated from nasal swab and viremia samples in *in vitro* experiments by spectrophotometry using the NanoDrop 2000 (ThermoScientific). The DNA was diluted such that 100 ng nasal swab transport media or 500 ng PBMC template DNA was used in each PCR reaction. *In vitro* sample DNA was used undiluted. Primers and the probe targeting the gB gene of EHV-1 were purchased from Integrated DNA Technologies, Inc. (Coralville, IA USA) or Sigma Aldrich with the sequences described. [10] For *in vitro* samples, the PCR reactions consisted of 10 μL TaqMan<sup>TM</sup> Fast Universal PCR Master Mix (2X), no AmpErase<sup>TM</sup> UNG (Applied Biosystems), 400 nM forward and reverse primers, 200 nM probe, with nuclease free water and DNA template added to a final reaction volume of 20 μL. For nasal swab and viremia samples, the PCR reactions consisted of 12.5 μL TaqMan<sup>™</sup> Fast Universal PCR Master Mix (2X), no AmpErase<sup>™</sup> UNG (Applied Biosystems), 400 nM forward and reverse primers, 200 nM probe, with nuclease free water and DNA template added to a final reaction volume of 25 µL. Plasmid DNA gene copies generated from a gB plasmid was quantified and included in 10-fold serial dilutions in each run in order to create a standard curve. Samples and standards were run in triplicate and duplicate, respectively. Notemplate negative controls were also included on each plate. Thermocycling was performed on the Applied Biosystems 7500 Fast Real-Time PCR system using the following conditions: One holding stage of 95 °C for 20 s followed by 40 cycles of 95 °C denaturing for 3 s and 60 °C annealing/extending for 30 s.

Analysis of virus neutralizing antibody response in blood serum

Virus neutralization assays (VN) for EHV-1 and EHV-4 were performed on all serums collected prior to the start of the study to screen for animals that had titers below 1:4 for EHV-1 and below 1:24 for EHV-4. In addition, VN for EHV-1 were performed on serum samples collected once weekly throughout the study. For this, serum was heat inactivated by incubating at 56 °C for 30 m and then frozen at -20 °C until further processing. VN assays were performed with final serial dilutions of serum from 1:4 to 1:4096 as previously described [77]. *Analysis of nasal cytokine expression* 

Nasal secretions were collected from horses by inserting a cotton/rayon tampon (Tampax) into the ventral nasal meatus for 30 m. After collection, tampons were centrifuged at 2000 x g for 20 m to separate the fluid. Nasal secretions were stored at -80 °C until processing. Equine cytokines (IL-4, IL-10, IL-17, IFN-α, and IFN-γ) were measured and quantified using a bead-based multiplex assay as described by Wagner and Freer, 2009 [78].

Detection of IR2P in nasal secretions of horses

Nasal secretions from horses were analyzed for presence of secreted IR2P using western blot analysis. Samples were boiled with RIPA lysis buffer and 5X Protein Loading Buffer containing DTT (National Diagnostics, Atlanta, GA, USA) and 20 ng of each sample were loaded onto 7.5 % Criterion TGX Precast midi protein gel (Bio-Rad, Hurcules, CA, USA) and separated by SDS-PAGE. Proteins were then transferred to a 0.2 µm PVDF membrane using the Trans-Blot Turbo transfer pack system (Bio-Rad). The blot was blocked for 1 h at room temperature with TBST (10 mM Tris-Cl [pH 7.5], 150 mM NaCl, and 0.1% Tween 20) containing 5% non-fat dried milk (Bio-Rad). The blot was then incubated overnight at 4 °C with polyclonal antibody to EHV-1 IEP OC33 (described in [69]) at a 1:10,000 dilution in TBST with

0.5% non-fat dried milk. The blot was rinsed 6 times for 5 m each with TBST and then incubated for 1 h at room temperature with secondary HRP conjugated goat anti-rabbit IgG antibody at a 1:12,500 dilution (Abcam, Cambridge, MA, USA) in TBST with 0.5% non-fat milk. The blot was rinsed 6 times for 5 m each and the membrane was then incubated for 1 m with SuperSignal West Dura Substrate (ThermoScientific) and visualized with the ChemiDoc XRS+ Imaging System (Bio-Rad).

# **Statistical Analysis**

All data were tested for normality and log transformed if necessary to perform parametric tests. Repeated measure data for body temperature, nasal viral shedding, and viremia were analyzed using a mixed effect model with Dunnett's post test to compare the means. Clinical score data, nasal cytokines, *in vitro* viral loads, and VN titers were analyzed using a Kruskal-Wallis test with Dunn's post-hoc analysis.

# **RESULTS**

# Ad vector generation

The EHV-1 IR2P is a truncated form of the IEP which lacks the TAD and SRT. Our previous results indicated that the IR2P inhibits EHV-1 gene expression and replication *in vitro* [70,71]. After transduction of NBL-6 cells with the Ad-IR2, western blot analyses with anti-IR2P antibody OC33 showed that a protein identical in size to 140-kDa IR2P expressed as the positive control was detected (Figure 2, lane 4).

# Ad-IR2 transduction reduces EHV-1 replication in NBL-6 and ARPE-19 cells

In ARPE-19 cells, Ad-IR2 reduced virus yield by 630-fold as compared to that of control medium at 48 h post EHV-1 inoculation (Figure 3A). In contrast, null Ad reduced virus production by 3.2-fold as compared to viral titers achieved in cells infected with control medium

(Figure 3A). In NBL-6 cells, Ad-IR2 reduced virus yield by 447-fold as compared to that of control medium at 48 h post EHV-1 inoculation (Figure 3B). In contrast, null Ad reduced virus production by 3.6-fold as compared to viral titers achieved in cells infected with control medium (Figure 3B). These results indicated that ectopic expression of the IR2P effectively inhibited EHV-1 replication in equine and human cell line monolayers.

# **IR2** transduction efficiency in ERECs

Prior to determining effect of IR2 transduction on EHV-1 replication, the transduction efficiency of Ad-IR2-GFP was determined in ERECs by measuring GFP fluorescence. With Ad-IR2-GFP added to the apical well at MOI=40, the percentage of GFP positive cells increased for 48 h post-transduction and began to decrease at 65 h (data not shown). Adding Ad vectors to the basolateral well did not improve transduction efficiency (data not shown). It was concluded that maximum transduction efficiency was 35-40% of cells expressing GFP, and this was achieved by incubating the apical side of EREC cultures with the Ad-IR2-GFP or null Ad-GFP for 6 h, removing the vector, and then further incubating the cells for 52 h prior to EHV-1 challenge (data not shown). Cytopathic effect was not observed at any timepoint following Ad-IR2-GFP or null Ad-GFP administration (data not shown).

# Ad-IR2-GFP or Ad-IR2 transduction does not reduce EHV-1 replication in ERECs

Transduction of ERECs with Ad-IR2-GFP (MOI = 40) did not reduce EHV-1 Ab4 growth as determined by TCID<sub>50</sub> when compared to null Ad-GFP or media transduced cells (data not shown). Because the *in vivo* experiments were to ultimately use Ad vectors without GFP, we performed a second experiment with Ad-IR2 (without GFP) or null Ad at a higher MOI of 100 in an attempt to enhance transduction efficiency. Following Ad-IR2 transduction at an MOI of 100, EHV-1 titers (strain Ab4) were not reduced compared to null Ad or media transduced ERECs

(data not shown). Finally, Ad-IR2 (MOI = 100) did not affect EHV-1 (strain RacL11) growth curves as determined by qPCR when compared to null Ad or media transduced cells. No EHV-1 DNA was detected in the negative control samples (data not shown).

## Effect of Ad-IR2 or null Ad on EHV-1 infection and disease in horses

Ad-IR2 and null Ad treatments reduced body temperatures and clinical disease

All horses developed primary fevers within 2 days post EHV-1 infection (p.i.), and all but two horses (n=1 control group; n=1 IR2 group) developed secondary fevers between day 4 and day 8 p.i. There were no fevers observed in any group prior to EHV-1 challenge, or after day 9 p.i. Body temperatures were significantly greater in control horses when compared to both Ad-IR2 and null Ad groups, and there were no differences between the Ad-IR2 and null Ad groups (Figure 4A).

Horses from each group showed clinical signs of respiratory disease (ocular discharge, nasal discharge, or cough) between day 1 p.i. and day 18 p.i. There were no differences in clinical score between groups prior to EHV-1 challenge. Clinical scores were significantly greater in control horses when compared to both Ad-IR2 and null Ad treated horses, and there was no difference between the Ad-IR2 and null Ad groups (Figure 4B).

Six of 16 horses demonstrated signs of neurologic disease at some point in the study (Ad-IR2 n=3; control n=3). Of these, 3 horses developed severe (grade 3) symptoms, including hindlimb ataxia and recumbency, and were humanely euthanized (Ad-IR2 n=1; control n=2). One horse (control) developed grade 2 symptoms (moderate hindlimb ataxia) and recovered completely. The remaining horses (Ad-IR2 n=2) demonstrated grade 1 symptoms (toe dragging or mild ataxia) and recovered completely.

Ad vector treatment did not affect nasal viral shedding

Following EHV-1 inoculation, every horse shed virus starting on day 1 p.i. and shed virus for 5-10 days following inoculation. No viral shedding was observed for any timepoint following day 10 p.i. in any group or in any horse prior to EHV-1 challenge. There were no significant differences between groups in levels or duration of nasal viral shedding (Figure 5A).

Ad-IR2 and null Ad treatments reduced viremia

All horses but one (IR2 group) developed viremia following EHV-1 challenge, and this same horse never developed a secondary fever. For the horses that developed viremia, the period of viremia ranged from day 4-10 p.i. for the null group, day 3-10 p.i. for the IR2 group, and day 2-10 p.i. for the control horses. Control horses showed significantly greater levels of EHV-1 viremia in PBMCs when compared to the null and IR2 groups (Figure 5B). None of the horses showed detectable viremia prior to EHV-1 challenge.

EHV-1 infection induces interferon expression in all horses and null Ad alters nasal cytokine response following EHV-1 challenge

Expression of IFN $\alpha$  and IFN $\gamma$  proteins in nasal secretions increased significantly in response to EHV-1 infection in all three groups when compared to baseline (Figure 6A, B). At baseline prior to EHV-1 infection, there was significantly more IFN $\gamma$  in the nasal secretions of control horses when compared to Ad-IR2 and null Ad treated horses, but post EHV-1 infection there were no differences between the groups (Figure 6B), and there were no differences between groups either at baseline or day 1 post EHV-1 infection for IFN $\alpha$  (Figure 6A).

For nasal IL-4 expression in the null Ad treated horses, there was a statistically significant increase following EHV-1 infection when compared to baseline values, and at day 1 post EHV-1 infection there was statistically significantly more IL-4 in null Ad treated horses

when compared to control horses (Figure 6C). There were no differences in IL-4 expression between groups at baseline (Figure 6C).

At baseline there was statistically significantly less IL-10 expression in control horses when compared to the Ad-IR2 treated horses and at day 1 post EHV-1 infection, there was statistically significantly less IL-10 expression when compared to both Ad-IR2 and null Ad treated horses (Figure 6D). There was no induction or reduction in IL-10 for any group in response to EHV-1 infection (Figure 6D).

There was no induction or reduction of nasal cytokines in the Ad-IR2 or null Ad groups following Ad vector treatment prior to EHV-1 challenge. There were no differences in IL-17 expression between groups or in any group in response to infection (data not shown).

Ad-IR2 and null Ad have no effect on VN titers

All horses developed EHV-1 neutralizing antibody titers following challenge infection but there were no significant differences observed between the treatment groups (Figure 7).

IR2 protein is not detectable in nasal secretions following Ad-IR2 administration

There was no detectable expression of IR2 protein in the nasal secretions of any horse at baseline, or days 1, 2, or 3 following Ad-IR2 or null Ad treatment (data not shown).

#### DISCUSSION

The early regulatory IR2 protein (IR2P) of EHV-1 is a truncated form of the immediate-early protein (IEP) and lacks the TAD and SRT essential for *trans*-activation and viral growth [70]. We hypothesized that recombinant adenovirus expressing the IR2 gene (Ad-IR2) would reduce replication of EHV-1 *in vitro* and that intranasal administration of Ad-IR2 in horses prior to EHV-1 challenge would protect from EHV-1 infection and disease. We were able to successfully produce recombinant Ad-IR2, and transduction with Ad-IR2 reduced EHV-1

replication in an equine (NBL-6) and a human cell line (ARPE-19). This is consistent with previous data, where we demonstrated that transgene expression of IR2P in plasmid transfected NBL-6 cells and in an IR2P expressing Vero cell line successfully inhibited EHV-1 replication [70,71].

Furthermore, we did observe a reduction of viremia and clinical disease in horses that received either the Ad-IR2 or null Ad compared to control horses. This somewhat surprising finding was interesting as it occurred regardless of IR2 expression. Similar phenomena have been observed previously where protective effects from pathogens are related to antigen exposure of non-related pathogens. It has been reported that children vaccinated with the Bacille Calmette-Guerin (BCG) vaccine against tuberculosis have lower mortality rates due to nontuberculosis related conditions, such as respiratory infections, diarrhea or malaria [79]. Additionally, measles vaccination has been associated with decreased mortality due to unrelated infectious diseases [80]. It is unknown through what mechanisms this non-specific protection may occur. However, a few theories have emerged in recent years. First, the concept of trained *immunity*, or innate immune memory, is the idea that innate leukocytes such as monocytes or NK cells can become "trained" via pattern-recognition receptor signaling. Once trained, these cells are capable of eliciting a more robust response following subsequent stimulation with other pathogens [81–83]. Furthermore, the traditional dichotomy of innate and adaptive immunity has recently been challenged, with evidence of a phenomenon known as *heterologous immunity*. [84,85] This occurs when lymphocytes specific for one antigen display protective effects against another. Specifically for adenoviruses, this has been observed in mice immunized with a null Ad vector that generated hepatitis C virus (HCV) specific cellular immunity in the absence of HCV antigen [86]. It is unknown in our study whether administration of Ad vector primed innate

immune cells or boosted cross-reactive EHV-1 immune responses, and if this contributed to the reduction of EHV-1 viremia and clinical disease severity. However, the concepts of trained and heterologous immunity following Ad vector treatment in horses warrants further investigation.

Additionally, induction of innate immunity likely occurred in the Ad vector treated horses, though this was not the primary focus of the study and thus was not fully investigated. Adenovirus vectors are well known to induce innate immune responses, including the induction of important antiviral responses such as chemokine and interferon expression [87]. These responses are often quick and independent of transgene expression, meaning that gene transfer is unnecessary for induction of innate antiviral immune responses [88–90]. EHV-1 is known to modulate features of innate immunity, including induction of chemokines and interferons [39,61–64,66]. Thus, induction of an antiviral immune responses in the nasal mucosa prior to EHV-1 challenge may have helped to counteract some of these features. In human epithelial cells, these antiviral pathways are stimulated within hours of Ad vector exposure, and this may explain why in our study we did not observe any changes in the small panel of protein cytokines we measured in nasal secretions 24 or 48 h following Ad vector administration in horses [89,90]. The panel of nasal cytokines investigated included IL-4, IL-10, IL-17, IFNγ, and IFNα. As expected, we did see an increase in interferons (IFNα and IFNγ) in all treatment groups in response to EHV-1 infection. This is consistent with previous observations where EHV-1 infection induces intranasal interferon responses in horses [22,76]. There were no differences in the interferon responses between treatment groups 24 h following EHV-1 challenge. However, interferon levels were only measured at one time point post-challenge, which may be less than ideal, as this type of response has been found to have quick onset and can change rapidly [42].

Control horses had higher IL-10 protein levels in nasal secretion compared to the Ad-IR2 and null Ad groups before and after EHV-1 infection. IL-10 is an immunoregulatory cytokine that protects against pathogenic inflammation in response to viral infection [91]. It is unknown whether the Ad vector treatments played a role in keeping IL-10 levels elevated in the horses following EHV-1 infection, however the low levels in the control group may help explain why these horses exhibited more severe clinical disease. Additionally, IL-4 expression was lower in control horses when compared to null Ad treated horses, and it decreased in response to EHV-1 infection in control horses but increased in the Ad-IR2 and null Ad groups. IL-4 is associated with a type 2 T-helper immune response. Changes in this cytokine may again indicate differences in local mucosal immunity and warrants further investigation. Clearly, more work is needed to more completely study immune factors in the nasal mucosa that could inform how differing early mucosal host immunity may impact clinical disease outcome following EHV-1 infection.

While intranasal administration of the Ad-IR2 or null Ad provided clinical protection and reduced viremia, we did not see an effect of Ad-IR2 treatment compared to null Ad in horses. Contrary to our hypothesis, we specifically did not observe a reduction in EHV-1 replication in the nasal secretions of Ad-IR2 treated horses and despite the inhibition of EHV-1 replication observed in the Ad-IR2 treated ARPE-19 and NBL-6 cell lines. We were also unable to reduce virus replication in ERECs with Ad-IR2 transduction. This indicates that IR2P expression was insufficient to effectively inhibit EHV-1 transcription and replication in the equine respiratory epithelium. These results may be due to limitations in transduction efficiency of the adenovirus vector in the epithelial cells of the upper respiratory tract. Consistent with this, we were unable to detect any IR2P in nasal secretions collected from horses for 3 consecutive days following Ad-

IR2 administration. However, there were limitations in *in vivo* sample collections, as we were only able to sample nasal secretions, which are non-cellular and it is possible that there was IR2P expression in the nasal epithelial cells that was not present in the extracellular samples we collected. Previous work in equine cells have shown that transduction efficiency differs for different primary cell types (bone marrow derived mesenchymal stem cells, chondrocytes, and synovial cells) [92]. However, to our knowledge, transduction efficiency of adenovirus vector has not been studied in equine respiratory epithelial cells. Interestingly, in mice, Ad vectors have a preference for alveolar epithelial cells, rather than tracheal epithelial cells [93]. This would corroborate human work that indicates the epithelium of the upper respiratory tract is resistant to Ad mediated gene therapy [94–96].

The inability of Ad-IR2 to reduce viral nasal shedding in horses mirrored the inefficiency of IR2 gene transfer to reduce EHV-1 replication in ERECs despite the inhibition of EHV-1 replication observed in the Ad-IR2 treated ARPE-19 and NBL-6 cell lines. ARPE-19 (human retinal epithelial) and NBL-6 (equine dermal) are commercial cell line monolayers, while ERECs (equine tracheal epithelial cells) are multilayered primary cells cultured at the air-liquid interface (ALI). The ERECs represent a polarized pseudo-stratified epithelium, with fully-differentiated and ciliated columnar cells at the apical surface, mimicking the luminal surface of the upper airway. Tight junctions prevent apical (luminal) access of pathogens to the basal cells below [35,38]. Furthermore, ERECs have been shown to be capable of epithelial innate immune responses, such as the secretion of cytokines and chemokines [37–39]. In these ways, EREC system provides a cell culture model of the natural equine airway that is more biologically relevant than commercial cell lines grown as monolayers. Consistent with our findings, optimal Ad vector gene transduction for mature human ALI respiratory epithelial cultures requires

prolonged incubation times when compared to monolayer cell line or immature primary epithelial cell cultures [97]. In our study we tested many transduction conditions, such as different MOI of Ad vector (40 and 100), increasing incubation time with Ad vector up to 65 h, and also including basolateral exposure to the vector. We ultimately found the optimal transduction conditions and achieved a maximal transduction efficiency of 40% of cells. Despite this, we were unable to effectively reduce viral replication in this system for two different EHV-1 strains, Ab4 or RacL11. The discrepancy of the ability of Ad-IR2 to inhibit EHV-1 replication between our monolayer and ALI cell culture systems is similar to the results of other studies on Ad vector gene therapy in humans. Work in human ALI cultures has revealed that in the polarized respiratory epithelium, Ad vectors are resistant to binding and entry to the apical cells. Instead, Ad vectors have preferential selection for binding and entry to the basal cells, due to the presence of high-affinity receptors [97–99]. This in vitro work is widely considered to explain the inefficiency of adenovirus-mediated gene transfer the upper respiratory tracts of mice and humans [94–96,100,101]. Interestingly, Chu, et al. found that adding EGTA media to ALI cultured epithelial cells allowed adenovirus vectors to better access the basal cells by opening the intracellular junctions and subsequently increased transgene expression in the trachea [100]. Similarly in ERECs, reducing the integrity of the intracellular junctions via EGTA enhances EHV-1 infection [35]. In our study, the addition of Ad-IR2 to the basolateral cell culture chamber did not improve transduction efficiency and more work is needed in the EREC system to see if transduction efficiency and IR2 inhibition of EHV-1 could be enhanced using a chelating agent such as EGTA. Nevertheless, the parallel effects of Ad-IR2 on EHV-1 replication in ALI cultures and in vivo airway may be due to the luminal ciliated epithelial cells

reluctance to Ad vector entry and highlight the utility of these cell culture systems to predict responses to treatment systems such as Ad vectors.

In conclusion, Ad-IR2 gene transfer was able to reduce EHV-1 replication in NBL-6 and ARPE-19 cells, but not ERECs or horses. While Ad-IR2 did not alter viral replication in the equine respiratory epithelium in vitro or in vivo, Ad-IR2 as well as the null Ad vector protected horses from viremia and clinical disease. We believe that intranasal exposure to the adenovirus capsid impacted host immunity in a way that altered the response to EHV-1 infection in a protective way. As viremia is a critical pre-requisite event in the pathogenesis of EHM, these results begin to suggest immune mechanisms that may contribute to protection from viremia and perhaps ultimately EHM. Our study was limited in that it was not designed to evaluate the immune responses to Ad vectors, which would have provided valuable information regarding the mechanisms surrounding this protection. However, future studies are warranted to investigate the protective effects of viral antigen exposure prior to EHV-1 challenge. Future work is also needed to determine an alternate delivery route for the IR2P in vivo. Our experiment revealed that the upper respiratory tract of horses is relatively resistant to adenovirus mediated gene transfer. Future studies should make use of the EREC system to evaluated potential transgene delivery methods prior to investigation in horses.

#### CONFLICT OF INTEREST

The authors declare that the research was conducted in the absence of any commercial or financial relationships that could be construed as a potential conflict of interest.

## **AUTHOR CONTRIBUTIONS**

LMZ, SKK, and GSH contributed to conception and design of the study. LMZ, SKK, YL, CLH, RKN, PSDW, & GSH performed the experiments. LMZ wrote the manuscript with contributions from SKK & GSH. All authors contributed to manuscript revisions, read, and approved the submitted version.

## **FUNDING**

This research was supported by National Research Initiative Competitive Grant 2013-67015-21311 from the USDA (NIFA) Cooperative State Research, Education and Extension Service, and by the National Institute of General Medical Sciences of the NIH under awards P30-GM110703.

## **ACKNOWLEDGMENTS**

The authors would like to thank the following colleagues for their help with this study.

David O'Daniel managed the animal facilities. Allison Davis McCauley, Rachel Baumgardner,

Julie Dau, and Elis Fisk assisted with animal husbandry and sample collection. Benjamin

Sorensen assisted with data analysis.

# **CHAPTER 3**

# A LIVE-ATTENUATED EQUINE INFLUENZA VACCINE STIMULATES IMMUNITY TO EQUINE HERPESVIRUS 1 IN EQUINE RESPIRATORY EPITHELIAL CELLS

Lila M. Zarski, Wendy E. Vaala, D. Craig Barnett, Fairfield T. Bain, Gisela Soboll Hussey

**ABSTRACT** 

**Background:** Equine herpesvirus 1 (EHV-1) ubiquitously infects horses worldwide and causes

respiratory disease, abortion, and equine herpesvirus myeloencephalopathy. Protection against

EHV-1 disease is elusive due to establishment of latency and immune modulatory features of the

virus. These include the interference with induction of interferons, cytokines, chemokines,

antigen presentation, and cellular immunity.

**Objectives:** Because these events are thought to occur at the site of first infection – the

respiratory epithelium, we hypothesized that the mucosal influenza vaccine Flu Avert<sup>®</sup> I.N. (Flu

Avert), which is known to stimulate strong antiviral responses, will enhance antiviral innate

immunity and that these responses would also provide protection from EHV-1 infection.

Study design: In vitro experiment

Methods: Primary equine respiratory epithelial cells (ERECs) were treated with Flu Avert and

innate immunity was evaluated for 10 days following treatment. Timing of Flu Avert treatment

was also evaluated for optimal effectiveness to reduce EHV-1 replication by changing early

immune responses to EHV-1. Induction of interferons, cytokine and chemokine mRNA

expression, and protein secretion was evaluated by high throughput qPCR and multiplex protein

analysis. Intracellular and extracellular EHV-1 titers were determined by qPCR.

**Results:** EHV-1 replication was most efficiently reduced in ERECs treated with Flu Avert 5

days prior to EHV-1 inoculation. Coinciding with the timing of optimal reduction in EHV-1

replication, Flu Avert treatment resulted in modulation of IL-8, CCL2 and CXCL9 starting on

days 5 and 6 post treatment.

Main limitations: EREC system lacks complete mucosal immune cell population.

38

**Conclusion:** Our results suggest that Flu Avert may be effective at counteracting some of the immune-modulatory properties of EHV-1 at the airway epithelium, and the peak for this response occurs 5-8 days post Flu Avert treatment. Future *in vivo* studies are needed to investigate Flu Avert as a prophylactic in situations where EHV-1 exposure may occur.

#### **KEYWORDS**

Horse

EHV-1

Equine influenza vaccine

Epithelial cell

Mucosal immunity

#### INTRODUCTION

Equine herpesvirus 1 (EHV-1) ubiquitously infects horses worldwide. It is responsible for causing respiratory disease, late term abortion in pregnant mares, or the crippling neurologic disease – equine herpesvirus myeloencephalopathy (EHM). Foals become infected within the first weeks or months of life, and infection results in respiratory illness [1–4]. Like many other herpesviruses, EHV-1 then establishes a life-long latent infection within the neurons or local lymphoid tissues [5–8]. Following primary infection, virus neutralizing (VN) antibodies can be detected in the serum and nasal mucosa and are associated with protection against clinical respiratory disease and nasal shedding upon re-exposure to the virus [53,54,102,103]. However, high serum antibody levels following vaccination or infection do not correlate with protection from viremia or subsequent secondary disease manifestations, such as abortion or EHM [4,21,54]. In contrast, high levels of cytotoxic lymphocyte (CTL) precursor frequencies are thought to be crucial for protection from viremia, abortion, and EHM [21,53,54].

In recent years the study of innate immunity to EHV-1 has also gained interest – particularly because it is known that innate immune events are critical for establishing and shaping pathogen-specific adaptive immunity, including cytotoxic T-cell responses [32–34]. As the first site of viral contact, the respiratory epithelium provides a physical barrier against inhaled pathogens. Tight junctions and respiratory epithelial integrity have been shown to be an important aspect of innate immune protection against EHV-1 infection [35]. Furthermore at this site, EHV-1 has been shown to upregulate pattern recognition receptors such as TLR3 and TLR9. Activation of these receptors signal downstream production of antiviral cytokines and chemokines [36–38]. Moreover, epithelial cells respond to EHV-1 infection by secreting interferons, which act as direct antivirals to limit viral replication [37–41]. Induction of INFα has also been shown to be a potent antiviral in vitro, and lower IFNα responses in nasal secretions of horses during early EHV-1 infection may increase the likelihood of developing EHM, indicating a role for early interferon production at the epithelium in disease protection [22,42]. In addition to direct antiviral molecules secreted by the epithelium, clearance of herpesviruses at the primary replication site requires recruitment of other immune cells. EHV-1 infection of equine respiratory epithelial cells induces expression of chemokines, such as IL-8, CCL2, CCL5, CXCL9, and CXCL10 and modulates chemotaxis [37–39,43,45]. This specific shaping of the recruitment of leukocytes is instrumental in protection against herpesviruses [32,34,46].

Interestingly, immunity following EHV-1 infection or vaccination is often insufficient and the main reason for this are the immune modulatory properties of the virus. Evasive strategies employed by EHV-1 include its ability to establish intracellular infection quickly to avoid detection by VN antibody [58–60]. The intracellular nature of EHV-1 also explains the finding that high levels of precursor CTLs are more likely to correlate with protection from

viremia and disease compared to serum VN titers [21,53,54]. However, EHV-1 is also known to interfere with antigen presentation via the downregulation of MHC-I, which hampers optimal CTL activation [37,39,55–57]. Ultimately though, most immune modulating events are likely to occur at the respiratory mucosa during initial infection with EHV-1. For example, the EHV-1 protein pUL56 is known to interfere with interferon production, and also induce expression of the anti-inflammatory gene IL-10 in equine respiratory epithelial cells [39]. Additionally, EHV-1 selectively interferes with the chemotaxis of leukocytes to the respiratory epithelium [61]. The EHV-1 protein pUL56 is known to modulate chemokine expression and neutrophil and monocyte chemotaxis in ERECs [39]. Glycoprotein G (gG) of EHV-1 has chemokine binding properties, which has been shown to interfere with IL-8 mediated chemotaxis of neutrophils in vitro [62,63]. Furthermore, in a murine in vivo model of EHV-1 infection, gG has shown to interfere with chemotaxis of inflammatory cells to the lung allowing for increased viral replication at this site [63,64]. Collectively, these immune evasive strategies of EHV-1, particularly during early infection, contribute to virulence in vivo and the inability of horses to develop lasting protective immunity following infection or vaccination.

Because early innate immunity is important for immediate protection as well as shaping adaptive immunity, counteracting immune modulation by EHV-1 during early epithelial infection could lead to a more robust innate immune response and consequently increased protective downstream adaptive immunity. To accomplish this, intranasal administration of live intranasal vaccines is an attractive method to stimulate mucosal innate immunity. These vaccines interact directly at the epithelium and are known to stimulate important features of mucosal innate immunity, including the secretion of inflammatory cytokines and chemokines, as well as promotion of maturation of resident antigen presentation cells [104]. For viral vaccines,

attenuated viruses are often able to induce antiviral innate immune responses because they retain their ability to replicate at the epithelium and it is known that live viral replication in the respiratory tract in horses is a potent stimulator of mucosal immunity [105,106].

Together with EHV-1, equine influenza virus (EIV) is one of the primary respiratory pathogens of horses. However, unlike EHV-1, EIV is not known for its immune modulatory properties. Instead, the fitness of influenza viruses relies on their ability to change through antigenic drift and shift. EIV infection in horses is known to induce powerful mucosal immune responses [105–107]. Furthermore, in humans it has been shown that both live attenuated influenza vaccine (LAIV) virus and wild-type influenza virus induce upregulation of pattern recognition receptors, interferons, and chemokines in the nasal mucosa as well as in respiratory epithelial cell culture systems, ultimately contributing to a diverse and potent adaptive immune response [32,34,105–113].

While current evidence is lacking, it stands to reason that an equine LAIV could induce antiviral mucosal immunity at the respiratory epithelium, and potentially overcome some of the immune-modulatory events that occur during EHV-1 infection. Flu Avert® I.N.A, is a commercially available equine LAIV, that has proven to be safe and efficacious at protecting horses against EIV [114–116]. We hypothesize that the equine LAIV, Flu Avert® I.N. (Flu Avert), induces innate immune responses at the respiratory epithelium that also provide protection against EHV-1 infection.

#### MATERIALS AND METHODS

## **Experimental design**

For this study, three experiments were conducted. A preliminary experiment evaluated the toxicity of Flu Avert in ERECs over a period of 7 days. The second experiment investigated

the effects of Flu Avert treatment on innate epithelial immune responses for 10 days after treatment of ERECs. A final experiment evaluated the effect of Flu Avert treatment for protection from EHV-1 and modulation of innate immune responses at varying times (1, 2, 5, or 7 days) prior to EHV-1 infection of ERECs. In this final experiment, EHV-1 viral titers as well as cytokine and chemokine mRNA and protein gene expression were evaluated.

#### Viruses

Flu Avert was propagated from Flu Avert® I.N.<sup>A</sup> commercial stock inoculated into Madin-Darby Canine Kidney cells (MDCK) with media consisting of Eagle's MEM (M5650)<sup>B</sup> supplemented with 0.3% Bovine Serum Albumin (A3059)<sup>B</sup>, 1% GlutaMAX <sup>C</sup>, 100 IU/mL penicillin, 100 μg/mL streptomycin, and 1 μg/mL trypsin. Cells were incubated at 33 °C and 5% CO<sub>2</sub> for 3-5 days until 90% of cells showed cytopathic effect (CPE). Cells and supernatants were collected, frozen to lyse the cells, thawed, and then centrifuged at 300 x g to remove cell debris and the stock was stored at -80 °C. The second passage was used for the experiments.

The Flu Avert titer was determined by plaque assay using serial dilutions of the propagated Flu Avert I.N. stock. Six-well plates seeded with MDCK cells were incubated with viral inoculum dilutions for 1 hr at 33 °C and 5% CO<sub>2</sub> after which 1.5% methylcellulose media was added and plates were incubated for an additional 4-5 days until plaques developed. The cells were fixed and stained with a 2% crystal violet/6% formalin solution. Viral plaques were counted, and the titer was expressed as plaque forming unit (pfu) per mL of original strength virus stock.

The EHV-1 strain Ab4 (GenBank Accession No. AY665713.1) was propagated in rabbit kidney 13 (RK-13) cells with MEM-10 (Minimum Essential Medium Eagle<sup>B</sup> supplemented with 100 IU / mL penicillin, 100  $\mu$ g / mL streptomycin, 1% GlutaMAX<sup>C</sup>, and 10% fetal bovine

serum) and incubated at 37 °C and 5% CO<sub>2</sub>. After viral propagation, the cell culture supernatants were collected, clarified, and stored as described above. The EHV-1 titer was determined by plaque assay using 10-fold serial dilutions of virus stock in RK-13 cells incubated at 37 °C and 5% CO<sub>2</sub> using the method described above.

# Animals and equine respiratory epithelial (EREC) cell cultures

Upper respiratory tract tissues were harvested from 8 horses (mean age 15 yrs; range 6-23 yrs) that were euthanized via intravenous overdose of pentobarbital sodium (≥ 86 mg/kg) for reasons unrelated to respiratory disease. All procedures were performed in compliance with the Institutional Animal Care and Use Committee of Michigan State University. Primary equine respiratory epithelial cells (ERECs) were isolated and cryopreserved as previously described [38]. Briefly, 6-8 inch sections of trachea were dissected from horses immediately following euthanasia and the mucosal surface was digested for 3-5 days at 4 °C in a 1.4 % Pronase<sup>D</sup> and 0.1% deoxyribonuclease I<sup>B</sup> solution in minimum essential medium without calcium or magnesium<sup>B</sup>. Following digestion, the cells were incubated for 2 hours in an uncoated petri dish at 37 °C to reduce fibroblast contamination after which the floating cells were collected and cryopreserved in liquid nitrogen until further use.

For each experiment, ERECs were thawed and cultured at the air-liquid interface by adding 2-3 million cells in 500  $\mu$ L of DMEM/F12<sup>C</sup> media supplemented with 5% FBS that was not heat inactivated, 1% MEM non-essential amino acid solution<sup>C</sup>, 100 IU/mL penicillin, 100  $\mu$ g/mL streptomycin, and 1.25  $\mu$ g/mL amphotericin to the top chamber of a collagen coated Transwell polyester membrane insert of a 12 well plate<sup>E</sup> as previously described [38]. One mL of the above media was added to the bottom chamber and the plates were incubated overnight at 37 °C with 5% CO<sub>2</sub>. The next day, the media in the top chamber was aspirated off and the media in

the bottom chamber was replaced with DMEM/F12<sup>C</sup> supplemented with 2% Ultroser G TM<sup>F</sup>, 100 IU/mL penicillin, 100  $\mu$ g/mL streptomycin, and 1.25  $\mu$ g/mL amphotericin B. Media in the bottom chamber was replaced every 2-4 days and the cultures were maintained for 3-4 weeks until fully differentiated. Fully differentiated cultures were used in the subsequent experiments.

# **Toxicity of Flu Avert in ERECs**

Cell culture and inoculation

Fully differentiated EREC cultures derived from tracheal tissues from three horses were washed with 500 µL DMEM/F12 media<sup>C</sup>. Cells were treated with Flu Avert I.N. (with multiplicities of infection (MOIs) of 0.1, 1 or 5) or media control (MOI of 0) at the apical side of the cell culture, in 500 µL DMEM/F12 media<sup>C</sup>. After two hours of incubation at 37 °C with Flu Avert, the inoculum was removed, and cells were washed twice with DMEM media<sup>C</sup> and incubated at 37 °C until cell collection. Cell pellets were collected 1, 2, 3, 4, 5, 6, and 7 days post Flu Avert treatment, and media supernatants in the bottom chamber were replaced every 4 days throughout the experiment. To collect the ERECs, cells were incubated with Accumax dissociation solution<sup>G</sup> for 2 cycles. For this, the top chamber was rinsed with 300 µL PBS, aspirated, and then incubated with 300 µL Accumax for 30 min at 37 °C. The dissociation solution was then collected on ice, and another 300 µL Accumax was added and further incubated for 20-45 minutes until all remaining cells were dissociated and this solution was added to the first aliquot. The top chamber was rinsed again with 300 µL PBS to collect any remaining cells and added to the Accumax/cell suspension. The cells were then pelleted by spinning at 300 x g for 10 minutes.

# Microscopic evaluation

Cultures for the toxicity experiment were evaluated by microscopy for evidence of cytopathic effect daily for 7 days following Flu Avert treatment. Images were taken and scored using the scale described in Table 3.

# Cell viability analysis

For the Flu Avert toxicity experiments, cell pellets were resuspended in PBS with 0.4% bovine serum albumin and 0.1% sodium azide and analyzed immediately following collection for cell viability using propidium iodide (PI) staining and flow cytometry. Twenty thousand events were collected from each sample both prior to and after staining with PI (10µg/mL). Positive events in stained and unstained samples were determined using frequency gating in Flowing Software version 2.5.1. The percent of dead cells for each sample was determined from the percent positive events for the PI stained samples.

# Effects of Flu Avert treatment on immune response in ERECs

Fully differentiated ERECs isolated from tracheal tissues of five horses were treated with Flu Avert (MOI=5) or media control on the apical side in 500 μL DMEM/F12 media<sup>C</sup>. After two hours of incubation at 37 °C with Flu Avert or media, the inoculum was removed, and cells were washed twice with DMEM media<sup>C</sup>. Cells were incubated at 37 °C and 5% CO<sub>2</sub> and the media was changed every 2-4 days until sample collection. ERECs were collected using Accumax dissociation solution<sup>G</sup> daily 2-10 days post Flu Avert or media treatment, as described in the previous experiment. The cell culture supernatants were collected 4, 5, 8, and 10 days post treatment for protein cytokine analysis. Cells were divided in half and the pellets stored as two separate aliquots at -80 °C until further processing for cytokine mRNA expression analyses. At

the same time, the cell culture supernatants were collected into separate aliquots and stored at -80 °C until further cytokine protein expression analyses.

## Effects of Flu Avert treatment and EHV-1 inoculation in ERECs

Fully differentiated ERECs isolated from tracheal tissues of five horses were treated with Flu Avert (MOI=5) or media control on the apical side of the cell culture as described above. After two hours of incubation at 37 °C with Flu Avert or media, the inoculum was removed, and cells were washed twice with DMEM media<sup>C</sup>. Cells were incubated at 37 °C and 5% CO<sub>2</sub> and the media was changed every 2-4 days until EHV-1 inoculation.

Following Flu Avert or media treatment ERECs were inoculated with EHV-1 strain Ab4 (MOI = 1) suspended in 500  $\mu$ L DMEM/F12<sup>C</sup> or media at 1, 2, 5, or 7 days post Flu Avert treatment. This dose was chosen based on previous studies [35,42,117] and the dose of the same virus typically used by our group in challenge infection experiments of horses [22,76]. After two hours of incubation at 37 °C with EHV-1 or media, the inoculum was removed, and cells were washed once with DMEM/F12 media<sup>C</sup> and incubated at 37 °C until collection. ERECs were collected using Accumax dissociation solution<sup>G</sup> at 24, 48, and 72 hours post EHV-1/Mock inoculation as described in the previous experiment. Cells were divided in half and the pellets stored as two separate aliquots at -80 °C until further processing for EHV-1 growth curves or cytokine mRNA expression analyses. At the same time, the cell culture supernatants were collected into separate aliquots and stored at -80 °C until further processing for EHV-1 growth curves and cytokine protein expression analyses.

## EHV-1 intracellular and extracellular growth curves

As part of the final experiment, EHV-1 viral load was determined from the cell pellets (intracellular) and supernatants (extracellular) by qPCR for the EHV-1 gB gene as previously

described [10]. DNA was isolated from all samples using the MagAttract 96 cador Pathogen Kit<sup>H</sup> and quantified using the NanoDrop 2000 spectrophotometer<sup>I</sup>. Reactions consisted of 10 μL TaqMan<sup>TM</sup> Fast Universal PCR Master Mix (2X), no AmpErase<sup>TM</sup> UNG<sup>J</sup>, 400 nM forward and reverse primers, 200 nM probe, with nuclease free water and DNA template added to a final reaction volume of 20 μL. Plasmid DNA gene copies generated from the gB gene product were quantified and included in 10-fold serial dilutions in each run in order to create a standard curve. Samples and standards were run in triplicate and duplicate, respectively. No-template controls were included on each plate. Thermocycling was performed on the Applied Biosystems 7500 Fast Real-Time PCR system using the following conditions: 20s holding stage at 95 °C followed by 37 cycles of 3s 95 °C denature and 30s at 60 °C anneal/extension. Viral load was expressed as EHV-1 copy number per ng of DNA for cell pellets and EHV-1 copy number per PCR reaction for supernatants.

# **Cytokine protein expression in EREC supernatants**

Cytokine protein expression for equine cytokines IL-4, IL-10, IL-17, IFNα, and IFNγ in cell culture supernatants was evaluated using a bead-based multiplex assay as previously described by Wagner and Freer (2009) at the Animal Health Diagnostic Center, Cornell University, Ithaca, NY [78].

## mRNA isolation

For gene expression analysis, cell pellets were lysed and homogenized using TRIzol Reagent<sup>I</sup> following the manufacturer's instructions. The aqueous phase was then collected, washed with 100% ethanol and the RNA was isolated using the RNeasy Mini Kit<sup>H</sup> according to the manufacturer's instructions. To eliminate genomic DNA contamination, deoxyribonuclease treatment<sup>H</sup> was applied to each sample according to the manufacturer's recommendation.

# RT-qPCR for mRNA expression analysis

RNA was quantified using the NanoDrop 2000 spectrophotometer<sup>I</sup> and 297 ng RNA was used in a 30 µL reverse transcription reaction with the High-Capacity cDNA Reverse Transcription Kit with RNAse inhibitor<sup>I</sup>. High throughput qPCR was then performed using the SmartChip Real-Time PCR System<sup>K</sup>. The chip was loaded and thermocycling performed following the manufacturer's recommendations – with reactions consisting of template cDNA, TaqMan Gene Expression Master Mix<sup>I</sup>, and the appropriate primer/probe combination. See Table 4 for details on primers and probes. Samples were run in triplicate, with 12 no-template control reactions per chip.

Three housekeeping genes (ACTB, B2M, and GUSB) were used to normalize the genes of interest, and the average of the untreated and mock inoculated cells was used as a calibrator. Relative expression was expressed as log fold change (the -ddCq value) from the calibrator for each gene of interest as described by Livak and Schmittgen, 2001 [118].

# **Statistical Analysis**

All statistical analysis was performed using R software version 3.4.2. For cell viability analysis, differences in viability between the MOIs were analyzed using the Kruskal-Wallis rank sum test (kruskal.test function). For analyzing the effect of Flu Avert treatment on cytokine responses in ERECs, statistical analysis was performed using either a Wilcoxon rank sum test (wilcox.test function) for RT-qPCR data or a Welch's two sample t-test (t.test function) for protein data. For analyzing the effect on Flu Avert treatment and subsequent EHV-1 inoculation on cytokine responses in ERECs, statistical analysis was performed using either a Kruskal-Wallis rank sum test with Dunn's post hoc analysis (dunn.test function, part of the dunn.test package) for RT-qPCR data or ANOVA (aov function) with Tukey's post hoc analysis

(TukeyHSD function) for protein expression. For EHV-1 replication, viral copy number was ranked, and a paired one tailed t-test was (t.test function) performed.

#### RESULTS

#### Flu Avert is non-toxic in ERECs

Before evaluation of the effect of Flu Avert on subsequent inoculation with EHV-1, we wanted to ensure that Flu Avert was not toxic for the EREC cultures over several days following Flu Avert inoculation. According to microscopic evaluation, there was no dose effect of Flu Avert on CPE scores (Figure 8A). A slight rise in score over time was observed for all doses including the media control (MOI=0). Propidium iodide viability staining confirmed the microscopic observations; there were no significant differences between groups, indicating there was no toxic effect of Flu Avert when used up to an MOI of 5 for 7 days following treatment (Figure 8B).

# Flu Avert induces cytokine responses in ERECs between days 5 and 10 post inoculation

Cytokine mRNA expression in Flu Avert treated and untreated cells were evaluated to determine the effects of Flu Avert on stimulation of immune gene expression over time in ERECs. CCL2, CCL5, CXCL9, CXCL10, and IL-8 mRNA expression was detected in the samples. Interestingly, there were no statistically significant differences in cytokine expression between Flu Avert and media treated cells until 6 days post treatment. On days 6-8 post treatment, IL-8 mRNA was significantly upregulated in Flu Avert treated cells (Figure 8C). CXCL9 was downregulated in Flu Avert treated cells when compared to media treated cells on day 5 (p = 0.06), and day 10 (p = 0.11) but differences were not quite statistically significant (Figure 8D). On day 6 post treatment, CCL2 was upregulated, but this trend was not statistically significant (Figure 8E). There were no differences observed in CXCL10 and CCL5 expression

(data not shown). Expression for IFN $\alpha$ , INF $\beta$ , IFN $\gamma$ , and IL-10 mRNA was positive in less than 10% of total samples (data not shown).

Protein secretion in EREC supernatants was also measured. IL-10 and IL-17 proteins were detected, but there were no differences between Flu Avert and media treatments (data not shown). Protein levels for IFN $\alpha$  and IL-4 were below the limit of detection for the assay and levels of IFN $\gamma$  were below 4 U/mL for all samples (data not shown).

# Flu Avert treatment reduces EHV-1 replication in ERECs

EHV-1 viral load in Flu Avert treated and untreated EHV-1 inoculated ERECs was determined for cell pellets (intracellular) and for supernatants (extracellular). In order to determine the Flu Avert treatment days that led to consistent reduction in EHV-1 titers, culture wells in which EHV-1 titers were lower in Flu Avert treated cultures compared to untreated cultures at 48 and 72 hours post EHV-1 inoculation were counted. We found that treatment day -5 resulted in the most cultures with reduced EHV-1 titers following Flu Avert treatment (8 of 10 wells for intracellular titers and 7/10 wells for extracellular titers) (Table 5). When titers were analyzed for each individual day post EHV-1 inoculation, there was little EHV-1 load and thus no differences observed in intracellular titer between Flu Avert and untreated cells at 24 hours post EHV-1 inoculation (Figure 9). At 48 hours post EHV-1 inoculation, there was a reduction in intracellular titer in cells treated with Flu Avert 2 days (p = 0.06) and 5 days (p = 0.07) prior to EHV-1 inoculation when compared to untreated cells (Figure 9). At 72 hours, there was again a reduction in titer in ERECs treated with Flu Avert 5 days prior to EHV-1 inoculation (p < 0.1) (Figure 9). For extracellular viral loads, there was a statistically significant reduction in titer in Flu Avert treated supernatants for treatment day -1 and day -5 when compared to the untreated supernatants at 72 hours post EHV-1 inoculation (Figure 10). Taking the combined results in

consideration, our data suggests that treatment with Flu Avert day -5 prior to EHV-1 inoculation most effectively resulted in a reduction of intracellular and extracellular EHV-1 titer in ERECs. All mock inoculated samples were negative for EHV-1 (data not shown). Four mock inoculated intracellular samples were excluded from analysis due to insufficient DNA isolation or contamination.

# Flu Avert treatment enhances cytokine response to EHV-1 infection in ERECs

At 24 hours post EHV-1 inoculation in untreated cells, a statistically significant induction of chemokine responses was not observed. In contrast, when ERECs were pretreated with Flu Avert treatment at days -5 or -7 prior to EHV-1 inoculation, IL-8 expression was significantly upregulated in Flu Avert/EHV-1 inoculated ERECs, compared to the untreated and uninfected ERECs (Figure 11A, B). A similar trend was observed for CXCL10 expression in ERECs treated with Flu Avert 7 days prior to EHV-1 or mock inoculation, although this trend was not statistically significant when compared to the media/mock inoculated ERECs (Figure 11D). There were no differences in IL-8 and CXCL10 expression for treatment day -1 or day -2 (data not shown) or in CXCL10 expression for treatment day -5 (Figure 11C). No differences were observed between groups for expression of CCL2, CCL5, or CXCL9 at 24 hours post EHV-1 inoculation (data not shown).

By 48 hours post EHV-1 inoculation, IL-8 expression was statistically significantly upregulated in all Flu Avert/EHV-1 inoculated ERECs when compared to untreated/mock inoculated ERECs for all Flu Avert treatment timepoints (Figure 12). IL-8 was also upregulated in untreated/EHV-1 inoculated ERECs for all treatment timepoints, and this was statistically significant for treatment day -1, day -5 and day -7. For CCL2 expression a similar trend was observed in ERECs 48 hours post EHV-1 inoculation that were pre-treated with Flu Avert on

days -2 and -7, but this trend was not statistically significant (Figure 12). Expression of CCL5, CXCL9, and CXCL10 was not different between groups 48 hours post EHV-1 infection (data not shown).

By 72 hours post EHV-1 infection, IL-8 was upregulated in EHV-1 inoculated ERECs pretreated with Flu Avert that was statistically significant for treatment day -2 and day -5 and untreated/EHV-1 inoculated ERECs for all treatment days besides for day -1 (data not shown). A similar trend (albeit not quite statistically significant) was observed for CCL2 expression where EHV-1 inoculation increased CCL2 compared to untreated/mock inoculated cells in cells pretreated with Flu Avert on day -2 (p = 0.12) and day -5 (p = 0.07) (Figure 13). In addition, ERECs treated with Flu Avert and inoculated with EHV-1 showed downregulated expression of CXCL9, and this was statistically significant in cells treated with Flu Avert 7 days prior to inoculation with EHV-1 (day -2 p = 0.07; day -5 p = 0.18; day -7 p < 0.05) (Figure 13). Furthermore, there was a downregulation in CXCL9 in EHV-1 inoculated ERECs treated with Flu Avert 5 days prior compared to untreated EHV-1 infected cells (p = 0.12) (Figure 13). There were no differences in mRNA expression of CCL2 or CXCL9 between ERECs for Flu Avert treatment day -1 (data not shown). There were no differences in expression of CCL5 and CXCL10 between groups at 72 hours post EHV-1 inoculation (data not shown).

Expression for IFN $\beta$  was low or near the limit of detection for all samples, and only ~17% of all samples were positive for this cytokine. Based on the low percent of positive samples, no relative quantitation was performed. However, EHV-1 infected samples appeared to be more likely to express IFN $\beta$  than mock inoculated samples. Of the 40 samples with detectable IFN $\beta$  mRNA expression, 30 were EHV-1 inoculated wells. Expression of IFN $\alpha$ , IFN $\gamma$ , and IL-10 mRNA was positive in less than 10% of total samples (data not shown).

Finally, EHV-1 inoculation downregulated IL-10 protein expression in EREC supernatants 72 hours post EHV-1 inoculation in both Flu Avert and untreated cells when compared to mock inoculated ERECs for treatment days -1, -2, and -5, but this was not quite statistically significant (data not shown). Interestingly, for treatment day -7, there was less downregulation of IL-10 observed in the supernatants from cells pre-treated with Flu Avert prior to EHV-1 inoculation when compared to mock inoculated groups (Figure 14). There were no differences in IL-17 protein expression between groups (data not shown). Expression of IFNα and IL-4 proteins were below the limit of detection of the assay, and expression of IFNγ proteins were below 4 U/mL in all sample (data not shown).

#### DISCUSSION

Our hypothesis was that exposure to a live-attenuated influenza vaccine (LAIV) would stimulate innate immunity in equine respiratory epithelial cells (ERECs), and that this response would protect cells against EHV-1 infection and replication. We found that Flu Avert stimulated epithelial immunity, and that these responses were optimal starting at day 5 post Flu Avert treatment. While it has been well established in humans that influenza virus infection or LAIV vaccination stimulates mucosal immunity, very little work has been done evaluating the equine respiratory epithelial innate immune response to EIV or equine LAIV. Here we show that Flu Avert treatment of ERECs stimulated induction of chemokine expression. In particular, we observed an upregulation of IL-8 and CCL2 expression following Flu Avert treatment, which agrees with other studies investigating mucosal chemokine responses to influenza vaccination. In humans, it has been shown that following LAIV treatment chemokine expression for CXCL9, CXCL10, CCL5, CCL2, and IL-8 are upregulated in human primary epithelial cell cultures [109,110].

Our data, along with these human studies, indicate that LAIVs such as Flu Avert act to stimulate epithelial mucosal immunity in primary cells of the upper respiratory tract, and may provide important information for how the natural airway will respond to treatment in the horse. In contrast to the human cell culture studies, we did not observe any effect on CCL5 or CXCL10 mRNA expression in our equine system. This may be attributed to different responses of human and equine cells to LAIV treatment, or be due to limits of detection in our system that was used at 37 °C (the optimal temperature for EHV-1 replication in vitro), while the human studies were conducted at 32 °C, which is known to more closely mimic the temperature of the human upper respiratory tract [119]. It is known that Flu Avert is a cold-adapted vaccine and previous work indicates that Flu Avert replicates more efficiently at 30 °C in MDBKs.[120] Because the magnitude of innate immune responses in epithelial cells depend on replication of viral RNA, optimal replication of LAIV may be necessary for optimal induction of chemokines [109]. However, even at suboptimal temperatures for Flu Avert replication, we did observe induction of IL-8 and CCL2. In addition, CXCL9 was downregulated in this experiment. Clearly, more work is needed to test Flu Avert treatment in horses and its effect on chemokine responses in the in vivo nasal mucosa and further downstream immune responses.

Stimulation of innate immunity is classically considered to occur quickly, often within hours, following virus infection. However, our data suggests that following treatment with Flu Avert, peak responses start at 5 days post treatment. This could be due to slow replication in the ERECs due to attenuation of the Flu Avert virus. In a study of LAIV treatment in human nasal epithelial cell cultures, it was also observed that peak cytokine responses occurred several days following treatment [109]. It has been shown that peak cytokine responses to LAIV correspond to expression of viral RNA in human epithelial cultures, and *in vivo* nasal IFN $\alpha$  peaks

corresponds with peak EIV viral titer and clinical disease [110,121]. While we did not measure Flu Avert RNA genome titers over time, it is likely that these peaked in ERECs at a similar timepoint where peak cytokine expression was observed.

In addition to chemokines, EIV infection is known to stimulate interferon production in nasal secretions of ponies beginning 2 days post infection [107]. In our study, interferon expression was near the detection limit, and we only detected interferon mRNA (IFNβ) expression in ERECs following treatment with Flu Avert in a few samples. In human epithelial cells, it is shown that LAIV stimulates many features of the interferon pathway, including the upregulation of pattern recognition receptors and expression of interferon stimulated genes (ISGs) [109,110]. However, in a cohort of human patients who received LAIV, only 21% had detectable levels of IFNα in nasal wash, while several ISGs were upregulated [111]. These results, along with ours, indicate that while the interferon pathway is stimulated by LAIV, the temporal regulation of different genes likely contribute to the timing of expression and ultimately detection of mRNA or proteins. The interferon pathway is stimulated through activation of pattern recognition receptors, including TLR3,[36,108] and in ERECs we have previously shown that either infection with wild type EIV or treatment with Flu Avert stimulated expression of TLR3 within 24 hours [120]. In our study, it is likely the interferon pathway was stimulated in ERECs in response to Flu Avert, however, IFN $\alpha$  and IFN $\beta$  as well as IFN $\gamma$  were at or below the limit of detection in our cultures. Though it has been shown that LAIV induces many aspects of the interferon pathway in epithelial cells, there is evidence that this response is more attributed to induction of type III interferon (IFNλ) which is unique to epithelial cells, [122] rather than type I (IFNα, IFNβ) interferons. Similarly, in mice, it was found that IFNλ was induced in epithelial cells to far greater levels than type I interferons in response to influenza challenge [123]. Future

studies should consider analyzing expression of IFN $\lambda$  or ISGs in addition to type I and II interferons in order to get a more complete picture of the role of Flu Avert on the interferon response.

Interestingly, peak chemokine modulation which occurred in ERECs on 5-8 days post Flu Avert treatment, also corresponded with optimal reduction in EHV-1 titers in the EHV-1 inoculated cells. The delayed peak in cytokine expression explains the timing of optimal EHV-1 reduction in our system, which was ultimately the goal of Flu Avert treatment. Here, the effects of Flu Avert on EHV-1 replication were investigated by generating EHV-1 intracellular and extracellular growth curves in ERECs. We found that treating with Flu Avert 5 days prior to EHV-1 inoculation was most likely to interfere with EHV-1 replication, particularly when intracellular and extracellular results were combined. However, the reduction in copy number was not complete, which is likely because the EREC system lacks the comprehensive immune system that the whole respiratory tract possesses. While antiviral cytokines and chemokines are expressed in ERECs, the leukocyte recruitment that would occur in the natural airway is absent and this recruitment and activation of leukocytes is critical for effective innate and adaptive immune responses and for effective pathogen elimination. Despite this limitation, the EREC system was useful at providing important information about the epithelial response to viral infection and to determine timing of optimal reduction in viral titers prior to further in vivo studies in the natural host.

The intention of this work is to investigate the suitability of the equine mucosal influenza virus vaccine to stimulate strong non-specific innate antiviral respiratory immunity to provide protection from another major equine respiratory virus, EHV-1. This could be particularly helpful, because it is known that EHV-1 modulates and suppresses innate respiratory immunity

[37,39,55–57,61–64]. In this study, it was observed that Flu Avert treatment modulated chemokine expression in EHV-1 infected cells. These chemokine responses of epithelial cells to EHV-1 are instrumental in promoting immune cell recruitment to the upper respiratory epithelium and ultimately protection from EHV-1 [32,34,124]. Specifically, we observed that ERECs treated with Flu Avert showed a significant upregulation of IL-8 expression by 24 hours post EHV-1 inoculation, whereas this increase was not seen in the untreated cells until 48 hours post EHV-1 inoculation. Influenza virus infection is known to stimulate IL-8 production in epithelial cells, supporting our finding that pre-treatment with Flu Avert enhanced IL-8 responses to EHV-1 in our study [112]. Similarly to IL-8 responses, we observed that Flu Avert treatment prior to EHV-1 inoculation enhanced the CCL2 expression in response to EHV-1. CCL2 and CCL5 act to recruit monocytes and memory T-cells, and influenza virus infection is known to stimulate both CCL2 and CCL5 production in epithelial cells [125,126]. Our data suggests that pre-treatment with Flu Avert may act similarly and might function to rescue CCL2 expression in respiratory epithelial cells during EHV-1 infection [125]. The modulation of IL-8 and CCL2 by EHV-1 is supported by studies showing that EHV-1 proteins, gG, and pUL56 suppress IL-8 protein responses and neutrophil chemotaxis, and play an important role in viral clearance [39,63,64]. Furthermore, EHV-1 pUL56 has been shown to suppress the expression of CCL2 in ERECs, and in PBMCs following EHV-1 infection [39,41]. The current theory is that EHV-1 selectively modulates recruitment of immune cells to its advantage by suppressing IL-8 and CCL2 and preventing recruitment of cells for viral clearance but not interfering with recruitment of cells that permit an establishment of viremia [61]. Interestingly, it has also been shown that neuro-pathogenic EHV-1 strains recruit monocytes via CCL2 and CCL5 expression more significantly than less neuro-pathogenic strains [45].

CXCL9 and CXCL10 are related chemokines that serve to recruit T-cells, including CTLs, and are thus of interest when considering induction of a robust immune response to herpesviruses [127]. In our study, we found that CXCL10 expression was enhanced in Flu Avert treated, but not media treated cells 24 hours following EHV-1 inoculation. On the other hand, we were surprised to observe a downregulation of CXCL9 in Flu Avert treated cells following EHV-1 inoculation. A previous study in ERECs showed a significant increase in both CXCL9 and CXCL10 expression following EHV-1 inoculation [43]. It has been shown that dramatic CXCL9 and CXCL10 expression is induced in PBMCs following EHV-1 infection, but this expression peaked at 10 hours post inoculation, and returned to baseline by 24 hours post inoculation [41]. Furthermore, influenza virus has been shown to induce rapid expression of CXCL9 and CXCL10 following infection in epithelial cells [128]. It is unclear why we observed an upregulation of CXCL10, but a downregulation of CXCL9 in ERECs following Flu Avert treatment and EHV-1 inoculation, given the related function of these two chemokines. One explanation is that our study investigated responses several days following initial Flu Avert treatment and not until 24 hours post EHV-1 infection, thus it is possible that the timepoints we investigated here were too late to observe an upregulation of CXCL9 expression. More work is needed to fully understand the complicated balance of these chemokine expression patterns following epithelial infection with Flu Avert and EHV-1 and its implications for EHV-1 related disease. However, it is clear that timing post Flu Avert administration must be considered in order to see the optimal response.

Previous work in ERECs have shown an increase in type I interferons (IFN $\alpha$  and IFN $\beta$ ) in response to EHV-1 infection [37,39,42]. In our study, levels of IFN $\alpha$  mRNA and proteins were below detectable levels. One explanation is that the previous studies were performed using

EHV-1 and a MOI of 10. In the present study, the inoculations were performed at a MOI of 1. This lower MOI is arguably more biologically relevant. Additionally, interferons are well known to be quickly and transiently expressed molecules of the innate immune system. In one study, Poelaert et al. found that type I interferon proteins were detectable as early as 10 hours post EHV-1 inoculation in ERECs and remained detectable up through 72 hours [42]. In our study, we measured mRNA, and thus it is possible the peak mRNA expression period in our system was missed with the timepoints chosen for sample collections. Additionally, type III, rather than type I, interferons are known to be specialized for epithelial responses, and have been shown to be the primary drivers of the interferon responses to influenza virus infection [122,123]. To our knowledge, IFNλ expression has not been evaluated in equine respiratory tissues, and may play a role in protection from EHV-1 infection.

Finally, IL-10 is an immunoregulatory cytokine that tempers excessive immune responses and is important for preventing immune-mediated damage to host tissues [91]. In our study, IL-10 mRNA was below the limit of detection of our assay, however, we were able to detect IL-10 proteins in EREC supernatants following EHV-1 infection. We found EHV-1 infection downregulated IL-10 expression; nevertheless, this response was less apparent in those cells treated with Flu Avert 7 days prior to EHV-1 inoculation, indicating that Flu Avert treatment at this time may have counteracted the suppressive effect of EHV-1. In addition to its anti-inflammatory role, IL-10 is known to contribute to B-cell activation, which at the site of the nasal epithelium could contribute to mucosal IgA antibody production [129]. Our finding that Flu Avert may reduce the IL-10 suppression by EHV-1 may be important when considering boosting mucosal humoral immunity.

In summary, this study revealed important information regarding the epithelial innate immune response to LAIV in equine respiratory epithelial cells. In this primary cell culture system, peak responses to this attenuated virus occurred several days following administration and this correlated with peak reduction in EHV-1 replication. These results suggest that Flu Avert may be effective at counteracting the immune-modulatory properties of EHV-1; however, more work is needed to understand whether the chemokine enhancing effects of Flu Avert at the site of the epithelium will translate to more protective adaptive immune responses *in vivo*. Finally, our study suggests that future *in vivo* research should consider the timing of administration of immune stimulants or mucosal vaccines during experimental design.

#### **AUTHORSHIP**

All authors contributed to study design, interpretation of data, and approval of the final manuscript. LMZ and GSH contributed to study execution, data analysis, and preparation of the manuscript.

#### **FUNDING**

This study was funded by MSD Animal Health

#### **COMPETING INTERESTS**

WEV, DCB, and FTB are employed by MSD Animal Health

## ETHICAL ANIMAL RESEARCH

Post-mortem tissues were collected from animals owned by Michigan State University and all work was performed with approval from Michigan State University's Institutional Animal Care and Use Committee.

#### OWNER INFORMED CONSENT

All animals were owned by Michigan State University.

#### ACKNOWLEDGEMENTS

The authors would like to thank Rahul Nelli for his contribution to primer design, Christi Harris, Emily Crisovan, and the Genomics Research and Technology Support Facility at Michigan State University for their assistance with the SmartChip Real-Time PCR System, and Christi Harris, Louis King, and the Flow Cytometry Research and Technology Support Facility at Michigan State University for their assistance with flow cytometry.

## **MANUFACTURERS' DETAILS**

- A. MSD Animal Health, Kenilworth, NJ USA
- B. Sigma Aldrich, St. Louis, MO USA
- C. GIBCO, Life Technologies, Carlsbad, CA USA
- D. Roche Applied Science, Indianapolis, IN USA
- E. Corning, Inc., Corning, NY USA
- F. Pall, Port Washington, NY USA
- G. Qiagen, Hilden, Germany
- H. Thermo Fisher, Waltham, MA USA
- I. Applied Biosystems, Waltham, MA USA
- J. Takara Bio Inc., Kusatsu, Shiga, Japan

## **CHAPTER 4**

# TRANSCRIPTOMIC PROFILING OF EQUINE AND VIRAL GENES IN PERIPHERAL BLOOD MONONUCLEAR CELLS IN HORSES DURING EQUINE HERPESVIRUS 1 INFECTION

Lila M. Zarski, Patty Sue D. Weber, Yao Lee, Gisela Soboll Hussey

#### **ABSTRACT**

Equine herpesvirus 1 affects horses worldwide and causes respiratory disease, abortions, and equine herpesvirus myeloencephalopathy (EHM). Following infection, a cell associated viremia is established in the peripheral blood mononuclear cells (PBMCs). This viremia is essential for transport of EHV-1 to secondary infection sites where subsequent immunopathology results in disease such as abortion or EHM. Because of the central role of PBMCs in EHV-1 pathogenesis, our goal was to establish a gene expression analysis of host and equine herpesvirus genes during EHV-1 viremia using RNA sequencing. When comparing transcriptomes of PBMCs during peak viremia to those prior to EHV-1 infection, we found 51 differentially expressed equine genes (48 upregulated and 3 downregulated). After gene ontology analysis, processes such as the interferon defense response, response to chemokines, the complement protein activation cascade, cell adhesion as well as coagulation were overrepresented during viremia. Additionally, transcripts for EHV-1, EHV-2, and EHV-5 were identified in pre and post EHV-1 infection samples. Looking at miRNAs, 278 known equine miRNAs and 855 potentially novel equine miRNAs were identified and 57 and 41 potentially novel miRNAs that mapped to the EHV-2 and EHV-5 genomes. Of those, 4 equine and 1 EHV-5 miRNAs were differentially expressed in PBMCs during viremia. In conclusion, this work expands our current knowledge about the role of PBMCs during EHV-1 viremia and will inform the focus on future experiments to identify host and viral factors that contribute to clinical EHM.

#### **KEYWORDS**

EHV-1

Herpesvirus

Horse

**PBMC** 

Transcriptomics

RNA sequencing

microRNA

gene expression

#### INTRODUCTION

The Herpesviridae are ubiquitous pathogens that infect most mammals, birds, and reptiles. They are enveloped, double stranded DNA viruses with the trademark ability to establish life-long latency in their hosts. The latent genome packages itself within the cell nucleus as a circular extra-chromosomal episome of viral genomic DNA [130]. Latent infections are typically subclinical, though reactivation or reinfection from another host can produce active clinical disease. In horses, the most commonly described herpesviruses include Equid alphaherpesvirus 1 (EHV-1), Equid gammaherpesvirus 2 (EHV-2), Equid alphaherpesvirus 4 (EHV-4), and Equid gammaherpesvirus 5 (EHV-5) [131]. These viruses fall into two main subfamilies: the alphaherpesvirinae (EHV-1 and EHV-4) and the gammaherpesvirinae (EHV-2 and EHV-5). Alphaherpesviruses are known for their rapid lytic replication in many cell types [131]. Alphaherpesviruses typically (though not exclusively) establish latency in the sensory ganglia of their host, however, EHV-1 is also known to establish latency in lymphoid tissues [5– 8,132]. On the other hand, gammaherpesviruses are more restrictive in their cell tropism and are known to establish latency primarily in lymphocytes as well as for their slow replication cycle [130,133].

In horses, alpha and gamma herpesviruses are ubiquitous and have been reported to be detected in their respective tissues of latency in over 75% of healthy animals [6,131,133]. For the

equine gammaherpesviruses, the role of infection in clinical disease is not well understood. However there are reports showing an association with pulmonary fibrosis, pharyngitis, dermatitis, lymphoma, as well as other conditions [133]. In contrast, active infection with the equine alphaherpesviruses EHV-1 and EHV-4 are primary causes of acute respiratory disease in younger animals, which is a major contributor to loss of training [18]. In addition, EHV-1 also can cause late-term abortion, neonatal death, ocular disease or the neurologic disease equine herpesvirus myeloencephalopathy (EHM) in up to 10% of infected cases [18]. This is in contrast to EHV-4 infection, which typically stays restricted to the respiratory tract and does not cause abortions or EHM [134].

The key reason for the difference in secondary clinical disease manifestations between EHV-1 and EHV-4 is the fact that EHV-1 establishes viremia, which is essential for transporting the virus from the respiratory tract to the secondary sites of infection. In contrast, viremia is not known to be a central feature of EHV-4 disease pathogenesis. EHV-1 establishes viremia in peripheral blood mononuclear cells (PBMCs) shortly after initial infection of the respiratory epithelium. Within the population of PBMCs, monocytes, T-cells, and B-cells are shown to become infected with EHV-1, and there are conflicting reports on which of these subpopulation the virus prefers [23,135–138]. Unlike the lytic life cycle of infected epithelial cells in which full transcription and replication of virions destroys cells and produces free virus, infection in PBMCs is characterized by a restricted viral gene expression, which delays viral replication until the cell has made contact with the vascular endothelium [28,29,60]. This allows the virus to effectively evade immune surveillance within the PBMCs while being transported to the secondary sites of infection. Furthermore, it is likely that viremia is an important step in the establishment of latency of EHV-1 in lymphoid tissues [132].

Thus, the period of viremia is a critical prerequisite for the development of secondary disease such as EHM and abortions. It has been shown that EHM generally develops during the end of the viremia phase and that longer duration and higher magnitude of viremia contribute to the likelihood of EHM [21]. It is presumed that the prolonged exposure to infected PBMCs increases the potential of viral transfer to the vascular endothelium. In addition to the necessity of viral transfer to the vascular endothelium, perhaps the most critical factor affecting vascular damage and subsequently the clinical outcome, is the immunopathology that occurs at this site. Because PBMCs are a robust immune and inflammatory cell population in the vasculature, as well as carriers of EHV-1 virus, they are an important focus of investigation of EHV-1 associated secondary diseases.

Despite the importance of PBMCs for the development of secondary EHV-1 associated diseases, limited information is available about the host or viral gene expression in these cells during this period. At this point, various cytokines, such as interleukin-10, interferon gamma (IFNγ), and tumor necrosis factor beta have been shown to be induced in the blood of horses during EHV-1 viremia [22,76]. In vitro, EHV-1 induces expression of interferons, cytokines, and chemokines in both epithelial cells and PBMCs [40,41]. However, a complete profile of host and viral mRNA expression has not yet been performed.

In addition, micro RNAs (miRNAs) may play a role in the regulation of host and viral gene expression in PBMCs during viremia. Micro RNAs are small (~22 bases) RNA molecules that block the translation of their target coding mRNAs [139]. It is becoming clear that host and viral miRNAs play an important role in the evasion from immune detection as a response to EHV-1 infection. Cellular (host) miRNAs have been shown to inhibit viral genome replication for HSV-1, which likely contributes to the virus' ability to persist in the cell undetected [140].

Virally-encoded miRNAs have been identified in several herpesviruses, and play an important role in viral persistence in cells by downregulating host immune responses [141]. At this time, the role of miRNAs are unknown for EHV-1 replication.

The goal of this study was to use RNA sequencing to analyze the mRNA and miRNA transcriptome of equine PBMCs before and during EHV-1 viremia as an unbiased and comprehensive approach to gene expression analysis. Our rationale was that this approach can be used to reveal mechanism involved in infection of the vascular endothelium and facilitate understanding of the events that contribute to EHV-1 secondary disease. This information is essential to aid in the development of prophylactics or treatments against secondary EHV-1 diseases and will inform the focus on future experiments to identify host and viral factors that contribute to EHM and abortions.

#### RESULTS

### Clinical disease and viremia

All horses were free from clinical signs of respiratory disease and had normal body temperatures prior to infection with EHV-1. As described previously, all horses developed fevers, shed virus in nasal secretions, and seroconverted following EHV-1 inoculation, indicating successful challenge infection (Figure 15A, C) [117]. One horse (horse 6) developed severe equine herpesvirus myeloencephalopathy and was euthanized day 11 post challenge. PBMC samples were analyzed for viremia for 10 days following challenge by qPCR. The day of peak viremia was identified for each horse and occurred days 5-8 p.i. (Figure 15B) [117].

## Horse mRNA sequencing and differential gene expression

The mapping summary statistics describing the number of total reads and uniquely mapped reads can be seen in Table 6. The read depth on average was 43,480,084 total reads per sample, and an average of 80.3% of reads uniquely mapped to the equine genome.

PCA plot analysis of regularized log transformed read-count data shows a clustering of samples based on timepoint (pre infection vs. post infection) (Figure 16A). When comparing pre-infection with post-infection samples, we found a total of 3,226 differentially expressed genes (DEG) with an adjusted p value (padj) < 0.05 (File S4.1). Due to the high number of DEGs and in order to highlight the most relevant biological processes in downstream enrichment analyses, we set the significance threshold at padj < 0.05 and log2 fold change greater than 3 or less than -3. At this threshold, there were 51 DEGs, 48 of which were significantly upregulated, and 3 significantly downregulated genes (Figure 16B).

Functional information for available genes from the *homo sapiens* uniprotKB database revealed numerous genes involved in various aspects of inflammation. The majority of upregulated genes belonged to the interferon pathway (such as *DDX60*, *MX2*, *MX1*, *GBP2*, *IFIT3*, *IFI44*, *OAS1*, *OASL*, *OAS3*, *TRIM22*, *OAS2*, *IFIT5*, *IFI6*, and *IRF7*). In addition, many chemotactic genes (*CXCL9*, *CXCL10*, *CXCL11*, *CCL8*) as well as genes involved in the complement system (*C1R*, *C3AR1*, *SERPING1*) were also upregulated, in addition to other genes which are shown in Table 7. The three downregulated genes included fibronectin (*FN1*), which encodes an adhesion molecule, as well as *DEFB1*, the gene that encodes the antimicrobial protein beta defensin 1, and the gene *FAM71A*.

## Gene ontology (GO) overrepresentation

Due to the low number of downregulated genes, GO overrepresentation analysis focused on processes involved in the upregulated gene list. Gene ontology overrepresentation analysis was performed on the 48 upregulated genes and 150 total GO terms for biological processes were enriched (File S4.2). After summarizing the list with a tool that summarizes lists of GO terms based on semantic similarity (REVIGO), 18 non-redundant enriched GO terms remained (Figure 17A). The most significantly enriched process was defense response to virus (GO:0051607), which also included the most genes (16) from our gene list. The other top significantly enriched process were: negative regulation of viral genome replication (GO:0045071), regulation of nuclease activity (GO:0043950), positive regulation of cAMP-mediated signaling (GO:0043950), and cellular response to chemokine (GO:1990869).

Genes associated with the top nine most significantly enriched GO terms are visualized in Figure 17B. These genes and processes cluster into 3 general groups. The largest group contains genes and processes involved in the defense response to viruses, negative regulation of viral genome replication, and regulation of nuclease activity and includes *DDX60*, *MX2*, *MX1*, *GBP2*, *IFIT3*, *IFI44*, *OAS1*, *OASL*, *OAS3*, *TRIM22*, *OAS2*, *IFIT5*, *IFI6*, and *IRF7*. The genes for chemokines *CCL8*, *CXCL9*, *CXCL10*, and *CXCL11* are involved with a second cluster of biological processes including cellular response to chemokine, positive regulation of cAMP-mediated signaling, and positive regulation of release of sequestered calcium ion into cytosol. The third main cluster includes three genes associated with the complement system; *C1R*, *SERPING1*, and *C3AR1* and are involved with the enriched terms regulation of protein activation cascade, protein activation cascade, and regulation of protein maturation.

## in silico cell sorting

Average cell fractions between pre- and post-infection samples and the averages +/- SEM for each cell type are shown in Table 8. Following challenge infection during peak viremia, there was a significant increase in  $\gamma\delta$  T-cells (p < 0.05) and M1 polarized macrophages (p < 0.1). Additionally, there was a significant reduction in CD8+ T-cells (p < 0.05), plasma cells (p < 0.1), and M0 macrophages (p < 0.1) post infection.

Relative cell percentages for 22 different leukocyte subpopulations in individual horses pre- and post-infection can be seen in Figure 18. Overall, the most abundant cell type identified in all samples was naïve B-cells, with around 40% of the estimated cell fraction followed by follicular T-helper cells with ~ 17%. Interestingly, horse #6, who was the only horse exhibiting clinical EHM, was also the only horse showing an increase in naïve B-cells, T-follicular helper cells and one of two horses exhibiting visible increases in the percentage of T-regulatory cells.

### Viral mRNA sequencing

Normalized read counts in transcripts per million (TPM) for EHV-1, EHV-2, and EHV-5 were identified and are shown in File S4.3. No reads mapped to the EHV-4 genome. Read coverage along the EHV-1 genome shows low level of transcription of viral reads in 5/7 of the horses prior to EHV-1 challenge (Figure 19). As expected, during EHV-1 viremia post challenge, read coverage of the EHV-1 genome increased and EHV-1 transcripts were present in all samples (Figure 19). Additionally, the horses with the highest levels of viremia corresponded to the samples with the most EHV-1 transcription post challenge (Figure 15B; Figure 19). TPM values for each gene were then averaged and the most abundant EHV-1 genes expressed post infection were ORF25, ORF34, and ORF75 (Figure 20A). The products of these genes include a capsid protein (ORF25) and a protein involved in the early step of virus egress (ORF34). ORF75 encodes a

membrane protein presumed to be involved in the virulence of certain EHV-1 strains [142,143]. The most abundant EHV-1 genes pre-infection were ORF59, ORF25, and ORF58 (Figure 20A). ORF59 encodes an early protein involved in viral growth and ORF58 encodes a nuclear non-structural protein [143,144]. Interestingly, three genes ORF59, ORF41 (encodes a membrane protein), and ORF55 (encodes a tegument protein) had higher levels of transcription in pre-infection PBMCs compared to PBMCs during viremia. This could indicate a role for these genes in EHV-1 persistence in PBMCs during clinical latency.

Additionally, transcription of the equine gammaherpesvirus (EHV-2 and EHV-5) genes were present in PBMCs prior to and post EHV-1 challenge (Figure 20B, C). No apparent differences were observed in TPM of EHV-2 or EHV-5 genes in response to EHV-1 infection.

#### **Identification of miRNAs**

MiRDeep2, a software tool for miRNA mapping and identification, identified 278 known mature equine miRNAs amongst the pooled samples. Furthermore, we identified 903 total novel miRNAs with a miRDeep2 score > 1 (File S4.4). Of these 903 novel miRNAs, 855 mapped to the equine genome, 57 mapped to the EHV-2 genome, and 41 mapped to the EHV-5 genome. The EHV-2 and EHV-5 miRNAs appeared to be relatively abundant given the low levels of their viral mRNA transcripts detected. The most abundant miRNA for EHV-2 had a total read count of 15,671 and for EHV-5 a count of 20,551. For EHV-2, the miRNAs clustered around three general regions on the genome: 38-44 kb and 176-182 kb on the plus strand, and 124-127 kb on the minus strand. For EHV-5, the miRNAs clustered around two general regions: 36-43 kb on the plus strand and 126-127 kb on the minus strand (File S4.4). Interestingly, no miRNAs were identified that mapped to either of the equine alpha herpesviruses, EHV-1 or EHV-4 (File S4.4).

## Differential expression of miRNAs

Novel miRNAs with a miRDeep2 cutoff > 1 were added to the list of known miRNAs for quantification in each sample and quantification was performed to identify differentially expressed miRNAs in horses pre and post EHV-1 infection. There was an average of 18,165,757 reads per sample with an average mapping of 49.7% (Table 9).

Interestingly, PCA plot analysis of these counts indicate that more variation occurred between individual horses, rather than within horses as a result of infection (Figure 21A). However, differential expression analysis revealed five total miRNAs that were differentially expressed in horses during viremia when compared to pre-infection levels (Table 10). Three of these miRNAs were upregulated in response to infection, and two were downregulated. The upregulated miRNAs included eca-miR-9104, eca-miR-2483, and eca-miR-652 (human ortholog hsa-miR-652-3p) (Figure 21B, C, D). In humans, hsa-miR-652-3p has been shown to interact with the endothelial repair gene, CCND2 and contributes to endothelial cell damage [145]. While the downregulated miRNA list did not include any known equine miRNAs, we did identify a "novel" equine miRNA with human ortholog hsa-miR-6852-5p to be downregulated in response to infection (Figure 21E). hsa-miR-6852-5p has been shown to induce cell cycle arrest and necrosis in humans [146]. Interestingly, a novel EHV-2 miRNA was also found to be downregulated in our samples (Figure 21F).

#### **DISCUSSION**

PBMCs are an important tissue involved in the pathogenesis of EHV-1 disease both as active immune cells in addition to being the site of EHV-1 viremia and potentially latency. In this study, we sought to characterize the host and viral transcriptome of equine PBMCs prior to and during acute equine herpesvirus 1 infection. In addition, we identified miRNA expression in

these cells as they likely contribute to the tight regulation of and switch between lytic and latent infection. Using next generation RNA sequencing (RNA seq) we were able to build an unbiased profile of equine and viral gene expression in PBMCs, and determined which genes were modulated during EHV-1 viremia.

In total 51 host genes were significantly differentially regulated in PBMCs of horses collected during peak EHV-1 viremia when compared to PBMCs collected pre-challenge infection. As expected, we found that numerous genes involved in the interferon pathway were upregulated during EHV-1 viremia. This included many classified as interferon stimulated genes (ISGs) including: *OAS1*, 2, and 3, *OASL*, *MX1* and 2, *IFIT3*, *IFIT5*, *IFI6*, *TRIM22*, *GBP1*, and *DDX60*.

The type I interferon response is considered to occur in three phases: 1) the stimulation of pattern recognition receptors and activations of tissue factors, including *IRF3* and *IRF7*, 2) induction of interferon alpha and interferon beta expression, and 3) the continued amplification and expression of ISGs through JAK/STAT signaling [147,148]. Similar to the observed upregulation of ISGs, we also observed the upregulation of the transcription factor, interferon regulatory factor 7 (*IRF7*). This gene is stimulated upon PRR stimulation and is involved in induction of the type I interferon response [147,149]. The type I interferon response pathway is a crucial aspect of antiviral innate immunity and is considered an important response against herpesviruses [147]. In humans, deficiencies in the responsiveness to type I interferons and the inability to induce ISGs, result in death from viral infections. In one case study, an infant with homozygous mutation in the *STAT1* gene succumbed to HSV-1 infection with uncontrolled encephalitis [150]. PBMCs from patients with atopic dermatitis complicated by exzema herpticum, show significantly lower type I interferon response to *ex vivo* HSV-1 infection

compared to PBMCs from patients without eczema herpeticum [151]. In addition, this study found that the regulating genes *IRF3* and *IRF7* were also downregulated in these patients [151]. Together, this data suggests that the type I interferon response is important for protection against disease caused by alphaherpesviruses. Less is known about the importance of the type I interferon response in PBMCs from horses. In previous studies, PBMCs have been found to produce type I interferon in response to EHV-1 infection in vitro [40,41]. Similarly, in other equine cell types, type I interferon has been shown to be upregulated in response to EHV-1 infection in vitro, including respiratory epithelial cells and endothelial cells [37–39,42,152,153]. In our study, it was interesting to notice that the interferon alpha or interferon beta genes themselves were not upregulated, but rather the ISGs were. This also was the case in a gene expression study of human PBMCs in response to a variety of viral infections, where they found multiple interferon inducible genes, yet no detectable interferons [154]. Type 1 interferons are known to be quickly and transiently expressed, and so timing likely plays a role in detection of these genes. In epithelial cells, type I interferon proteins have been shown to be detectable as early as 10 hours post EHV-1 inoculation in vitro and remained detectable up through 72 hours [42]. It might also be considered that the persistence of the antiviral transcriptome is maintained without further induction of type 1 interferons. In fact, it has been shown that ISGs are expressed in the absence of interferon alpha/beta signaling through IRF7 mediated pathways [155]. This indicates that future studies interested in the interferon response may consider investigating downstream molecules of this pathway, such as the numerous ISGs we found here.

Another major group of genes upregulated in PBMCs during EHV-1 viremia were chemokines (*CXCL9*, *CXCL10*, *CXCL11*, and *CCL8*). More specifically, we found upregulation of chemokines important for induction of cell-mediated immunity, and recruitment of T-cells,

monocytes, and NK cells. CXCL9, CXCL10, and CXCL11 are related chemokines that are well known for their chemotactic activity, as their receptor (CXCR3) can be found on type 1 CD4+ T helper cells, CD8+ cytotoxic lymphocytes, and NK cells [156]. Previous work has also found strong induction of these chemokines in PBMCs in response to EHV-1 infection in vitro [41]. In addition, these chemokines have been shown to be stimulated in epithelial and endothelial cell cultures following EHV-1 inoculation [43,157]. The gene encoding CCL8 (also known as monocyte chemotactic protein-2; MCP-2) was also found to be upregulated in PBMCs during EHV-1 viremia in our study. This protein, as its name suggests, is chemotactic for monocytes, as well as NK cells, T-cells, eosinophils and basophils [158]. Not much is known about the role of CCL8 during EHV-1 infection, however, it has been shown to be upregulated in endothelial cell cultures [157]. The CXCR3 ligands, as well as CCL8 are known to be induced by type II interferon (interferon gamma) [156,158]. Interferon gamma is secreted by T-cells and NK cells, and is considered a correlate of an active cell-mediated immune response [159,160]. Cellular immunity, particularly CD8+ T-cells, are considered to be an important correlate of protection from EHV-1 [21,53,54]. Re-stimulation assays have found that T-cells in horses infected with EHV-1 increase interferon gamma secretion, indicative of activated T-cell responses [21,161– 163]. The fact that all three of the CXCR3 ligands were upregulated in our samples, along with previous work, suggests that these chemokines are consistently stimulated during EHV-1 infection, and T-cell activation and recruitment plays a role during EHV-1 infection and possibly in the protection from EHM and EHV-1 abortions. However, the exact role of these chemokines in the pathogenesis of EHV-1 mediated disease remains unknown.

A third cluster of genes with related functions in protein activation cascades were upregulated in PBMCs during EHV-1 viremia. The complement cascade is a pathway of the

innate immune system that involves a series of protein activation and cleavages that enhance antibody mediated clearance of pathogens. We found two components of this system (C1R and C3ARI) as well as an inhibitor to this cascade (SERPINI) all upregulated during infection. EHV-1 and other herpesviruses are known to evade the complement system by "hiding" antigen within the PBMCs [67,164]. However, components of the complement system have also been shown to play a role in adaptive immunity through B-cell and T-cell related functions. The complement receptor encoded by CIR has been shown to have a central role in B-cell responses [165]. In humans about 15% of T-cells express C1R, and this molecule is upregulated in CD4+ and CD8+ T-cells upon activation [166–168]. Similarly, C3AR1 is not expressed on naïve T-cells, but it is induced upon activation [169]. While these characteristics have not been described in equine lymphocytes, it is possible the differential regulation of these genes during EHV-1 infection corresponds with activation of lymphocytes. Additionally, the proteins involved in the complement cascade have also been shown to be associated with the coagulation cascade [170]. For example, the C1 inhibitor (SERPINI) not only regulates the complement cascade, but also has been shown to inactivate coagulation factors [171]. This is of particular interest because the coagulation cascade is known to be induced in horses during EHV-1 viremia, and it is thought that this is a major contributor to endothelial damage and subsequent immunopathology causing secondary disease such as EHM [24–27]. Regulation of hemostasis is critical during health and disease with a tightly regulated balance between anticoagulation and pro-coagulation factors. In a healthy individual, the body holds this balance towards a slight anti-coagulation state. However, in times of disease or vascular damage, coagulation factors are released to form a protective fibrin clot. These factors are tightly regulated so as to prevent clotting disorders

[170,172] Therefore it is not surprising that we see gene expression for components (C1R and C3ARI), as well as regulators (SERPINI) of the complement and coagulation cascades.

Upon infection with EHV-1, we observed a change in the cell fraction percent of certain cell populations. We saw a decrease in M0 macrophages and an increase in M1 macrophages, which indicates activation and polarization of macrophages to an M1 phenotype. This phenotype is considered to correspond with the antiviral and antinflammatory macrophage phenotype [173]. Additionally, there was an increase in γδ T-cells. γδ T-cells are known for their expression of IL-17, and while they do express a T-cell receptor they can also be stimulated via cytokines, making them similar to innate lymphoid cells [174]. During viremia, EHV-1 infects monocytes, T-cells, and B-cells, however, only 1-10 out of 10<sup>7</sup> PBMCs are estimated to be infected with EHV-1, therefore, it is unlikely that drastic cell population changes are a result of EHV-1 infection of a certain subtype [23,30,135–138]. EHV-1 infection is marked by lymphopenia, and previous reports attributed this specifically to T-cells [175,176]. This was confirmed by Charan et al. (90) who showed that post-EHV-1 infection autologous sera collected from horses contained increased levels of transforming growth factor beta and caused both non-specific and EHV-1 specific suppression of T-cell responses. Furthermore, we have previously shown suppression of both CD4+ and CD8+ T-cell responses in ponies on day 7 post-infection with EHV-1 [76]. In the present study, we found a decrease in CD8+ T cells during infection. CD4+ T-cells were also decreased although this decrease was not statistically significant. It is known that CD4+ type 1 helper T-cells and CD8+ T-cells are crucial for protection against EHV-1 disease, and the decrease in circulating PBMC population could be explained by the recruitment of these cells towards sites of infection, i.e., the nasal epithelial tissue and secondary sites of infection [21,53,54]. These results also correspond with the observed increases in the chemokine genes

CXCL9, CXCL10, CXCL11, and CCL8 during peak viremia. Similarly, the reduction of plasma B-cells we observed, may be a sign of these cells being recruited out of circulation to the site of primary infection. However, we estimated cell populations using CIBERSORTx, which is a new tool for digital cytometry, and allows for cell population estimations of heterogenous populations based on bulk RNA sequencing data [177]. It must be noted that the results from this *in silico* analysis should be interpreted with caution, as the estimation of cell fractions were computed using a reference file based on the transcriptome of human leukocytes that Newman et al. developed [177]. In order to generate a more accurate estimation, a reference should be generated based on the transcriptome of classically sorted equine cells. Otherwise, the expensive technology of single-cell RNA sequencing could be used to characterize gene expression in individual cells and more precisely estimate populations.

While the majority of the PBMC transcriptome belongs to host genes, it was another goal to identify which EHV-1 viral transcripts were present in the samples. It was interesting to see that many EHV-1 transcripts were identified in 5 of 7 horses prior to EHV-1 challenge, despite horses being negative for viral genome using qPCR. However, the depth of sequencing of our samples was approximately 43 million reads per sample, so we could identify low levels of viral transcription. It is possible this depth of next generation sequencing is more sensitive than our qPCR assay, and it is also possible that viral transcripts are more abundant in samples than latent genomic DNA. While the trigeminal ganglia is the trademark site for EHV-1 latency, many studies have reported EHV-1 latency in lymphoid tissues and PBMCs as well as in additional ganglia and lymphoid tissues [5–8,132]. It is presumed that most horses become primarily infected with EHV-1 at a very young (days to weeks of age) [1–4]. While the horses used in our study were seronegative for EHV-1 serum VN antibodies prior to challenge, it is presumed they

still may have previously been exposed to the virus and established latency. We propose the transcription of EHV-1 found in the pre-infection PBMCs are from a previously acquired, but clinically "latent" virus. An important distinction must be made between clinical latency – the period of time after an infection when the host no longer has disease, and cellular latency – when the viral genome is present within the cell but does not produce progeny virions [130]. Cellular latency is often characterized by a restricted gene expression pattern, and a characteristic latency associated transcript. This transcript has not yet been identified for EHV-1, and we are unable to speculate whether the transcription observed in our pre-challenge samples represents true cellular latency, an "arrested" state of virus replication, or a mixture of lytic and latent gene expression pattern in different cells. However, we identified three genes that exhibited higher average expression in pre-challenge samples compared to post challenge. These included ORF59, ORF41, and ORF 55. ORF59 was also the most abundant transcript overall in pre-challenge samples. This gene encodes an early protein involved in viral growth and has been found to be essential for EHV-1 replication in culture [144]. Interestingly, ORF59 is one of a few genes without a positional homolog in HSV-1 or HSV-2. The homolog exists in other varicelloviruses including VZV and PRV, and while it is essential for PRV replication it has been found to be non-essential for VZV replication in culture [178,179]. The ORF25 gene was found to be relatively highly expressed in both pre and post challenge samples. This gene encodes a capsid protein. While not much is known about the role of this protein in EHV-1 infection, the VZV homolog (ORF23) has been found to be important for infection and lesion formation on human skin xenografts in a murine model of VZV pathogenesis [180]. During viremia, we also found ORF75 to be one of the most abundantly expressed genes. This gene is one of 6 genes that have been deleted from the KyA laboratory strain of EHV-1. KyA has been found to be attenuated and avirulent in horses and does not cause detectable viremia [142]. Creation of an ORF75 deletion mutant has identified that this gene is not essential for EHV-1 replication and does not alter the clinical virulence *in vivo* [181,182]. However, the complete function of ORF75 remains unknown.

In addition to transcription of EHV-1 genes, we found transcripts from both equine gammaherpesviruses, EHV-2 and EHV-5. This is unsurprising given that the site of persistence for these viruses are B-cells [183,184]. We found EHV-2 transcripts in 4/7 horses both pre and post EHV-1 challenge. We found EHV-5 transcripts in 5/7 and 3/7 pre and post EHV-1 challenge, respectively. In a previous study of EHV-1 challenged horses, we found EHV-5 in PBMCs of 76% of horses prior to challenge and 52% seven and ten days post EHV-1 challenge [185]. It is possible the rate of EHV-5 detection drops below the detectable limit in PBMCs during EHV-1 viremia due to increased immune activity of the circulating lymphocytes. However, since we still see EHV-2 and EHV-5 transcripts during acute EHV-1 infection, it is likely that the gammaherpesviruses are resilient and persistent in this site of latency even in the face of systemic immunity.

Notably, no miRNAs mapped to the EHV-1 genome prior to or during EHV-1 viremia. However, we identified 98 total miRNAs mapping to the two gammaherpesvirus genomes. MicroRNAs are known to be involved in herpesvirus biology and the establishment of latency [141]. The differences we observed in miRNA between the gammaherpesviruses EHV-2 and EHV-5, and the alphaherpesvirus EHV-1 may be explained by the differences in these subfamilies' latency tropism. The classical theory of herpesvirus biology describes sensory ganglia as the primary target for latency of alphaherpesviruses and lymphocytes as the primary latency site for gammaherpesviruses [130]. While several reports have identified lymphoid

tissues as a site of latency for EHV-1, genome detection in circulating PBMC via qPCR is often negative in non-clinically affected animals [5–8,132,186]. In contrast, EHV-2 and EHV-5 can be routinely detected in PBMC samples of healthy animals [186,187]. This indicates that these two subfamilies employ differing transcription strategies in latency and persistence in lymphocytes, likely including the use of miRNA transcription.

In contrast to mRNA gene expression, we found very few differentially expressed host or viral miRNAs in this study. We found five significantly differentially expressed miRNAs, two of which had human orthologs identified. Interestingly, *hsa-miR-652-3p* (the equine ortholog was upregulated in our study) is known to contribute to endothelial damage, and knockdown of this miRNA has been shown to promote endothelial cell repair [145]. As damage of the vascular endothelium is part of EHM pathogenesis, and PBMCs interact directly with the endothelium during viremia, further investigation of this miRNA in horses and its role in EHM development would be interesting.

In conclusion, we characterized the transcriptome of equine PBMCs pre and post EHV-1 challenge infection using a repeated measure design. We used RNA deep sequencing to comprehensively investigate equine mRNA and miRNA transcripts, as well as those from four common equine herpesviruses, EHV-1, EHV-2, EHV-4, and EHV-5. Notably, after gene expression analysis, we were able to characterize the immune response of PBMCs during viremia and found significant upregulation of multiple genes involved in processes including the interferon pathway, T-cell chemotaxis, and protein activation cascades such as the complement and coagulation system. More work is needed to fully elucidate how these mechanisms are involved in either protection from or contribution to EHV-1 associated secondary diseases, such as abortion and EHM. Nevertheless, this work expands our current knowledge about the role of

PBMCs during EHV-1 viremia and will inform the focus on future experiments to identify host and viral factors that contribute to clinical EHM.

#### MATERIALS AND METHODS

#### Viruses

EHV-1 strain Ab4 (NCBI RefSeq: NC\_001491.2) was propagated in NBL-6 cells (ATCC® CCL-57<sup>TM</sup>) with MEM-10 (Minimum Essential Medium Eagle [Sigma-Aldrich, St. Louis, MO, USA] supplemented with 100 IU / mL penicillin, 100 μg / mL streptomycin, 1% GlutaMAX [GIBCO, Life Technologies, Carlsbad, CA, USA], 1 mM sodium pyruvate, 1% non-essential amino acids [M7145, Sigma-Aldrich], and 10% fetal bovine serum). After incubation at 37 °C and 5 % CO<sub>2</sub> for 3-4 days, the cells were frozen and thawed, and cellular debris removed by centrifugation at 300 \* g for 10 min. The stock was stored at -80 °C. Prior to inoculation in horses, the stock was thawed and sonicated for three cycles of 30 sec at 50-1 amplification and diluted to a titer of 10<sup>6</sup> PFU/mL for inoculation of horses.

#### **Animals**

Seven 1-year old horses (5 males, 2 females) were used in this experiment. Horses were screened prior to inclusion in the study to ensure virus neutralization assays (VN) blood serum titers were below 1:4 for EHV-1 and below 1:24 for EHV-4. Animals were housed in a building with natural ventilation with multiple horses per pen and nose-to-nose contact between pens. The horses had access to grass hay and water *ad libitum* for the entirety of the study. All animal maintenance and procedures were performed in compliance with Michigan State University's Institutional Animal Care and Use Committee.

## **Experiment design**

The horses used in this study were part of a separate experiment evaluating the use of a human adenovirus vector expressing the EHV-1 inhibitory gene, IR2, for prevention of nasal viral shedding [117]. In this study, horses received intranasal instillation of either 3 x  $10^{10}$  particles of a human adenovirus vector expressing the EHV-1 IR2 protein (n=3, 2 males, 1 female) or 1.5 x  $10^{10}$  particles of a null adenovirus vector (n=4, 3 males, 1 female) by intranasal instillation two days prior to EHV-1 challenge [117]. Because no effect was observed as a result of IR2 treatment in any of the clinical, virological, or immunological parameters evaluated, for the purpose of the current study all horses were considered as one group [117]. Horses were challenged with 5 x  $10^7$  plaque forming units (pfu) of EHV-1 Ab4 via intranasal instillation.

## **Sample collection**

One hundred mL of whole blood was collected into heparinized syringes via jugular venipuncture from all horses 13 days prior to experimental infection with EHV-1 and daily for 10 days post challenge infection to ensure we had samples for each horse's day of peak viremia. Samples were immediately transported back to the laboratory for PBMC isolation. For isolation of RNA and library preparation, PBMCs were separated by density gradient centrifugation over Histopaque-1077 (Sigma-Aldrich) as previously described [76] and cell pellets of 6 x 10<sup>7</sup> were stored at -80 °C until RNA isolation. An additional aliquot of 1 x 10<sup>7</sup> PBMCs was stored at -80 °C for quantification of viremia using qPCR as previously described [22]. The day post challenge for peak viral load in PBMCs was determined for each horse. Additionally, physical exams to evaluate respiratory disease and rectal body temperature were performed daily and nasal swabs collected for viral quantification using qPCR, as previously described. [22]

## RNA isolation, library preparation, and sequencing

A summary of the data analysis can be seen in Figure 22. RNA for RNA Sequencing analysis was isolated from PBMCs from each horse pre-challenge, as well as the day of peak viremia. Cell pellets were lysed and homogenized using TRIzol Reagent (Thermo Fisher) following the manufacturer's instructions. The aqueous phase was then collected, washed with 100% ethanol and total RNA was isolated using the miRNeasy Mini Kit (Qiagen) according to the manufacturer's instructions. To eliminate genomic DNA contamination, deoxyribonuclease treatment (Qiagen) was applied to each sample according to the manufacturer's recommendation. Concentration of RNA was determined using fluorometric quantification with the Qubit 1.0. RNA quality was evaluated using the Agilent 2100 Bioanalyzer with the RNA 6000 Pico Assay, and samples with RIN score ≥ 8.90 were submitted for sequencing. Library preparation and next generation sequencing was performed Michigan State University's Genomics Research and Technology Support Facility. Briefly, stranded mRNA cDNA library preparation was preformed using the Illumina TruSeq Stranded mRNA kit with IDT for Illumina Unique Dual Index adapters according to manufacturer's recommendations. MicroRNA cDNA libraries were prepared using Illumina TruSeq Small RNA Library Preparation Kit following manufacturer's recommendations. Completed libraries were quality controlled and quantified using a combination of Qubit dsDNA HS and Advanced Analytical Fragment Analyzer High Sensitivity DNA assays. The mRNA libraries were pooled in equimolar quantities for sequencing and the pool quantified using the Kapa Biosystems Illumina Library Quantification qPCR kit. This pool was loaded onto two (2) lanes of an Illumina HiSeq 4000 flow cell and sequencing was performed in a 2x150 bp paired end format using HiSeq 4000 SBS reagents. The small libraries were pooled in equimolar amounts for multiplexed sequencing and the pool quantified using the Kapa Biosystems Illumina Library Quantification qPCR kit. This pool was loaded onto one (1) lane of an Illumina HiSeq 4000 flow cell and sequencing was performed in a 1x50 bp single read format using HiSeq 4000 SBS reagents. Base calling was done by Illumina Real Time Analysis (RTA) v2.7.7 and output of RTA was demultiplexed and converted to FastQ format with Illumina Bcl2fastq v2.19.1. All raw sequencing reads are available in the NCBI sequence read archive (SRA) under BioProject Ascension number *PRJNA681404*.

## Genome guided mRNA alignment

Read quality was assessed using FastQC software v0.11.7. Reads were mapped to the *Equus caballus* genome (assembly EquCab3.0, ENSEMBL release-95) using HISAT2 v 2.1.0. with these options: --rna-strandness RF --dta. The accepted hits .BAM files were sorted by name using SAMtools v1.5 and read counts generated using htseq-count (built in with Python v3.6.4) with the following options: -- format=bam, --stranded=reverse, and -order=name [188–190]. The reference annotation .GTF file was downloaded from ENSEMBL resease-95.

## Host and viral miRNA identification and quantification

Read quality was assessed before and after quality and adaptor trimming using FastQC software v0.11.7 [191]. Raw reads were trimmed using cutadapt v1.16. Options included trimming the Illumina adaptor sequence (option -a TGGAATTCTCGGGTGCCAAGG), reads shorter than 15 bp discarded (option -m 15), and the 3' end trimmed with a quality score cutoff of 20 (option -q 20) [192]. After trimming, miRDeep2 v2.0.0.8 was used to identify all miRNAs present in the samples, including putative novel miRNAs, as well as known miRNAs [193]. For this, reads from all samples were first pooled. Next, a combined reference genome was created from combining the horse (EquCab3.0; downloaded from ENSEMBL release-95) with the genome of the four most common equine herpesviruses (EHV-1 NCBI RefSeq NC\_001491.2, EHV-2 NCBI RefSeq

NC\_001650.2, EHV-4 NCBI RefSeq NC\_001844.1, and EHV-5 NCBI RefSeq NC\_026421.1) and indexed using the bowtie-build function of Bowtie v1.2.2. The mapper.pl function of miRDeep2 was used on the pooled reads to the reference genome to create a .fasta file with processed reads and a .arf file with mapped reads. Next, miRDeep2.pl function was performed on these outputs using equine miRNAs as the main reference. Since the equine miRNA database is still very incomplete, mouse and human known miRNAs were used as related species lists. Known equine, mouse, and human miRNAs were download from the miRbase database (release 22.1) [194]. Novel RNAs with a miRDeep score < 1 were removed for subsequent analysis.

In order to perform differential gene expression analysis, the miRNAs were quantified in each sample. For this the quantifier.pl tool from the miRDeep2 package was used. For this, all novel mature and precursor miRNAs were added to the list of known miRNAs from horse, mouse, and human. Quantifier.pl was run with the processed reads .fasta file as input and the -k option was used to consider precursor-mature mappings that have different ids.

## Differential gene expression

Differential gene expression analyses for both mRNA gene counts and miRNA counts were performed using the DESeq2 package v1.22.2, in R v3.5.3 [195]. The design formula used was "~ horse + timepoint" so that the variable of interest was "timepoint" (pre infection vs. post infection), and controlling for the effect of "horse." Genes or miRNAs with less than 5 total read counts were filtered out prior to analysis. The default DESeq2 analysis was performed using the *DESeq* function. P values were adjusted using the Benjamini-Hochberg method (the default for DESeq2). Significance was set at adjusted p value (padj) < 0.05 and log2FoldChange > |3| for mRNA and padj < 0.05 and log2FoldChange > |1| for miRNA.

## Gene enrichment analysis

Gene enrichment analysis for gene ontology (GO) terms was performed on the gene lists derived from the differential expression analysis. Horse ENSEMBL IDs were converted to gene symbol based on the gene names identified in the EquCab3.0 .GTF file (ENSEMBL release-95). GO enrichment analysis for biological processes was performed using the enrichGO function from the clusterProfiler package [196]. The database used was the human "org.Hs.eg.db", and the background created from the gene symbols associated with all genes present in our samples [197]. P values were adjusted using Benjamini-Hochberg correction and statistical significance set at p < 0.05. After generating lists of enriched GO terms, redundant terms were removed using REVIGO [198]. Enriched GO terms, along with their associated adjusted p value were provided as input, and the allowed similarity was small (0.5). The default settings were used, which included selecting the whole UniProt database to determine GO term sizes and using the SimRel semantic similarity measure for the analysis.

## Viral gene identification and counting

In order to identify viral reads within the samples, a combined reference genome was created from combining the horse (EquCab3.0; ENSEMBL release-95) with the genome of the four most commonly studied equine herpesviruses (EHV-1 NCBI RefSeq NC\_001491.2, EHV-2 NCBI RefSeq NC\_001650.2, EHV-4 NCBI RefSeq NC\_001844.1, and EHV-5 NCBI RefSeq NC\_026421.1). This allowed for subsequent normalization of viral read counts to consider total gene expression from the host. Alignment to this genome was performed for each sample using HISAT2, as described above. Gene counts were then generated using StringTie v1.3.5 as described in the StringTie manual (accessed June 2020) [190]. Initially, gene counts are generated for each sample using the equine reference .GTF file. Then, a new annotation in .GTF format was generated

based on the genes and transcripts present in our samples. Finally, the .BAM file for each sample was re-ran with StringTie to generate gene counts for each sample using the new merged .GTF as the reference annotation and included the -B and -e options. Transcript per million (TPM) values for each gene were extracted from the gene abundance files generated using the -A option. Raw read coverages of samples on the EHV-1 genome were visualized using Integrative Genomics Viewer (IGV) v2.4.10 [199].

#### in silico cell sorting

Normalized read counts expressed as counts per million (CPM) were determined using EdgeR v3.24.3 and values of redundant genes were merged together [200]. Cell fractions were imputed using CIBERSORTx [177]. The included LM22 (22 immune cell types based on human immune cell gene signatures) was used as the signature matrix file. The mixture file included the CPM values for each gene from all samples, identified with gene symbol. B-mode batch correction was performed, and quantile normalization was disabled (recommended for RNA sequencing data). Permutations for significance analysis was set at 100. The run was performed in relative mode (default). Each cell type was represented as a percentage of total cells for each sample, and a Wilcoxon signed rank test performed on the percentages for each cell type using R.

#### SUPPLEMENTARY MATERIALS

The following are available online; File S4.1, File S4.2, File S4.3, and File S4.4.

#### **AUTHOR CONTRIBUTIONS**

All authors have read and agree to the published version of the manuscript.

Conceptualization, L.M.Z, P.S.D.W., and G.S.H.; experiment and sample collection, L.M.Z., and Y.L., computational data analysis, L.M.Z.; writing—original draft preparation, L.M.Z and G.S.H; writing—review and editing, all authors.; funding acquisition, P.S.D.W. and G.S.H.

#### **FUNDING**

This research was funded by the Michigan State University College of Veterinary Medicine's Endowed Research Fund and the Freeman Fund for Equine Research.

#### **ACKNOWLEDGEMENTS**

The authors would like to thank the following colleagues and facilities for their help with this study. David O'Daniel managed the animal facilities. Allison McCauley, Rachel Baumgardner, Julie Dau, and Elis Fisk assisted with animal husbandry and sample collection. Emily Crisovan and the Genomics Research and Technology Support Facility at Michigan State University assisted with technical advice and performed the library preparation and next generation sequencing. The Institute for Cyber-Enabled Research at Michigan State University provided the computational resources.

#### **CONFLICTS OF INTEREST**

The authors declare no conflicts of interest.

## **CHAPTER 5**

## IDENTIFICATION OF HOST FACTORS ASSOCIATED WITH THE DEVELOPMENT OF EQUINE HERPESVIRUS MYELOENCEPHALOPATHY IN HORSES BY TRANSCRIPTOMIC ANALYSIS OF PERIPHERAL BLOOD MONONUCLEAR CELLS

Lila M. Zarski, Kim S. Giessler, Sarah I. Jacob, Patty Sue D. Weber, Allison G. McCauley, Yao Lee, Gisela Soboll Hussey

#### **ABSTRACT**

Equine herpesvirus-1 is the cause of respiratory disease, abortion, and equine herpesvirus myeloencephalopathy (EHM) in horses worldwide. EHM affects as many as 14% of infected horses and a cell-associated viremia is thought to be central for EHM pathogenesis. While EHM is infrequent in younger horses, up to 70% of aged horses develop EHM. The aging immune system likely contributes to EHM pathogenesis, however little is known about the host factors associated with clinical EHM. Here, we used the "old horse model" to induce EHM following EHV-1 infection. PBMCs of horses prior to infection and during viremia were collected and RNA sequencing with differential gene expression was used to compare the transcriptome of horses that did (EHM group) and did not (non-EHM group) develop clinical EHM. Interestingly, horses exhibiting EHM did not show respiratory disease, while non-EHM horses showed significant respiratory disease starting on day 2 post infection. Multiple immune pathways differed in EHM horses in response to EHV-1. These included an upregulation of IL-6 gene expression, a dysregulation of T-cell activation through AP-1 and responses skewed towards a Thelper 2 phenotype. Further, a dysregulation of coagulation and an upregulation of elements in the progesterone response were observed in EHM horses.

## **KEYWORDS**

EHM
Pathogenesis
Herpesvirus
Horse
PBMC

EHV-1

Transcriptomics

RNA sequencing

microRNA

Gene expression

#### INTRODUCTION

Equine herpesvirus 1 (EHV-1) affects horses worldwide. It is the cause of upper respiratory disease, late term abortion or the crippling neurologic disease, equine herpesvirus myeloencephalopathy (EHM). While respiratory disease can contribute to temporary loss of training, severe disease manifestations such as EHM can have devastating effects on animal welfare and economic impact [18]. In a recent U.S. outbreak, as many as 14% of infected animals died or were euthanized due to EHM and to date, no vaccine is effective at preventing EHM [15,16]. This means strict biosecurity and quarantines during an outbreak remain the most effective strategy to control losses due to EHM. In order to limit these devastating consequences, the current recommendation is that state animal health officials issue quarantines of premises with EHV-1 confirmed cases for 21 days from the onset of disease of the latest case [17].

Following primary exposure, EHV-1 establishes a latent lifelong infection in the sensory ganglia or peripheral blood mononuclear cells (PBMCs) [5–8]. Despite this early natural infection and/or vaccination, horses remain susceptible particularly to secondary disease following a repeat exposure or reactivation of latent virus. During an acute infection, EHV-1 replicates in the nasal epithelium and causes upper respiratory disease in younger horses [9]. In the period of 4-14 days following exposure, EHV-1 is detectable in the PBMCs and transported throughout the body during a period of cell-associated viremia [10]. Viremia is a prerequisite event in the pathogenesis of EHM and facilitates the transfer of the virus to the vascular

endothelial cells of the central nervous system [11,12]. It has been demonstrated that duration and magnitude of viremia contribute to likelihood of EHM development, which suggests that increasing the exposure of the vascular endothelium to infected PBMCs increases likelihood of CNS damage [21–23,201]. Further supportive of this are studies showing that a single nucleotide polymorphism in the DNA polymerase gene of the virus, which encodes an aspartic acid residue at position 752 (genotype D<sub>752</sub>), has been associated with more neurologic disease during outbreaks than that which encodes an asparagine at this position (genotype N<sub>752</sub>) [18,19]. Many challenge infection experiments in horses have confirmed that infection with the neuropathogenic D<sub>752</sub> strain is associated with higher magnitude and longer duration of EHV-1 viremia during a challenge infection when compared to the lower neuropathogenic N<sub>752</sub> strain, and this corresponded to increased likelihood of EHM [20–23,201].

Clinical EHM is typically observed towards the end of the viremic phase, suggesting that endothelial infection most likely occurs during peak levels of viremia [202]. Following infection of the vascular endothelium it is thought that a vasculitis, thrombosis, and neuronal damage develop and lead to clinical neurologic disease. Because of this, dysregulation of blood-brain barrier (BBB) integrity is considered to be a critical event for clinical neurological disease during EHM. The BBB is comprised of the vascular endothelial cells of the CNS microvasculature and are connected with tight junctions and adherens junctions, forming a protective barrier protecting neurons from damage [203,204]. The intact BBB protects against neuronal damage resulting from leukocytic infiltration [203]. Due to similarities in the damaging events at the BBB, EHM pathogenesis can be compared to human ischemic stroke. In human and mouse models of stroke, BBB integrity and permeability can be damaged as a result of an inciting event, such as hypoxia (via thrombosis) [203,205–207]. In horses, the coagulation cascade is known to be induced

during EHV-1 viremia, and it is thought that this is a contributor to hypoxic BBB damage and neuronal damage resulting from microthrombosis [24–27]. In addition to ischemic damage via thrombosis, inflammation is another key factor in the development of BBB damage and EHM

However, while viremia is a key feature of EHV-1 infection, and a large percentage of infected horses become viremic, only a small percentage of infected horses go on to develop clinical EHM. While some virus factors have been identified that increase the neuropathogenic potential of EHV-1 infection, it is clear that there are a number of host factors involved in the response to EHV-1 that correlate with the development of EHM [22]. While significant respiratory disease is more common in younger horses, it has been shown that older animals are more likely to develop EHM [21,31,65,202]. In addition, there is some evidence, that in mares over 20 years of age the incidence of clinical EHM is up to 70% [21,208]. The propensity of older animals to get EHM may be related to immunosenescence, which is a commonly observed feature of aging. In horses as well as humans this immunosenescence involves reduced levels of naïve lymphocytes, increase in the memory lymphocytes, and the reduction of T memory cell activation and proliferation following stimulation [209,210]. Additionally, aging is often associated with low levels of chronic inflammation, known as "inflamm-aging," which is thought to contribute to the pathogenesis of other inflammatory diseases of older humans and horses [209,210].

In order to identify which host factors are directly linked with the development of EHM, we thought to utilize the "old horse model" to reliably induce EHM and then compare which host factors are changed in horses with clinical EHM compared to horses that are infected and viremic but do not exhibit clinical EHM. For this, we conducted a challenge infection with a neuropathogenic strain of EHV-1 in both young and old horses in order to ensure animals with

both phenotypes (those that progressed to clinical EHM and those that did not). Based on the central role of viremia for systemic host immunity and EHM pathogenesis and in induction of BBB dysfunction, the goal of our study was to use deep RNA sequencing and a repeated measure design to identify the differences in the host and virus transcriptome in PBMCs of horses that did and did not develop clinical EHM following an EHV-1 challenge infection.

#### MATERIALS AND METHODS

#### **Animals**

Fourteen horses of mixed breeds (5 males, 9 females) were used in this study. The study consisted of two challenge infection experiments that occurred several months apart. One experiment used 2-year old horses (n=7; 5 males, 2 females) and a separate experiment was performed in aged (18-21 year old; n=7; 7 females) horses. For both experiments, animals were housed in a building with natural ventilation with multiple horses per pen and nose-to-nose contact between pens. Horses had access to grass hay and water *ad libitum* for the entirety of the study. All animal maintenance and procedures were performed in compliance with Michigan State University's Institutional Animal Care and Use Committee.

#### Viruses

The neuropathic strain EHV-1 Ab4 (GenBank Accession No. AY665713.1) was propagated in NBL-6 cells (ATCC® CCL-57<sup>TM</sup>) with MEM-10 (Minimum Essential Medium Eagle [Sigma-Aldrich, St. Louis, MO, USA] supplemented with 100 IU / mL penicillin, 100 μg / mL streptomycin, 1% GlutaMAX [GIBCO, Life Technologies, Carlsbad, CA, USA], 1 mM sodium pyruvate, 1% non-essential amino acids [M7145, Sigma-Aldrich], and 10% fetal bovine serum). After incubation at 37 °C and 5 % CO<sub>2</sub> for 3-4 days, the cells were frozen and thawed, and cellular debris removed by centrifugation at 300 \* g for 10 min. The stock was stored at -80

°C. Prior to inoculation in horses, the stock was thawed and sonicated for three cycles of 30 sec at 50-1 amplification.

## **Experimental design and sample collection**

Prior to inclusion in the study, serum was screened for virus neutralizing antibodies for EHV-1. The 2-year old horses had pre-challenge titers  $\leq 1.8$  for EHV-1 and the aged horses had pre-challenge titers of  $\leq 1.32$  for EHV-1. Horses were inoculated with intranasal instillation of 5 x 10<sup>7</sup> pfu of EHV-1 Ab4. Physical examinations were conducted prior to infection and daily following challenge and included evaluation of nasal discharge, ocular discharge, cough, and rectal body temperature as well as a neurological exam using the simplified version of the Mayhew scale, as described by Allen [21]. Peripheral blood mononuclear cells (PBMCs) were isolated from horses prior to challenge and daily for 10 days post challenge. One hundred mL whole blood was collected in heparinized syringes via jugular venipuncture and immediately transported to the laboratory for processing. PBMCs were separated by density gradient centrifugation over Histopaque-1077 (Sigma-Aldrich) as previously described and cell pellets of 6 x 10<sup>7</sup> were stored at -80 °C until RNA isolation [76]. An additional aliquot of 1 x 10<sup>7</sup> PBMCs were used for quantification of viremia using qPCR as previously described [22]. The day post challenge for peak viral load in PBMCs was determined for each horse and RNA for RNA Seq analysis was isolated from PBMCs from each horse pre-challenge, as well as on the day of peak viremia. Statistical analysis was performed using a 2-way ANOVA with significance of p < 0.05.

#### RNA isolation, library preparation, and sequencing

Cell pellets were lysed and homogenized using TRIzol Reagent (Thermo Fisher) following the manufacturer's instructions. The aqueous phase was then collected, washed with 100% ethanol and total RNA was isolated using the miRNeasy Mini Kit (Qiagen) according to

the manufacturer's instructions. To eliminate genomic DNA contamination, deoxyribonuclease treatment (Qiagen) was applied to each sample according to the manufacturer's recommendation. The concentration of RNA was determined using fluorometric quantification with the Qubit 1.0. RNA quality was evaluated using the Agilent 2100 Bioanalyzer with the RNA 6000 Pico Assay and samples with a RIN score > 6.70 were submitted for sequencing. Library preparation and next generation sequencing was performed at Michigan State University's Genomics Research and Technology Support Facility. Stranded mRNA cDNA library preparation was preformed using the Illumina TruSeq Stranded mRNA kit with IDT for Illumina Unique Dual Index adapters according to manufacturers' recommendations. MicroRNA cDNA libraries were prepared using the Illumina TruSeq Small RNA Library Preparation Kit following manufacturer's recommendations. Completed libraries were quality controlled and quantified using a combination of Qubit dsDNA HS and Agilent 4200 TapeStation HS DNA1000 assays. The stranded mRNA cDNA libraries were divided into 5 pools for multiplexed sequencing; four of these pools contained 8 libraries and the fifth pool contained 7. Pools were quantified using the Kapa Biosystems Illumina Library Quantification qPCR kit. Each pool was loaded onto one lane of an Illumina HiSeq 4000 flow cell and sequencing was performed in a 2x150bp paired end using HiSeq 4000 SBS reagents. The small RNA cDNA libraries were divided into two pools and the pools quantified using the Kapa Biosystems Illumina Library Quantification qPCR kit. Each pool was loaded onto one lane of an Illumina HiSeq 4000 flow cell and sequencing was performed in a 1x50 bp single read format using HiSeq 4000 SBS reagents. Base calling was done by Illumina Real Time Analysis (RTA) v2.7.7 and output of RTA was demultiplexed and converted to FastQ format with Illumina Bcl2fastq v2.19.1. All raw sequencing reads are available in the NCBI sequence read archive (SRA) under BioProject ascension number TBD.

## Genome guided mRNA alignment

Read quality was assessed before and after quality and adaptor trimming using FastQC software (version 0.11.7) [191]. Illumina adapters were trimmed from files using Trimmomatic (version 0.38) with the additional options for quality trimming: LEADING:2, TRAILING:2, SLIDINGWINDOW:4:2, and MINLEN:25 [211]. Reads were mapped to the *Equus caballus* genome (assembly EquCab3.0, ENSEMBL release-95) using HISAT2 (version 2.1.0). The accepted hits .BAM files were sorted by name using SAMtools (version 1.5) and read counts generated using htseq-count (built in with Python version 3.6.4) with the following options: -- format=bam, --stranded=reverse, and --order=name [188–190].

## Host and viral miRNA identification and quantification

Read quality was assessed before and after quality and adaptor trimming using FastQC software v0.11.7 [191]. Raw reads were trimmed using cutadapt v1.16. Options included trimming the Illumina adaptor sequence (option -a TGGAATTCTCGGGTGCCAAGG), reads shorter than 15 bp discarded (option -m 15), and the 3' end trimmed with a quality score cutoff of 20 (option -q 20) [192]. After trimming, miRDeep2 v2.0.0.8 was used to identify all miRNAs present in the samples, including putative novel miRNAs, as well as known miRNAs [193]. For this, reads from all samples were first pooled. Next, a combined reference genome was created from combining the horse (EquCab3.0; downloaded from ENSEMBL release-95) with the genome of the four most common equine herpesviruses (EHV-1 NCBI RefSeq NC\_001491.2, EHV-2 NCBI RefSeq NC\_001650.2, EHV-4 NCBI RefSeq NC\_001844.1, and EHV-5 NCBI RefSeq NC\_026421.1) and indexed using the bowtie-build function of Bowtie v1.2.2. The mapper.pl function of miRDeep2 was used on the pooled reads to the reference genome to create a .fasta file with processed reads and a .arf file with mapped reads. Next, miRDeep2.pl function

was performed on these outputs using equine miRNAs as the main reference. Since the equine miRNA database is still very incomplete, mouse and human known miRNAs were used as related species lists. Known equine, mouse, and human miRNAs were download from the miRbase database (release 22.1) [194]. Novel RNAs with a miRDeep score < 1 were removed for subsequent analysis.

In order to perform differential gene expression analysis, the miRNAs were quantified in each sample. For this the quantifier.pl tool from the miRDeep2 package was used. For this, all novel and known mature and precursor miRNAs from the miRDeep2 step above were used as input reference sequences. Quantifier.pl was run with the processed reads .fasta file as input and the -k option was used to consider precursor-mature mappings that have different ids.

# Differential gene expression analysis

An overview of the data analysis pipeline is described in Figure 23 and Figure 24. A repeated measure study design was used to assess differential gene expression in response to EHV-1 challenge both *between* groups (EHM vs. no EHM) and *within* groups (pre vs. post infection). The between group, "contrast" comparison was performed which compared the response (pre vs. post) in the EHM group to the response (pre vs. post) in the non-EHM group in order to identify differences between the EHM and non-EHM horses that contribute to or protect from EHM. To expand on this and identify additional potential contributing or protective mechanisms, we also performed the within group comparison. For this, we determined which genes were up or down regulated (pre vs. post challenge) uniquely in either non-EHM (protective from disease) or EHM horses (contributing to disease).

Differential expression analyses for both mRNAs and microRNAs were performed using the edgeR package (version 3.24.3), in R (version 3.5.3) [200]. We analyzed differences between

groups (the "contrast" comparison of EHM vs. Non-EHM) and within groups (prior to and after EHV-1 challenge for each group) using a repeated measure type design as described in the EdgeR manual section 3.5 (last revised 2020 [212]). For this, the model matrix was designed as: ~group + group:horse + group:timepoint, where "group" indicated normal or EHM, "horse" were individual horses, and "timepoint" referred to pre or post EHV-1 challenge. Preprocessing of the data were performed as recommended in the edgeR user manual and included filtering to eliminate low expressed genes (filterByExpr function), TMM normalization (calcNormFactors function), and dispersion estimations (estimateDisp function). We then fit a genewise general linear model (GLM) using the glmFit function, and then performed likelihood ratio testing (LRT) for comparisons using the glmLRT function. Three LRT comparisons were made as explained above: genes that respond differently to the virus in EHM horses compared to how they respond in normal horses (contrast comparison between groups), genes responding to the virus in EHM horses (within group), and genes responding to the virus in non-EHM horses (within group). Benjamini-Hochberg adjustment was used on the p values and statistical significance was set at an FDR < 0.05 and log fold change > |1|.

## Gene ontology (GO) enrichment analysis

Enrichment analysis for gene ontology (GO) terms was performed on the gene lists derived from the differential expression analysis in order to meaningfully interpret and consolidate the up- or down-regulated gene lists and identify relevant functions associated with these genes. GO is a system of classification for genes based on their biologic functions, and genes can be classified to any number of GO terms. Over-representation analysis identifies which of the GO terms are statistically more likely (or "over-represented") based on proportion

of genes in the data set compared to the proportion of all genes in that species that are classified to a certain term.

Horse ENSEMBL IDs were converted to gene symbol based on the annotations in the EquCab3.0 GTF file (ENSEMBL release-95). GO enrichment analysis for biological processes was performed using the enrichGO function from the clusterProfiler package [196]. The database used was the human "org.Hs.eg.db", and the background consisted of all genes present in our samples [197]. P values were adjusted using Benjamini-Hochberg correction and statistical significance set at p < 0.05. After generating lists of enriched GO terms, redundant terms were removed using REVIGO [198]. Enriched GO terms, along with their associated adjusted p value were provided as input, and the allowed similarity was small (0.5). The default settings were used, which included selecting the whole UniProt database to determine GO term sizes and using the SimRel semantic similarity measure for the analysis.

## In silico cell sorting

Cell fractions were imputed using CIBERSORTx [177]. The included LM22 (22 immune cell types) was used as the signature matrix file. The mixture file included the CPM values for each gene from all of our samples, identified with gene symbol, and CPM values of redundant genes were merged together. B-mode batch correction was performed, and quantile normalization was disabled (recommend for RNA-seq data). Permutations for significance analysis was set at 100. The run was performed in relative mode (default). The data was determined to be non-normally distributed as determined by Shapiro-Wilk testing. Therefore, a Wilcoxon signed-rank test was used to compare the paired data for each group.

# Whole blood cytokine RT-qPCR

In order to validate changes in cytokine mRNA expression between groups, RNA was isolated from whole blood collected via jugular venipuncture into PAXgene RNA Blood Tubes (BD Biosciences, San Jose, CA, USA). Samples were collected prior to EHV-1 challenge and day 7 post challenge. RNA was isolated following the manufacturer's instructions. RNA was reverse transcribed using the High-Capacity cDNA Reverse Transcription Kit with RNAse inhibitor (Applied Biosystems, Waltham, MA USA). Real time PCR was performed using the SmartChip Real-Time PCR System (Takara Bio Inc., Kasatsu, Shiga, Japan) following the manufacturer's recommendations. Reactions consisted of template cDNA, TaqMan Gene Expression Master Mix (Applied Biosystems) and TaqMan Gene Expression assays for equine target genes (Thermo Fisher, Waltham, MA USA). Target genes included CCL5, CXCL10, IRF7, IRF9, MMP9, THBS1, GUSB, ACTB, and YWHAZ. The negative delta delta Cq (-ddCq) was calculated following the Livak and Schmittgen method [118]. For this, three housekeeping genes (GUSB, ACTB, and YWHAZ) were averaged to normalize the gene of interest and average of pre-challenge values for each group were used as calibrators. Statistical differences between -ddCq values between non-EHM and EHM groups were determined for each gene of interest using a Wilcoxon rank sum test in R and significance set at p < 0.05.

#### **RESULTS**

#### Clinical disease and viremia

The clinical data presented here were collected as part of a separate study by our laboratory still in preparation, but are also being reported here to provide clinical context to our RNA sequencing results. All horses were free from clinical signs of respiratory disease, had normal body temperatures, and were negative for EHV-1 genome in nasal swab and PBMC

samples when tested by real-time PCR prior to challenge infection with EHV-1. All horses developed fevers and shed virus in nasal secretions following EHV-1 inoculation, indicating successful challenge infection (Figure 25A, B). The EHM group consisted of all seven of the horses from the aged horse group and 1 horse from the young group; all horses that developed EHM were female. Neurologic symptoms in the EHM group appeared as early as 6 days post challenge and all 7 old horses developed severe ataxia/paralysis and were humanely euthanized day 9 or 10 post challenge. The one horse from the young horse group developed moderate ataxia and recovered from neurologic symptoms by the end of the study (data not shown). The non-EHM group consisted of the remaining young horses and did not develop neurologic clinical signs (1 female and 5 males).

The fever response to EHV-1 infection is often characterized by a primary fever (corresponding to peak nasal viral shedding) and a secondary fever (corresponding to peak viremia). Looking closer at the body temperatures, all the non-EHM horses showed a primary fever immediately following challenge infection (days 1-4), while all but one EHM horse did not develop a primary fever (Figure 25A). Additionally, non-EHM horses developed more severe clinical respiratory disease (nasal discharge and cough) compared to EHM horses, which showed only very mild symptoms (unpublished data). Finally, non-EHM horses showed significantly more nasal viral shedding when compared to EHM horses (Figure 25B). In contrast, EHM horses developed significantly greater viremia levels when compared to non-EHM horses (Figure 25C). The day of peak viremia was identified for each horse and occurred days 6-10 post challenge.

## Horse mRNA sequencing and differential gene expression

After paired-end sequencing, there was an average of 43,730,408 reads per sample, and 85.2% of total reads uniquely mapped to the EquCab3.0 genome (Table 11). Principal component analysis of regularized log transformed read-count data shows a clustering of samples, with a few exceptions, based on timepoint (pre infection vs. post infection) and group (EHM vs. Non-EHM) (Figure 26).

A repeated measure study design was used to assess differential gene expression in response to EHV-1 challenge both *between* groups and *within* groups. The between group comparison (contrast comparison) identified the differentially expressed genes between the response to the virus in EHM vs. non-EHM horses. This was performed in order to identify the potential host factors or biological responses that contribute to EHM pathogenesis. We then supported these findings by identifying additional genes that are uniquely found to be differentially regulated in either EHM or non-EHM horses in response to infection, but not in both groups. For this, we identified the *within* group responses by determining the response to challenge (pre vs. post challenge) in the EHM and non-EHM groups and then selecting which of these genes were unique to each group (unique to EHM or unique to non-EHM). Significance was set at FDR < 0.05 and log fold change > |1|.

For the between group comparison (contrast), there were 181 DEGs (37 upregulated and 144 downregulated in EHM horses compared to non-EHM horses) (Figure 28A, File S5.1).

For the within group response for non-EHM horses, there were a total of 113 DEGs (109 upregulated during infection and 4 downregulated during infection) (Figure 28B, File S5.1). When looking at the within group response for the EHM horses, there were a total of 490 DEGs (239 upregulated during infection and 251 downregulated during infection) (Figure 28C, File S5.1). In order to identify genes that were uniquely upregulated and downregulated in either

group during EHV-1 infection, we used a Venn diagram. There were 93 commonly upregulated and 1 commonly downregulated gene shared between EHM and non-EHM horses. There were 146 uniquely upregulated and 250 uniquely downregulated genes in EHM horses (potential risk factors) and 16 uniquely upregulated and 3 uniquely downregulated in non-EHM horses (potentially protective factors) (Figure 27A, B).

## Gene ontology overrepresentation

A list of all enriched GO terms for the between group contrast comparison and also for the within group comparison unique to EHM horses can be seen in File S5.2. Due to the limited number of uniquely regulated genes in non-EHM horses, GO overrepresentation analysis did not result in any enriched terms.

After removing redundant GO terms using REVIGO analysis, for the between group contrast comparison, there were 5 enriched biological process (with 8 associated genes) from upregulated genes in EHM horses compared to non-EHM horses (Table 12, Figure 29A, Figure 30A), and 12 enriched biological processes from the downregulated genes (with 36 associated genes) (Table 12, Figure 29B, Figure 30B). When looking at the genes differentially regulated in response to challenge uniquely in EHM horses, a total of 12 biological processes were enriched (with 39 associated genes) and 7 biological processes downregulated (with 41 associated genes) (Table 13).

For the between group contrast comparison, the gene associated with the most biological processes upregulated in EHM horses compared to non-EHM horses was IL6, which was involved in 4/5 enriched biological processes (Figure 31A). IL6 encodes the interleukin-6 (IL-6) protein, which is implicated in several diseases involving immune mediated damage of the vascular endothelium and serves as an important biomarker in human stroke [213,214].

Additional upregulated responses included positive regulation of type II immune response (IL6, RSAD2), positive regulation of cytokine production (NOX1, RSAD2, IL1RL1, IL6, LPL) and regulation of cellular pH (NOX1, SLC4A9, SLC9B1) and upregulation of the interferon stimulated gene (RSAD2; Figure 31B). As seen in the between group contrast comparison, the gene involved with the most enriched process uniquely upregulated within EHM horses was also IL6. Additionally, upregulated functions and the associated genes were largely related to the defense response to virus and the type 1 interferon response pathway (CYBB, ACOD1, ZBP1, IRF9, TGM2, NR1H3, IL15, IRF7, CCL8, ISG20, NMI, CD180, ISG15, TIMP1, ADAR, AIM2, EIF2AK2, CXCL10, RTP4, IL6, TRIM56, LPL, TLR3, LAG3, SLPI) (Figure 31A, C).

For the processes that were downregulated in the between group contrast comparison, JUN and FOS, the genes which encode the subunits for the AP-1 transcription factor (also important for T-cell activation) were downregulated (Figure 31D, E). FOS (encoding c-fos protein) and JUN (encoding c-jun protein) are proto-oncogenes well known for their role in cell proliferation [215]. The downregulation of FOS and JUN corresponds to the many other genes (KLF4, INSR, JUN, PDGFB, FGFR1, CCL5, EPHA4, NLRP12, DUSP1, ATF3, DUSP6) we observed downregulated that are known to be related to either positive or negative regulation of the mitogen-activated protein kinase cascades (such as the extracellular signal-related kinase cascade) which are important in T-cell activation and proliferation [52]. Furthermore, a key proinflammatory cytokine expressed by activated T-cells, IFNG, was downregulated in EHM horses (Figure 31F). Other functions downregulated included leukocyte migration (IFNG, KLRK1, TREM1, PLCB1, NLRP12, CCL5, MMP9, CD244, PDGFB, SLC7A11, DUSP1, CX3CR1, DAPK2, TBX21), regulation of apoptosis (ACER2, IFNG, KLRK1, JUN, NLRP12, CCL5, PLK2, ATF3, FGFR1, MMP9, KLF4, SLC7A11, DUSP1, CX3CR1, DAPK2, GSN, DUSP6),

regulation of transcription (JUN, ATF3, KLF4, EGR2, FOS, TBX21), regulation of cell adhesion (KLF4, IFNG, INSR, CX3CR1, CCL5, EPHA4, PLCB1, DUSP1, SLC7A11, ACER2), vascular endothelial cell growth and proliferation (PDGFB, FGFR1, SLC7A11), oxidative stress (MMP9, SLC7A11), and NK cell activation (KLRK1, CD244, TBX21). Additional downregulated functions were identified when evaluating the within group comparison for EHM horses including those associated with fibrinogen complex formation (THBS1, FN1), as well as additional JUN/FOS genes (JUND and FOSB).

Due to the limited number of uniquely regulated genes in non-EHM horses which may predict protective functions, GO overrepresentation analysis did not result in any enriched terms. Instead, we investigated the individual functions of the differentially expressed genes, which can be found in (Table 14). These genes had different functions and include: upregulated (BFSP2, NFE2, HEY1, CILP, SCD, CISH, TCF7L1, DUSP6, FAM111B, FRMD4A, LZTS1, SHISA5) and downregulated (CGA, SYTL2, WWTR1). General functions of the upregulated genes include positive or negative regulation of signal transduction (CISH, TCF7L1, DUSP6), regulation of cell growth (LZTS1), scaffolding (FRMD4A, CILP), repression of transcription (HEY1), and a transcription factor subunit for NF-E2 (NFE2). Functions of the downregulated genes include hormone signaling (CGA), cytotoxic granule exocytosis in lymphocytes (SYTL2), and negative regulation of cell proliferation (WWTR1).

## In silico cell sorting

The most abundant cell type identified in all groups was naïve B-cells, with 23-37% of the cell population identifying with this fraction (Table 15). In EHM horses, we observed higher percent (~8%) of CD8+ T-cells pre-infection than non-EHM horses (~2%). Additionally, in EHM horses, there was an increase in percentage of M1 and M2 macrophages, resting

dendritic cells, and eosinophils following infection with EHV-1. There was a decrease in percentage of CD8+ T-cells, regulator T-cells, resting NK cells, M0 macrophages, and activated mast cells. In the non-EHM horses, there was an increase in plasma cells and CD4+ activated memory T-cells and a decrease in naïve B-cells and follicular helper T-cells. In both groups, there was an increase in percentages of  $\gamma\delta$  T-cells and activated dendritic cells (Table 15).

## Whole blood cytokine RT-qPCR

In order to validate the differential gene expression results of our RNA seq analysis, RT-qPCR cytokine gene expression for select genes was determined from whole blood RNA collected pre-challenge and day 7 post challenge. In agreement with RNA seq differential gene expression results from PBMCs, RT-pPCR from whole blood showed CCL5, MMP9, and THBS1 were significantly downregulated in the EHM group when compared to non-EHM horses (Figure 32A, G, I). Also in agreement with RNA seq data, CXCL10 and IRF9 expressions were significantly upregulated in the EHM group when compared to non-EHM horses (Figure 32C, E). IRF7 was upregulated in EHM horses when compared to non-EHM horses, though this was not significant (p = 0.14) (data not shown). For a convenient comparison, the normalized count data obtained from the RNA seq analysis from PBMCs for these genes have been expressed as delta-CPM (post CPM value – group average of pre challenge CPM) and can be seen in Figure 32.

## Viral mRNA sequencing

Normalized read counts expressed as transcripts per million (TPM) for EHV-1, EHV-2, and EHV-5 are found in File S5.3. No reads mapped to the EHV-4 genome. There was low level of transcription of a single EHV-1 gene in two of the EHM horses prior to EHV-1 challenge (File S5.3). As expected, during EHV-1 viremia post challenge EHV-1 transcripts were present

in all samples. The most abundant EHV-1 genes expressed in EHM horses during peak viremia were ORF34, ORF25, ORF18, and ORF75 (Figure 33). The products of these genes include a protein involved in the early step of virus egress (ORF34) and a capsid protein (ORF25), a DNA polymerase processivity factor (ORF18) and a membrane protein presumed to be involved in the virulence of certain EHV-1 strains (ORF75) [142,143]. The most abundant EHV-1 genes induced in non-EHM horses during viremia were ORF34, ORF18, ORF51, and ORF42 (Figure 33). ORF51 encodes the pUL11 protein which appears to have differing roles in viral replication depending on the strain; however, it has shown to be essential for replication of strain Ab4 in cell culture [216,217]. ORF42 encodes a capsid protein [143]. Additionally, transcription of the equine gammaherpesvirus (EHV-2 and EHV-5) genes were present in PBMCs prior to and post EHV-1 challenge in both non-EHM and EHM groups (File S5.3). EHV-2 transcripts were identified in 1/8 and 2/8 EHM horses pre and post EHV-1 challenge, respectively, and 3/6 and 4/6 non-EHM horses pre and post EHV-1 challenge, respectively. EHV-5 transcripts were identified in 2/8 and 3/8 EHM horses pre and post EHV-1 challenge, respectively, and 4/6 and 3/6 non-EHM horses pre and post EHV-1 challenge, respectively (File S5.3).

#### **Identification of miRNAs**

MiRDeep2, a software tool for miRNA mapping and identification, identified 285 known mature equine miRNAs amongst the pooled samples. Furthermore, we identified 962 total novel miRNAs with a miRDeep2 score > 1 (File S5.4). Of these novel miRNAs, 860 mapped to the equine genome, 52 mapped to the EHV-2 genome, and 50 mapped to the EHV-5 genome. For EHV-2, the miRNAs clustered around three general regions on the genome: 38-44 kb and 176-182 kb on the plus strand, and 125-127 kb on the minus strand. For EHV-5, the miRNAs clustered around two general regions: 36-43 kb on the plus strand and 125-127 kb on the minus

strand (File S5.4). Interestingly, no miRNAs were identified that mapped to either of the equine alpha herpesviruses, EHV-1 or EHV-4 (File S5.4).

# **Differential expression of miRNAs**

Novel miRNAs with a miRDeep2 cutoff > 1 were added to the list of known miRNAs for quantification in each sample and quantification was performed to identify differentially expressed miRNAs in horses pre and post EHV-1 infection. There was an average of 14,122,680 reads per sample with an average mapping of 59.7% (Table 16). Principal component analysis plot analysis of these counts indicate that samples clustered based on group (EHM vs. non-EHM), rather than within horses as a result of infection (Figure 34). Thus, it was not surprising to have limited numbers of miRNAs differentially expressed as a result of EHV-1 challenge. For the contrast comparison comparing the differences in response to infection between groups, two miRNAs were upregulated and 7 miRNAs were downregulated in EHM horses compared to non-EHM horses (Table 17). For the within group comparisons, there were no miRNAs differentially expressed in non-EHM horses pre vs. post EHV-1 challenge. However, in the within group comparison for EHM horses, there were 5 miRNAs upregulated and 5 miRNAs downregulated in response to EHV-1 challenge (Table 17).

All of the upregulated genes for both the contrast and within group comparisons identified as novel miRNAs. However, these included one with the murine ortholog *mmu-miR*-7059-5p which has been shown to be involved with the downregulation of immunoregulatory genes and pathways [218]. Another miRNA upregulated in EHM horses included one with the human ortholog *hsa-miR-7108-3p*, which has been shown to be upregulated in the serum of human stroke patients compared to controls (Figure 35A-E) [219].

Most of the downregulated genes in EHM horses were known equine miRNAs, though not much is currently understood about their biological function in horses. In addition, while miRNAs may play a role in many biological processes, current knowledge of the functions for specific miRNAs is limited to those that have been elucidated from experimental investigation for particular diseases of interest. Thus, there is much unknow regarding function of many miRNAs, particularly in horses. Expression levels of all downregulated miRNAs can be visualized in Figure 35F-N. The human or murine orthologs of most of our downregulated miRNAs (hsa-miR-199a-3p [220,221], hsa-miR-34a-5p [221,222], hsa-miR-542-5p [223,224], hsa-miR-10a-5p [225], hsa-miR-328-3p [226,227], and hsa-miR-138-5p [228]) have been shown to be involved in cell cycle control, apoptosis, or cancer, with the majority having a tumor suppressor function. In horses, many of these (eca-miR-138, eca-miR-328, eca-miR-10b, ecamiR-34, and eca-miR-199) have also been identified in the male reproductive tract and are presumed to be involved in cell motility and viability of equine spermatozoa [229]. Additionally, eca-miR-34c has been shown to also be downregulated in equine ocular squamous cell carcinoma tissue, and it is presumed that the downregulation promotes tumorigenesis by providing a metabolic advantage through fatty acid synthesis [230]. We also found eca-miR-146a/eca-miR-146a downregulated in EHM horses compared to non-EHM horses. In humans, hsa-miR-146a-5p targets factors to reduce p38/JNK mediated inflammation in adipocytes [231], and in horses eca-miR-146a has been identified in the male reproductive tract [229]. Finally, ecamiR-328 and eca-miR-483 have been previously shown to be differentially expressed in the serum of certain breeds, which is interesting considering pony breeds are less likely to acquire EHM compared to other breeds [18,232]. In the serum of ponies, eca-miR-328 was shown to be

downregulated and *eca-miR-483* upregulated compared to warmblood breed horses [232]. In our study, both of these miRNAs were downregulated in EHM horses compared to non-EHM horses.

#### DISCUSSION

In this experiment we utilized the "old mare model" (female horses > 18 years old) to reliably induce EHM and to compare infection with EHV-1 between EHM and non-EHM "protected" horses. This approach was based on the fact that EHM typically only occurs sporadically in EHV-1 infected horses and is challenging to induce experimentally [202]. However, EHM has been shown to occur in >70% of experimentally infected aged horses, and is more likely to occur in mares [21,208]. The increased propensity of older horses to develop EHM following EHV-1 infection is presumed to be a result of differing host immunity. Our goal was to take advantage of this phenomenon and use RNA sequencing to analyze the transcriptomic profile of PBMCs in horses that did and did not develop EHM to elucidate potential host mechanisms involved in the pathogenesis of EHM.

Evaluating this comparison, we found an upregulation of *IL6* expression in the PBMCs of EHM horses when compared to non-EHM horses. Excessive IL-6 production is a key feature of the condition known as "cytokine storm" and is considered to be a major contributor to vascular damage during disorders such as sepsis or systemic inflammatory response syndrome [214]. In PBMCs, monocytes and T-cells are the likely sources of IL-6 during an infection [233]. IL-6 is also widely known for its role in immunopathology of several diseases including stroke [213]. Ischemic stroke in humans shares many characteristics with the pathogenesis of EHM, namely the damage to the brain blood barrier (BBB) resulting in leukocytic inflammation and damage to the CNS. Serum IL-6 routinely predicts the severity of the CNS lesions as well as the clinical outcome in ischemic stroke patients [213,234–237]. Il-6 is thought to contribute to BBB damage

in multiple ways. More specifically, IL-6 can act on endothelial cells to increase their expression of adhesion factors, which contribute to leukocyte adhesion, infiltration, and damage to the BBB [238]. Furthermore, IL-6 also plays a role in promoting thrombosis, another critical feature of BBB damage and neuropathology [239]. In horses, IL-6 has been implicated in equine diseases including equine metabolic syndrome and osteoarthritis, both of which tend to occur in older animals [240,241]. Due to its relevance in vascular damage and immune mediated disease, in addition to the upregulation we observed in the present study, IL-6 is a candidate for use as a biomarker to predict EHM severity in EHV-1 infected horses.

Consistent with the fact that IL-6 is known to play a role in thrombosis and neuropathology [239], we also identified a number of genes related to fibrin clot formation and changes in vascular permeability to be significantly downregulated in EHM horses. Physiologically, hemostasis is tightly regulated by the body, as dysfunction in either timely coagulation or fibrinolysis can results in pathogenic hemorrhage or clotting disorders [172]. In horses, the coagulation cascade is known to be induced during EHV-1 viremia, and it is thought that this is a major contributor to endothelial damage and the immunopathology that leads to EHM [24–27]. In this study, we found two genes related to fibrin clot formation (THBS1 and FN1) as well as MMP9, which is associated with increasing permeability of blood vessels, to be downregulated in PBMCs of EHM horses compared to non-EHM horses. Previously, in PBMCs we found upregulation of genes encoding proteins involved in coagulation during EHV-1 viremia [242]. In humans, decreases of THBS1 expression by endothelial cells infected with hantavirus is linked to hemorrhagic disease, and elevated serum levels have been seen in stroke patients [243,244]. Elevated levels of FN1, and also MMP9 predicts endothelial damage and hemorrhage after stroke in response to thrombolytic therapy [245]. While it is unclear what

precise role the downregulation of these genes in PBMCs have in the pathogenesis of EHM, our results further support a role of hemostasis (dys)regulation in EHM.

We also observed an upregulation of several interferon stimulated genes (ISGs) in EHM horses. These genes tend to typically be related to the innate immune response to viruses. Many of these ISGs were upregulated in both EHM and Non-EHM horses, which is in agreement with our previous observations [242]. However, EHM horses appeared to have more significantly upregulated genes related to the antiviral defense and type 1 interferon response than the non-EHM group, such as the pattern recognition receptor, TLR3, the interferon regulatory factors IRF7 and IRF9, and interferon stimulated genes, such as RSAD2. An early and rapid induction of interferons has been shown critical for protection from viral diseases and we have previously demonstrated significantly lower amounts of IFNa in the nasal secretions of horses that went on to develop EHM when compared to horses that did not develop EHM at 24 hours after EHV-1 challenge infection [22]. Confirming this observation, the EHM horses in this study also exhibited significantly lower IFNa secretion in the nasal secretion at 24 and 48 hours post infection when compared to the non-EHM horses (unpublished data). In viral infection, the timing of type 1 IFN pathway induction in relation to peak viral replication can dictate the severity of downstream immunopathology and disease, because delayed IFN responses to increased viral titers contribute to immunopathology, presumably through exaggerated proinflammatory cytokine response and leukocytic activation [246–248]. The present study does not provide information on the timing of the interferon response or whether there is a delay in induction of IFN response in PBMCs resulting from the lower interferon levels in the nasal secretions and the reduced nasal shedding early on in EHM horses. There also is no information on how this contributes to propensity for the development of higher viremia and EHM. However, the higher viremia levels in EHM horses likely explain the increased defense response genes observed in this group and could contribute to the downstream immunopathology of the CNS vasculature. Future work should focus on the expression patterns of the interferon associated genes over time.

While IL-6 and associated inflammatory factors likely play a major role in the immunopathology of the CNS, the dysregulation of the development of an appropriate T cell response also appears to be involved in the likelihood to develop EHM. In our study, FOS, the gene encoding the c-fos protein and the direct product of the ERK cascade, was downregulated as well as the gene encoding the other AP-1 subunit, JUN. Many genes associated with or influenced by the MAPK/ERK cascades also appeared to be differentially regulated in EHM horses. Previously, in vitro experiments have shown that EHV-1 infection of PBMCs stimulates the MAPK pathway in infected cells, and thus enhances cell adhesion and viral transfer with the vascular endothelial cells [29,249]. In our study, we are focused on the entire PBMC population, not only infected cells. The differential expression of MAPK pathways in the PBMCs of EHM horses points to the importance of this pathway in the pathogenesis of EHM from an immunological perspective. Taken together with the literature on immunosenescence, our gene expression data support the idea that impairment of T-cell activation and cellular immunity plays an important role in EHM pathogenesis. Increased age has been identified as a s a risk factor for development of EHM [21,31]. This was confirmed in our study where EHM developed in 7/7 aged horses and only 1/7 young horses. Immunosenescence is a well-known phenomenon affecting aged individuals, with T-cells being considered the most affected immune cell population [250,251]. One of the key features of immunosenescence is the resistance of T-cells to activate and proliferate upon antigenic stimulation [209]. Ligand/Receptor binding (such as T- cell receptor stimulation by antigen) triggers a variety of signal transduction pathways, which ultimately result in transcription factor production. Interleukin-2 (IL-2) expression is the hallmark feature of T-cell activation and proliferation. Binding of several transcription factors to the IL-2 promotor, including the transcription factor AP-1 are required for full activation of IL-2 production [52]. The signal transduction pathway responsible for AP-1 production is the mitogen activated protein kinase (MAPK) cascade. This cascade involves the production of extracellular signal-related kinase (ERK), which then enters the nucleus to facilitate transcription of the FOS gene and phosphorylation of the c-fos protein. The c-fos and c-jun proteins form the subunits of AP-1, the transcription factor involved in IL-2 production [52]. Activity of AP-1 has been shown to be impaired in aged mice, and this is related to a decrease in FOS expression [252]. In humans, age related impairments in AP-1 activity has also been shown to be associated with decreased IL-2 production in T-cells [253]. Aging is known to reduce MAPK activation and the ERK1/ERK2 cascade [253–255]. Further, impairment of activation of the ERK pathway is known to be associated with decreased IL-2 production by T-cells in response to stimulation in aged humans [256]. Finally, age-related immunosenescence is also known to be associated with a decreased lymphoproliferative response in humans [257]. In horses, it has been shown that PBMCs from aged horses exhibit a reduced lymphoproliferative response in vitro when exposed to mitogens when compared to younger horses [258–260]. In our study, there was a significant upregulation of CD4+ memory cell activation in non-EHM horses, which is a response we did not observe in EHM horses. Furthermore, we have previously shown that lymphopenia, as well as decreased T-cell responses are part of the immune response to EHV-1 infection, even in horses that do not develop EHM [76,175,176]. Consistent with this, our data indicate there is a downregulation of AP-1 production (through FOS/JUN downregulation) in horses that develop

EHM when compared to non-EHM horses, most likely through dysregulation of MAPK/ERK cascades.

In persistent viral infections (as occurs with many herpesviruses) reactivation is suppressed by constant immune surveillance. It has been suggested for human herpesviruses that this chronic antigenic stimulation contributes to immunosenescence, specifically in CD4+ and CD8+ memory T-cells [261]. This is thought to be because after a lifetime of replication, the memory cell population enters a late stage of effector differentiation and senescence [209,262]. It appears different herpesviruses may affect this in different ways. For example, VZV specific CD4+ T-cells are shown to decline with age, while human cytomegalovirus specific T-cell clones can grow to become a prominent proportion of the memory T-cells [209,263,264]. Nevertheless, frequent antigenic stimulation throughout the life of the horse likely influences the EHV-1 specific T-cell population in aged horses, though more work is needed to verify this.

In addition to the dysregulation of MAPK cascades, JUN/FOS expression, and the presumed decrease in T-cell activation, we also observed an apparent skew towards a T-helper type 2 (Th2) immune response in the EHM horses when compared to the non-EHM group. The T-helper 1 (Th1) cytokine genes IFNG and TBX21 were downregulated in EHM horses. Though many phenotypes of CD4+ T cells have been identified, the classic dichotomy dictates that CD4+ Th cells express a repertoire of cytokines that fit either a Th1 (pro-inflammatory) or Th2 (anti-inflammatory) upon activation. Th1 immunity contributes to effective clearance of viral infections and encourages CTL responses, which are the only known correlate for protection from EHV-1 [21,53,54]. In further support of a transition to a Th2 immune response and its contribution to EHM, the horses that developed EHM in our study showed higher levels of IL-10 in nasal secretions and CSF and lower IFNα and IL-17 in nasal secretions when compared to

non-EHM horses (unpublished data). Furthermore, EHM horses induced a greater EHV-1 IgG(T) antibody sub-isotype response following EHV-1 challenge compared to non-EHM horses (unpublished data). This sub-isotype has been associated with a Th2 immune response in horses [265]. The observed skew from Th1 to Th2 immunity in horses that develop EHM indicates that proper Th1 mediated immune responses are important protective features against EHV-1 infection and EHM and a shift to Th2 responses may predispose horses to clinical EHM.

We also saw some differential expression of chemokines in EHM horses compared to non-EHM horses. CXCL10 is best known for its T-cell chemotactic activity and its receptor can be found on Th1 cells, CD8+ cytotoxic lymphocytes, and NK cells [156]. We observed an upregulation of CXCL10 in EHM horses, but not in non-EHM horses. This is in contrast to our previous study where we found a statistically significant increase in CXCL10 expression in PBMCs following EHV-1 challenge [242]. Additionally, infection of PBMCs in vitro has been shown to increase CXCL10 expression [41]. Thus, it was surprising to see that CXCL10 was only significantly upregulated in the EHM horses in this study. However upon further examination it was apparent that CXCL10 was upregulated in the non-EHM horses in this study as well but this difference was not statistically significant (FDR = 0.16, log fold change = 1.5). Additionally, we saw a CCL5 was downregulation in EHM horses. Also known as "regulated upon activation normal T-cell expressed and secreted" or "RANTES", CCL5 acts as a chemotactic agent for monocytes, T-cells, NK cells, dendritic cells, eosinophils, and basophils [266]. Aging may have an impact on the sensitivity of PBMCs to secrete CCL5 following stimulation. In human PBMCs, T-cells from the elderly produced more CCL5, while NK cells produced less when compared to PBMCs from younger people [267]. While the role of the

downregulation of CCL5 from PBMCs is unknown in EHM pathogenesis, it likely reflects differences in cell populations, activation status, and responsiveness between these two groups.

In addition to host transcripts, we were able to identify viral transcription in the PBMCs using RNA sequencing analysis. EHV-1 transcription was detected in all samples post EHV-1 infection, but no noticeable differences in gene expression between EHM and non-EHM horses were observed. We found very little EHV-1 transcription in PBMCs prior to EHV-1 challenge, and only two pre-challenge samples (0/6 non-EHM horses and 2/8 EHM horses) were positive for EHV-1 transcripts. This is in contrast to our previous study, where we found low-level transcription in 5 of 7 horses prior to EHV-1 challenge, which likely indicated latent infection [242]. It is possible that the previously described horses were latently infected with EHV-1, while the majority of the horses in the present study were not. However, this is unlikely as most horses are exposed to EHV-1 at a young age, often before 1 year of age [1–4]. Another explanation could be differences in the sensitivities of the two analyses. However, while the RNA quality was slightly better in our previous study, the depth of sequencing and mapping quality was comparable between the two. Another explanation is that there is a difference in the "depth" of latency in PBMCs between the different herds in this experiment. It is thought that EHV-1 exhibits several gene expression profiles during latency and "deeper" latency is characterized by lower transcription [132]. It is possible different factors between the herds contributed to modulation of EHV-1 depth of latency in the PBMCs. We additionally identified transcripts from the gammaherpesviruses EHV-2 and EHV-5 in several samples both pre and post EHV-1 challenge with no apparent effect of EHV-1 challenge, which is what we observed previously [242]. We did observe that EHV-2 transcripts were more prevalent in the non-EHM

group – which may indicate that younger horses are more likely to have active transcription of EHV-2.

Small RNA sequencing and analysis identified several known and novel host and viral miRNAs expressed in the PBMC samples of these horses. Interestingly, and in agreement with our previous findings [242], no miRNAs mapped to the EHV-1 or EHV-4 genomes, even during peak EHV-1 viremia. Also in agreement with our previous study, several miRNAs were identified for the equine gammaherpesviruses, EHV-2, and EHV-5. The gammaherpesviruses are known for their persistence in lymphocytes [186,187]. Given our findings, it is presumed that miRNA expression plays a role in the maintenance of latent lymphocytic infection of gammaherpesviruses. The lack of EHV-1 miRNAs indicate that EHV-1 likely does not make use of miRNA expression during lymphocytic infection during peak viremia. We also identified numerous equine (host) miRNAs expressed by the PBMCs. However, very few of these were differentially expressed as a result of EHV-1 infection. Of the few miRNAs altered during EHV-1 infection, the majority were downregulated in EHM horses during infection. The human and murine orthologs of these miRNAs have routinely been associated with cancer, and presumably due to their role in regulation of the cell cycle [220–228]. It is unknown what the role of these miRNAs are in EHM development, but the differences between EHM and non-EHM horses may indicate differences in the proliferative activity of PBMCs between the two groups.

For this study, we used the "old mare model" in order to reliably induce EHM in horses using EHV-1 challenge infection. It has been well established aged female horses are significantly more likely to develop EHM during acute EHV-1 infection, and we also observed this in our study where all aged (but only one young) horses developed EHM, all of which were female [21,31,202]. It is known that factors associated with age and sex also play a role in the

development of EHM [18,21]. It is also known that EHV-1 associated abortions are rare when infection occurs in early pregnancy, but more frequent when it occurs in late pregnancy. It is presumed that changes to the hormonal microenvironment of the pregnant uterus predisposes this site to vasculitis and thrombosis at different stages of pregnancy [268]. In our study, we observed genes associated with the response to progesterone upregulated in EHM horses following EHV-1 challenge. It was not within the scope of this study to tease out specific differences between ages and sexes of horses, but rather to reliably induce EHM. More work is needed to study factors in a larger cohort of younger and male horses that develop EHM. Additionally, focusing on more timepoints, specifically looking at early immune events in the PBMCs and the respiratory tract on day 1 or 2 following challenge could help to further elucidate host factors important for protection from EHM.

In summary, the features we found to be associated with EHM such as elevated IL-6 expression and decreased T-cell activation through reduced AP-1 production can be explained with the phenomena associated with the aging immune system. Regardless, these mechanisms are also likely involved in EHM development in younger horses and were observed in the young horse exhibiting EHM in our study as well. Further host mechanisms identified to be associated with EHM included factors involved in coagulation, cell adhesion and the response to progesterone. Future studies should follow up on these factors identified as risk factors (or protective factors) for EHM in cohorts of horses of all age groups and of both sexes as well as in different breeds. In conclusion, this study provides an unbiased insight into differences in systemic responses during peak viremia of horses with and without EHM during EHV-1 infection and identifies inhibition of IL-6, regulation of hemostasis, and mechanisms to activate

T-cells, and shifting immune responses toward Th1 cell-mediated immunity as interesting targets for protection from EHM.

## SUPPLEMENTARY MATERIALS

The following are available online: File S5.1, File S5.2, File S5.3, and File S5.4

### **AUTHOR CONTRIBUTIONS**

All authors have read and agree to the published version of the manuscript.

Conceptualization, L.M.Z, P.S.D.W., and G.S.H.; experiment and sample collection, all authors; computational data analysis, L.M.Z.; writing—original draft preparation, L.M.Z and G.S.H; writing—review and editing, all authors.; funding acquisition, P.S.D.W. and G.S.H.

#### **FUNDING**

This research was funded by the Grayson Jockey Club Research Foundation.

#### **ACKNOWLEDGEMENTS**

The authors would like to thank the following colleagues and facilities for their help with this study. Amanda Wiel assisted with the experiment. Tristan Foster and the Veterinary Research Farm at Michigan State University managed the animal facilities. Emily Crisovan and the Genomics Research and Technology Support Facility at Michigan State University assisted with technical advice and performed the library preparation and next generation sequencing. The Institute for Cyber-Enabled Research at Michigan State University provided the computational resources.

#### **CONFLICTS OF INTEREST**

The authors declare no conflict of interest. The funders had no role in the design of the study; in the collection, analyses, or interpretation of data; in the writing of the manuscript, or in the decision to publish the results.

# **CHAPTER 6**

# CONCLUSIONS AND FUTURE DIRECTIONS

#### CONCLUSIONS AND FUTURE DIRECTIONS

In this dissertation I describe my work dedicated to further the understanding of equine immunity to equine herpesvirus 1 infection. My initial experiment was not *per se* designed to investigate host immunity, however, the unexpected results lead to my speculation that the interplay between innate and adaptive systemic immune responses are complex and important for protection against EHV-1 viremia. As viremia is the central pre-requisite for secondary diseases such as EHM, this speculation deserved to be further investigated. In this experiment, I hypothesized that delivery of the IR2 gene (a gene inhibitory for EHV-1 replication) using a human adenovirus vector would reduce EHV-1 replication in the nasal epithelium and thereby reduce clinical disease and viremia. Contrary to my hypothesis, I found no reduction in nasal viral shedding, but instead, horses that received either the IR2 vector or the null (empty) viral vector had a decrease in viremia compared to horses that received no adenovirus treatment. It is my belief that delivery of the adenovirus to the nasal epithelium 2 days prior to EHV-1 challenge initiated an anti-viral innate immune response and "primed" the horses to mount a more effective systemic immune response upon EHV-1 challenge infection.

This lead to my second experiment, which investigated the efficacy of an intranasal live-attenuated influenza virus (LAIV) vaccine treatment to provide protection from EHV-1. Prior to investigating this hypothesis *in vivo*, I performed an *in vitro* experiment with equine respiratory epithelial cell (EREC) cultures. The goal of this was to determine at what day post LAIV treatment was optimal immune induction achieved, as measured by expression of cytokine mRNA and protein, specifically interferons and chemokines. I found that LAIV treatment in ERECs, particularly 5 days prior to EHV-1 inoculation, did improve immune responses to EHV-1 and reduced EHV-1 replication. The intention was to then vaccinate horses with intranasal

LAIV a few days prior to EHV-1 challenge infection and measure immunological, virologic, and clinical signs of disease. Unfortunately, a naturally occurring outbreak of EHV-4 spread through the research herd prior to the experiment. Due to the similarities of EHV-4 and EHV-1 and antibody cross reactivity between the two viruses, it was determined these horses should not continue in the study. Resource limitations indefinitely postponed this *in vivo* experiment.

While the first two experiments focused on innate immune events at the respiratory epithelium and their role in protection from EHV-1, it is my ultimate goal to protect horses particularly from EHM. Therefore, the next experiments were focused on the systemic host immune responses in PBMCs during viremia. As a the carriers of EHV-1 to secondary infection sites, as well as important inflammatory cells PBMCs are an important tissue to study the mechanisms surrounding EHM pathogenesis. These experiments used next-generation RNA sequencing to create an unbiased gene expression profile of the samples. The first experiment was initially designed as a pilot study to the study described in chapter 5, in order to ensure the data analysis would be successful with a larger number of samples. However, analysis of this "pilot" data revealed many previously unknown features of viremia. For example, I found type 1 interferon response to be robustly upregulated in PBMCs. In addition, I found PBMCs to be sources of chemokines (especially the CXCR3 ligands) as well as components of the complement and coagulation protein activation cascades.

While this study provided previously unknown data at the gene expression responses in PBMCs during EHV-1 viremia, the question remained as to which mechanisms are different in horses that go on to develop clinical EHM. The experiment described in chapter 5 was designed to compare horses with and without EHM disease in order to identify systemic host immune mechanisms ultimately responsible for the disease. I identified features such as IL-6

overexpression, defects in T-cell activation, and a skew from Th1 to Th2 immunity to be likely contributors to EHM.

The work in this dissertation identifies some potential directions for future studies: Firstly, this work identifies IL-6 as a biomarker and potentially a target for EHM disease. IL-6 is an important cytokine involved in the immunopathology of many diseases involving vascular permeability and endothelial damage [213]. In humans, serum IL-6 expression can be used as a biomarker to predict severity of stroke in addition to clinical outcome [213,234–237]. Based on the mRNA expression we observed in PBMCs, it would be a logical and exciting next step to analyze serum IL-6 levels in these horses, as well as any other available clinical or research samples to identify the ability of IL-6 to predict EHM incidence in horses. Serum samples are relatively easy for clinicians and researchers to obtain and should serum IL-6 prove to useful for predicting EHM would allow for expansion of current research using larger samples and more diverse study designs. In addition to being a marker of disease, IL-6 also likely plays a direct role in immunopathology leading to EHM clinical disease. As such, IL-6 inhibition is an interesting idea to explore as target for treatment or protection from EHM.

Secondly, the inability of current EHV-1 vaccines to induce protection against EHM has been thought to be associated with the difficulty in in stimulating cell-mediated immunity [53,54]. The work described in this dissertation further supports the idea that T-cell activation deficiencies, especially in older horses, may contribute to the pathogenesis of EHM. Similarly, deficits in T-cell mediated immunity has been implicated in shortcomings of varicella-zoster virus (VZV) vaccines to protect against herpes zoster (HZ) disease in older humans [269]. A recent new vaccine (brand name Shingrix, manufactured by GlaxoSmithKline) has recently been shown to outperform previously approved vaccines for HZ, and is recommended as the

"preferred shingles vaccine" according to the Centers for Disease Control and Prevention [269,270]. The success of Shingrix has been attributed to the adjuvant, AS01. This adjuvant contains two stimulants: *Quillaja saponaria* Molina, fraction 21 (QS-21), which stimulates innate immunity and recruitment and activation of dendritic cells, and 3-*O*-desacyl-4'-monophosphoryl lipid A (MPL), which acts as a TLR-4 agonist. These two stimulants act in a synergistic way to boost cell-mediated immune responses [269,271–273]. Given the similarities between EHV-1 and VZV life-cycles and cell tropism, in addition to the problems generating protective immunity of older individuals, investigation of similar technology in adjuvants for EHV-1 vaccination is warranted.

Finally, additional host mechanisms contributing to EHM may be identified or clarified by comparing the transcriptome of PBMCs in age and sex matched horses with EHV-1 infection to those with EHV-4 infection. EHV-4 is the other major alphaherpesvirus affecting horses, and is genetically and antigenically very similar to EHV-1. While both viruses cause respiratory disease in younger horses, the hallmark difference between these two viruses is that EHV-4 causes little to no viremia, and is not known to result in EHM, even in aged horses [274]. We have previously investigated differences in host responses to EHV-4 genes by replacing the glycoprotein D gene of EHV-1 with that of EHV-4, and we found delays and reductions in viremia [22]. Virological factors (such as glycoproteins) may explain part of the differences in clinical diseases between these two viruses. However, cell tropism and viremia establishment may not be explain the whole story. In fact, I performed deep sequencing analysis of PBMCs of horses with EHV-4 infection and found that EHV-4 transcription occurred in all 5 horses sampled (unpublished data). This indicates that EHV-4 viremia may be more prevalent than previously thought, and viremia alone cannot account for the different propensities of these two

viruses to cause neurologic disease. In light of the results presented in this thesis, a more comprehensive analysis of systemic host immunity to these two viruses, ideally a repeated measure design and experimental challenge infection of aged matched older horses. To help shape this hypothesis, I have collected and performed RNA deep sequencing on 5 young horses with EHV-4 infection and can compare to the transcriptome post infection of the young horses with EHV-1 presented in Chapter 4 or 5. A limitation to this is there were no pre-samples collected for the EHV-4 infected horses (as these were collected during an unexpected natural EHV-4 outbreak). However, the analysis may provide useful information to shape a future study investigating differential host responses to these two viruses.

# **APPENDIX**

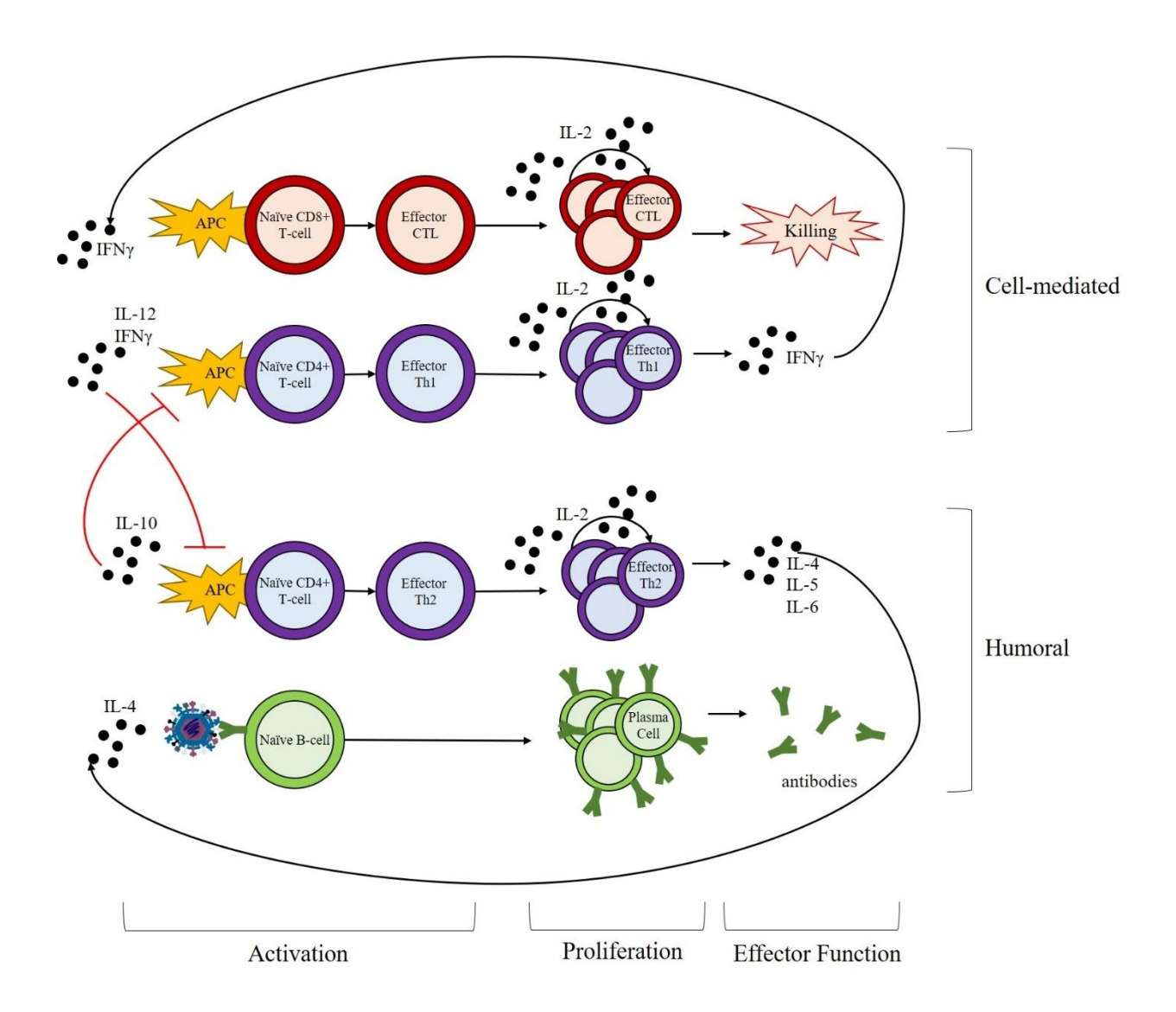


**Figure 1. Overview of adaptive immunity involved in protection from EHV-1.** Cytokines expressed from and Th cells, as well as other surrounding cells, dictate the polarization of responses following antigen presentation and activation. Th1 cells produce IFNγ, which further promotes Th1 cell differentiation, as well as CTL activation. Th2 cells produce cytokines such as IL-4, which promote humoral immune responses. Th1 cytokines block activation of Th2 cells, while Th2 cytokines block activation of Th1 cells, further contributing to the polarity of these responses. Following activation, T-cells produce IL-2 which acts in an autocrine manner to stimulate proliferation of that clone.

**Table 1. Experimental design.** Groups consisted of Ad-IR2 treated horses (n=4), null Ad treated horses (n = 4), or no Ad vector controls (n=8). Ad-IR2 or null Ad treatment was performed on day -2. EHV-1 challenge was performed on all groups on day 0. Pre samples were collected between days -13 and -3. X indicates daily sampling. ad indicates sampling on alternating days. Y indicates sampling for only the Ad-IR2 and null Ad groups. \*sample collections on day 0 were performed prior to EHV-1 challenge. Physical exams were performed to collect clinical score and body temperature data. VN – virus neutralizing serum titer.

Experimental design																
	pre	-2	-1	0	1	2		7		10	11	12	13	14		20
Physical	X		X		X	X	X	X	X	X	X	X	X	X	ad	ad
exams																
Nasal	X				X	X	X	X	X	X	X	X				
Shedding																
Viremia	X				X	X	X	X	X	X						
VN titers	X							X						X		X
Nasal	X		Y	Y*	X											
cytokines																
Nasal	X		Y	Y*	X											
IR2P																

**Table 2. Clinical score grading criteria**. For each sampling session, a grade was assigned for each component (cough, nasal discharge, and ocular discharge) for each horse and summed for a total clinical score.

Clinical Score Criteria								
Score	Cough	Nasal Discharge	Ocular Discharge					
0	No coughing during	No discharge or	No discharge					
	sampling time	slight serous						
		discharge						
0.5	Single cough during	Copious serous	Serous discharge					
	sampling time	discharge						
1	Two coughs during	Slight mucopurulent	Slight mucopurulent					
	sampling time	discharge	discharge					
2	$\geq$ 3 coughs during	Moderate or severe	Moderate or severe					
	sampling time	mucopurulent	mucopurulent					
		discharge	discharge					

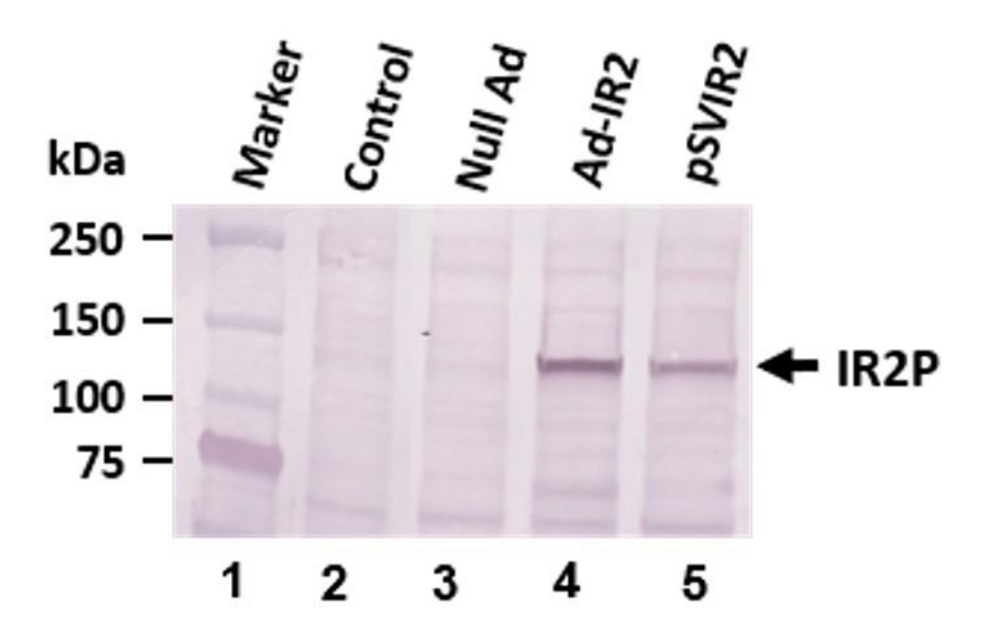


**Figure 2. Detection of IR2P in NBL-6 cells by western blot analysis**. NBL-6 cells were transduced with the newly created IR2P-expressing recombinant adenovirus (Ad-IR2) vector or null vector (null Ad) at an MOI of 5, harvested, and analyzed with anti-IEP (IR2P) OC33 antibody [69]. As a positive control, the IR2P were expressed from the IR2 expression vector pSVIR2.

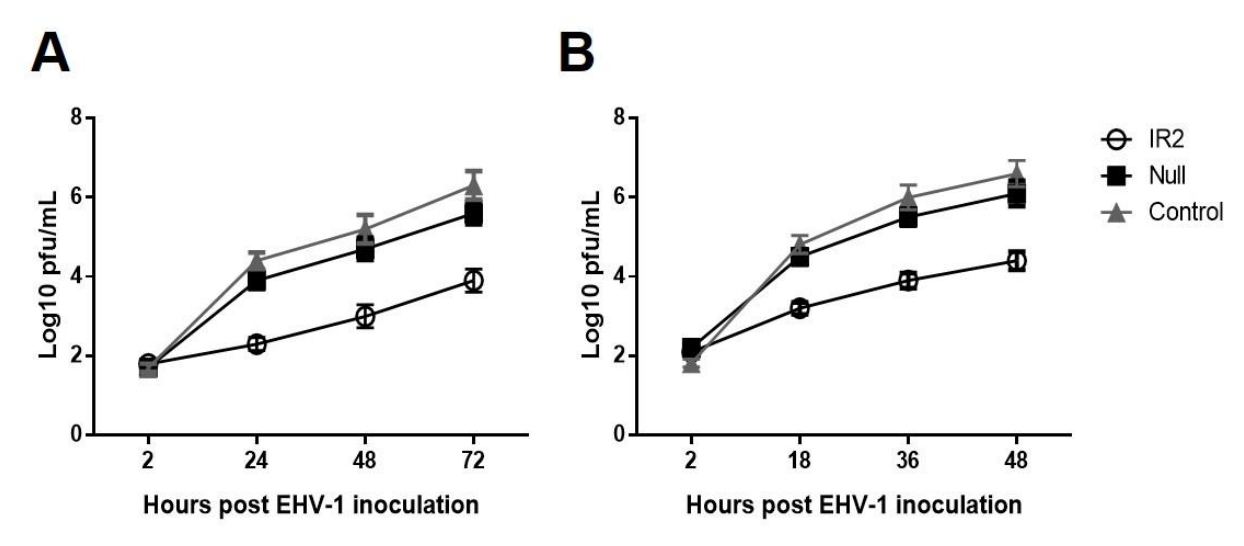


Figure 3. IR2P-expressing recombinant adenovirus (Ad-IR2) reduces EHV-1 yield. (A) ARPE-19 cells and (B) NBL-6 cells were inoculated with the Ad-IR2 and an MOI of 30 and 24 h later inoculated with EHV-1 RacL11 at an MOI of 0.02 At the indicated time post EHV-1 inoculation, the cell culture was harvested for use in a plaque assay. EHV-1 titers were determined by plaque assay on NBL6 cells. Each sample was assayed in triplicate and data are presented as means  $\pm$  SD.

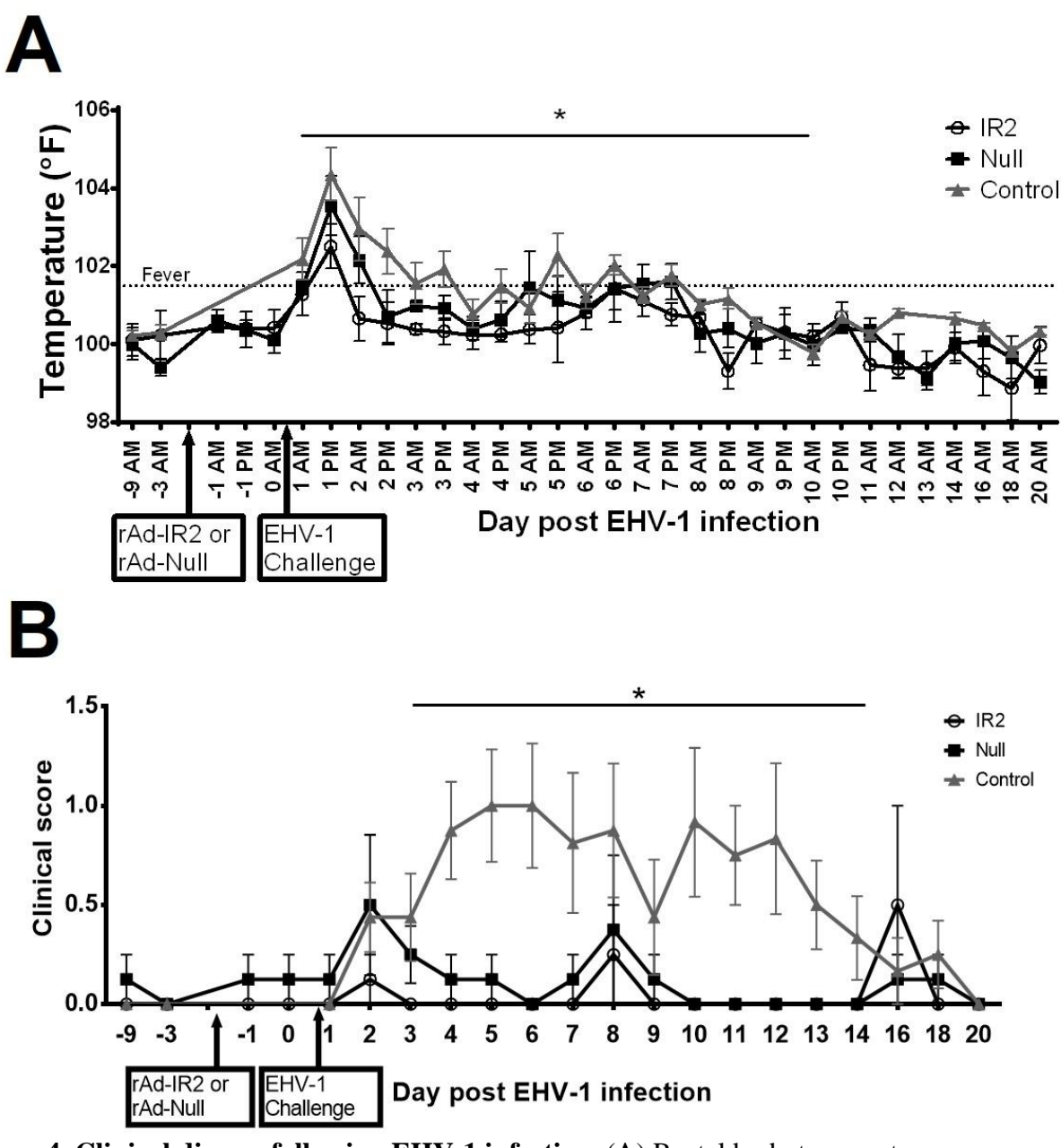
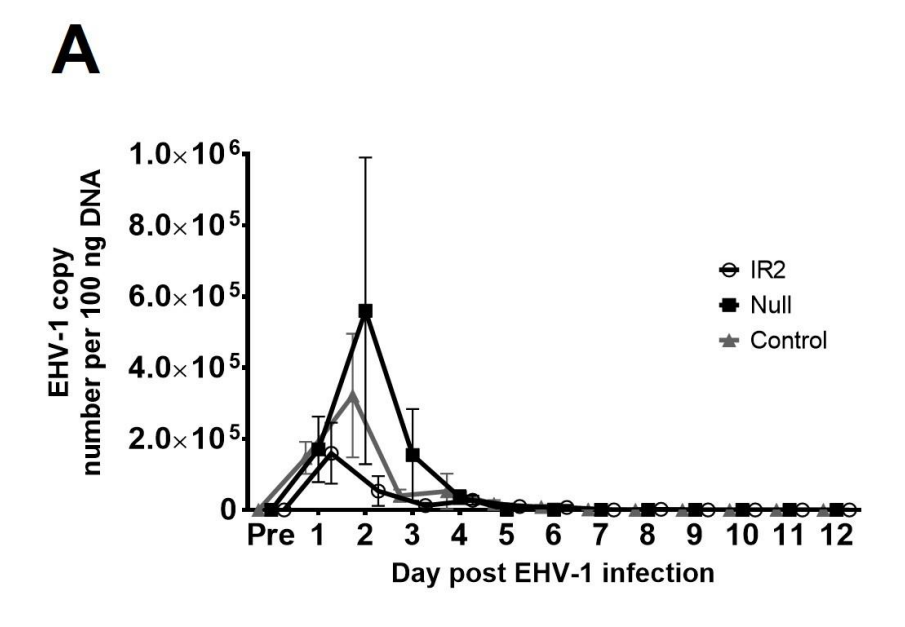
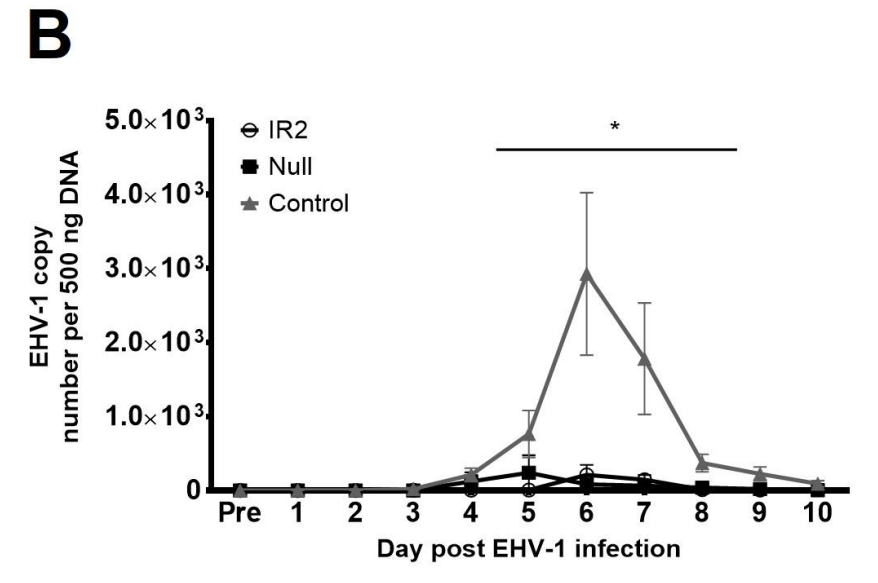


Figure 4. Clinical disease following EHV-1 infection. (A) Rectal body temperature was measured at the indicated timepoints. Fever is indicated by the line at 101.5 °F. (B) Total clinical score was assessed during the physical examination and calculated for each individual horses by adding scores for cough, nasal discharge, and ocular discharge following the criteria in table 2. All data are presented as means  $\pm$  SEM. \* indicates statistically significant difference between the control group when compared to the Ad-IR2 and the null Ad groups (p  $\leq$  0.05).





**Figure 5. Viral load following EHV-1 infection.** (**A**) Nasal viral shedding. Nasal swab samples were collected from each horse at the indicated timepoints and stored at -80 °C until further processing. (**B**) Viremia. Whole blood was collected by jugular venipuncture into heparinized tubes at the timepoints indicated for each horse. Immediately following blood collection, PBMCs were isolated by density gradient centrifugation as previously described [76] and stored at -80 °C until further processing. Viral load was determined for all frozen samples via qPCR as previously described [10]. Data are presented as means  $\pm$  SEM. \* indicates statistically significant difference between the control group when compared to the Ad-IR2 and the null Ad groups ( $p \le 0.05$ ).

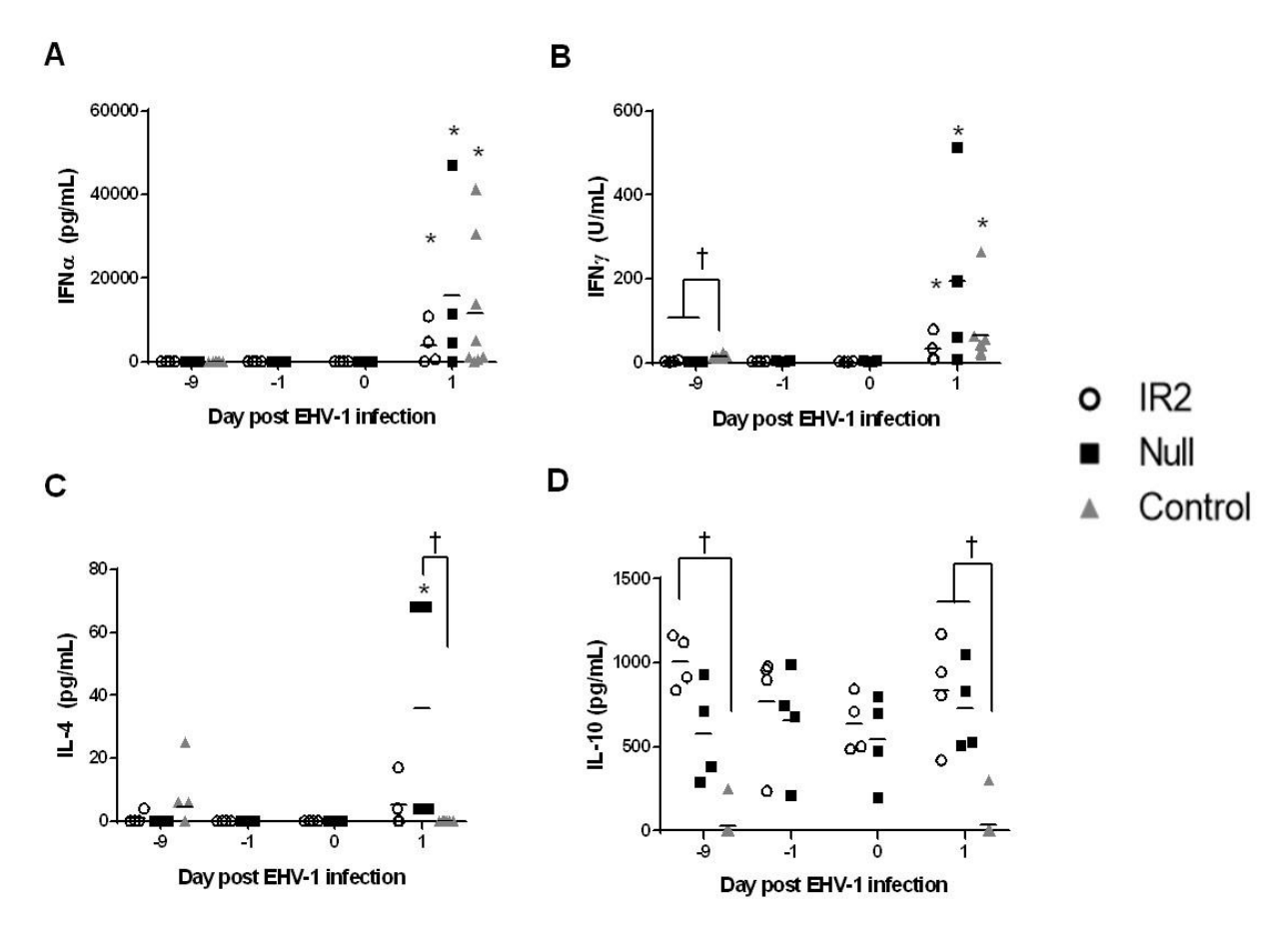


Figure 6. Nasal cytokine protein expression. (A) IFN $\alpha$  (B) IFN $\gamma$  (C) IL-4 (D) IL-10. Nasal secretion samples were collected at the indicated timepoints by inserting and absorbent tampon into the central nasal meatus of each horse. After 30 m, the tampon was removed and centrifuged for 20 m at 2,000 x g to collect the fluid. Fluid was stored at -80 °C until further processing. Protein expression was quantified using a bead-based multiplex assay as described previously [78]. Ad-IR2 or null Ad administration occurred on day -2 and EHV-1 challenge occurred on day 0 after sampling occurred. Data are presented as means  $\pm$  SEM. \* indicates statistically significant difference compared to baseline (day -9) values (p  $\leq$  0.05). † indicates statistically significant difference between the indicated groups on that day (p  $\leq$  0.05).

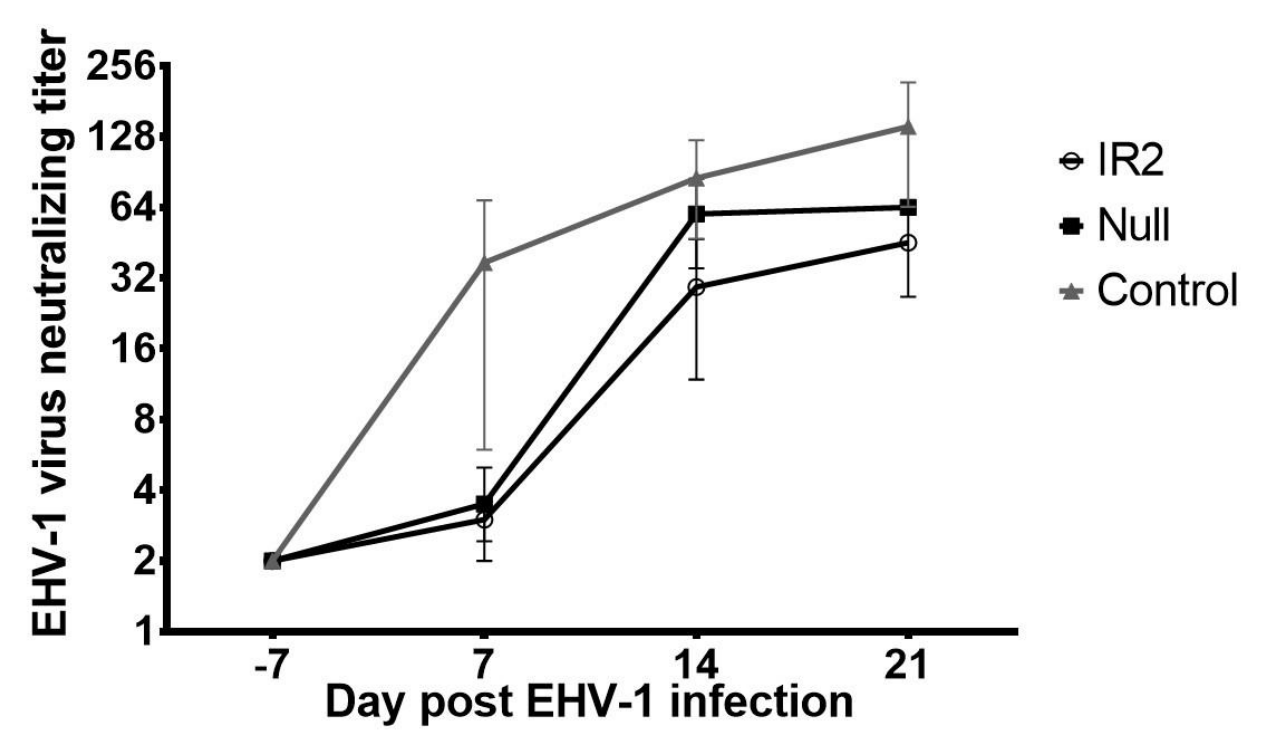


Figure 7. Virus neutralizing (VN) antibody titers in blood serum following EHV-1 infection. Blood serum was collected via jugular venipuncture at the indicated timepoints. VN assays were performed with final serial dilutions of serum from 1:4 to 1:4096 as previously described [77]. Data are presented as means  $\pm$  SEM.

Table 3. Grading criteria for Flu Avert toxicity in EREC cultures.

Grade	Criteria
0	Cells appear healthy
1	Cell clumping or mucus in <50% of well or minor clumping/mucus
2	Cell clumping or mucus in >50% of well or severe clumping/mucus
3	Same as grade "2" plus cells peeling off of culture membrane

Table 4. Primer and probe source list.

	Primer and probe source list					
Gene	Source					
CCL2	TaqMan® Gene Expression assay no: Ec03468496_ml (Thermo Fisher)					
CCL5	TaqMan® Gene Expression assay no: Ec03468106_ml (Thermo Fisher)					
CXCL9	TaqMan® Gene Expression assay no: Ec03469470_ml (Thermo Fisher)					
CXCL10	TaqMan® Gene Expression assay no: Ec03469403_ml (Thermo Fisher)					
IL-8	TaqMan® Gene Expression assay no: Ec03468860_ml (Thermo Fisher)					
IFN-γ	TaqMan® Gene Expression assay no: Ec03468606_ml (Thermo Fisher)					
IFN-α	Designed in house;					
	Forward 5'-CGGAAGCCTCAAGCCATCT-3'					
	Reverse 5'-TCTGTGCTGAAGAGGTGGAAGA-3'					
	Probe 5'-TGCGGTCCATGAGACGATCCAACA-3'					
IFN-β	Young Go, et al. 2014 [275]					
IL-10	TaqMan® Gene Expression assay no: Ec03468647_ml (Thermo Fisher)					
ACTB	TaqMan® Gene Expression assay no: Ec04176172_gH (Thermo Fisher)					
B2M	TaqMan® Gene Expression assay no: Ec03468699_ml (Thermo Fisher)					
GUSB	TaqMan® Gene Expression assay no: Ec03470630_m1 (Thermo Fisher)					

Table 5. Intracellular and extracellular EHV-1 virus.

Intracell	Intracellular Virus				
Flu Avert treatment day	# of cultures where viral load is reduced by >10 <sup>4</sup> gB DNA copies				
Day -1	7/10				
Day -2	8/10				
Day -5	8/10				
Day -7	4/10				
Extracellular Virus					
Extracell	ular Virus				
Extracell Flu Avert treatment day	# of cultures where viral load is reduced by >500 gB				
Flu Avert	# of cultures where viral load is reduced				
Flu Avert treatment day	# of cultures where viral load is reduced by >500 gB DNA copies				
Flu Avert treatment day  Day -1	# of cultures where viral load is reduced by >500 gB DNA copies 7/10				

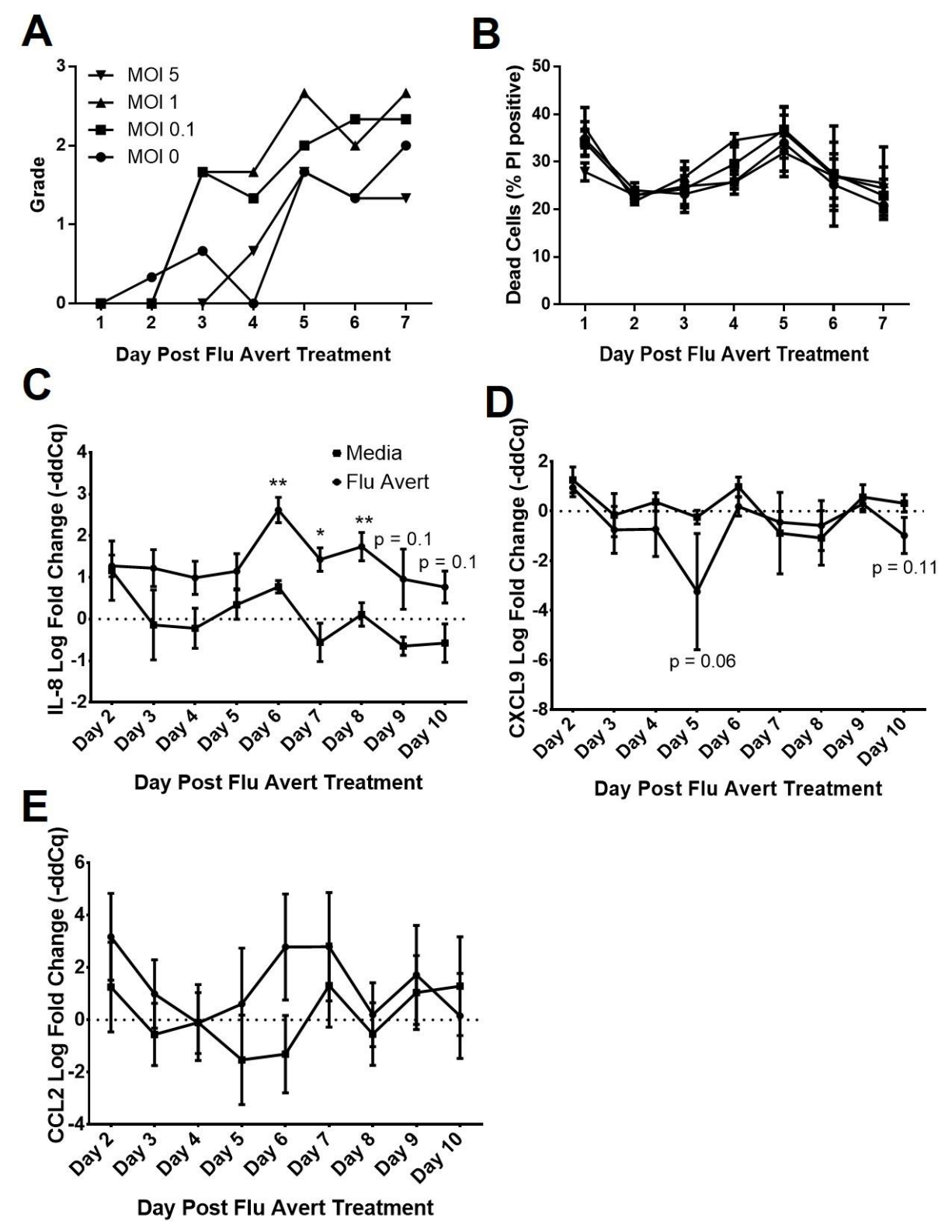
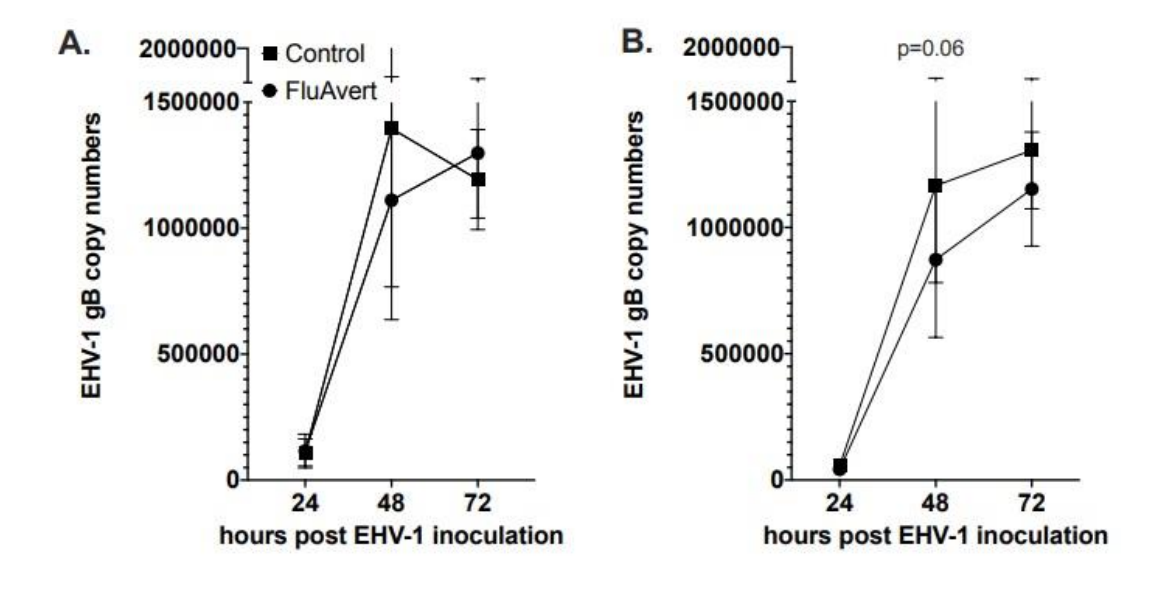
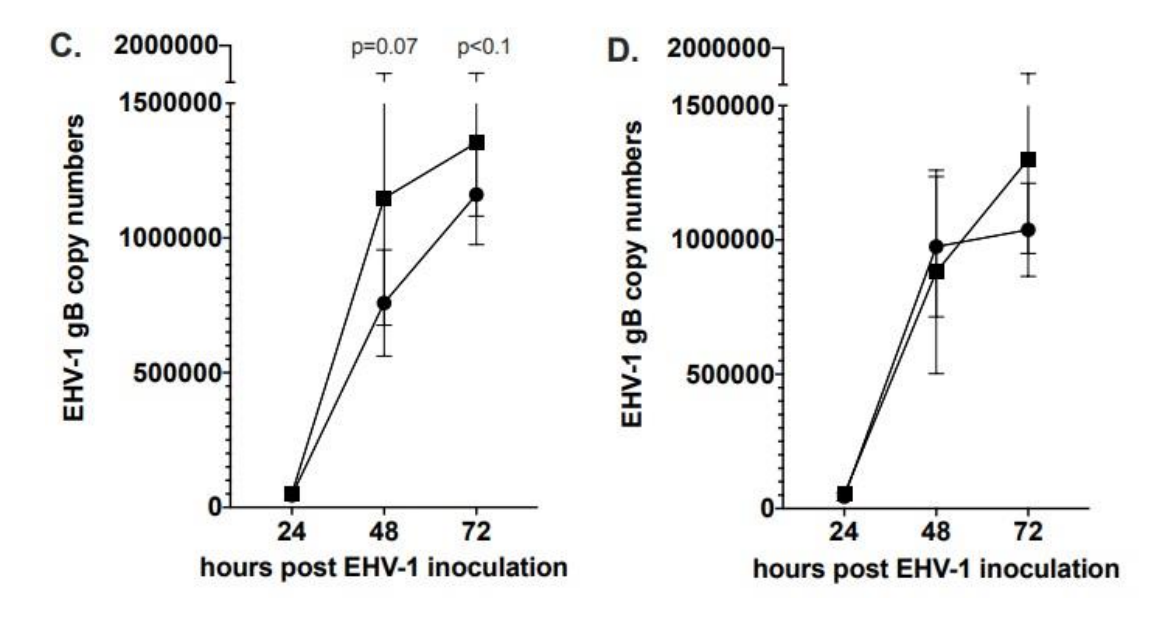


Figure 8. Cell viability and chemokine mRNA expression following Flu Avert treatment in ERECs. A. Microscopic analysis of EREC cultures. Mean grades from cells of three horses

**Figure 8.** (Cont'd) following Flu Avert treatment at different MOI. Grade 0 indicates cells appear healthy. Grade 1 indicates cell clumping or mucus in < 50% of well or minor clumping or mucus. Grade 2 indicates cell clumping or mucus in > 50% of the well or severe clumping or mucus. Grade 3 criteria is same as for grade 2, plus cells peeling off of the membrane. B. Cell viability analysis. Mean percent positive cells  $\pm$  SEM of three horses at each MOI as determined with propidium iodide staining. Black circle is MOI = 0. Black square is MOI = 0.1. Black upright triangle is MOI = 1. Black upside down triangle is MOI = 5. C. IL-8 mRNA expression. D. CCL2 mRNA expression. E. CXCL9 mRNA expression. Values are mean log fold change (-ddCq)  $\pm$  SEM. Black square represents untreated (media) treated ERECs. Black circle represents Flu Avert treated ERECs. \* and \*\* indicates statistically significant difference at p  $\leq$  0.05 and p < 0.01, respectively, between media and Flu Avert treatment groups.





**Figure 9. Difference in EHV-1 copy number between Flu Avert treated and media treated ERECs.** A. Intracellular copy number in cells treated with Flu Avert or media at day-1 prior to EHV-1 inoculation; B. Intracellular copy number in cells treated with Flu Avert or media at day-2 prior to EHV-1 inoculation; C. Intracellular copy number in cells treated with Flu Avert or media at day-5 prior to EHV-1 inoculation; D. Intracellular copy number in cells treated with Flu Avert or media at day-7 prior to EHV-1 inoculation.

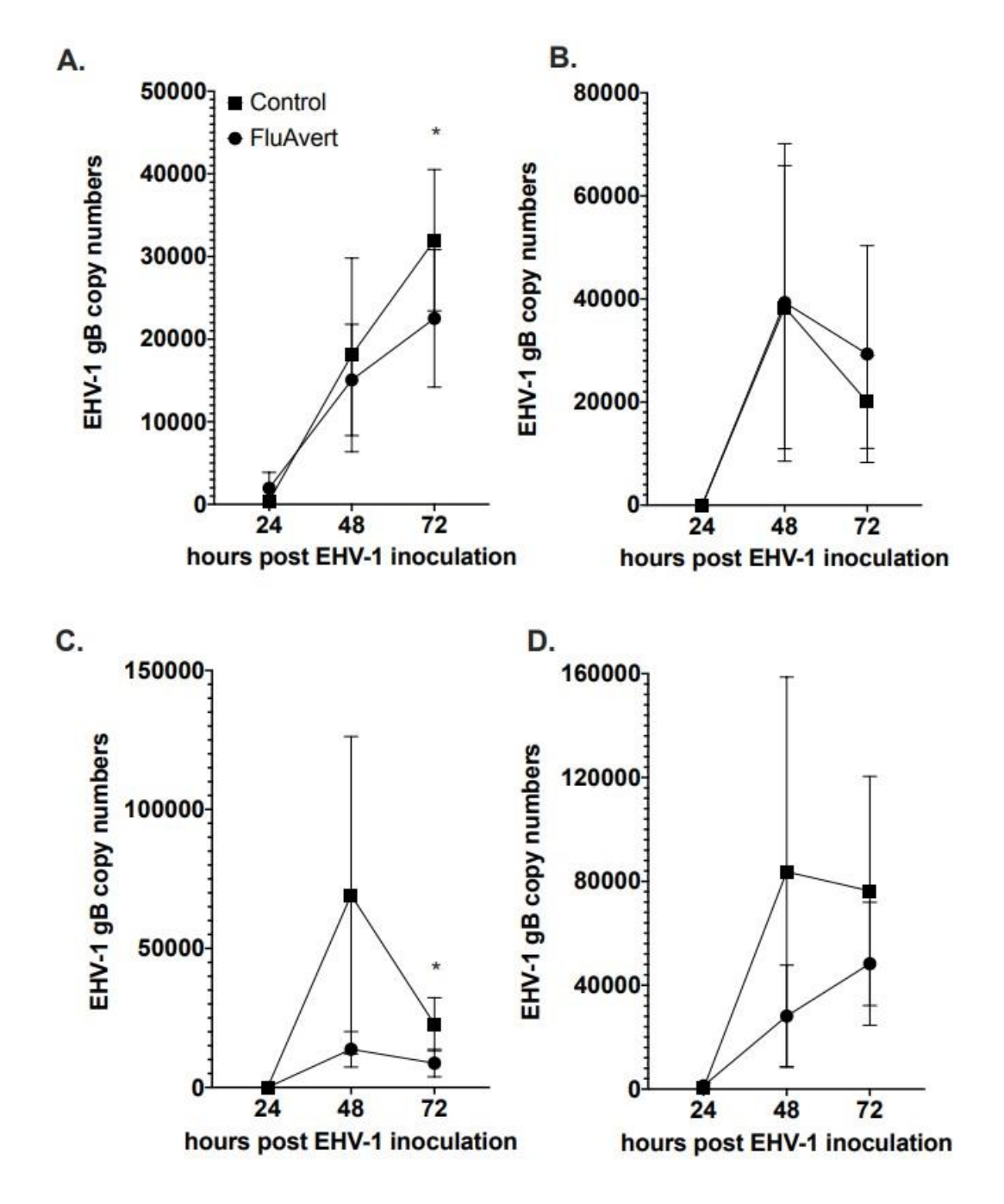


**Figure 10. Difference in EHV-1 copy number between Flu Avert treated and media treated ERECs.** A. Extracellular copy number in cells treated with Flu Avert or media at day-1 prior to EHV-1 inoculation; B. Extracellular copy number in cells treated with Flu Avert or media at day-2 prior to EHV-1 inoculation; C. Extracellular copy number in cells treated with Flu Avert or media at day-5 prior to EHV-1 inoculation; D. Extracellular copy number in cells treated with Flu Avert or media at day-7 prior to EHV-1 inoculation. \* p<0.05.

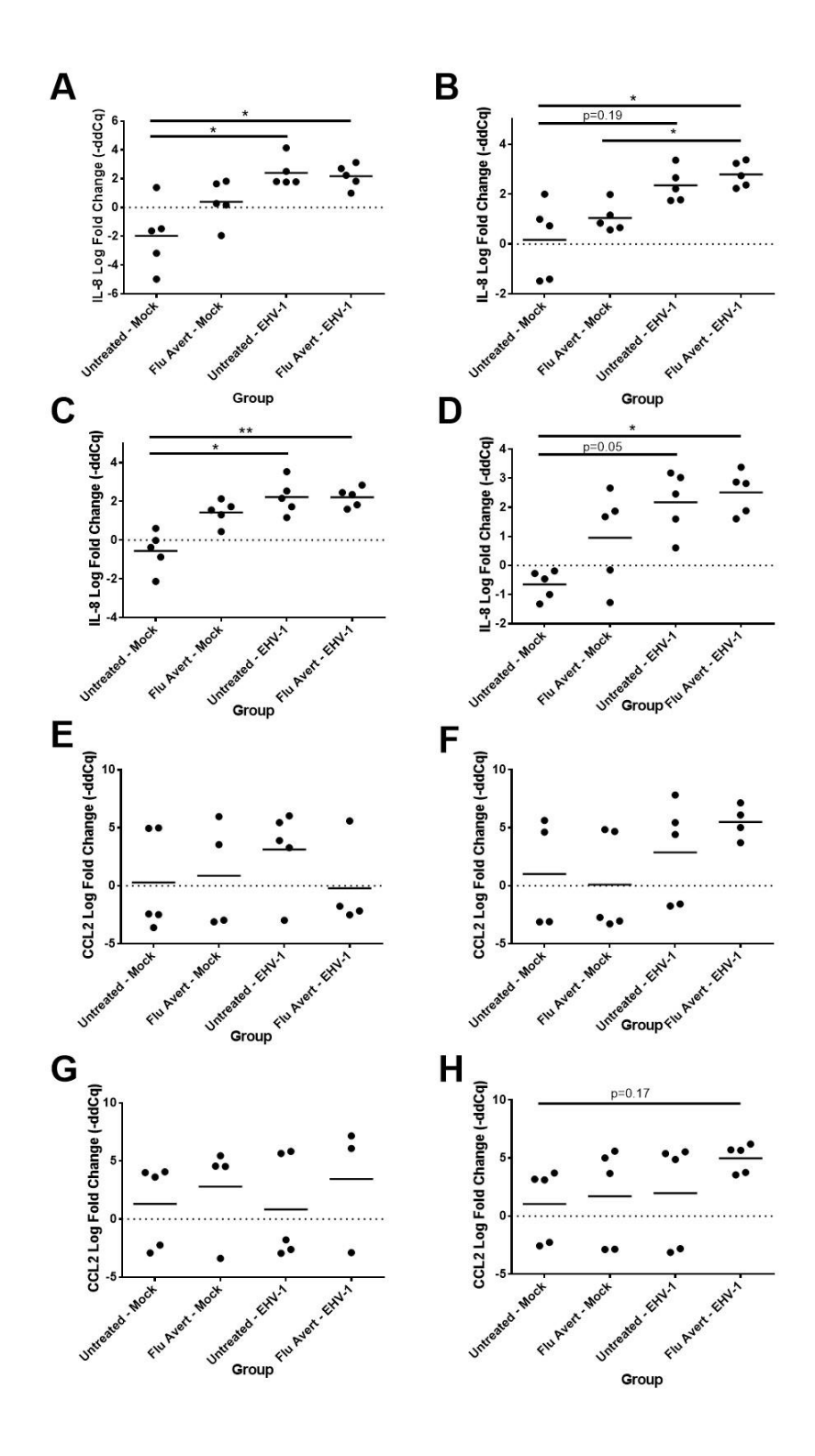


**Figure 11.** Effect of Flu Avert treatment on chemokine mRNA expression in ERECs 24 hours following EHV-1 inoculation. A. IL-8 mRNA expression in ERECs that were treated with Flu Avert on day -5 prior to EHV-1 inoculation. B. IL-8 mRNA expression in ERECs that **Figure 11.** (Cont'd) were treated with Flu Avert on day -7 prior to EHV-1 inoculation. C. CXCL10 mRNA expression in ERECs that were treated with Flu Avert on day -5 prior to EHV-1

inoculation. D. CXCL10 mRNA expression in ERECs that were treated with Flu Avert on day -7 prior to EHV-1 inoculation. The mean log fold change (-ddCq) is represented by a bar. \* indicates statistically significant difference (p < 0.05).

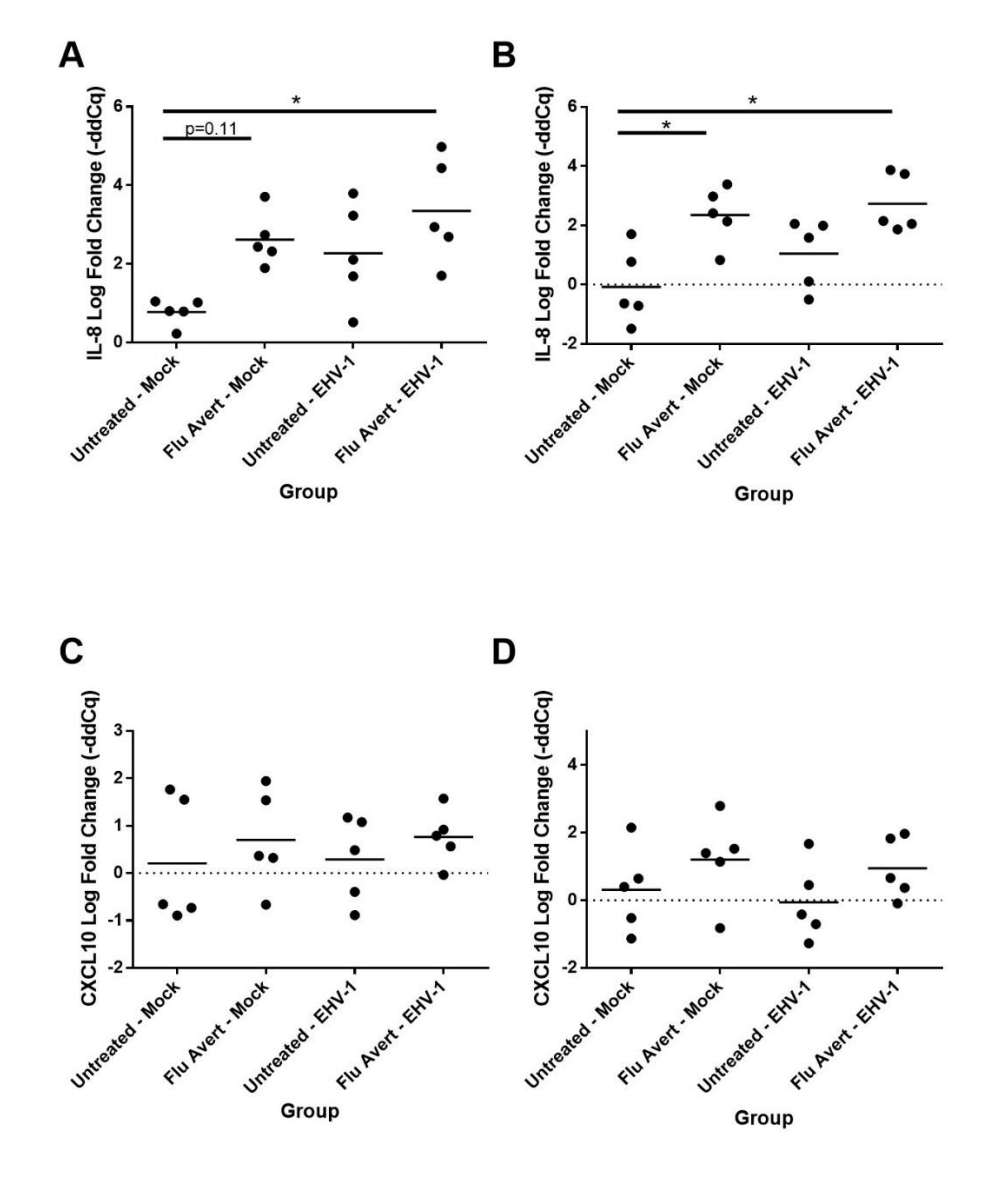


**Figure 12. Effect of Flu Avert treatment on chemokine mRNA expression in ERECs 48 hours following EHV-1 inoculation.** A. IL-8 mRNA expression in ERECs that were treated with Flu Avert on day -1 prior to EHV-1 inoculation. B. IL-8 mRNA expression in ERECs that were treated with Flu Avert on day -2 prior to EHV-1 inoculation. C. IL-8 mRNA expression in ERECs that were treated with Flu Avert on day -5 prior to EHV-1 inoculation. D. IL-8 mRNA expression in ERECs that were treated with Flu Avert on day -7 prior to EHV-1 inoculation. E. CCL2 mRNA expression in ERECs that were treated with Flu Avert on day -1 prior to EHV-1 inoculation. F. CCL2 mRNA expression in ERECs that were treated with FluAvert on day -2 prior to EHV-1 inoculation. G. CCL2 mRNA expression in ERECs that were treated with Flu Avert on day -5 prior to EHV-1 inoculation. H. CCL2 mRNA expression in ERECs that were treated with Flu Avert on day -7 prior to EHV-1 inoculation. The mean log fold change (-ddCq) is represented by a bar. \*\* indicates statistically significant difference (p<0.01). \* indicates statistically significant difference (p<0.05).

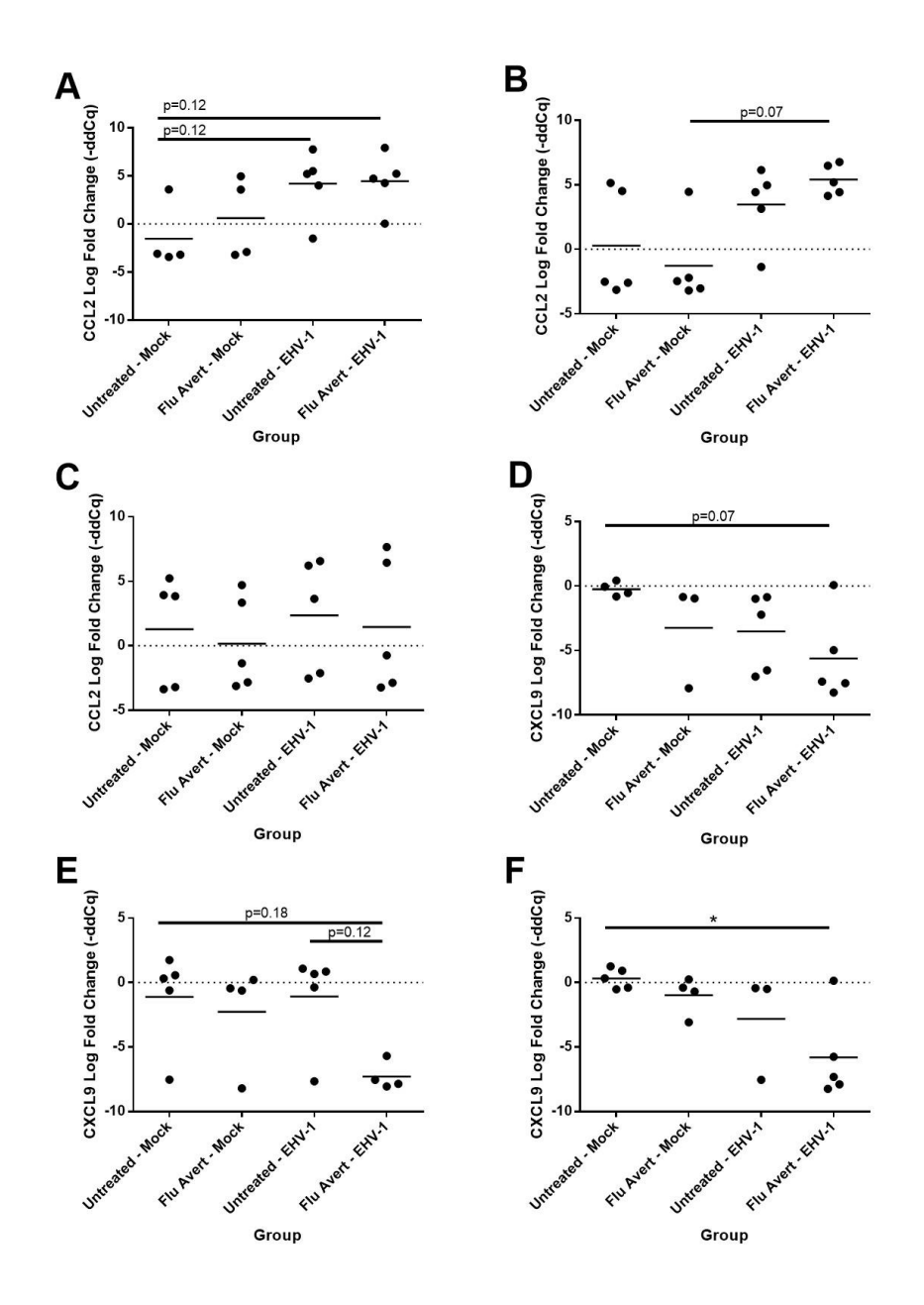


**Figure 13.** Effect of Flu Avert treatment on chemokine mRNA expression in ERECs 72 hours following EHV-1 inoculation. A. CCL2 mRNA expression in ERECs that were treated with Flu Avert on day -2 prior to EHV-1 inoculation. B. CCL2 mRNA expression in ERECs that were treated with Flu Avert on day -5 prior to EHV-1 inoculation. C. CCL2 mRNA expression in ERECs that were treated with Flu Avert on day -7 prior to EHV-1 inoculation. D. CXCL9 mRNA expression in ERECs that were treated with Flu Avert on day -2 prior to EHV-1 inoculation. E. CXCL9 mRNA expression in ERECs that were treated with Flu Avert on day -5 prior to EHV-1 inoculation. F. CXCL9 mRNA expression in ERECs that were treated with Flu Avert on day -7 prior to EHV-1 inoculation. The mean log fold change (-ddCq) is represented by a bar. \* indicates statistically significant difference (p < 0.05).

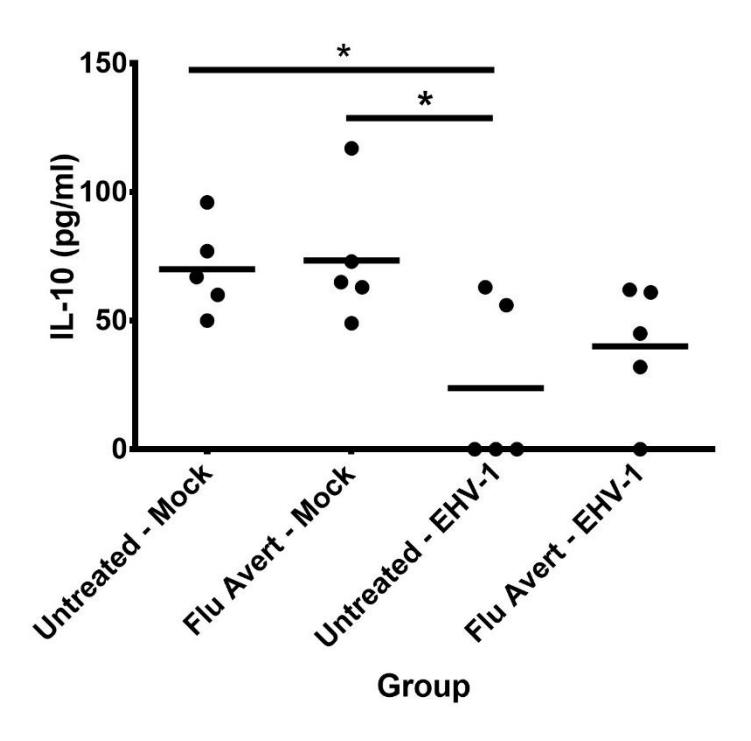


Figure 14. IL-10 protein expression in EREC supernatants 72 hours post EHV-1 infection. The mean concentration (pg/ml) is represented by a bar. \* represents statistically significant difference (p < 0.05).

**Table 6. Mapping summary statistics of mRNA sequencing.** Total reads after sequencing and the number and percent that uniquely mapped to the EquCab3.0 genome are shown for each sample.

Mapping summary statistics of mRNA sequencing							
Sample ID	Total reads	Uniquely mapped (number of	Uniquely mapped				
		reads)	(%)				
H1_PRE	26999513	21296243	78.9				
H1_POST	27536037	20976540	76.2				
H2_PRE	35256030	29155433	82.7				
H2_POST	42517852	33582323	79.0				
H3_PRE	56397724	45505043	80.7				
H3_POST	63282694	51758322	81.8				
H5_PRE	93180427	75568952	81.1				
H5_POST	27862507	23309213	83.7				
H6_PRE	50453360	40889209	81.0				
H6_POST	24740083	19062322	77.1				
H7_PRE	26710306	20926895	78.3				
H7_POST	52898636	43121055	81.5				
H9_PRE	51887615	42716415	82.3				
H9_POST	28998398	23182557	79.9				
Average	43480084	35075037	80.3				

Table 7. Differentially expressed genes.

Symbol	Log2FoldChange	Padj	PANTHER family/subfamily	Function – UniProtKB (homo
		Upregulat		sapiens ortholog)
ENSECAG00000034754	6.4	3.8E-22	Interferon-induced	No UniProtKB function listed
ENSECAG00000034734	0.4	3.6E-22	transmembrane protein	No Unificial function fisted
			3 (PTHR13999:SF4)	
DDX60	6.1	1.1E-65	ATP-dependent RNA	Positively regulates DDX58/RIG-I-
DDA00	0.1	1.112-03	helicase DDX60-	and IFIH1/MDA5-dependent type I
			related	interferon and interferon inducible
			(PTHR44533:SF3)	gene expression in response to viral
			(1111114-1333.513)	infection.
MX2			Interferon-induced	Interferon-induced dynamin-like
1,1112			GTP-binding protein	GTPase with potent antiviral activity
			MX2	against human immunodeficiency
	5.8	1.4E-64	(PTHR11566:SF46)	virus type 1 (HIV-1).
APOBEC3Z1B	5.8		DNA DC-DU-editing	No UniProtKB function listed
			enzyme APOBEC-3G	
		1.8E-07	(PTHR13857:SF20)	
			Subfamily not named	No UniProtKB function listed
ENSECAG00000032492	5.0	1.7E-52	(PTHR44533:SF5)	
			C-X-C motif	Cytokine that affects the growth,
			chemokine 9	movement, or activation state of
			(PTHR10179:SF44)	cells that participate in immune and
				inflammatory response. Chemotactic
CXCL9	4.8	5.7E-34		for activated T-cells.
NRGN			none	Acts as a 'third messenger' substrate
				of protein kinase C-mediated
				molecular cascades during synaptic
	4.6	8.6E-04		development and remodeling.

Table 7. (Cont'd)

Symbol	Log2FoldChange	Padj	PANTHER	Function – UniProtKB (homo
			family/subfamily	sapiens ortholog)
		Upregulat	. — —	
			Tumor necrosis factor	Mediates activation of NF-kappa-B.
			ligand superfamily	Inhibits vascular endothelial growth
			member 15	and angiogenesis (in vitro).
			(PTHR11471:SF24)	Promotes activation of caspases and
TNFSF15	4.5	4.9E-04		apoptosis.
			Interferon-induced	No UniProtKB function listed
			protein with	
			tetratricopeptide	
			repeats 1	
ENSECAG00000004433	4.5	1.5E-70	(PTHR10271:SF30)	
	4.4		Granzyme B	No UniProtKB function listed
ENSECAG00000015137		1.5E-03	(PTHR24271:SF53)	
			C-X-C motif	Chemotactic for interleukin-
			chemokine 11	activated T-cells but not
			(PTHR10179:SF28)	unstimulated T-cells, neutrophils or
CXCL11	4.4	1.5E-07		monocytes.
			C3A anaphylatoxin	Receptor for the chemotactic and
			chemotactic receptor	inflammatory peptide anaphylatoxin
			(PTHR24225:SF28)	C3a. This receptor stimulates
				chemotaxis, granule enzyme release
C3AR1	4.4	1.6E-05		and superoxide anion production.

Table 7. (Cont'd)

Symbol	Log2FoldChange	Padj	PANTHER family/subfamily	Function – UniProtKB (homo sapiens ortholog)			
	Upregulated genes Upregulated genes						
		Oproguiac	C-X-C motif chemokine 10 (PTHR10179:SF47)	Pro-inflammatory cytokine that is involved in a wide variety of processes such as chemotaxis, differentiation, and activation of peripheral immune cells, regulation of cell growth, apoptosis and modulation of angiostatic effects. Plays thereby an important role during viral infections by stimulating the activation and migration of immune cells to the			
CXCL10	4.3	3.9E-21		infected sites.			
ENSECAG00000001555	4.3	5.4E-04	Metallothionein-2 (PTHR23299:SF24)	No UniProtKB function listed			
ENSECAG00000032756	4.3	1.4E-07	DNA DC-DU-editing enzyme APOBEC-3G (PTHR13857:SF20)	No UniProtKB function listed			
SAMD9L			Sterile alpha motif domain-containing protein 9-like (PTHR16155:SF18)	May be involved in endosome fusion. Mediates down-regulation of growth factor signaling via internalization of growth factor			
	4.2	5.3E-53	,	receptors.			
				Interferon-induced dynamin-like GTPase with antiviral activity against a wide range of RNA viruses			
MX1	4.2	5.8E-79		and some DNA viruses.			

Table 7. (Cont'd)

Symbol	Log2FoldChange	Padj	PANTHER family/subfamily	Function – UniProtKB (homo sapiens ortholog)			
	Upregulated genes						
BCL2L14	4.0	7.4E-08	Apoptosis facilitator BCL-2-like protein 14 (PTHR14965:SF1)	Plays a role in apoptosis.			
			Guanylate-binding protein 1 (PTHR10751:SF96)	Hydrolyzes GTP to GMP in 2 consecutive cleavage reactions. Exhibits antiviral activity against influenza virus. Promotes oxidative killing and delivers antimicrobial peptides to autophagolysosomes,			
GBP1	3.9	2.2E-56		providing broad host protection against different pathogen classes.			
			Cis-Aconitate Decarboxylase (PTHR16943:SF11)	Involved in the inhibition of the inflammatory response. Acts as a negative regulator of the Toll-like receptors (TLRs)-mediated inflammatory innate response by stimulating the tumor necrosis factor alpha-induced protein TNFAIP3 expression via reactive oxygen species (ROS) in LPS-tolerized macrophages. Involved in antimicrobial response of innate immune cells; ACOD1-mediated itaconic acid production contributes to the antimicrobial activity of			
ACOD1	3.9	5.5E-39		macrophages.			

Table 7. (Cont'd)

Symbol	Log2FoldChange	Padj	PANTHER family/subfamily	Function – UniProtKB (homo sapiens ortholog)
		Upregulat		suprens of thology
		<u> </u>	Interferon-induced protein with	IFN-induced antiviral protein which acts as an inhibitor of cellular as
			tetratricopeptide	well as viral processes, cell
			repeats 3	migration, proliferation, signaling,
IFIT3	3.9	8.2E-91	(PTHR10271:SF3)	and viral replication.
C1R			Complement C1R	C1r B chain is a serine protease that
			subcomponent	combines with C1q and C1s to form
			(PTHR24255:SF25)	C1, the first component of the
				classical pathway of the
	3.8	2.3E-19		complement system.
ALPK1			Alpha-protein kinase 1	Serine/threonine-protein kinase that
			(PTHR46747:SF1)	detects bacterial pathogen-
				associated molecular pattern
				metabolites (PAMPs) and initiates
				an innate immune response, a
				critical step for pathogen
				elimination and engagement of
	3.8	2.2E-03		adaptive immunity.
			Metallothionein-2	No UniProtKB function listed
ENSECAG00000028889	3.6	3.3E-04	(PTHR23299:SF24)	
IFI44			Interferon-induced	
			protein 44	This protein aggregates to form
	3.6	1.2E-100	(PTHR14241:SF3)	microtubular structures.

Table 7. (Cont'd)

Symbol	Log2FoldChange	Padj	PANTHER family/subfamily	Function – UniProtKB (homo sapiens ortholog)			
	Upregulated genes						
			Interferon-induced protein with tetratricopeptide repeats 1B	No UniProtKB function listed			
ENSECAG00000033029	3.6	8.0E-15	(PTHR10271:SF16)				
HSD11B1	3.5	1.1E-11	Corticosteroid 11- Beta-dehydrogenase isozyme 1 (PTHR44279:SF1)	Catalyzes reversibly the conversion of cortisol to the inactive metabolite cortisone.			
			2'-5'-oligoadenylate synthase 1 (PTHR11258:SF13)	Interferon-induced, dsRNA- activated antiviral enzyme which plays a critical role in cellular innate antiviral response. In addition, it may also play a role in other cellular processes such as apoptosis, cell growth, differentiation and gene			
OAS1	3.5	5.4E-79		regulation.			
SERPING1	3.5	3.3E-13	Plasma protease C1 inhibitor (PTHR11461:SF159)	Activation of the C1 complex is under control of the C1-inhibitor.			
ENSECAG00000031838	3.5	7.1E-04	unknown	No UniProtKB function listed			
CCL8	3.5	1.0E-14	C-C Motif Chemokine 8 (PTHR12015:SF168)	Chemotactic factor that attracts monocytes, lymphocytes, basophils and eosinophils.			
OASL	3.4	6.1E-89	2'-5'-oligoadenylate synthase-like protein (PTHR11258:SF16)	Does not have 2'-5'-OAS activity, but can bind double-stranded RNA.			

Table 7. (Cont'd)

Symbol	Log2FoldChange	Padj	PANTHER family/subfamily	Function – UniProtKB (homo sapiens ortholog)			
	Upregulated genes						
MYO1D	3.4	5.1E-06	Unconventional myosin-ID (PTHR13140:SF417)	Unconventional myosin that functions as actin-based motor protein with ATPase activity.			
			Interferon-induced helicase C domain- containing protein 1 (PTHR14074:SF14)	Innate immune receptor which acts as a cytoplasmic sensor of viral nucleic acids and plays a major role in sensing viral infection and in the activation of a cascade of antiviral responses including the induction of type I interferons and			
IFIH1	3.3	2.2E-56		proinflammatory cytokines.			
ENSECAG00000035315	3.2	5.9E-05	Leukocyte immunoglobulin-like receptor subfamily B member 4 (PTHR11738:SF174)	No UniProtKB function listed			
			2'-5'-oligoadenylate synthase 3 (PTHR11258:SF4)	Interferon-induced, dsRNA- activated antiviral enzyme which plays a critical role in cellular innate antiviral response. In addition, it may also play a role in other cellular processes such as apoptosis, cell growth, differentiation and gene			
OAS3	3.2	1.2E-69		regulation.			

Table 7. (Cont'd)

Symbol	Log2FoldChange	Padj	PANTHER	Function – UniProtKB (homo			
			family/subfamily	sapiens ortholog)			
	Upregulated genes						
			Myelin protein P0	Is an adhesion molecule necessary			
			(PTHR13869:SF7)	for normal myelination in the			
				peripheral nervous system. It			
				mediates adhesion between adjacent			
				myelin wraps and ultimately drives			
MPZ	3.1	1.6E-03		myelin compaction			
			Interferon alpha-	Plays a role in apoptosis, negatively			
			inducible protein 6	regulating the intrinsinc apoptotic			
			(PTHR16932:SF25)	signaling pathway and TNFSF10-			
				induced apoptosis. However, it has			
				also been shown to have a pro-			
				apoptotic activity. Has an antiviral			
				activity towards hepatitis C			
				virus/HCV by inhibiting the EGFR			
				signaling pathway, which activation			
				is required for entry of the virus into			
IFI6	3.1	1.8E-70		cells.			
			Interferon regulatory	Key transcriptional regulator of type			
			factor 7	I interferon (IFN)-dependent			
			(PTHR11949:SF2)	immune responses and plays a			
				critical role in the innate immune			
				response against DNA and RNA			
IRF7	3.1	4.9E-12		viruses.			
ENSECAG00000012132			2'-5'-oligoadenylate	No UniProtKB function listed			
	_		synthase-like protein 2				
	3.1	2.0E-55	(PTHR11258:SF7)				

Table 7. (Cont'd)

Symbol	Log2FoldChange	Padj	PANTHER family/subfamily	Function – UniProtKB (homo sapiens ortholog)		
Upregulated genes Upregulated genes						
		o paragram	Interferon-induced	No UniProtKB function listed		
			protein with			
			tetratricopeptide			
			repeats 5			
ENSECAG00000032818	3.1	8.9E-49	(PTHR10271:SF28)			
RF01955	3.0	1.5E-02	Unknown	No UniProtKB function listed		
			Solute carrier family	No UniProtKB function listed		
			23 member 4			
ENSECAG00000017970	3.0	1.3E-04	(PTHR11119:SF22)			
			Protein-glutamine	Catalyzes the cross-linking of		
			gamma-	proteins, such as WDR54, and the		
			glutamyltransferase 2	conjugation of polyamines to		
TGM2	3.0	2.6E-18	(PTHR11590:SF6)	proteins.		
			E3 ubiquitin-protein	Interferon-induced antiviral protein		
			ligase TRIM22	involved in cell innate immunity.		
			(PTHR24103:SF650)	The antiviral activity could in part be		
				mediated by TRIM22-dependent		
TRIM22	3.0	2.0E-139		ubiquitination of viral proteins.		
			2'-5'-oligoadenylate	Interferon-induced, dsRNA-		
			synthase 2	activated antiviral enzyme which		
			(PTHR11258:SF3)	plays a critical role in cellular innate		
OAS2	3.0	6.5E-66		antiviral response.		

Table 7. (Cont'd)

Symbol	Log2FoldChange	Padj	PANTHER family/subfamily	Function – UniProtKB (homo			
Upregulated genes Sapiens ortholog							
		Opregulat	Interferon-induced	Interferon-induced RNA-binding			
			protein with	protein involved in the human innate			
			tetratricopeptide	immune response. Has a broad and			
			repeats 5	adaptable RNA structure recognition			
			(PTHR10271:SF28)	important for RNA recognition			
IFIT5	3.0	7.4E-09	(= ====================================	specificity in antiviral defense.			
			Excitatory amino acid	Sodium-dependent, high-affinity			
			transporter 1	amino acid transporter that mediates			
			(PTHR11958:SF24)	the uptake of L-glutamate and also			
SLC1A3	3.0	8.3E-06		L-aspartate and D-aspartate.			
		Downregula	ated genes				
			Protein FAM71A	No UniProtKB function listed			
FAM71A	-4.6	2.4E-08	(PTHR22574:SF15)				
			unknown	Fibronectins bind cell surfaces and			
				various compounds including			
				collagen, fibrin, heparin, DNA, and			
				actin. Fibronectins are involved in			
				cell adhesion, cell motility,			
				opsonization, wound healing, and			
FN1	-4.0	6.3E-19		maintenance of cell shape.			
			Beta-defensin 1	Has bactericidal activity.			
DEFB1	-3.3	1.7E-04	(PTHR21388:SF9)				

**Table 8. Average fraction of cell population fractions.** Cell population fractions for each sample was estimated using CIBERSORTx [177] and the reference gene signature "LM22" included with the software, which is based off of the transcriptome of human PBMC samples with pre-determined cell populations. Wilcoxon signed-rank test was performed. \* indicates  $p \le 0.1$  and \*\* indicates  $p \le 0.05$ .

Average fraction of cell populations						
	Pre-challenge (%	Post-challenge (%				
	of total cell	of total cell				
	population)	population)				
B cells naive	$42.07 \pm 0.02$	$39.89 \pm 0.01$				
B cells memory	$0.00 \pm 0.00$	$0.62 \pm 0.01$				
Plasma cells	$0.38 \pm 0.00$	$0.00 \pm 0.00*$				
T cells CD8	$2.37 \pm 0.00$	$0.46 \pm 0.00**$				
T cells CD4 naive	$5.52 \pm 0.02$	$6.95 \pm 0.02$				
T cells CD4 memory resting	$1.34 \pm 0.01$	$1.04 \pm 0.01$				
T cells CD4 memory activated	$5.55 \pm 0.01$	$3.28 \pm 0.01$				
T cells follicular helper	$17.75 \pm 0.02$	$16.69 \pm 0.01$				
T cells regulatory (Tregs)	$0.88 \pm 0.00$	$1.05 \pm 0.01$				
T cells gamma delta	$1.11 \pm 0.00$	$4.00 \pm 0.00**$				
NK cells resting	$2.32 \pm 0.01$	$1.32 \pm 0.01$				
NK cells activated	$0.18 \pm 0.00$	$0.51 \pm 0.00$				
Monocytes	$4.38 \pm 0.01$	$4.71 \pm 0.01$				
Macrophages M0	$1.49 \pm 0.00$	$0.00 \pm 0.00$ *				
Macrophages M1	$0.00 \pm 0.00$	$2.14 \pm 0.01*$				
Macrophages M2	$2.39 \pm 0.00$	$3.18 \pm 0.00$				
Dendritic cells resting	$0.00 \pm 0.00$	$0.66 \pm 0.00$				
Dendritic cells activated	$4.98 \pm 0.00$	$5.84 \pm 0.01$				
Mast cells resting	$0.00 \pm 0.00$	$0.64 \pm 0.01$				
Mast cells activated	$2.89 \pm 0.01$	$1.54 \pm 0.01$				
Eosinophils	$4.22 \pm 0.01$	$4.92 \pm 0.01$				
Neutrophils	$0.15 \pm 0.00$	$0.55 \pm 0.00$				

**Table 9. Mapping summary statistics for miRNA**. Total reads after sequencing and the number and percent that uniquely mapped to the combined genome consisting of horse (EquCab3.0), EHV-1 (NCBI RefSeq NC\_001491.2), EHV-2 (NCBI RefSeq NC\_001650.2), EHV-4 (NCBI RefSeq NC\_001844.1), and EHV-5 (NCBI RefSeq NC\_026421.1 genome are shown for each sample.

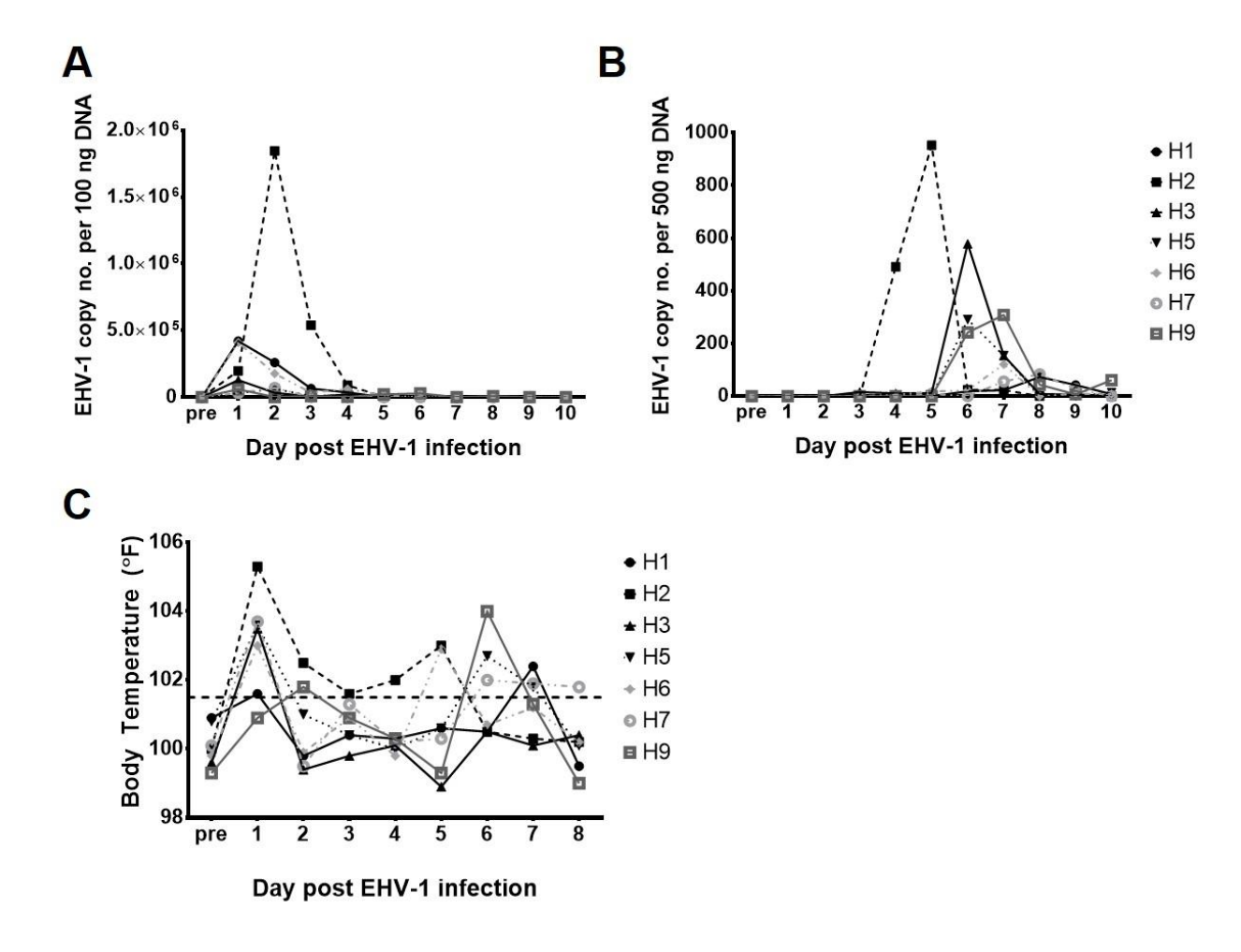
Table	Table 3. Mapping summary statistics for miRNA						
Sample ID	Total reads	Mapped reads (number of reads)	Mapped reads (%)				
H1_PRE	20352241	11692423	57.5				
H1_POST	23676872	13834897	58.4				
H2_PRE	20994711	10117799	48.2				
H2_POST	20255481	9999105	49.4				
H3_PRE	20651994	10458273	50.6				
H3_POST	19113616	9805906	51.3				
H5_PRE	20352426	9223249	45.3				
H5_POST	18477943	9073071	49.1				
H6_PRE	14388881	6751730	46.9				
H6_POST	12035002	6261094	52.0				
H7_PRE	17643353	8970565	50.8				
H7_POST	13916919	6010956	43.2				
H9_PRE	13712739	6613096	48.2				
H9_POST	18748418	8506104	45.4				
Average	18165757	9094162	49.7				

**Table 10. Differentially expressed miRNAs.** Differentially expressed (adjusted p value < 0.05 and log 2 fold change > |1| were determined for miRNAs. Upregulated refers to miRNAs upregulated during viremia compared to pre-challenge infection and downregulated refers to miRNAs downregulated during viremia compared to pre-challenge infection.

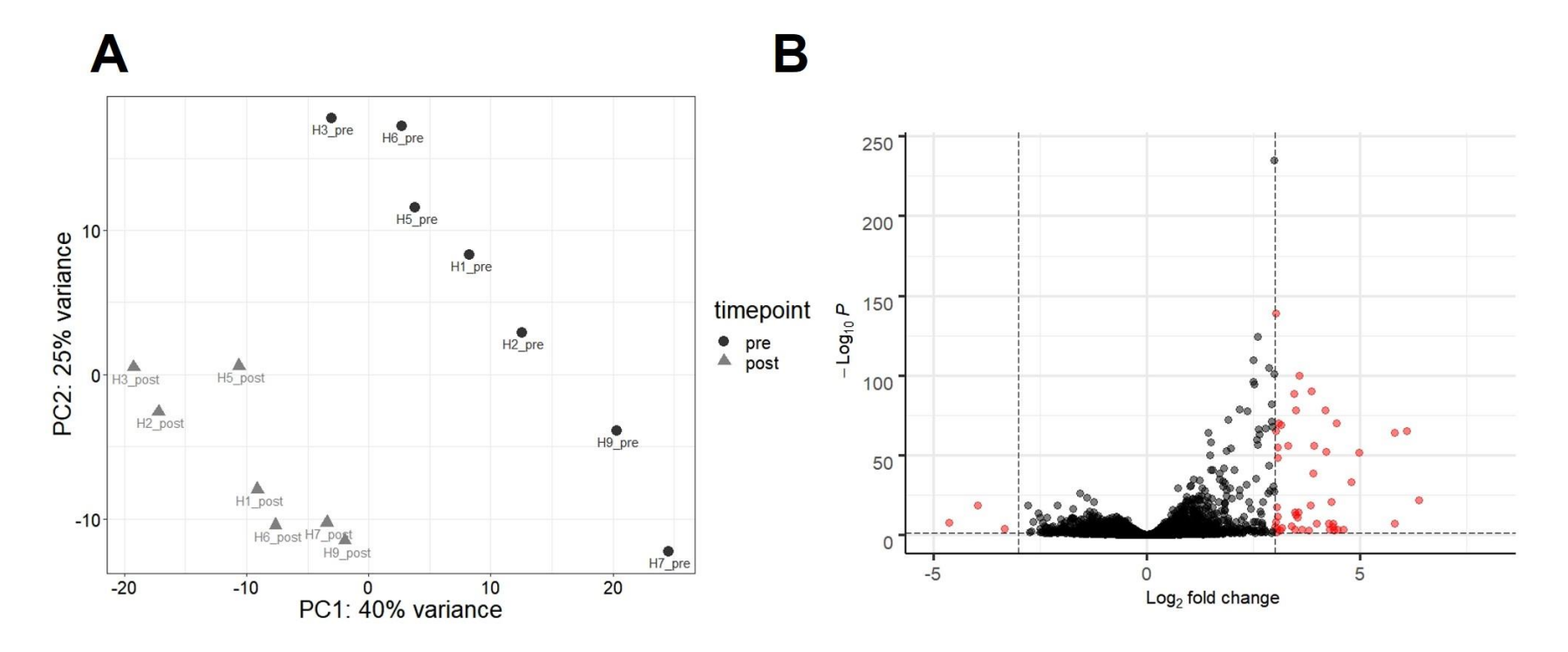
Differentially expressed miRNAs						
	log2 Fold		mirBase	Human		
ID	Change	padj	ID	ortholog	mature sequence	precursor sequence
				Upregi	ulated miRNAs	-
						GAGTGGCTGGGCTCAGCAGGGC
						GGAGGGTC
						AGGAGGTGAGCTTGGCTG
Equine_chr11_		3.5E	eca-miR-		CTGACCTGAGGCCTCT	ACCTGAGG
2567	1.2	-08	9104		GCTGCA	CCTCTGCTGCA
						CAACCCTAGGAGAGGGTGCCAT
						TCACATAGA
Equine_chrX_		1.3E	eca-miR-	hsa-miR-	AATGGCGCCACTAGG	CTATAATTGAATGGCGCCACTAG
44985	1.1	-17	652	652-3p	GTTG	GGTTG
						TCTGTCAACCATCCAGCTGTTTG
						GGGTGATG
Equine_chrX_		2.0E	eca-miR-		TCTGTCAACCATCCAG	CAAACAACATCTAGTTGGTTGA
45803	1.1	-03	2483		CTGTTT	GAGAAT

Table 10. (Cont'd)

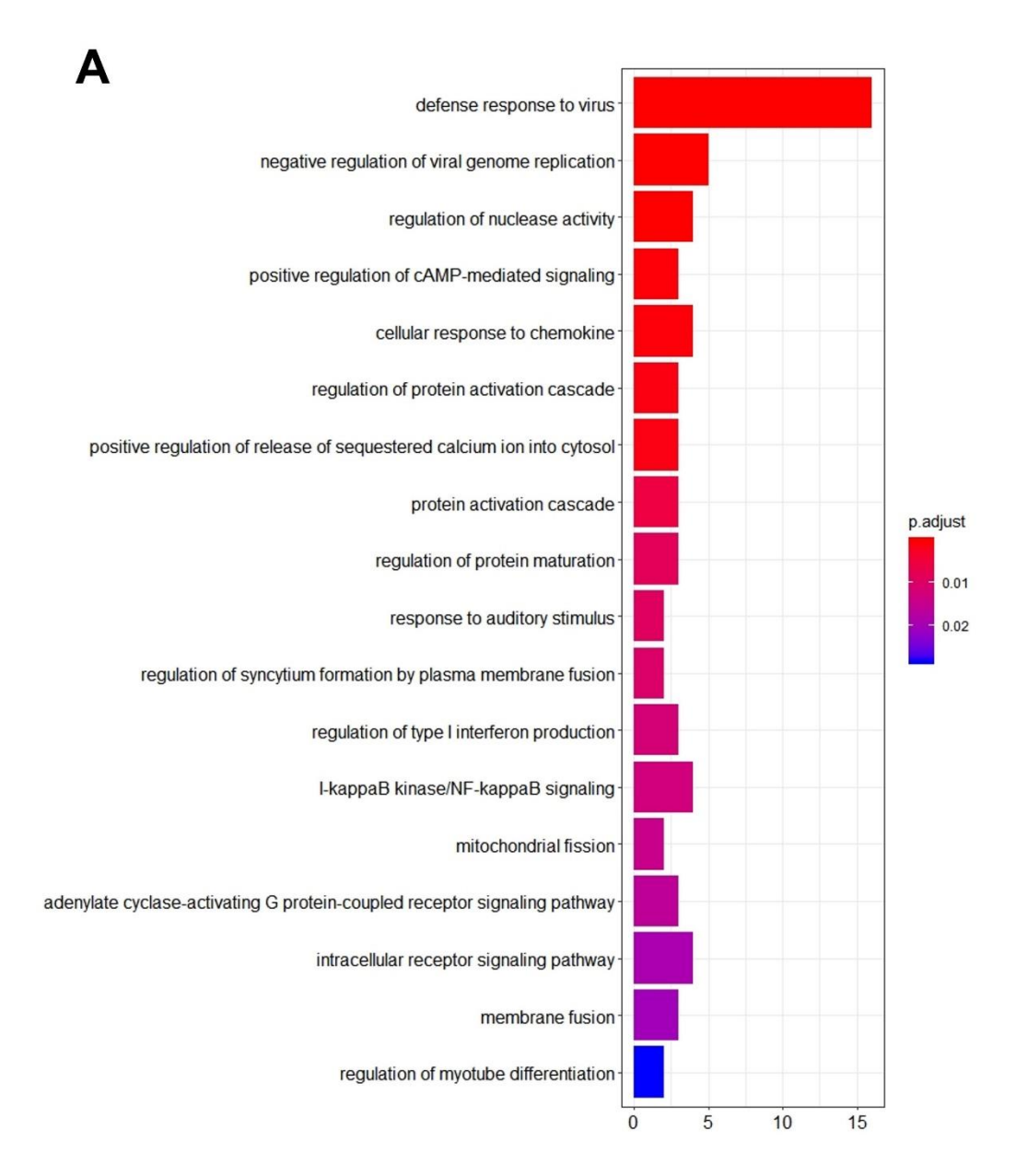
Differentially expressed miRNAs						
	log2					
	Fold		mirBase	Human		
ID	Change	padj	ID	ortholog	mature sequence	precursor sequence
				Downre	gulated miRNAs	
						ACCTGGGGATCTGAGGAGGCCC
						TTCCAGCCC
						CAAGGCTGGGAATGCTCCTGGTC
Equine_chr15_		1.4E		hsa-miR-	ACCTGGGGATCTGAG	CCCTTTCTT
10631	-1	-02	ī	6852-5p	GAG	GC
						TATGATAGTCCATACCCTTAAGT
						TTGATAAGTA
		1.0E			TATGATAGTCCATACC	AAAAATTTAAGTACGTGGACTGT
EHV-2_38	-1	-02	-		CTTAAGT	CAACA



**Figure 15. Clinical and virological disease post EHV-1 challenge.** (A) EHV-1 nasal shedding. Data is expressed as EHV-1 copy number per 100 ng template DNA as determined by qPCR. (B) Viremia. Data is expressed as EHV-1 copy number per 500 ng template DNA as determined by qPCR. (C) Body temperature. Fever is any body temperature over 101.5 °F, which is indicated by the horizontal dashed line.

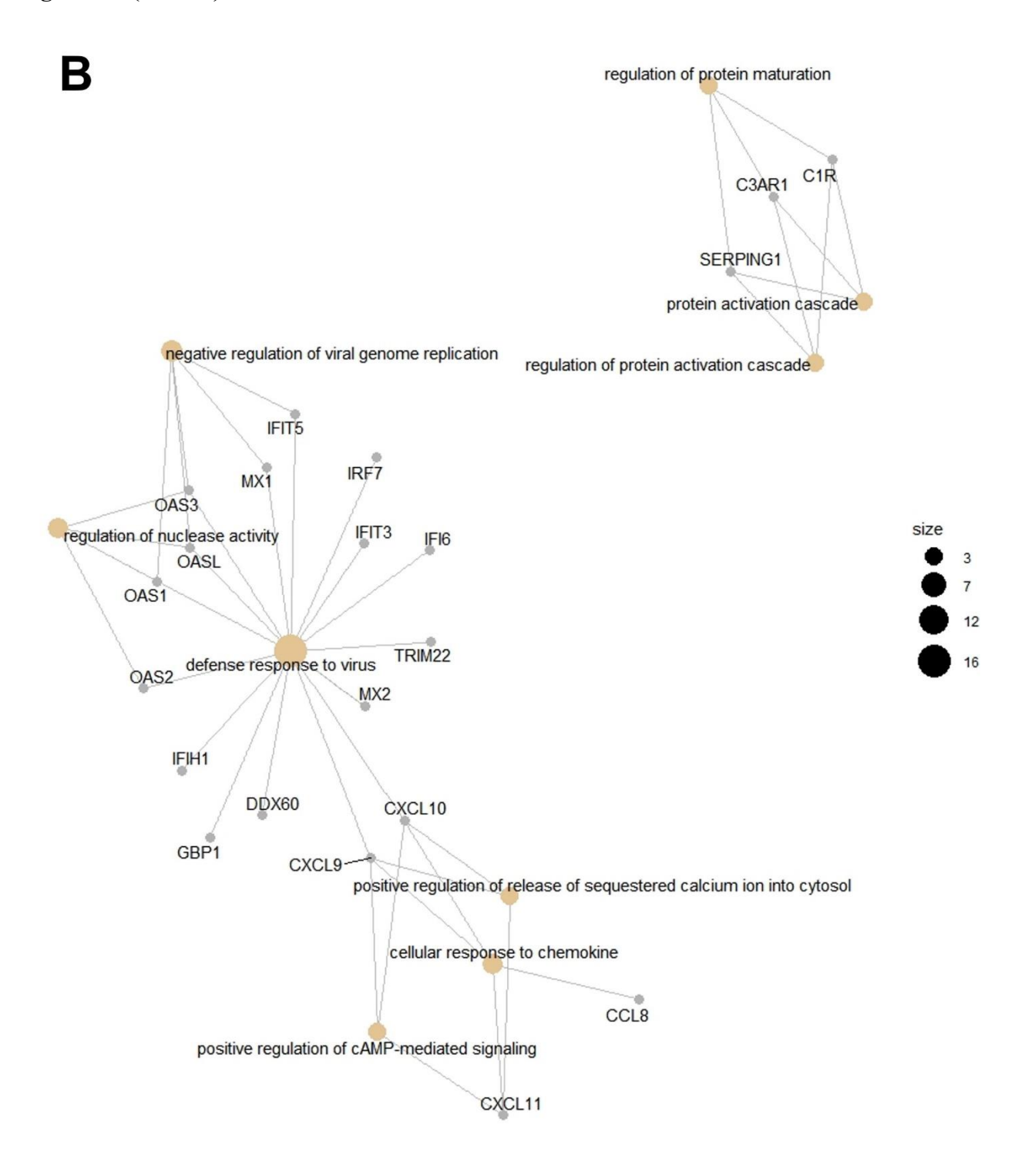


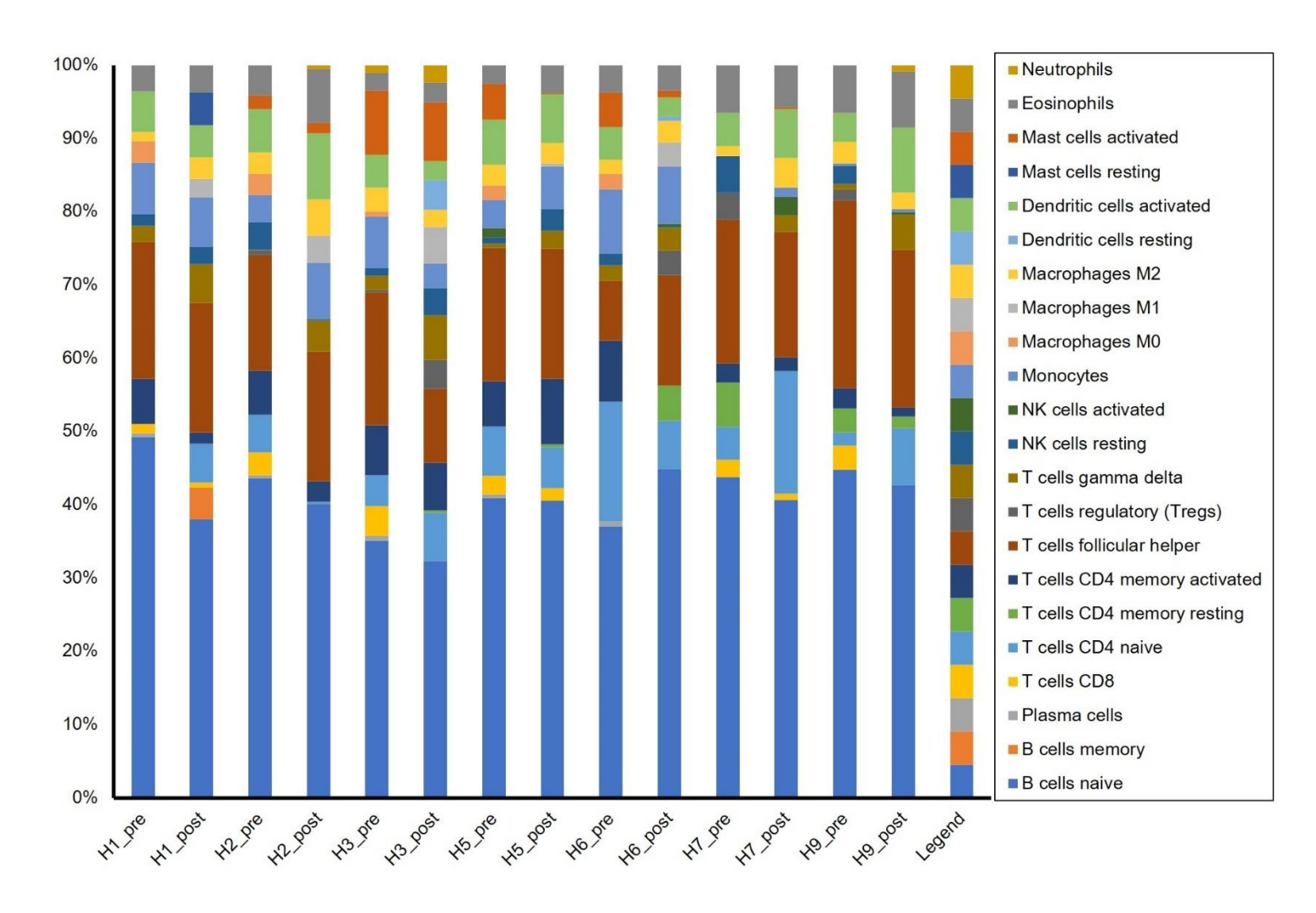
**Figure 16. Principal component analysis and differentially expressed genes.** (A) Principal component analysis. Samples from horses pre-infection (gray) cluster separately from samples during viremia (black). (B) Differentially expressed genes in horses pre-infection vs. post-infection. Genes with positive Log2 fold change (x-axis) indicate genes upregulated in PBMCs during EHV-1 infection compared to pre-infection while negative Log2 fold change values indicate genes downregulated in PBMCs during infection. P values are expressed on the y-axis, with more significantly differentially expressed genes towards the top of the plot. Genes highlighted in red passed the threshold of significance set at adjusted p-value < 0.05 and Log2 fold change > |3|.



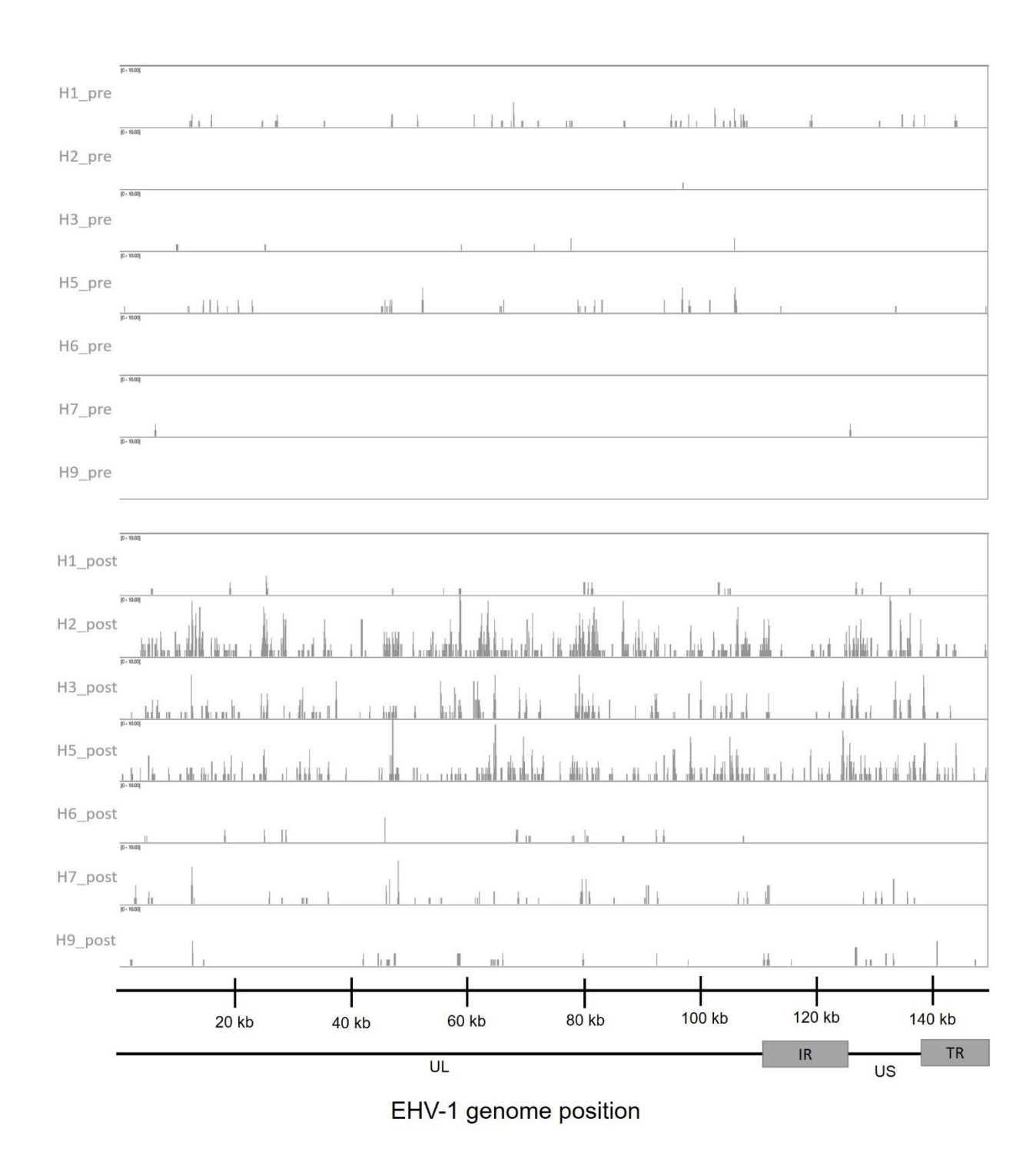
**Figure 17. Gene ontology enrichment results.** (A) GO terms for biological processes overrepresented in horses during EHV-1 infection. GO term enrichment analysis was performed using the enrichgo function of the clusterprofiler package in R. The resulting terms were filtered for redundancy using REVIGO. The 18 non-redundant enriched GO terms are visualized here. The most significantly enriched terms are at the top and listed in decreasing significance (increasing p.adjust). The number of genes from our gene list are indicated on the x-axis. (B) Net plot of the most significantly enriched GO terms and associated genes. The ten non-redundant GO terms with the lowest p.adjust values are listed here with the associated genes from our gene list. Tan nodes represent the GO term and gray nodes represent genes. The size of the GO term nodes indicate the number of genes from our list associated with that term. The biological processes and the associated genes cluster based on similarity.

Figure 17. (Cont'd)





**Figure 18. Cell population fractions in PBMC samples.** Cell population fractions for each sample was estimated using CIBERSORTx and the reference gene signature "LM22" included with the software, which is based off of the transcriptome of human PBMC samples with pre-determined cell populations. Twenty-two cell subpopulations are represented by different colors. Fractions are expressed as percent of the total population (y-axis) for each sample (x-axis).



**Figure 19. Read coverage plot of the EHV-1 genome.** The top 7 tracks are the pre-infection samples, and the bottom 7 tracks are post infection samples. Reads were aligned to EHV-1 strain Ab4 genome (NCBI RefSeq NC\_001491.2). UL = unique long region, IR = internal repeat region, US = unique small region, and TR = terminal repeat region as described in [143].

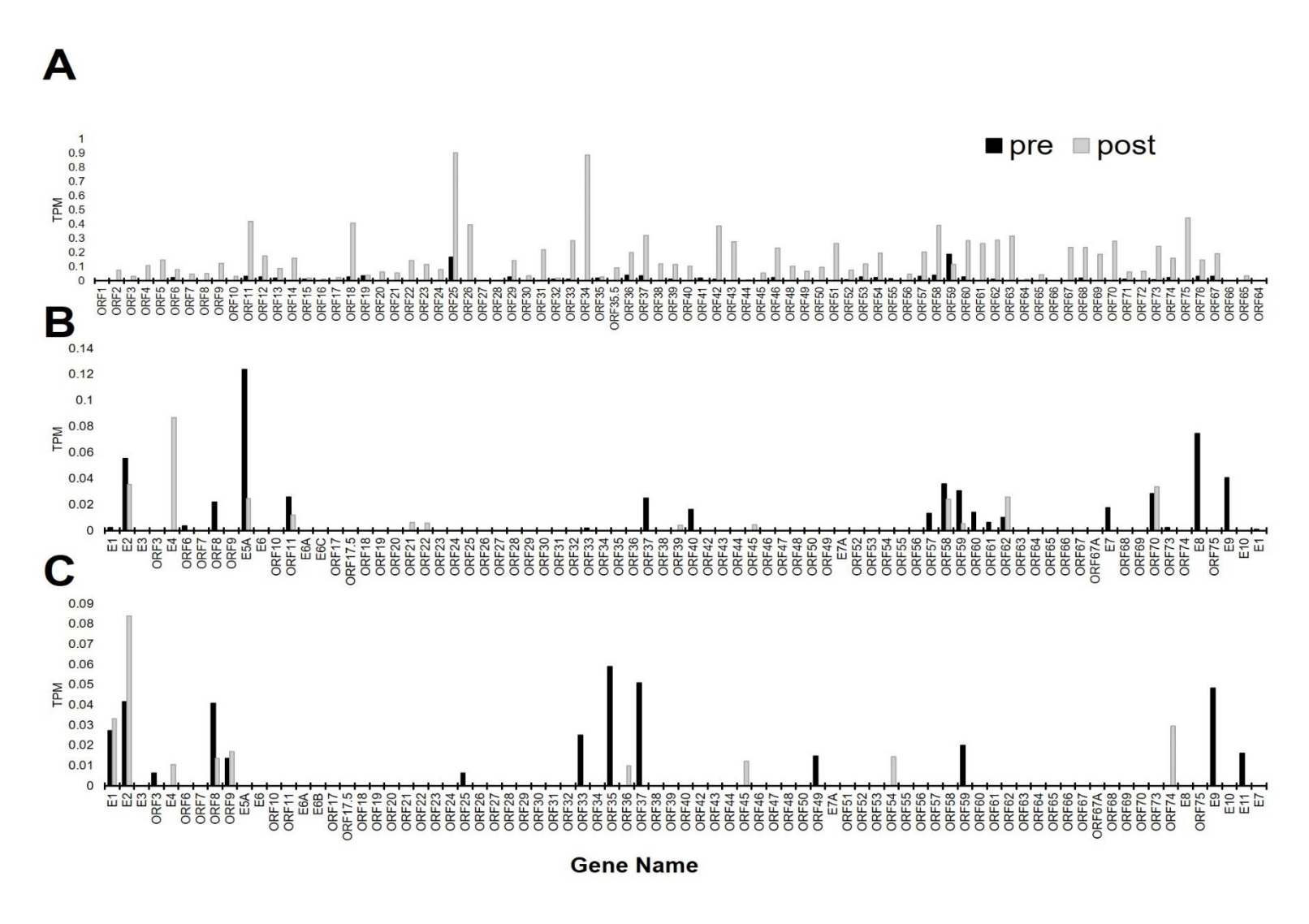


**Figure 20. Normalized counts of viral genes.** Data represents the average transcripts per million (TPM) of EHV-1 (A), EHV-2 (B), and EHV-5 (C). The gray line is pre-EHV-1 challenge infection and the black line is post EHV-1 challenge.

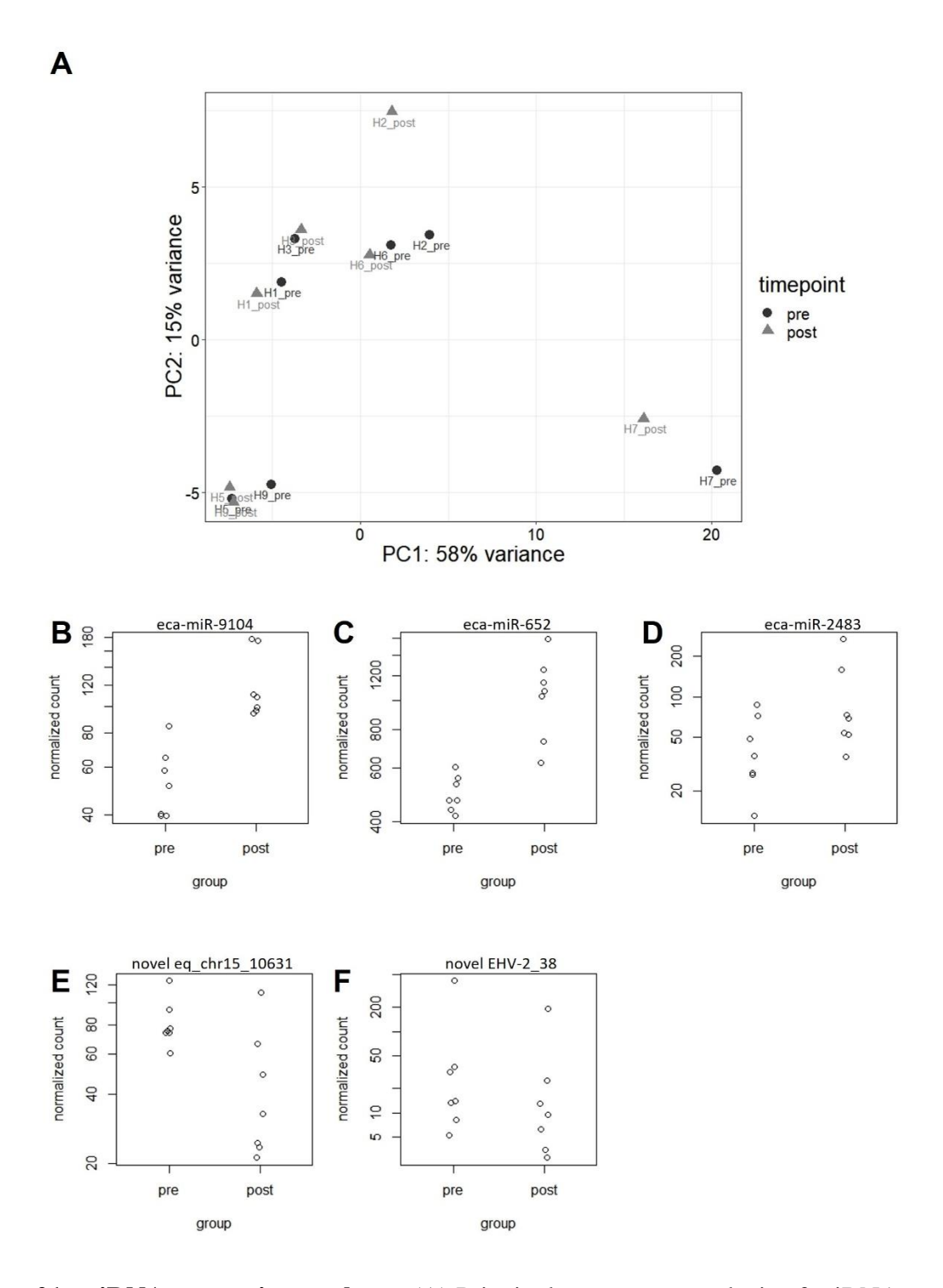


**Figure 21. miRNA expression analyses.** (A) Principal component analysis of miRNA samples. Samples cluster based on horse rather than from infection status (pre-infection (gray) vs. during infection (black). Normalized read counts of differentially expressed miRNAs.

**Figure 21 (Cont'd)** (B) eq\_chr11\_2567 identified with *eca-miR-9104* (C) eq\_chrx\_44985 identified with *eca-miR-652* and the human ortholog *hsa-miR-652-3p* (D) eq\_chrx\_45803 identified with *eca-miR-2483* (E) eq\_chr15\_10631 identified with the human ortholog *hsa-miR-6852-5p* (F) EHV-2\_38 which aligned to the EHV-2 viral genome. Details regarding these miRNAs can be found in Table 10.

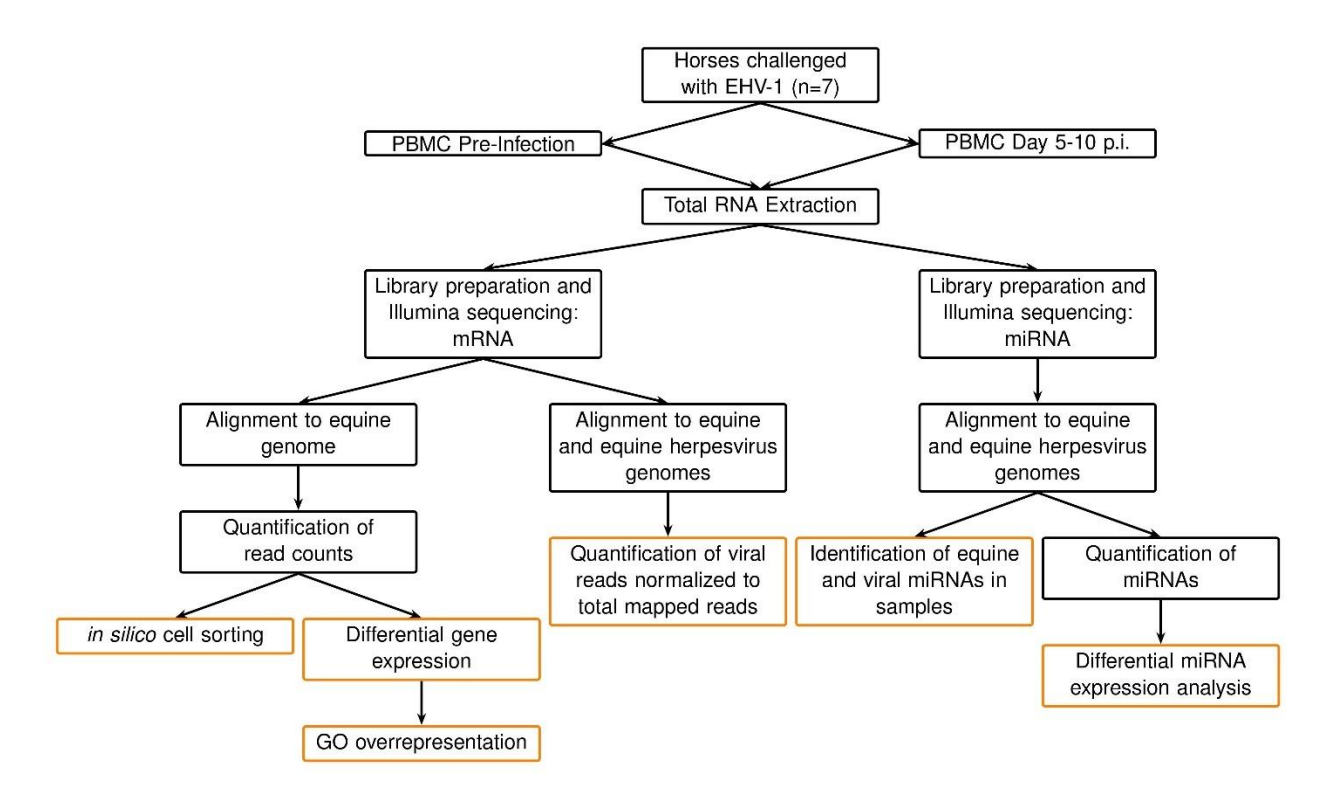


**Figure 22. Summary of data analysis.** RNA was extracted from PBMCs from horses prior to and during EHV-1 challenge infection. Total RNA was processed with next generation RNA sequencing for mRNA and miRNA. Black boxes represent upstream data analysis processes, while the red boxes represent processes that resulted in output reported in the results.

**Table 11. Mapping summary statistics of mRNA sequencing.** Total reads after sequencing and the number and percent that uniquely mapped to the EquCab3.0 genome are shown for each sample.

Mapping summary statistics							
Sample ID	Total reads	Uniquely mapped (number of	Uniquely mapped				
_		reads)	(%)				
EHM_PRE_H1	44184310	37923518	85.8				
EHM_POST_H1	40599945	34218921	84.3				
EHM_PRE_H2	40137880	34895454	86.9				
EHM_POST_H2	47149254	39078943	82.9				
EHM_PRE_H3	45889974	39613428	86.3				
EHM_POST_H3	39483290	32787239	83.0				
EHM_PRE_H4	47767833	41484855	86.9				
EHM_POST_H4	38260560	31521306	82.4				
EHM_PRE_H5	49226922	42871550	87.0				
EHM_POST_H5	40912839	34362844	84.0				
EHM_PRE_H7	38847518	33686604	86.7				
EHM_POST_H7	38231216	32466324	84.9				
EHM_PRE_H9	35120357	30748238	87.6				
EHM_POST_H9	42198521	35572673	84.3				
EHM_PRE_H15	47675687	40789167	85.6				
EHM_POST_H15	39075706	32534599	83.3				
CONT_PRE_H16	49819781	42630558	85.6				
CONT_POST_H16	39358775	32872086	83.5				
CONT_PRE_H26	51958124	44491095	85.6				
CONT_POST_H26	53090751	45842652	86.4				
CONT_PRE_H27	48454087	41617390	85.9				
CONT_POST_H27	38965552	31684566	81.3				
CONT_PRE_H28	44791662	38284817	85.5				
CONT_POST_H28	43886029	37670974	85.8				
CONT_PRE_H34	53040512	45283021	85.4				
CONT_POST_H34	38011582	32238800	84.8				
CONT_PRE_H35	48119400	41310875	85.9				
CONT_POST_H35	40193344	35081080	87.3				
Average	43730408	37270128	85.2				

**Table 12. Enriched GO terms for contrast comparison between group comparison between EHM and Non-EHM horses.** GO term enrichment was performed on the up and down regulated gene lists generated from the between group (contrast) comparison. Upregulated terms are those based on the genes upregulated in EHM horses compared to Non-EHM horses. Downregulated terms are those based on the genes downregulated in EHM horses compared to Non-EHM horses.

ID	Description	Gene Ratio	Bg Ratio	pvalue	p.adjust	qvalue	Gene ID	Gene Count				
	Upregulated											
GO:0006885	regulation of pH	3/21	73/13991	0.00016	0.00964	0.00702	NOX1/SLC9B1/SLC4 A9	3				
GO:0002830	positive regulation of type 2 immune response	2/21	14/13991	0.00019	0.00964	0.00702	RSAD2/IL6	2				
GO:0001819	positive regulation of cytokine production	5/21	368/13991	0.00017	0.00964	0.00702	NOX1/RSAD2/IL1RL 1/IL6/LPL	5				
GO:0048661	positive regulation of smooth muscle cell proliferation	3/21	83/13991	0.00024	0.01082	0.00789	NOX1/TGM2/IL6	3				
GO:0010883	regulation of lipid storage	2/21	41/13991	0.00169	0.03597	0.02622	IL6/LPL	2				
		D	ownregulate	d								
							DAPK2/CCL5/CX3CR 1/CD244/KLRK1/ MMP9/TBX21/PLCB1 /DUSP1/SLC7A11/ NLRP12/PDGFB/TRE					
GO:0050900	leukocyte migration	13/106	349/13991	2.28E-06	0.00596	0.00521	M1 CCL5/FGFR1/INSR/J UN/DUSP1/ATF3/ EPHA4/DUSP6/NLRP	13				
GO:0070372 GO:0007611	regulation of ERK1 and ERK2 cascade learning or memory	9/106	278/13991	8.18E-06 6.39E-05	0.01070	0.00936	12/PDGFB/KLF4 CX3CR1/FOS/PLK2/P LCB1/MAP1A/ INSR/JUN/EGR2/SLC 7A11	9				
GO:0007011	cellular response to cadmium ion	4/106	25/13991	3.48E-05	0.02237	0.01956	MMP9/FOS/JUN/GSN	4				
GO:0033002	muscle cell proliferation	8/106	187/13991	8.66E-05	0.02266	0.01982	CCL5/MMP9/FGFR1/ ABCC4/IFNG/ JUN/PDGFB/KLF4	8				

Table 12. (Cont'd)

								Gene			
ID	Description	Gene Ratio	Bg Ratio	pvalue	p.adjust	qvalue	Gene ID	Count			
	Downregulated										
	reactive nitrogen species metabolic						CX3CR1/KLRK1/INS				
GO:2001057	process	5/106	68/13991	0.00016	0.02324	0.02032	R/IFNG/KLF4	5			
							CX3CR1/KLRK1/INS				
GO:0046209	nitric oxide metabolic process	5/106	67/13991	0.00015	0.02324	0.02032	R/IFNG/KLF4	5			
							BAMBI/MMP9/PLK2/				
							IFNG/EPHA4/				
GO:0051099	positive regulation of binding	7/106	166/13991	0.00026	0.0278	0.02431	KLF4/DACT1	7			
							DAPK2/PTK6/FGFR1/				
							INSR/JUN/				
							EPHA4/NLRP12/PDG				
GO:0046777	protein autophosphorylation	8/106	220/13991	0.00026	0.0278	0.02431	FB	8			
	pri-miRNA transcription by RNA						FOS/JUN/PDGFB/KL				
GO:0061614	polymerase II	4/106	42/13991	0.00027	0.02811	0.02458	F4	4			
							SCD/LIPE/CD244/FG				
							FR1/ACER2/				
							NUDT4/PLCB1/IFNG/				
GO:0006066	alcohol metabolic process	9/106	302/13991	0.00047	0.03531	0.03088	APOBR	9			
							CX3CR1/KLRK1/INS				
GO:0042136	neurotransmitter biosynthetic process	5/106	90/13991	0.00059	0.03732	0.03264	R/IFNG/KLF4	5			

**Table 13. Enriched GO terms based on differentially expressed genes in EHM horses.** GO term enrichment was performed on the gene list of within group up and downregulated genes unique to EHM horses.

ID	Description	Gene Ratio	Bg Ratio	pvalue	p.adjust	qvalue	geneID	Count
				Upr	egulated			
GO:0051607	defense response to virus	13/92	175/13 991	1.1E-10	2.1E-07	1.8E-07	EIF2AK2/TRIM56/ADAR/CXCL10/ IRF9/RTP4/ISG15/AIM2/IRF7/TLR3/ IL6/ISG20/IL15	13
GO:0032479	regulation of type I interferon production	8/92	104/13 991	3.9E-07	1.3E-04	1.1E-04	TRIM56/UBA7/NMI/ISG15/IRF7/ ACOD1/TLR3/ZBP1	8
GO:0042107	cytokine metabolic process	7/92	101/13 991	4.4E-06	6.8E-04	5.9E-04	LAG3/NMI/IGF2BP3/IRF7/TLR3/ IL6/CYBB	7
GO:0043900	regulation of multi- organism process	11/92	313/13 991	6.3E-06	9.0E-04	7.9E-04	EIF2AK2/ADAR/PPID/ISG15/ CD180/AIM2/ACOD1/ISG20/ IL15/SLPI/TIMP1	11
GO:0048771	tissue remodeling	7/92	150/13 991	5.8E-05	4.5E-03	3.9E-03	TGM2/CD38/SNX10/IL6/IL15/ VDR/TIMP1	7
GO:0032570	response to progesterone	4/92	38/139 91	1.1E-04	6.7E-03	5.9E-03	CD38/ACOD1/NR1H3/RAMP2	4
GO:0010883	regulation of lipid storage	4/92	41/139 91	1.5E-04	7.9E-03	6.9E-03	IL6/LPL/NR1H3/MSR1	4
GO:0015012	heparan sulfate proteoglycan biosynthetic process	3/92	23/139 91	4.4E-04	1.8E-02	1.6E-02	EXT1/TCF7L2/EXTL2	3
GO:0010743	regulation of macrophage derived foam cell differentiation	3/92	25/139 91	5.7E-04	2.1E-02	1.9E-02	LPL/NR1H3/MSR1	3
GO:0070661	leukocyte proliferation	7/92	231/13 991	8.1E-04	2.6E-02	2.2E-02	TNFSF13B/CD38/CD180/IL6/GAPT/ IL15/CCL8	7
GO:0090077	foam cell differentiation	3/92	30/139 91	9.8E-04	2.8E-02	2.4E-02	LPL/NR1H3/MSR1	3
GO:0097050	type B pancreatic cell apoptotic process	2/92	10/139 91	1.9E-03	4.7E-02	4.1E-02	IL6/TCF7L2	2

Table 13. (Cont'd)

ID	Description	Gene Ratio	Bg Ratio	pvalue	p.adjust	qvalue	geneID	Count					
Downregulated													
GO:0030335	positive regulation of cell migration	20/18	441/13 991	1.1E-06	8.4E-04	7.6E-04	DAPK2/MMP9/DOCK5/FGFR1/CASS4/ CCL5/FN1/HSPA5/THBS1/JUN/INSR/ ADAM8/PDGFB/PDGFD/SEMA6C/ SEMA4C/TNFSF14/GATA2/RHOB/ GPNMB	20					
GO:0031952	regulation of protein autophosphorylation	6/181	43/139 91	1.8E-05	8.9E-03	8.0E-03	NLRP12/JUN/PDGFB/PDGFD/ERRFI1/ GPNMB	6					
GO:0046777	protein autophosphorylation	12/18 1	220/13 991	2.9E-05	1.3E-02	1.1E-02	DAPK2/PTK6/FGFR1/NLRP12/JUN/ INSR/PDGFB/PDGFD/ERRFI1/INSRR/ BMX/GPNMB	12					
GO:0070371	ERK1 and ERK2 cascade	13/18	292/13 991	1.1E-04	3.0E-02	2.7E-02	FGFR1/CCL5/FN1/NLRP12/FBLN1/ JUN/INSR/PDGFB/PDGFD/ERRFI1/ INSRR/ ZFP36L2/GPNMB	13					
GO:0032103	positive regulation of response to external stimulus	12/18 1	260/13 991	1.5E-04	3.6E-02	3.3E-02	DAPK2/FGFR1/CCL5/FAM19A3/ NLRP12/THBS1/MAPK13/ADAM8/ PDGFB/PDGFD/NPY/TNFSF14	12					
GO:0010035	response to inorganic substance	17/18 1	491/13 991	2.2E-04	4.6E-02	4.2E-02	EEF1A2/MMP9/HSPA5/THBS1/ MAPK13/JUN/SELENOP/PDGFD/ PTCH1/GSN/FOSB/FOS/SLC40A1/ CHP2/JUND/RHOB/IL1A	17					
GO:0071248	cellular response to metal ion	9/181	161/13 991	2.5E-04	4.6E-02	4.2E-02	MMP9/HSPA5/JUN/GSN/FOSB/FOS/ SLC40A1/CHP2/JUND	9					

**Table 14. Differentially expressed genes unique to non-EHM horses.** Differentially expressed genes (adjusted p value < 0.05 and log 2 fold change > |1|) are displayed here. Upregulated refers to genes upregulated during viremia compared to pre-challenge, and downregulated refers to genes downregulated during viremia compared to pre-challenge. The PANTHER family and subfamily category is listed for the equine gene [276] and the UniProtKB function for the protein associated with the orthologous human gene is shown [277].

	Log fold		PANTHER	
Symbol	change	FDR	family/subfamily	Function - UniProtKB (homo sapiens ortholog)
			Upregulated genes	
				Required for the correct formation of lens intermediate
		1.5E-03	Phakinin	filaments as part of a complex composed of BFSP1, BFSP2
BFSP2	2.2		(PTHR23239:SF32)	and CRYAA
			Transcription factor NF-E2	
		1.5E-02	45 KDA subunit	Component of the NF-E2 complex essential for regulating
NFE2	2.0		(PTHR24411:SF26)	erythroid and megakaryocytic maturation and differentiation.
			C-type lectin domain	
		3.8E-02	family 4 member M	
ENSECAG00000021212	1.6		(PTHR22802:SF197)	Human ortholog unavailable
				Transcriptional repressor which binds preferentially to the
			Hairy/enhancer-of-split	canonical E box sequence 5'-CACGTG-3' Downstream
			related with YRPW motif	effector of Notch signaling required for cardiovascular
		3.0E-03	protein 1	development. Specifically required for the Notch-induced
HEY1	1.5		(PTHR10985:SF78)	endocardial epithelial to mesenchymal transition
			Cartilage intermediate layer	
		4.6E-02	protein 1	Probably plays a role in cartilage scaffolding. May act by
CILP	1.4		(PTHR15031:SF3)	antagonizing TGF-beta1 (TGFB1) and IGF1 functions.
				Stearyl-CoA desaturase that utilizes O <sub>2</sub> and electrons from
				reduced cytochrome b5 to introduce the first double bond into
		6.1E-12	Acyl-CoA desaturase	saturated fatty acyl-CoA substrates. Plays an important role in
SCD	1.4		(PTHR11351:SF73)	body energy homeostasis.
				SOCS family proteins form part of a classical negative
				feedback system that regulates cytokine signal transduction.
				CIS is involved in the negative regulation of cytokines that
				signal through the JAK-STAT5 pathway such as
		2 27 62	Cytokine-inducible SH2-	erythropoietin, prolactin and interleukin 3 (IL3) receptor.
		2.2E-03	containing protein	Inhibits STAT5 trans-activation by suppressing its tyrosine
CISH	1.4		(PTHR10155:SF9)	phosphorylation.

 ${\bf Table~14.~Differentially~expressed~genes~unique~to~non-EHM~horses.}$ 

	Log fold	FDR	PANTHER	
Symbol	change		family/subfamily	Function - UniProtKB (homo sapiens ortholog)
			<b>Upregulated genes</b>	
				Participates in the Wnt signaling pathway. Binds to DNA and
		1.8E-02	Transcription factor 7-like	acts as a repressor in the absence of CTNNB1, and as an
TCF7L1	1.3		1 (PTHR10373:SF25)	activator in its presence.
			Carcinoembryonic antigen-	
			related cell adhesion	
		8.5E-04	molecule 1	
ENSECAG00000009762	1.3		(PTHR44427:SF1)	No human ortholog available
				Inactivates MAP kinases. Has a specificity for the ERK family
			Dual specificity protein	Promotes cell differentiation by regulating MAPK1/MAPK3
		1.4E-02	phosphatase 6	activity and regulating the expression of AP1 transcription
DUSP6	1.3		(PTHR10159:SF45)	factors
		8.6E-03	Protein FAM111B	
FAM111B	1.2		(PTHR14389:SF4)	No function listed
		1.7E-02	C-type lectin-like domain	
ENSECAG00000022644	1.1		family 1 (PTHR46746:SF4)	No human ortholog available
			FERM domain-containing	Scaffolding protein that regulates epithelial cell polarity by
		1.1E-02	protein 4A	connecting ARF6 activation with the PAR3 complex. Plays a
FRMD4A	1.1		(PTHR46079:SF3)	redundant role with FRMD4B in epithelial polarization.
		1.8E-04	Apolipoprotein L2	
ENSECAG00000019430	1.1		(PTHR14096:SF27)	No human ortholog available.
				Involved in the regulation of cell growth. May stabilize the
			Zipper putative tumor	active CDC2-cyclin B1 complex and thereby contribute to the
		4.1E-02	suppressor 1-related	regulation of the cell cycle and the prevention of uncontrolled
LZTS1	1.1		(PTHR19354:SF5)	cell proliferation.
		1.3E-02	Protein SHISA-5	Can induce apoptosis in a caspase-dependent manner and
SHISA5	1.0		(PTHR31395:SF14)	plays a role in p53/TP53-dependent apoptosis.

Table 14. (Cont'd)

	Log fold	FDR	PANTHER	
Symbol	change		family/subfamily	Function - UniProtKB (homo sapiens ortholog)
			Downregulated genes	
				Shared alpha chain of the active heterodimeric glycoprotein
				hormones thyrotropin/thyroid stimulating hormone/TSH,
				lutropin/luteinizing hormone/LH, follitropin/follicle
			Glycoprotein hormones	stimulating hormone/FSH and choriogonadotropin/CG. These
		2.8E-05	alpha chain	hormones bind specific receptors on target cells that in turn
CGA	-1.2		(PTHR11509:SF0)	activate downstream signaling pathways.
				Isoform 1 acts as a RAB27A effector protein and plays a role
		2.2E-03	Synaptotagmin-like protein	in cytotoxic granule exocytosis in lymphocytes. It is required
SYTL2	-1.0		2 (PTHR45716:SF5)	for cytotoxic granule docking at the immunologic synapse.
				Transcriptional coactivator which acts as a downstream
				regulatory target in the Hippo signaling pathway that plays a
			WW domain-containing	pivotal role in organ size control and tumor suppression by
			transcription regulator	restricting proliferation and promoting apoptosis. Regulates
		7.0E-03	protein 1	embryonic stem-cell self-renewal, promotes cell proliferation
WWTR1	-1.0		(PTHR17616:SF6)	and epithelial-mesenchymal transition.

Table 15. Average fractions of cell populations in PBMCs. Cell population fractions for each sample was estimated using CIBERSORTx [177] and the reference gene signature "LM22" included with the software, which is based off of the transcriptome of human PBMC samples with pre-determined cell populations. Wilcox signed-rank test was performed on the paired samples for each group \* indicates a significant difference at  $p \le 0.1$ , and \*\* indicates  $p \le 0.05$  in cell fraction between pre and post challenge samples for each group (EHM and non-EHM).

group (Errivi and non Errivi).	EHM pre-challenge (% of total cell population)	EHM post-challenge (% of total cell population)	Non-EHM pre- challenge (% of total cell population)	Non-EHM post- challenge (% of total cell population)
B cells naive	$23.03 \pm 1.84$	$24.75 \pm 3.23$	$37.03 \pm 1.53$	32.55 ± 1.14 **
B cells memory	$0.60 \pm 0.60$	$0.41 \pm 0.41$	$0.03 \pm 0.03$	$0.00 \pm 0.00$
Plasma cells	$0.27 \pm 0.12$	$0.46 \pm 0.29$	$0.28 \pm 0.15$	0.74 ± 0.06 *
T cells CD8	$7.92 \pm 1.56$	2.36 ± 1.59 *	$2.18 \pm 0.79$	$2.21 \pm 1.03$
T cells CD4 naive	$1.64 \pm 0.66$	$4.60 \pm 2.05$	$6.21 \pm 2.25$	$10.26 \pm 1.62$
T cells CD4 memory resting	$0.77 \pm 0.55$	$1.34 \pm 0.77$	$0.02 \pm 0.02$	$0.00 \pm 0.00$
T cells CD4 memory activated	$7.88 \pm 0.86$	$9.55 \pm 1.62$	$0.55 \pm 0.26$	1.71 ± 0.52 *
T cells follicular helper	$16.62 \pm 1.58$	$14.86 \pm 1.84$	$23.27 \pm 0.80$	19.43 ± 1.44 *
T cells regulatory (Tregs)	$1.82 \pm 0.62$	0.16 ± 0.16 **	$1.48 \pm 0.49$	$0.41 \pm 0.41$
T cells gamma delta	$0.88 \pm 0.33$	2.84 ± 0.66 *	$0.79 \pm 0.32$	2.67 ± 0.82 *
NK cells resting	$6.43 \pm 1.10$	2.75 ± 1.08 **	$2.24 \pm 0.82$	$0.86 \pm 0.35$
NK cells activated	$0.13 \pm 0.13$	$0.34 \pm 0.22$	$0.63 \pm 0.42$	$0.53 \pm 0.26$
Monocytes	$12.71 \pm 2.75$	$13.85 \pm 3.72$	$7.27 \pm 0.57$	$11.85 \pm 2.22$
Macrophages M0	$2.99 \pm 0.91$	0.00 ± 0.00 **	$1.77 \pm 1.01$	$0.15 \pm 0.15$
Macrophages M1	$0.00 \pm 0.00$	0.98 ± 0.30 **	$0.00 \pm 0.00$	$0.00 \pm 0.00$
Macrophages M2	$6.34 \pm 0.57$	8.54 ± 0.80 *	$4.22 \pm 0.84$	$5.54 \pm 0.93$
Dendritic cells resting	$0.04 \pm 0.04$	0.86 ± 0.37 *	$0.37 \pm 0.29$	$0.35 \pm 0.30$
Dendritic cells activated	$2.92 \pm 0.48$	4.88 ± 0.89 *	$4.24 \pm 0.32$	5.99 ± 0.42 *
Mast cells resting	$0.33 \pm 0.33$	$0.23 \pm 0.22$	$0.00 \pm 0.00$	$0.00 \pm 0.00$
Mast cells activated	$4.51 \pm 0.78$	1.80 ± 0.99 *	$5.43 \pm 2.04$	$2.32 \pm 1.80$
Eosinophils	$1.63 \pm 0.77$	3.83 ± 0.58 **	$1.74 \pm 0.60$	$1.56 \pm 0.50$
Neutrophils	$0.54 \pm 0.23$	$0.60 \pm 0.24$	$0.25 \pm 0.25$	$0.86 \pm 0.56$

**Table 16. Mapping summary statistics of miRNA sequencing.** Total reads after sequencing and the number and percent that uniquely mapped to the combined equine and viral genomes are

shown for each sample.

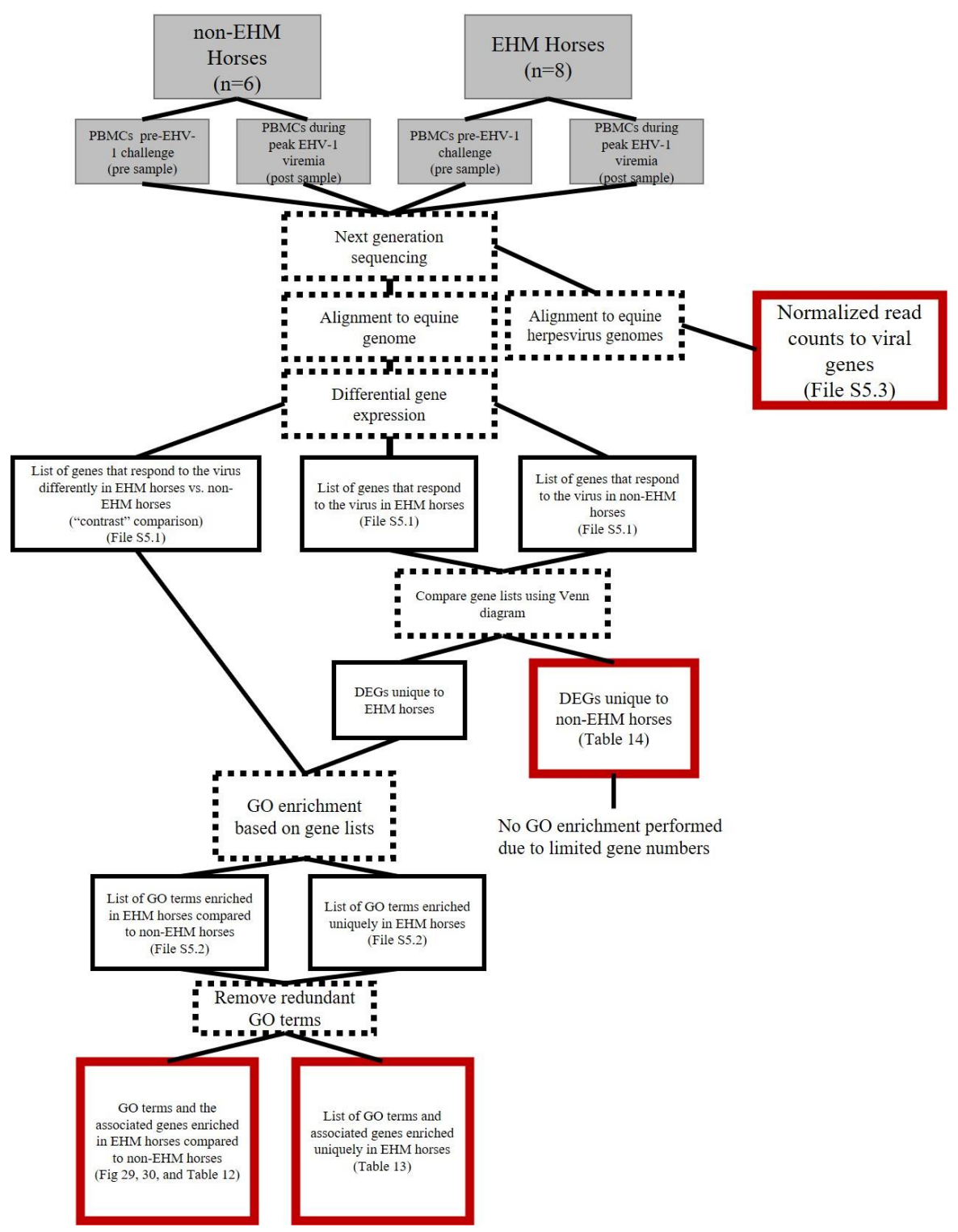
Table 6. Mapping summary statistics for miRNA								
Sample ID	Total reads	Mapped reads (number of reads)	Mapped reads (%)					
EHM_POST_H15	10565453	6343105	60.0					
EHM_PRE_H15	13441490	8441676	62.8					
CONT_POST_H16	16333781	9902090	60.6					
CONT_PRE_H16	18666363	10063969	53.9					
EHM_POST_H1	16138773	10132028	62.8					
EHM_PRE_H1	14579372	8401412	57.6					
CONT_POST_H26	20738238	13052381	62.9					
CONT_PRE_H26	12620476	7639817	60.5					
CONT_POST_H27	14478575	9121947	63.0					
CONT_PRE_H27	14274791	8648212	60.6					
CONT_POST_H28	11650722	6770100	58.1					
CONT_PRE_H28	13958536	8185342	58.6					
EHM_POST_H2	10003035	6177560	61.8					
EHM_PRE_H2	27603885	18045362	65.4					
CONT_POST_H34	14229914	7987735	56.1					
CONT_PRE_H34	16414130	8970337	54.7					
CONT_POST_H35	12721783	7562530	59.4					
CONT_PRE_H35	12118767	6341040	52.3					
EHM_POST_H3	13411346	7434254	55.4					
EHM_PRE_H3	16196518	9932650	61.3					
EHM_POST_H4	13378608	8204075	61.3					
EHM_PRE_H4	14230204	8689707	61.1					
EHM_POST_H5	12190031	6308410	51.8					
EHM_PRE_H5	11389204	7010810	61.6					
EHM_POST_H7	11022200	6965796	63.2					
EHM_PRE_H7	6538519	3809812	58.3					
EHM_POST_H9	17781885	11311463	63.6					
EHM_PRE_H9	8758431	5622680	64.2					
Average	14122680	8467011	59.7					

Table 17. Differentially expressed miRNAs. Differentially expressed (FDR < 0.05 and log 2 fold change > |1|) miRNAs are shown here. The top two lists indicate the miRNAs identified in the between group (contrast) comparison. Upregulated terms are those based on the genes upregulated in EHM horses compared to Non-EHM horses. Downregulated terms are those based on the genes downregulated in EHM group (pre vs post challenge). Upregulated refers to genes upregulated during viremia compared to prechallenge, and downregulated refers to genes downregulated during viremia compared to pre-challenge. There were no differentially expressed miRNAs in the non-EHM horses pre vs post challenge. ID numbers next to novel miRNAs indicate the arbitrary ID given to those without corresponding equine, murine, or human IDs. Gene expression of these miRNAs can be visualized in Figure 35.

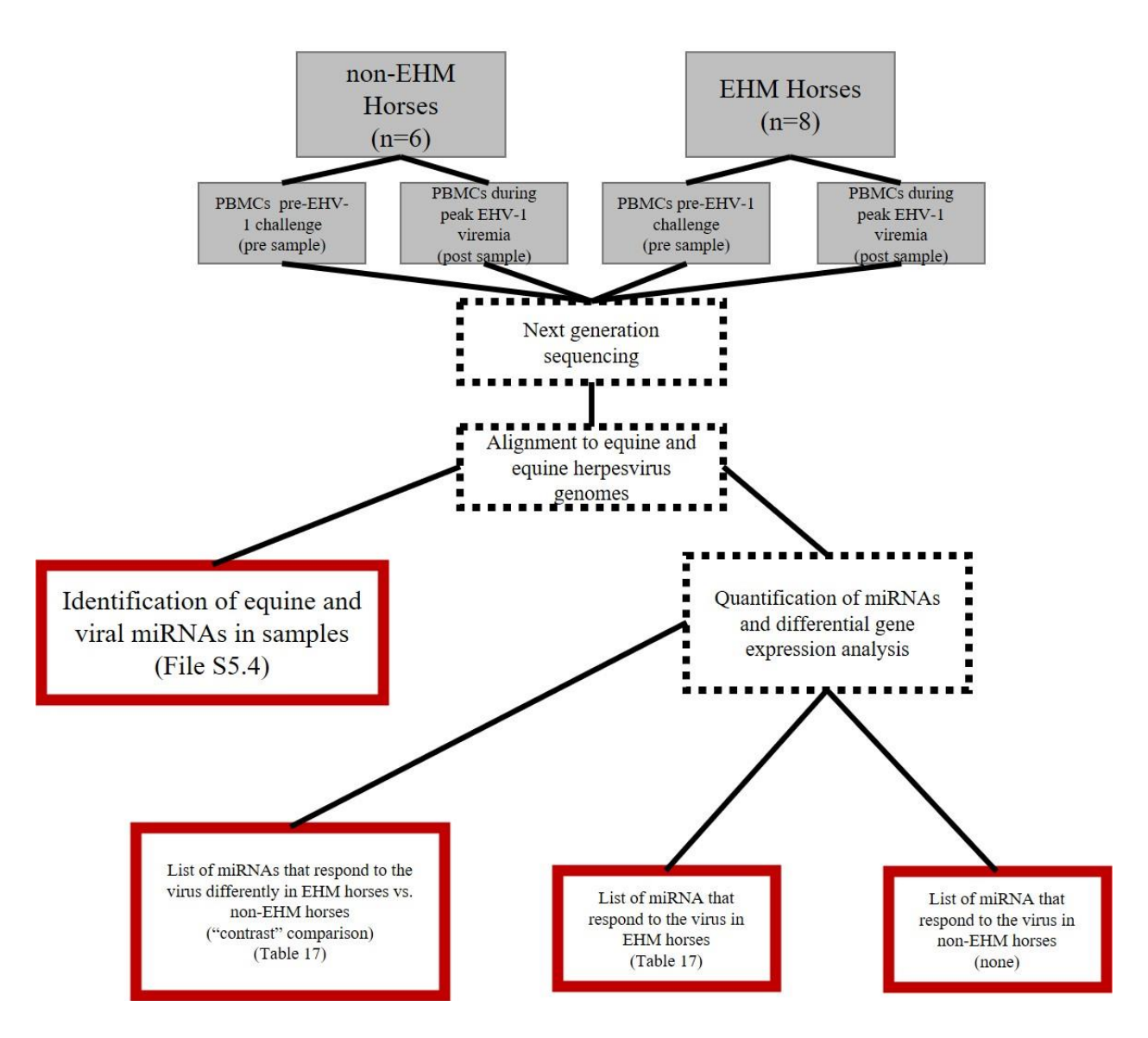
· D ID	Mouse or Human		I FC	EDD					
mirBase ID	Ortholog	mature sequence	logFC	FDR					
Upregulated in EHM vs non-EHM horses: contrast comparison (between groups)									
novel (id: 764)	unknown	CCCGCCGGCCGGCCGCC	2.633433	0.037716					
novel	mmu-miR-7059-5p	GCCGGGGAGCCCGGCGGC	2.007236	0.031695					
Downreg	gulated in EHM vs non-E	EHM horses: contrast comparison (betwe	en groups)						
novel	mmu-miR-669k-5p	TGTGCATGTGTGCATGTAGGCAG	-1.35402	0.047318					
eca-miR-199a-5p,									
eca-miR-199b-5p	hsa-miR-199a-3p	ACAGTAGTCTGCACATTGGTT	-1.32914	0.008					
eca-miR-34c	hsa-miR-34a-5p	AGGCAGTGTAGTTAGCTGATTGC	-1.29981	0.008					
novel	hsa-miR-542-5p	TCGGGGATTCAGGTGGCTGTTC	-1.24093	0.008					
eca-miR-10b	hsa-miR-10a-5p	TACCCTGTAGAACCGAATTTGT	-1.20325	0.035115					
eca-miR-328	hsa-miR-328-3p	CTGGCCCTCTCTGCCCTTCCGT	-1.1001	0.010824					
eca-miR-146a	hsa-miR-146a-5p	TGAGAACTGAATTCCATGGGTT	-1.05304	0.000473					
	Uniquely upregul	lated in EHM horses (within group)							
novel (id: 764)	unknown	CCCGCCCGGCCCGCCC	2.310828	0.000781					
novel (id: 983)	unknown	CCGCCGCCGCCGCC	1.741133	0.010356					
novel (id: 187)	unknown	CCCGCCGCCGCCGCC	1.726318	0.010904					
novel	hsa-miR-7108-3p	CCCCGCCGCCGCCGCCG	1.700159	0.009829					
novel	mmu-miR-7059-5p	GCCGGGGAGCCCGGCGGC	1.591515	0.002068					

Table 17. (Cont'd)

mirBase ID	Mouse or Human Ortholog	mature sequence	logFC	FDR
	Uniquely downregul	lated in EHM horses (within group)		
eca-miR-483	unknown	CACTCCTCTCCCGTCTTCT	-1.80772	4.23E-12
eca-miR-146a	hsa-miR-146a-5p	TGAGAACTGAATTCCATGGGTT	-1.49104	1.19E-20
eca-miR-34c	hsa-miR-34a-5p	AGGCAGTGTAGTTAGCTGATTGC	-1.34093	3.29E-07
eca-miR-138	hsa-miR-138-5p	AGCTGGTGTTGTGAATCAGGCCG	-1.31391	0.000642
eca-miR-199b-5p	hsa-miR-199a-3p	ACAGTAGTCTGCACATTGGTT	-1.034	0.000266



**Figure 23. Summary of mRNA sequencing data analysis.** RNA was extracted from PBMCs from horses prior to and during EHV-1 challenge infection. The gray boxes represent experimental design. The dashed outline boxes are data analysis processes (actions). Black and red boxes represent output. The red outline indicates final output used for interpretation.



**Figure 24. Summary of miRNA sequencing data analysis**. RNA was extracted from PBMCs from horses prior to and during EHV-1 challenge infection. The gray boxes represent experimental design. The dashed outline boxes are data analysis processes (actions). Black and red boxes represent output. The red outline indicates final output used for interpretation.

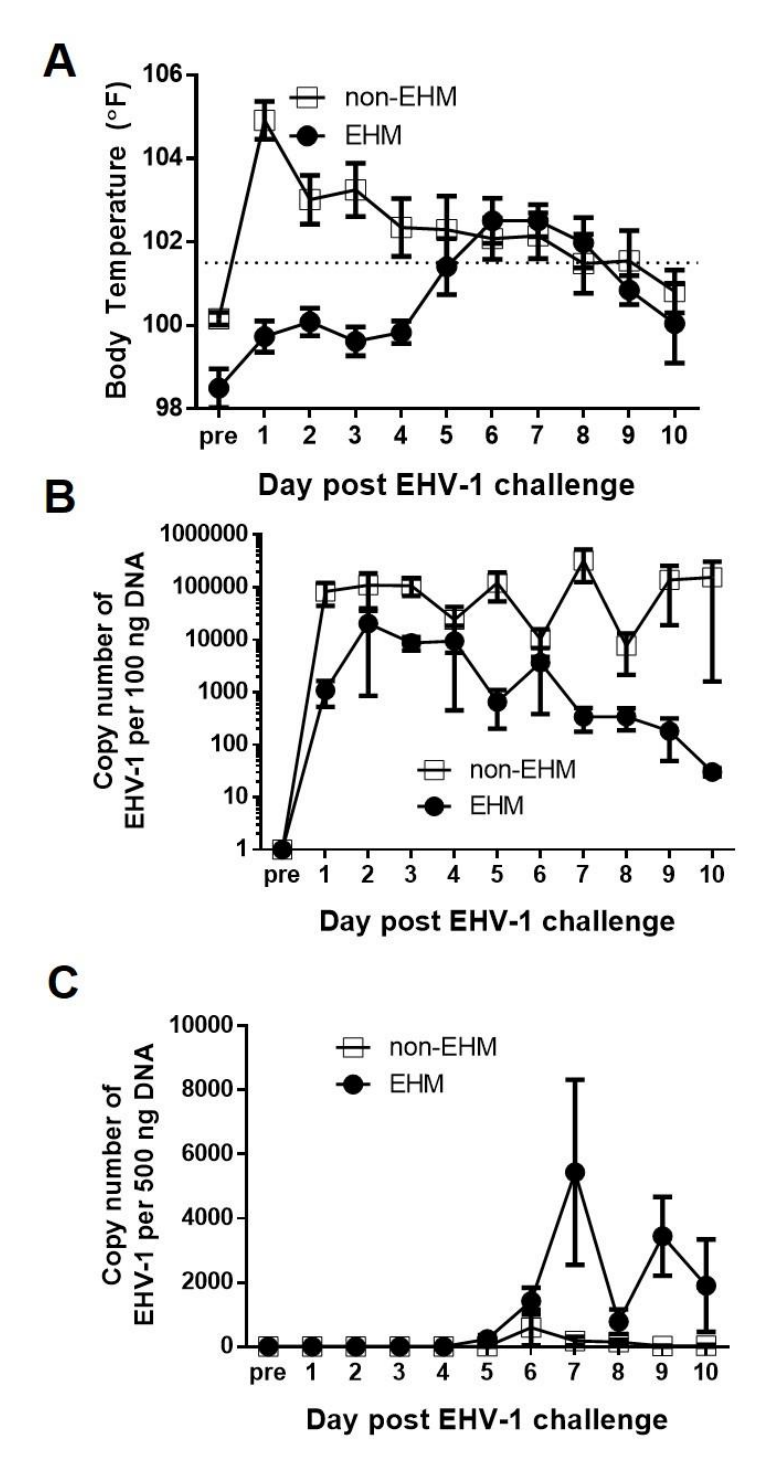


**Figure 25.** Clinical and virological disease between EHM and non-EHM horses. (A) Body temperature. Fever is any body temperature over 101.5 °F and is indicated by the horizontal dashed line. (B) EHV-1 nasal shedding. Data is expressed as EHV-1 copy number per 100 ng template DNA as determined by qPCR. (C) Viremia. Data is expressed as EHV-1 copy number per 500 ng template DNA as determined by qPCR. This data was obtained in conjunction with another study (manuscript in preparation).

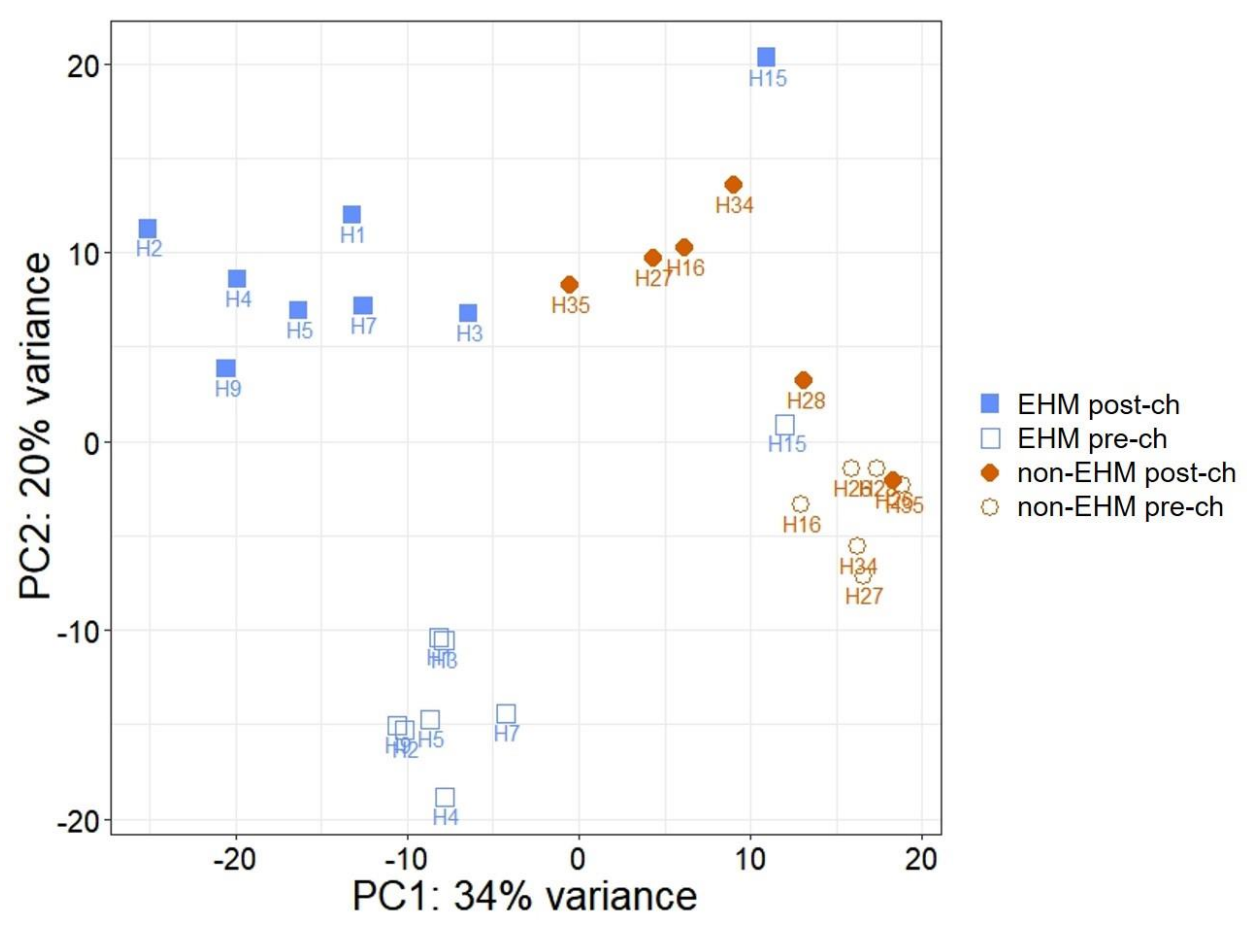


**Figure 26. Principal component analysis (PCA) plot.** Principal component analysis was performed on the read count data obtained after mRNA sequencing. Red closed circles indicate samples from non-EHM horses post EHV-1 challenge, red open circles indicate samples from non-EHM horses prior to EHV-1 challenge, blue closed squares indicate samples from EHM horses post EHV-1 challenge, and blue open squares indicate samples from EHM horses prior to EHV-1 challenge.

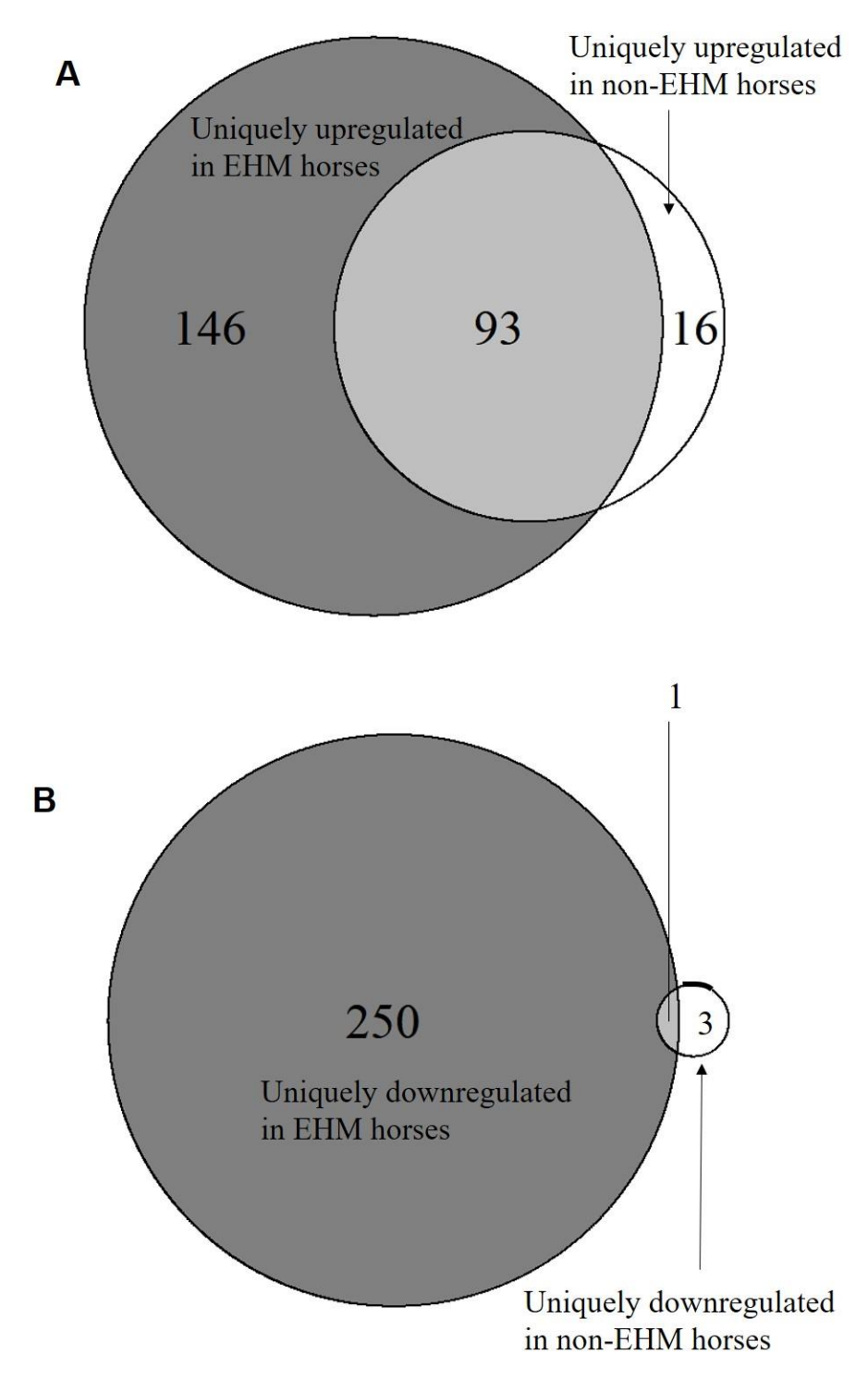
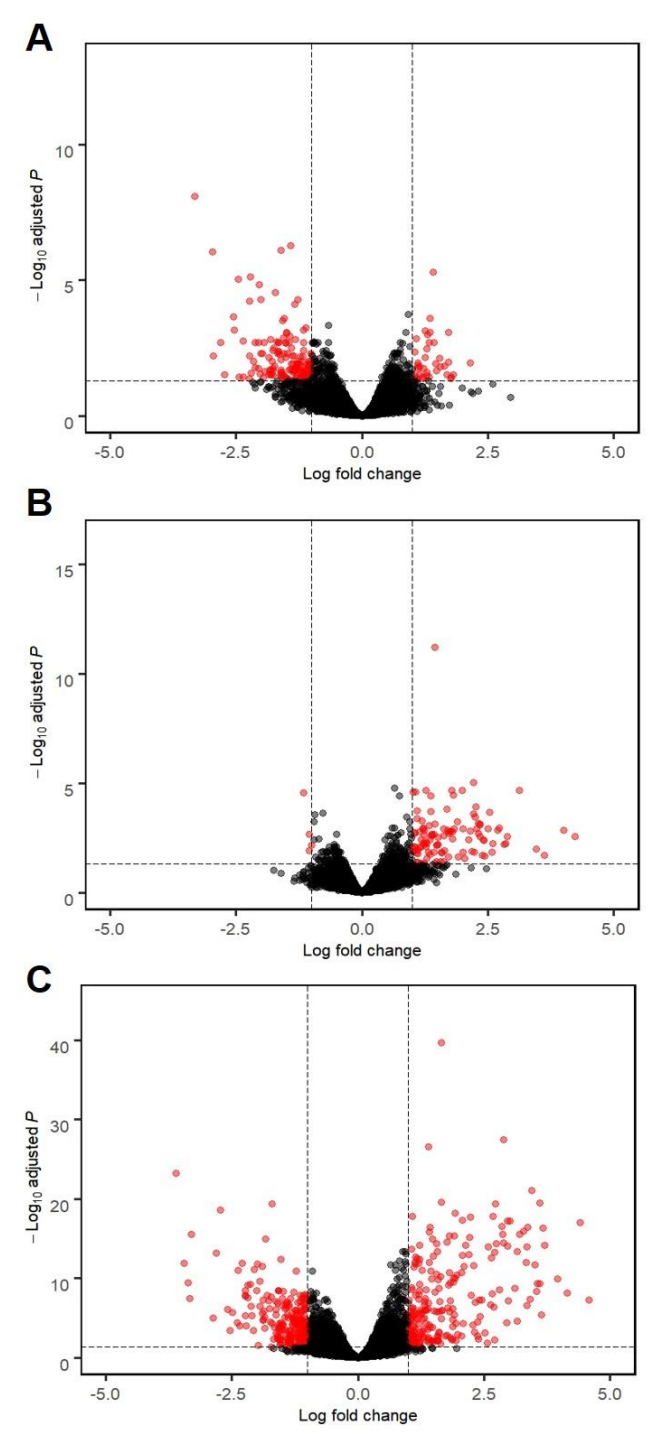


Figure 27. Venn diagrams of up- and down- regulated genes in response to EHV-1 challenge. The within group comparisons for EHM and non-EHM horses were compared using a Venn diagram to determine genes uniquely (A) upregulated and (B) downregulated for each group.



**Figure 28. Volcano plots of differentially expressed genes.** (A) Genes differentially expressed between EHM and non-EHM horses. Genes with a positive log fold change represent genes upregulated in EHM horses compared to non-EHM horses, while genes with a negative log fold change represent genes downregulated in EHM horses compared to non-EHM horses. (B) Genes differentially expressed within Non-EHM horses. Genes with a positive log fold change represent genes upregulated in non-EHM horses post-challenge compared to pre-challenge,

**Figure 28 (Cont'd)** while genes with a negative log fold change represent genes downregulated. (C) Genes differentially expressed within EHM horses. Genes with a positive log fold change represent genes upregulated in EHM horses post-challenge compared to pre-challenge, while genes with a negative log fold change represent downregulated genes. P values are expressed on the y-axis, with more significantly differentially expressed genes towards the top of the plot. Genes highlighted in red passed the threshold of significance set at adjusted p-value < 0.05 and Log fold change > |1|.

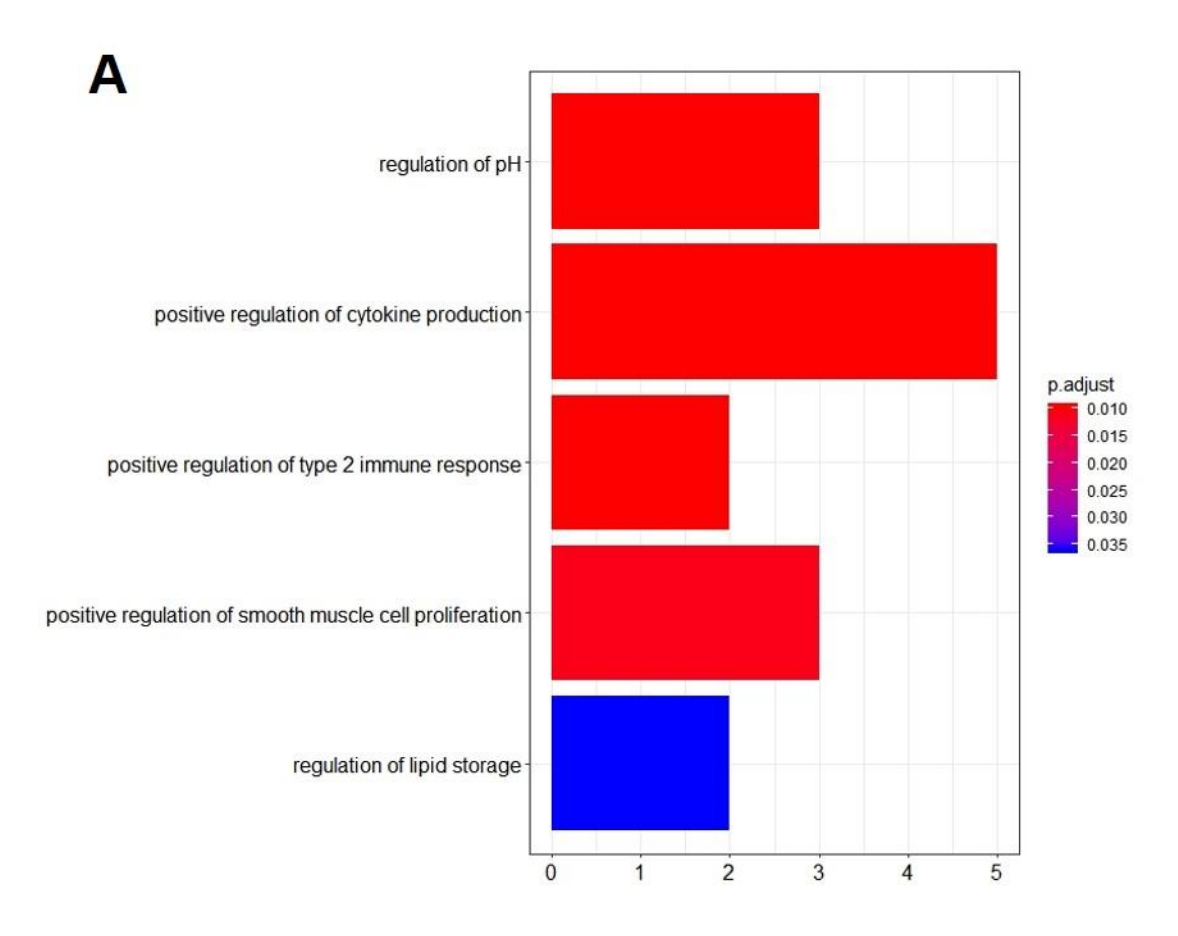
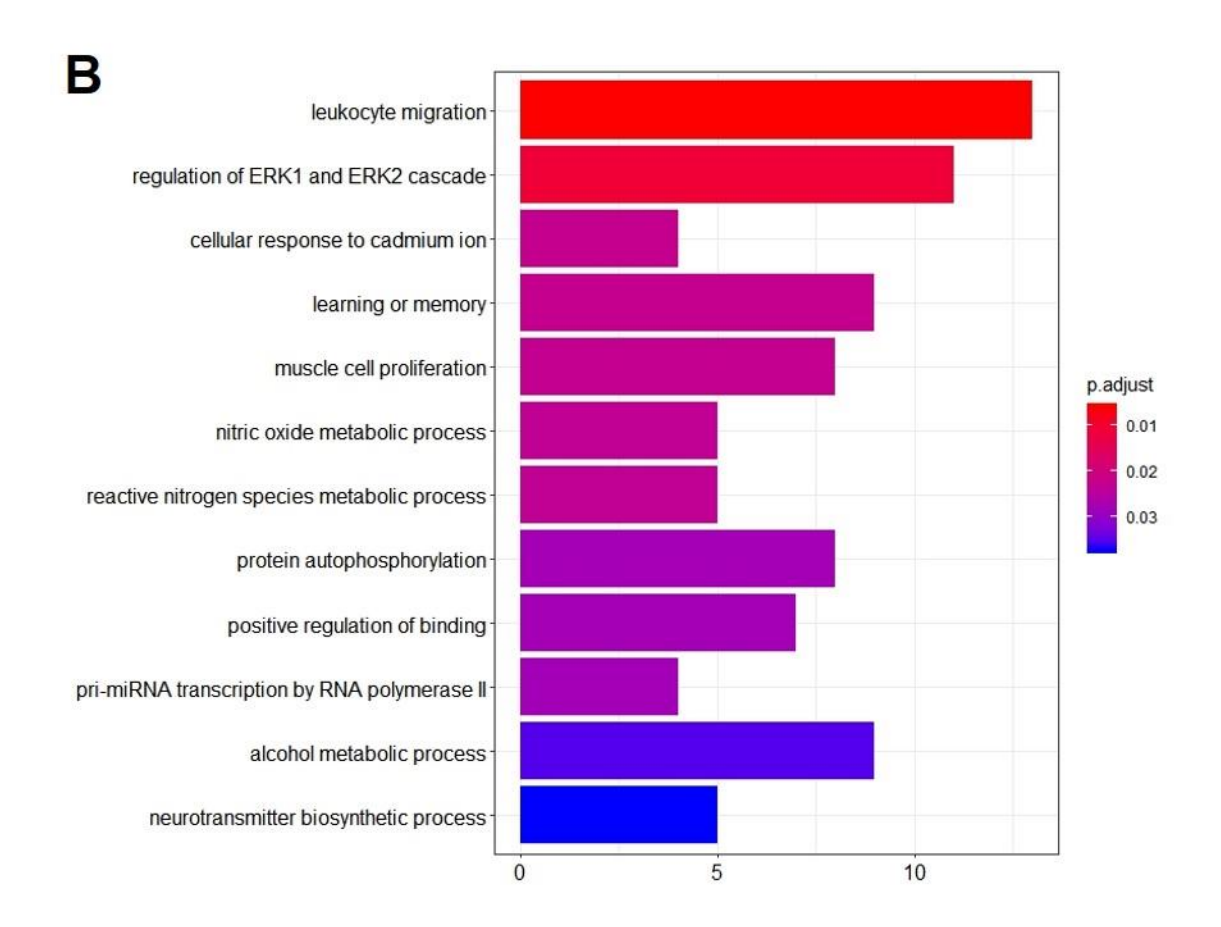


Figure 29. GO terms for biological processes overrepresented in EHM horses compared to non-EHM horses. (A) upregulated biological process and (B) downregulated biological processes. GO term enrichment analysis was performed using the enrichgo function of the clusterprofiler package in R. The resulting terms were filtered for redundancy using REVIGO. The non-redundant enriched GO terms are visualized here. The most significantly enriched terms are at the top and listed in decreasing significance (increasing p.adjust). The number of genes from our gene list are indicated on the x-axis.

Figure 29. (Cont'd)



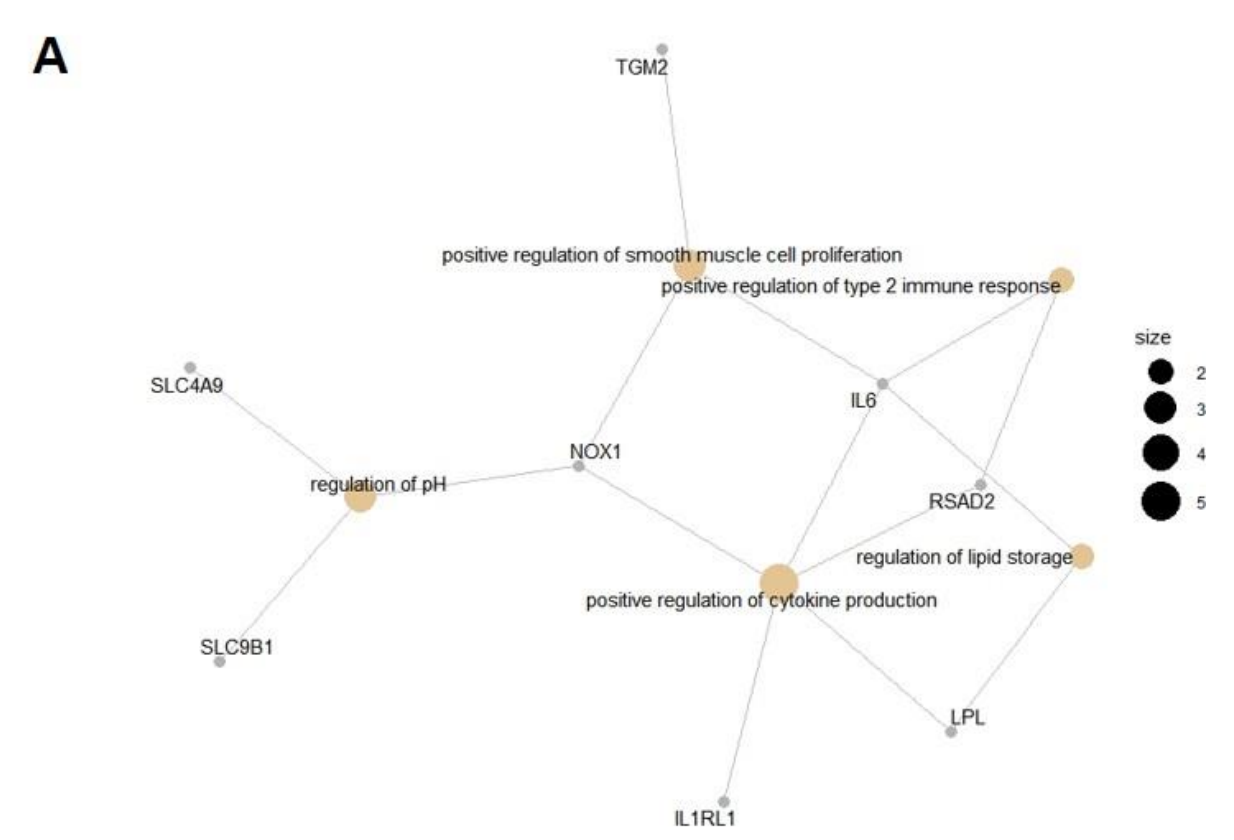
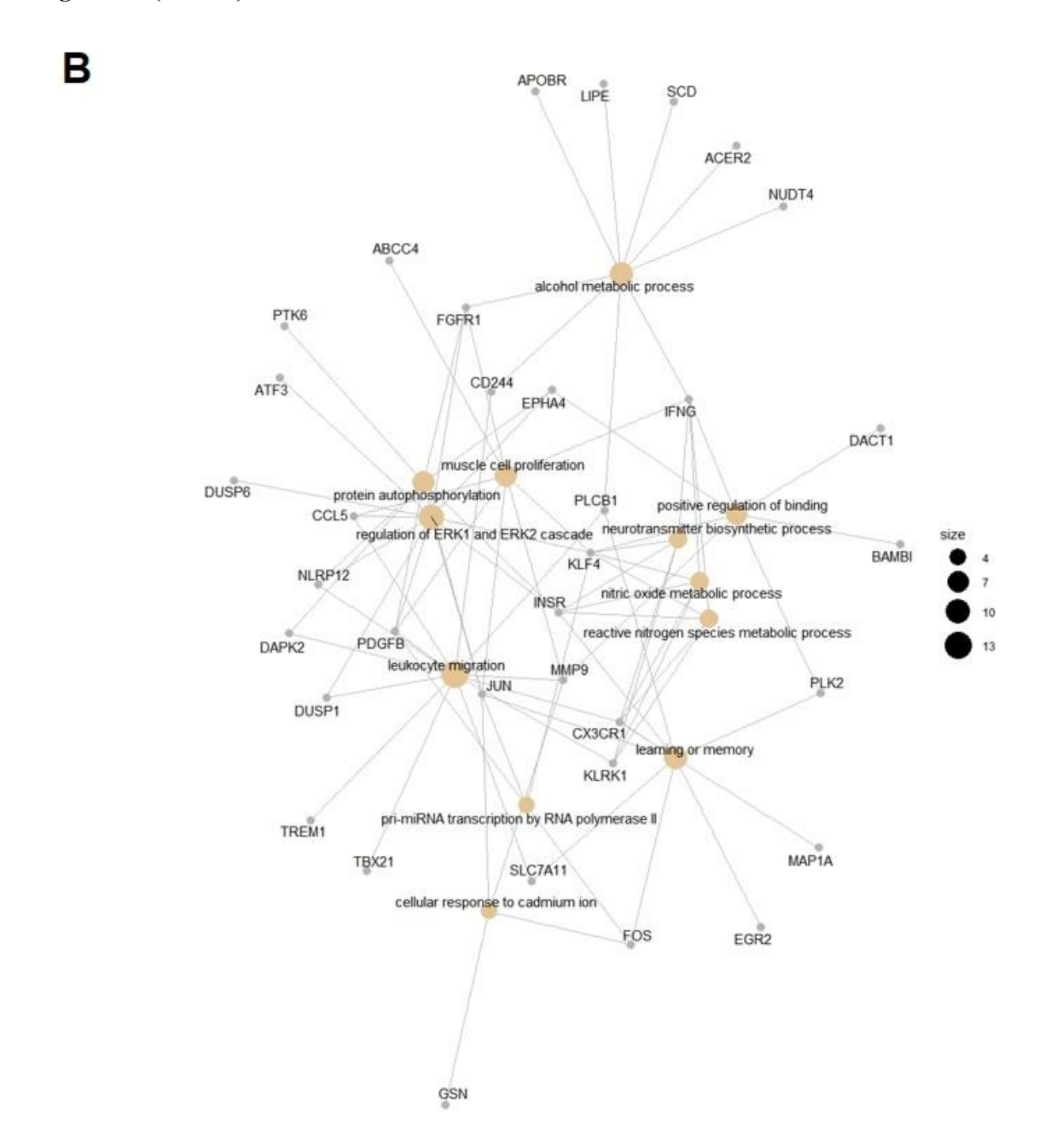


Figure 30. Net plot of the most significantly enriched GO terms and associated genes. (A) upregulated biological process and (B) downregulated biological processes. The non-redundant GO terms are listed here with the associated genes from our gene list. Tan nodes represent the GO term and gray nodes represent genes. The size of the GO term nodes indicate the number of genes from our list associated with that term. The biological processes and the associated genes cluster based on similarity.

Figure 30. (Cont'd)



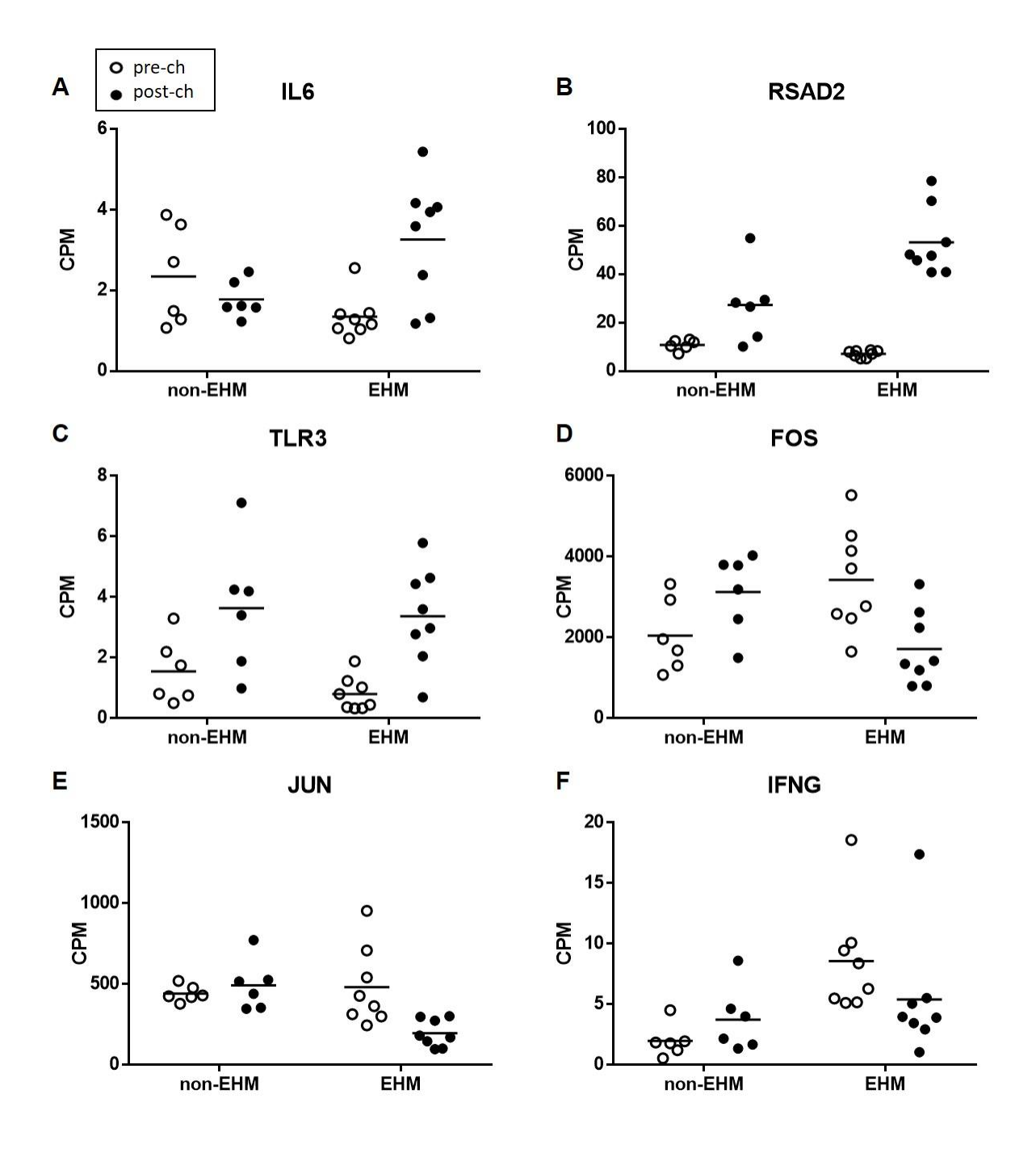
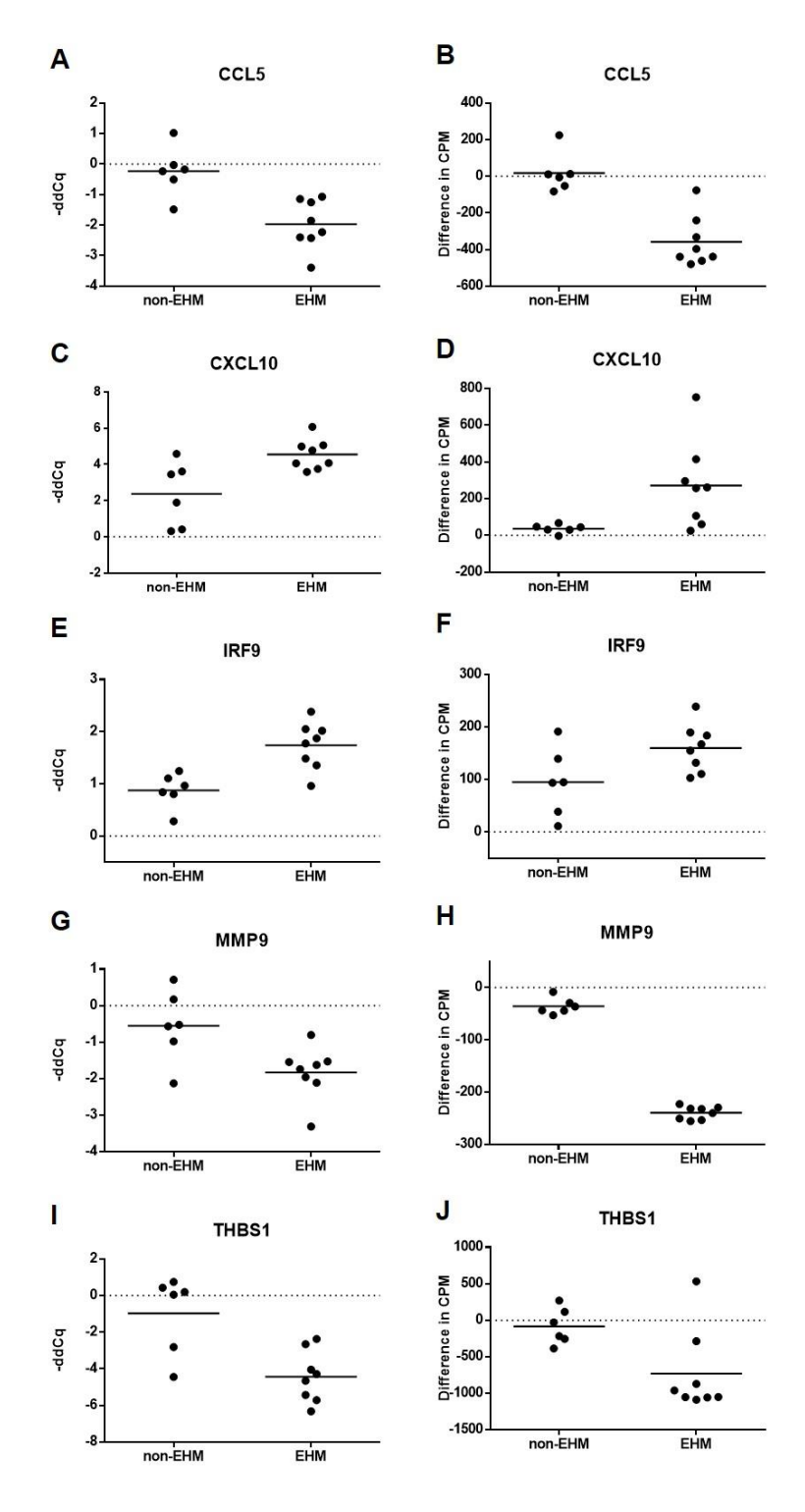
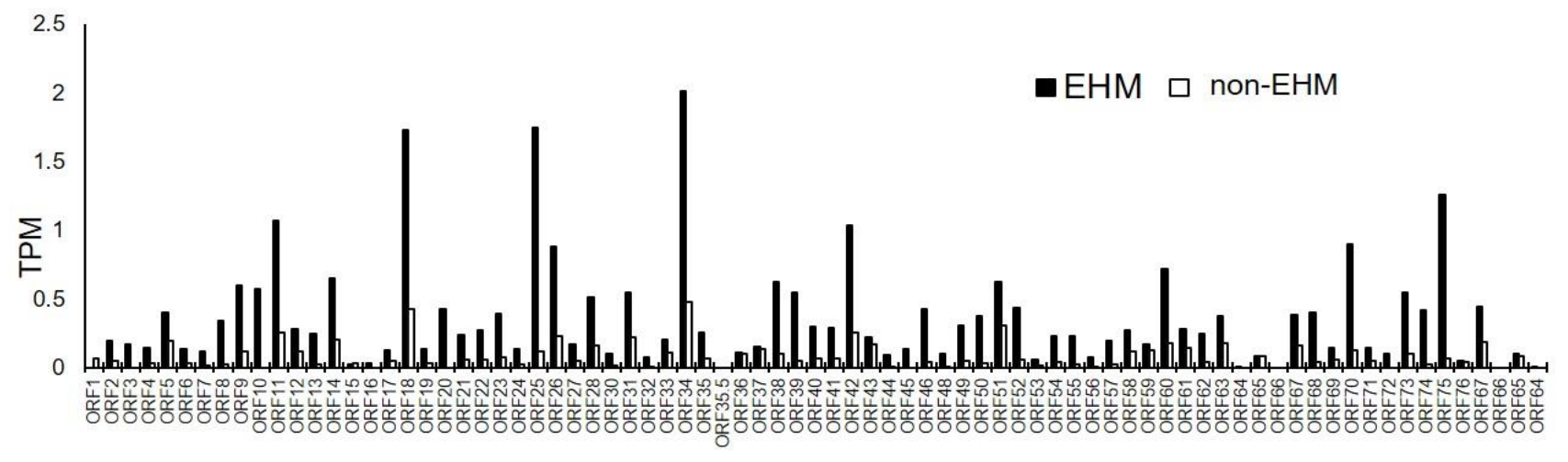


Figure 31. Normalized read counts (cpm) of selected genes in PBMCs of horses. (A) IL6 (B) RSAD2 (C) TLR3 (D) FOS (E) JUN (F) IFNG.



**Figure 32.** Gene expression as determined by RT-qPCR and RNA sequencing. RT-qPCR data from whole blood is expressed as the negative delta-delta-Cq value for (A) CCL5, (C) CXCL10, (E) IRF9, (G) MMP9, and (I) THBS1, where the average pre-challenge data for each group used as a calibrator and values above zero represent an upregulation and below zero

**Figure 32 (Cont'd)** represent a downregulation. RNA sequencing data from PBMCs are shown for comparison and expressed as delta-CPM (post-challenge CPM value – group average of prechallenge CPM) for (B) CCL5, (D) CXCL10, (F) IRF9, (H) MMP9, and (J) THBS1. Differences between groups were statistically significant as described in the methods for all genes visualized here.



**Figure 33. Normalized counts of viral genes post EHV-1 challenge.** Data represents the average transcripts per million (TPM). The gray line is non-EHM horses and the black line is EHM horses.

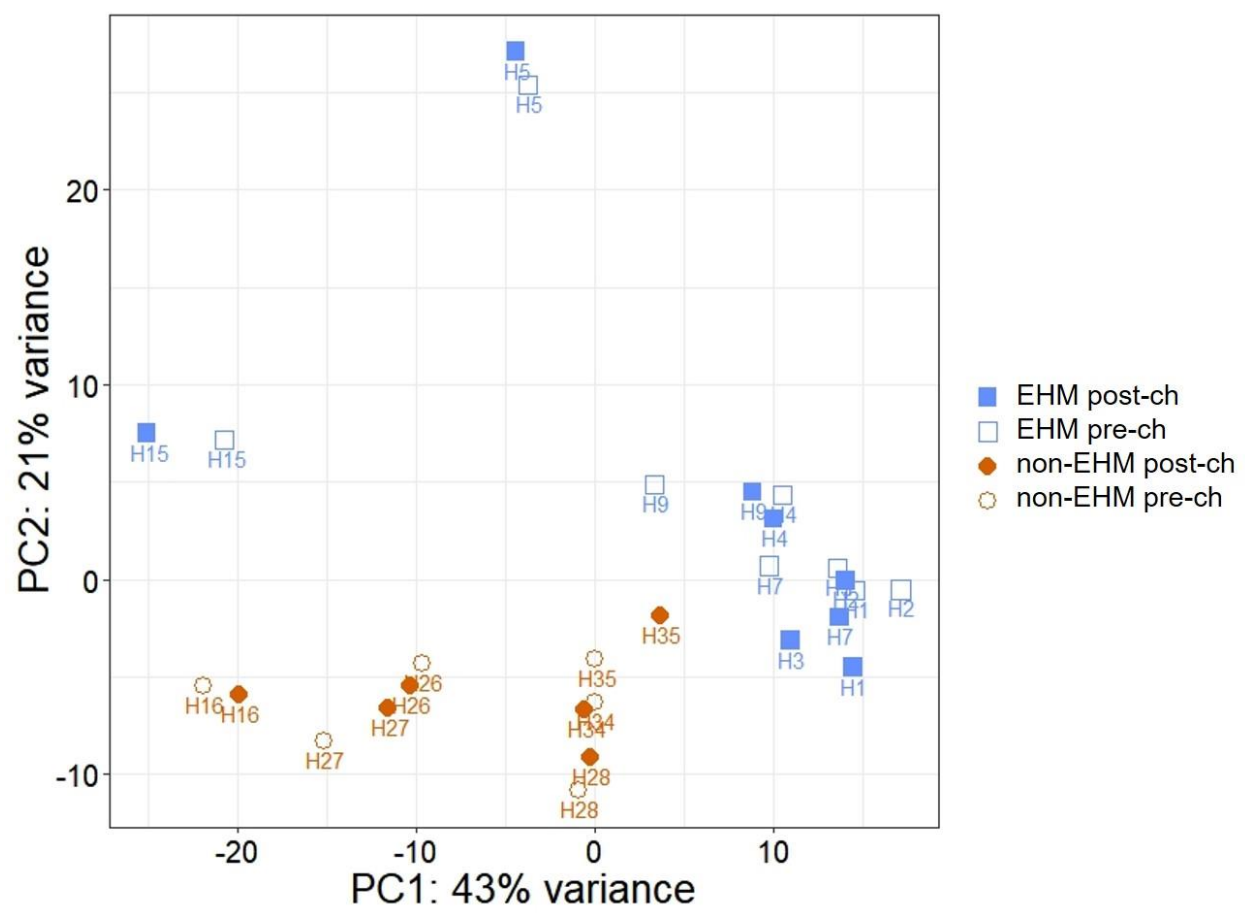


**Figure 34. Principal component analysis (PCA) plot for miRNA read counts.** Principal component analysis was performed on the read count data obtained after miRNA sequencing. Red closed circles indicate samples from non-EHM horses post EHV-1 challenge, red open circles indicate samples from non-EHM horses prior to EHV-1 challenge, blue closed squares indicate samples from EHM horses post EHV-1 challenge, and blue open squares indicate samples from EHM horses prior to EHV-1 challenge.

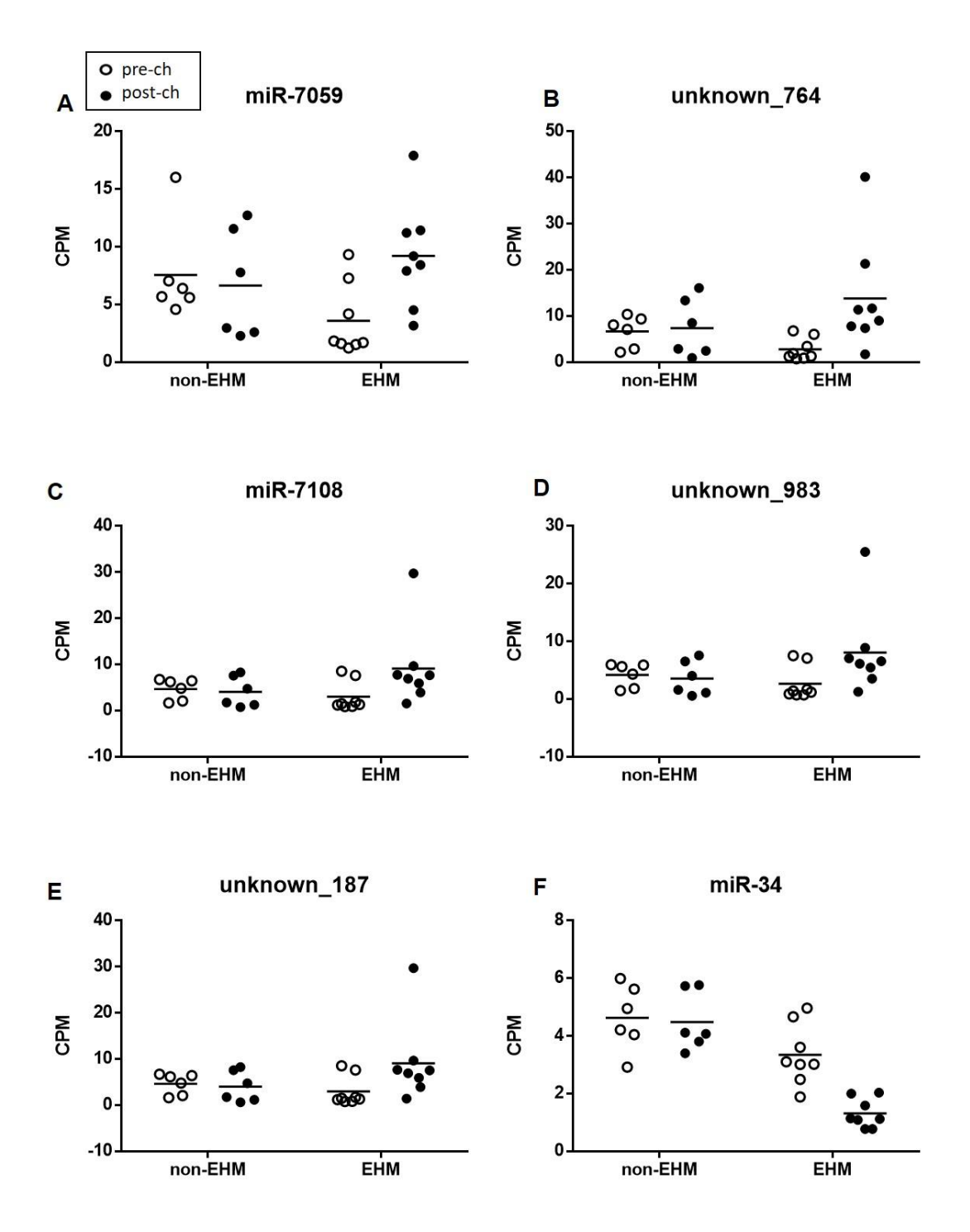
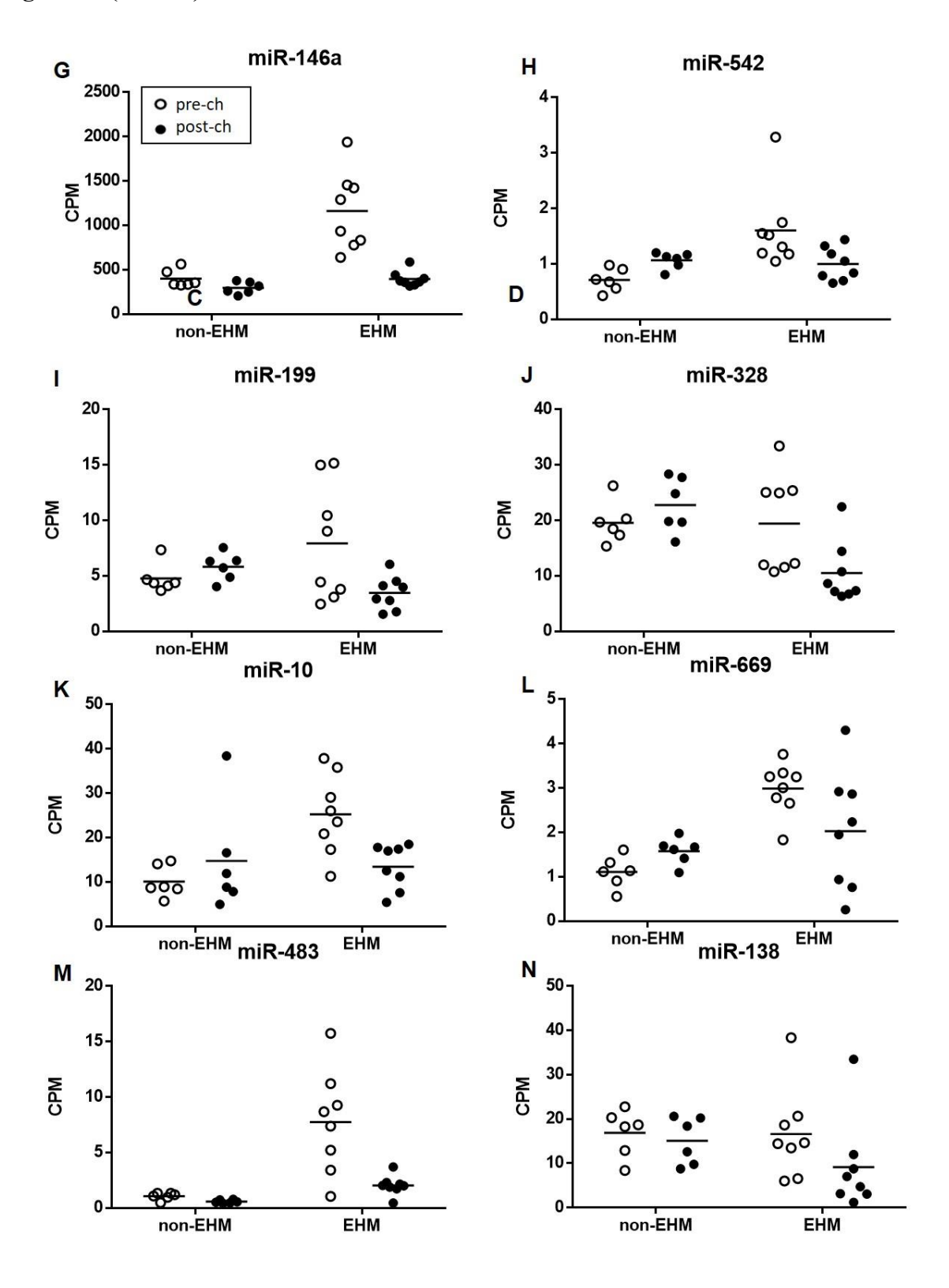


**Figure 35. Differentially expressed miRNAs.** Details regarding these miRNAs can be seen in Table 17. miRNAs upregulated in EHM horses included (A) miR-7059, (B) novel miRNA (id: 764), (C) miR-7108, (D) novel miRNA (id: 983), and (E) novel miRNA (id: 187) miRNAs downregulated in EHM horses include (F) miR-34, (G) miR-146a, (H) miR-542, (I) miR-199, (J) miR-328, (K) miR-10, (L) miR-669, (M) miR-483, and (N) miR-138.

Figure 35 (Cont'd)



## **REFERENCES**

## REFERENCES

- 1. Gilkerson, J.R.; Whalley, J.M.; Drummer, H.E.; Studdert, M.J.; Love, D.N. Epidemiological studies of equine herpesvirus 1 (EHV-1) in Thoroughbred foals: a review of studies conducted in the Hunter Valley of New South Wales between 1995 and 1997. *Vet. Microbiol.* **1999**, *68*, 15–25, doi:10.1016/S0378-1135(99)00057-7.
- 2. Gilkerson, J.R.; Whalley, J.M.; Drummer, H.E.; Studdert, M.J.; Love, D.N. Epidemiology of EHV-1 and EHV-4 in the mare and foal populations on a Hunter Valley stud farm: are mares the source of EHV-1 for unweaned foals. *Vet. Microbiol.* **1999**, *68*, 27–34, doi:10.1016/S0378-1135(99)00058-9.
- 3. Foote, C.E.; Love, D.N.; Gilkerson, J.R.; Whaley, J.M. Detection of EHV-1 and EHV-4 DNA in unweaned Thoroughbred foals from vaccinated mares on a large stud farm. *Equine Vet. J.* **2010**, *36*, 341–345, doi:10.2746/0425164044890634.
- 4. Mumford, J.A.; Rossdale, P.D.; Jessett, D.M.; Gann, S.J.; Ousey, J. Serological and virological investigations of an equid herpesvirus 1 (EHV-1) abortion storm on a stud farm in 1985. *J. Reprod. Fertil. Suppl.* **1987**, *35*, 509–518.
- 5. Pusterla, N.; Mapes, S.; Wilson, W.D. Prevalence of equine herpesvirus type 1 in trigeminal ganglia and submandibular lymph nodes of equids examined postmortem. *Vet. Rec.* **2010**, *167*, 376–378, doi:10.1136/vr.c3748.
- 6. Allen, G.P. Antemortem detection of latent infection with neuropathogenic strains of equine herpesvirus-1 in horses. *Am. J. Vet. Res.* **2006**, *67*, 1401–1405, doi:10.2460/ajvr.67.8.1401.
- 7. Allen, G.P.; Bolin, D.C.; Bryant, U.; Carter, C.N.; Giles, R.C.; Harrison, L.R.; Hong, C.B.; Jackson, C.B.; Poonacha, K.; Wharton, R.; et al. Prevalence of latent, neuropathogenic equine herpesvirus-1 in the Thoroughbred broodmare population of central Kentucky. *Equine Vet. J.* **2008**, *40*, 105–110, doi:10.2746/042516408X253127.
- 8. Slater, J.D.; Borchers, K.; Thackray, A.M.; Field, H.J. The trigeminal ganglion is a location for equine herpesvirus 1 latency and reactivation in the horse. *J. Gen. Virol.* **1994**, 75, 2007–2016, doi:10.1099/0022-1317-75-8-2007.
- 9. Kydd, J.H.; Townsend, H.G.G.; Hannant, D. The equine immune response to equine herpesvirus-1: The virus and its vaccines. *Vet. Immunol. Immunopathol.* **2006**, *111*, 15–30, doi:10.1016/j.vetimm.2006.01.005.
- 10. Hussey, S.B.; Clark, R.; Lunn, K.F.; Breathnach, C.; Soboll, G.; Whalley, J.M.; Lunn, D.P. Detection and quantification of equine herpesvirus-1 viremia and nasal shedding by real-time polymerase chain reaction. *J. Vet. Diagnostic Investig.* **2006**, *18*, 335–342,

- doi:10.1177/104063870601800403.
- 11. Patel, J.R.; Edington, N.; Mumford, J.A. Variation in cellular tropism between isolates of Equine herpesvirus-1 in foals. *Arch. Virol.* **1982**, *74*, 41–51, doi:10.1007/BF01320781.
- 12. Osterrieder, N.; Van de Walle, G.R. Pathogenic potential of equine alphaherpesviruses: The importance of the mononuclear cell compartment in disease outcome. *Vet. Microbiol.* **2010**, *143*, 21–28, doi:10.1016/j.vetmic.2010.02.010.
- 13. Edington, N.; Smyth, B.; Griffiths, L. The role of endothelial cell infection in the endometrium, placenta and foetus of equid herpesvirus 1 (EHV-1) Abortions. *J. Comp. Pathol.* **1991**, *104*, 379–387, doi:10.1016/S0021-9975(08)80148-X.
- 14. Edington, N.; Bridges, C.G.; Patel, J.R. Endothelial cell infection and thrombosis in paralysis caused by equid herpesvirus-1: Equine stroke. *Arch. Virol.* **1986**, *90*, 111–124, doi:10.1007/BF01314149.
- 15. USDA; APHIS Equine Herpesvirus (EHV-1) FINAL Situation Report Available online: https://www.aphis.usda.gov/vs/nahss/equine/ehv/ehv\_2011\_final\_sitrep\_062311.pdf (accessed on Oct 24, 2018).
- 16. USDA; APHIS; VS; CEAH Equine herpesvirus myeloencephalopathy: a potentially emerging disease Available online: https://www.aphis.usda.gov/animal\_health/emergingissues/downloads/ehv1final.pdf (accessed on Oct 24, 2018).
- 17. USAHA Equine Herpesvirus Myeloencephalopathy Incident Guidelines for State Animal Health Officials Available online: http://www.usaha.org/upload/Publication/Top Specific/EHM\_Guidance\_Document\_Revised\_Fe.pdf (accessed on Oct 24, 2018).
- 18. Lunn, D.P.; Davis-Poynter, N.; Flaminio, M.J.B.F.; Horohov, D.W.; Osterrieder, K.; Pusterla, N.; Townsend, H.G.G. Equine herpesvirus-1 consensus statement. *J. Vet. Intern. Med.* **2009**, *23*, 450–461.
- 19. Nugent, J.; Birch-Machin, I.; Smith, K.C.; Mumford, J.A.; Swann, Z.; Newton, J.R.; Bowden, R.J.; Allen, G.P.; Davis-Poynter, N. Analysis of equid herpesvirus 1 strain variation reveals a point mutation of the DNA polymerase strongly associated with neuropathogenic versus nonneuropathogenic disease outbreaks. *J. Virol.* **2006**, *80*, 4047–4060.
- 20. Allen, G.P.; Breathnach, C.C. Quantification by real-time PCR of the magnitude and duration of leucocyte-associated viraemia in horses infected with neuropathogenic vs. non-neuropathogenic strains of EHV- 1. *Equine Vet. J.* **2006**, *38*, 252–257, doi:10.2746/042516406776866453.
- 21. Allen, G.P. Risk factors for development of neurologic disease after experimental

- exposure to equine herpesvirus-1 in horses. *Am. J. Vet. Res.* **2008**, *69*, 1595–1600, doi:10.2460/ajvr.69.12.1595.
- 22. Holz, C.L.; Nelli, R.K.; Eilidh Wilson, M.; Zarski, L.M.; Azab, W.; Baumgardner, R.; Osterrieder, N.; Pease, A.; Zhang, L.; Hession, S.; et al. Viral genes and cellular markers associated with neurological complications during herpesvirus infections. *J. Gen. Virol.* **2017**, *98*, doi:10.1099/jgv.0.000773.
- 23. Goodman, L.B.; Loregian, A.; Perkins, G.A.; Nugent, J.; Buckles, E.L.; Mercorelli, B.; Kydd, J.H.; Palù, G.; Smith, K.C.; Osterrieder, N.; et al. A point mutation in a herpesvirus polymerase determines neuropathogenicity. *PLoS Pathog.* **2007**, *3*, e160, doi:10.1371/journal.ppat.0030160.
- 24. Yeo, W.M.; Osterrieder, N.; Stokol, T. Equine herpesvirus type 1 infection induces procoagulant activity in equine monocytes. *Vet. Res.* **2013**, *44*, 16, doi:10.1186/1297-9716-44-16.
- 25. Stokol, T.; Yeo, W.M.; Burnett, D.; DeAngelis, N.; Huang, T.; Osterrieder, N.; Catalfamo, J. Equid Herpesvirus Type 1 Activates Platelets. *PLoS One* **2015**, *10*, e0122640.
- 26. Goehring, L.S.; Soboll Hussey, G.; Gomez Diez, M.; Benedict, K.; Maxwell, L.K.; Morley, P.S.; Sloet van Oldruitenborgh-Oosterbaan, M.M.; Lunn, D.P. Plasma D-Dimer Concentrations during Experimental EHV-1 Infection of Horses. *J. Vet. Intern. Med.* **2013**, *27*, 1535–1542, doi:10.1111/jvim.12203.
- 27. Wilson, M.E.; Holz, C.L.; Kopec, A.K.; Dau, J.J.; Luyendyk, J.P.; Soboll Hussey, G. Coagulation parameters following equine herpesvirus type 1 infection in horses. *Equine Vet. J.* **2019**, *51*, 102–107, doi:10.1111/evj.12843.
- 28. Laval, K.; Favoreel, H.W.; Nauwynck, H.J. Equine herpesvirus type 1 replication is delayed in CD172a+ monocytic cells and controlled by histone deacetylases. *J. Gen. Virol.* **2015**, *96*, 118–130, doi:10.1099/vir.0.067363-0.
- 29. Laval, K.; Favoreel, H.W.; Poelaert, K.C.K.; Van Cleemput, J.; Nauwynck, H.J. Equine herpesvirus type 1 enhances viral replication in CD172a+ monocytic cells upon adhesion to endothelial cells. *J. Virol.* **2015**, *89*, 10912–10923, doi:10.1128/JVI.01589-15.
- 30. van der Meulen, K.; Caij, B.; Pensaert, M.; Nauwynck, H. Absence of viral envelope proteins in equine herpesvirus 1-infected blood mononuclear cells during cell-associated viremia. *Vet. Microbiol.* **2006**, *113*, 265–273, doi:10.1016/j.vetmic.2005.11.048.
- 31. Henninger, R.W.; Reed, S.M.; Saville, W.J.; Allen, G.P.; Hass, G.F.; Kohn, C.W.; Sofaly, C. Outbreak of Neurologic Disease Caused by Equine Herpesvirus-1 at a University Equestrian Center. *J. Vet. Intern. Med.* **2008**, *21*, 157–165, doi:10.1111/j.1939-1676.2007.tb02942.x.

- 32. Kato, A.; Schleimer, R.P. Beyond inflammation: airway epithelial cells are at the interface of innate and adaptive immunity. *Curr. Opin. Immunol.* **2007**, *19*, 711–720, doi:10.1016/j.coi.2007.08.004.
- 33. Iwasaki, A.; Medzhitov, R. Regulation of adaptive immunity by the innate immune system. *Science* (80-. ). **2010**, 327, 291–295, doi:10.1126/science.1183021.
- 34. Sokol, C.L.; Luster, A.D. The chemokine system in innate immunity. *Cold Spring Harb. Perspect. Biol.* **2015**, 7, doi:10.1101/cshperspect.a016303.
- 35. Van Cleemput, J.; Poelaert, K.C.K.; Laval, K.; Maes, R.; Hussey, G.S.; Van den Broeck, W.; Nauwynck, H.J. Access to a main alphaherpesvirus receptor, located basolaterally in the respiratory epithelium, is masked by intercellular junctions. *Sci. Rep.* **2017**, *7*, 16656, doi:10.1038/s41598-017-16804-5.
- 36. Thompson, M.R.; Kaminski, J.J.; Kurt-Jones, E.A.; Fitzgerald, K.A. Pattern recognition receptors and the innate immune response to viral infection. *Viruses* **2011**, *3*, 920–940, doi:10.3390/v3060920.
- 37. Soboll Hussey, G.; Ashton, L. V; Quintana, A.M.; Lunn, D.P.; Goehring, L.S.; Annis, K.; Landolt, G. Innate immune responses of airway epithelial cells to infection with equine herpesvirus-1. *Vet. Microbiol.* **2014**, *170*, 28–38, doi:10.1016/j.vetmic.2014.01.018.
- 38. Quintana, A.M.; Landolt, G.A.; Annis, K.M.; Hussey, G.S. Immunological characterization of the equine airway epithelium and of a primary equine airway epithelial cell culture model. *Vet. Immunol. Immunopathol.* **2011**, *140*, 226–36, doi:10.1016/j.vetimm.2010.12.008.
- 39. Soboll Hussey, G.; Ashton, L. V; Quintana, A.M.; Van de Walle, G.R.; Osterrieder, N.; Lunn, D.P. Equine herpesvirus type 1 pUL56 modulates innate responses of airway epithelial cells. *Virology* **2014**, *464–465*, 76–86, doi:https://doi.org/10.1016/j.virol.2014.05.023.
- 40. Wagner, B.; Wimer, C.; Freer, H.; Osterrieder, N.; Erb, H.N. Infection of peripheral blood mononuclear cells with neuropathogenic equine herpesvirus type-1 strain Ab4 reveals intact interferon-alpha induction and induces suppression of anti-inflammatory interleukin-10 responses in comparison to other viral strains. *Vet. Immunol. Immunopathol.* **2011**, *143*, 116–124, doi:10.1016/j.vetimm.2011.06.032.
- 41. Wimer, C.L.; Damiani, A.; Osterrieder, N.; Wagner, B. Equine herpesvirus type-1 modulates CCL2, CCL3, CCL5, CXCL9, and CXCL10 chemokine expression. *Vet. Immunol. Immunopathol.* **2011**, *140*, 266–274, doi:10.1016/j.vetimm.2011.01.009.
- 42. Poelaert, K.C.K.; Van Cleemput, J.; Laval, K.; Favoreel, H.W.; Soboll Hussey, G.; Maes, R.K.; Nauwynck, H.J. Abortigenic but Not Neurotropic Equine Herpes Virus 1 Modulates the Interferon Antiviral Defense. *Front. Cell. Infect. Microbiol.* **2018**, 8, 312,

- doi:10.3389/fcimb.2018.00312.
- 43. Poelaert, K.C.K.; Van Cleemput, J.; Laval, K.; Xie, J.; Favoreel, H.W.; Nauwynck, H.J. Equine herpesvirus 1 infection orchestrates the expression of chemokines in equine respiratory epithelial cells. *J. Gen. Virol.* **2019**, jgv001317, doi:10.1099/jgv.0.001317.
- 44. Babcock, G.J.; Decker, L.L.; Volk, M.; Thorley-Lawson, D.A.; Anagnostopoulos, I.; Hummel, M.; Kreschel, C.; Stein, H.; Beaufils, P.; Choquet, D.; et al. EBV persistence in memory B cells in vivo. *Immunity* **1998**, *9*, 395–404, doi:10.1016/S1074-7613(00)80622-6.
- 45. Zhao, J.; Poelaert, K.C.K.; Van Cleemput, J.; Nauwynck, H.J. CCL2 and CCL5 driven attraction of CD172a(+) monocytic cells during an equine herpesvirus type 1 (EHV-1) infection in equine nasal mucosa and the impact of two migration inhibitors, rosiglitazone (RSG) and quinacrine (QC). *Vet. Res.* **2017**, *48*, 14, doi:10.1186/s13567-017-0419-4.
- 46. Wuest, T.R.; Carr, D.J.J. The role of chemokines during herpes simplex virus-1 infection. *Front. Biosci.* **2008**, *13*, 4862–4872, doi:10.2741/3045.
- 47. Owen, J.A.; Punt, J.; Stransford, S.A.; Jones, P.P.; Kuby, J. Chapter 11. T-Cell activation, differentiation, and memory. In *Kuby immunology*; W.H. Freeman and Company: New York, NY, USA, 2013; pp. 357–384.
- 48. Owen, J.A.; Punt, J.; Stranford, S.A.; Jones, P.P.; Kuby, J. Chapter 12. B-Cell activation, differentiation, and memory generation. In *Kuby immunology*; W.H. Freeman and Company: New York, NY, USA, 2013; pp. 385–414.
- 49. Goehring, L.S.; Wagner, B.; Bigbie, R.; Hussey, S.B.; Rao, S.; Morley, P.S.; Lunn, D.P. Control of EHV-1 viremia and nasal shedding by commercial vaccines. *Vaccine* **2010**, 28, 5203–5211, doi:10.1016/j.vaccine.2010.05.065.
- 50. Goodman, L.B.; Wagner, B.; Flaminio, M.J.B.F.; Sussman, K.H.; Metzger, S.M.; Holland, R.; Osterrieder, N. Comparison of the efficacy of inactivated combination and modified-live virus vaccines against challenge infection with neuropathogenic equine herpesvirus type 1 (EHV-1). *Vaccine* **2006**, *24*, 3636–3645, doi:10.1016/j.vaccine.2006.01.062.
- 51. Breathnach, C.C.; Yeargan, M.R.; Sheoran, A.S.; Allen, G.P. The mucosal humoral immune response of the horse to infective challenge and vaccination with Equine herpesvirus-1 antigens. *Equine Vet. J.* **2001**, *33*, 651–657, doi:10.2746/042516401776249318.
- 52. Owen, J.A.; Punt, J.; Stranford, S.A.; Jones, P.P.; Kuby, J. Chapter 3. Receptors and signaling: B and T-Cell Receptors. In *Kuby immunology*; W.H. Freeman and Company: New York, NY, USA, 2013; pp. 65–104.
- 53. O'Neill, T.; Kydd, J.H.; Allen, G.P.; Wattrang, E.; Mumford, J.A.; Hannant, D.

- Determination of equid herpesvirus 1-specific, CD8+, cytotoxic T lymphocyte precursor frequencies in ponies. *Vet. Immunol. Immunopathol.* **1999**, *70*, 43–54, doi:10.1016/S0165-2427(99)00037-9.
- 54. Kydd, J.H.; Wattrang, E.; Hannant, D. Pre-infection frequencies of equine herpesvirus-1 specific, cytotoxic T lymphocytes correlate with protection against abortion following experimental infection of pregnant mares. *Vet. Immunol. Immunopathol.* **2003**, *96*, 207–217, doi:10.1016/j.vetimm.2003.08.004.
- 55. Rappocciolo, G.; Birch, J.; Ellis, S.A. Down-regulation of MHC class I expression by equine herpesvirus-1. *J. Gen. Virol.* **2003**, *84*, 293–300, doi:10.1099/vir.0.18612-0.
- 56. Ma, G.; Feineis, S.; Osterrieder, N.; Van de Walle, G.R. Identification and characterization of equine herpesvirus type 1 pUL56 and its role in virus-induced downregulation of major histocompatibility complex class I. *J. Virol.* **2012**, *86*, 3554–3563, doi:10.1128/JVI.06994-11.
- 57. Ambagala, A.P.N.; Gopinath, R.S.; Srikumaran, S. Peptide transport activity of the transporter associated with antigen processing (TAP) is inhibited by an early protein of equine herpesvirus-1. *J. Gen. Virol.* **2004**, *85*, 349–353, doi:10.1099/vir.0.19563-0.
- 58. KYDD, J.H.; SMITH, K.C.; HANNANT, D.; LIVESAY, G.J.; MUMFORD, J.A. Distribution of Equid herpesvirus-1 (EHV-1) in the respiratory tract of ponies: implications for vaccination strategies. *Equine Vet. J.* **1994**, *26*, 466–469, doi:10.1111/j.2042-3306.1994.tb04051.x.
- 59. KYDD, J.H.; SMITH, K.C.; HANNANT, D.; LIVESAY, G.J.; MUMFORD, J.A. Distribution of Equid herpesvirus-1 (EHV-1) in respiratory tract associated lymphoid tissue: implications for cellular immunity. *Equine Vet. J.* **1994**, *26*, 470–473, doi:10.1111/j.2042-3306.1994.tb04052.x.
- 60. Poelaert, K.C.K.; Van Cleemput, J.; Laval, K.; Favoreel, H.W.; Couck, L.; Van den Broeck, W.; Azab, W.; Nauwynck, H.J. Equine herpesvirus 1 bridles T-lymphocytes to reach its target organs. *J. Virol.* **2019**, JVI.02098-18, doi:10.1128/JVI.02098-18.
- 61. Van de Walle, G.R.; Jarosinski, K.W.; Osterrieder, N. Alphaherpesviruses and Chemokines: Pas de Deux Not Yet Brought to Perfection. *J. Virol.* **2007**, *82*, 6090 LP 6097.
- 62. Bryant, N.A.; Davis-Poynter, N.; Vanderplasschen, A.; Alcami, A. Glycoprotein G isoforms from some alphaherpesviruses function as broad-spectrum chemokine binding proteins. *EMBO J.* **2003**, 22, 833–846, doi:10.1093/emboj/cdg092.
- 63. Van de Walle, G.R.; May, M.L.; Sukhumavasi, W.; von Einem, J.; Osterrieder, N. Herpesvirus chemokine-binding glycoprotein G (gG) efficiently inhibits neutrophil chemotaxis in vitro and in vivo. *J. Immunol.* **2007**, *179*, 4161–4169,

- doi:10.4049/jimmunol.179.6.4161.
- 64. Van de Walle, G.R.; Sakamoto, K.; Osterrieder, N. CCL3 and viral chemokine-binding protein gg modulate pulmonary inflammation and virus replication during equine herpesvirus 1 infection. *J. Virol.* **2008**, *82*, 1714–1722, doi:10.1128/JVI.02137-07.
- 65. Slater, J. Chapter 14 Equine Herpesviruses. In; Sellon, D.C., Long, M.T.B.T.-E.I.D. (Second E., Eds.; W.B. Saunders: St. Louis, 2014; pp. 151-168.e8 ISBN 978-1-4557-0891-8.
- of equine herpesvirus 1 and other herpesviruses of veterinary importance. *Vet. Immunol. Immunopathol.* **2006**, *111*, 31–40, doi:10.1016/j.vetimm.2006.01.006.
- 67. van der Meulen, K.M.; Nauwynck, H.J.; Pensaert, M.B. Absence of viral antigens on the surface of equine herpesvirus-1-infected peripheral blood mononuclear cells: a strategy to avoid complement-mediated lysis. *J. Gen. Virol.* **2003**, *84*, 93–97, doi:10.1099/vir.0.18864-0.
- 68. Caughman, G.B.; Lewis, J.B.; Smith, R.H.; Harty, R.N.; O'Callaghan, D.J. Detection and intracellular localization of equine herpesvirus 1 IR1 and IR2 gene products by using monoclonal antibodies. *J. Virol.* **1995**, *69*, 3024–3032.
- 69. Harty, R.N.; Callaghan, D.J. An early gene maps within and is 3' coterminal with the immediate-early gene of equine herpesvirus 1. *J. Virol.* **1991**, *65*, 3829 LP 3838.
- 70. Kim, S.K.; Ahn, B.C.; Albrecht, R.A.; O' Callaghan, D.J. The Unique IR2 Protein of Equine Herpesvirus 1 Negatively Regulates Viral Gene Expression. *J. Virol.* **2006**, *80*, 5041 LP 5049, doi:10.1128/JVI.80.10.5041-5049.2006.
- 71. Kim, S.K.; Kim, S.; Dai, G.; Zhang, Y.; Ahn, B.C.; O'Callaghan, D.J. Identification of functional domains of the IR2 protein of equine herpesvirus 1 required for inhibition of viral gene expression and replication. *Virology* **2011**, *417*, 430–442, doi:10.1016/j.virol.2011.06.023.
- 72. Wilson, J.M. Adenoviruses as gene-delivery vehicles. *N. Engl. J. Med.* **1996**, *334*, 1185–1187, doi:10.1056/NEJM199605023341809.
- 73. Sambrook, J.; Fritsch, E.F.; Maniatis, T. *Molecular cloning: A laboratory manual*; 2nd ed.; Cold Spring Harbor Laboratory Press: Cold Spring Harbor, NY, 1989; ISBN 0 87969 309 6.
- 74. Smith, R.H.; Caughman, G.B.; O'Callaghan, D.J. Characterization of the regulatory functions of the equine herpesvirus 1 immediate-early gene product. *J. Virol.* **1992**, *66*, 936–945.
- 75. Reed, L.J.; Muench, H. A simple method of estimating fifty per cent endpoints,. *Am. J.*

- Epidemiol. 1938, 27, 493–497.
- 76. Soboll Hussey, G.; Hussey, S.B.; Wagner, B.; Horohov, D.W.; Van de Walle, G.R.; Osterrieder, N.; Goehring, L.S.; Rao, S.; Lunn, D.P. Evaluation of immune responses following infection of ponies with an EHV-1 ORF1/2 deletion mutant. *Vet. Res.* **2011**, *42*, doi:10.1186/1297-9716-42-23.
- 77. Soboll, G.; Hussey, S.B.; Whalley, J.M.; Allen, G.P.; Koen, M.T.; Santucci, N.; Fraser, D.G.; Macklin, M.D.; Swain, W.F.; Lunn, D.P. Antibody and cellular immune responses following DNA vaccination and EHV-1 infection of ponies. *Vet. Immunol. Immunopathol.* **2006**, *111*, 81–95, doi:10.1016/j.vetimm.2006.01.011.
- 78. Wagner, B.; Freer, H. Development of a bead-based multiplex assay for simultaneous quantification of cytokines in horses. *Vet. Immunol. Immunopathol.* **2009**, *127*, 242–248, doi:10.1016/j.vetimm.2008.10.313.
- 79. Netea, M.G.; van Crevel, R. BCG-induced protection: effects on innate immune memory. *Semin. Immunol.* **2014**, *26*, 512–517, doi:10.1016/j.smim.2014.09.006.
- 80. Aaby, P.; Samb, B.; Simondon, F.; Seck, A.M.; Knudsen, K.; Whittle, H. Non-specific beneficial effect of measles immunisation: analysis of mortality studies from developing countries. *BMJ* **1995**, *311*, 481–485, doi:10.1136/bmj.311.7003.481.
- 81. Negi, S.; Das, D.K.; Pahari, S.; Nadeem, S.; Agrewala, J.N. Potential Role of Gut Microbiota in Induction and Regulation of Innate Immune Memory. *Front. Immunol.* **2019**, *10*, 2441, doi:10.3389/fimmu.2019.02441.
- 82. Netea, M.G.; Quintin, J.; van der Meer, J.W.M. Trained immunity: a memory for innate host defense. *Cell Host Microbe* **2011**, *9*, 355–361, doi:10.1016/j.chom.2011.04.006.
- 83. Netea, M.G.; Joosten, L.A.B.; Latz, E.; Mills, K.H.G.; Natoli, G.; Stunnenberg, H.G.; O'Neill, L.A.J.; Xavier, R.J. Trained immunity: A program of innate immune memory in health and disease. *Science* **2016**, *352*, aaf1098–aaf1098, doi:10.1126/science.aaf1098.
- 84. Selin, L.K.; Cornberg, M.; Brehm, M.A.; Kim, S.-K.; Calcagno, C.; Ghersi, D.; Puzone, R.; Celada, F.; Welsh, R.M. CD8 memory T cells: cross-reactivity and heterologous immunity. *Semin. Immunol.* **2004**, *16*, 335–347, doi:https://doi.org/10.1016/j.smim.2004.08.014.
- 85. Berg, R.E.; Crossley, E.; Murray, S.; Forman, J. Memory CD8+ T cells provide innate immune protection against Listeria monocytogenes in the absence of cognate antigen. *J. Exp. Med.* **2003**, *198*, 1583–1593, doi:10.1084/jem.20031051.
- 86. Singh, S.; Vedi, S.; Samrat, S.K.; Li, W.; Kumar, R.; Agrawal, B. Heterologous Immunity between Adenoviruses and Hepatitis C Virus: A New Paradigm in HCV Immunity and Vaccines. *PLoS One* **2016**, *11*, e0146404–e0146404, doi:10.1371/journal.pone.0146404.

- 87. Muruve, D.A. The innate immune response to adenovirus vectors. *Hum. Gene Ther.* **2004**, *15*, 1157–1166, doi:10.1089/hum.2004.15.1157.
- 88. Liu, Q.; Zaiss, A.K.; Colarusso, P.; Patel, K.; Haljan, G.; Wickham, T.J.; Muruve, D.A. The role of capsid-endothelial interactions in the innate immune response to adenovirus vectors. *Hum. Gene Ther.* **2003**, *14*, 627–643, doi:10.1089/104303403321618146.
- 89. Borgland, S.L.; Bowen, G.P.; Wong, N.C.; Libermann, T.A.; Muruve, D.A. Adenovirus vector-induced expression of the C-X-C chemokine IP-10 is mediated through capsid-dependent activation of NF-kappaB. *J. Virol.* **2000**, *74*, 3941–3947, doi:10.1128/jvi.74.9.3941-3947.2000.
- 90. Bowen, G.P.; Borgland, S.L.; Lam, M.; Libermann, T.A.; Wong, N.C.W.; Muruve, D.A. Adenovirus vector-induced inflammation: capsid-dependent induction of the C-C chemokine RANTES requires NF-kappa B. *Hum. Gene Ther.* **2002**, *13*, 367–379, doi:10.1089/10430340252792503.
- 91. Rojas, J.M.; Avia, M.; Martin, V.; Sevilla, N. IL-10: A Multifunctional Cytokine in Viral Infections. *J. Immunol. Res.* **2017**, 2017, 6104054, doi:10.1155/2017/6104054.
- 92. Ishihara, A.; Zachos, T.A.; Bartlett, J.S.; Bertone, A.L. Evaluation of permissiveness and cytotoxic effects in equine chondrocytes, synovial cells, and stem cells in response to infection with adenovirus 5 vectors for gene delivery. *Am. J. Vet. Res.* **2006**, *67*, 1145–1155, doi:10.2460/ajvr.67.7.1145.
- 93. Damjanovic, D.; Zhang, X.; Mu, J.; Fe Medina, M.; Xing, Z. Organ distribution of transgene expression following intranasal mucosal delivery of recombinant replication-defective adenovirus gene transfer vector. *Genet. Vaccines Ther.* **2008**, *6*, 5, doi:10.1186/1479-0556-6-5.
- 94. Grubb, B.R.; Pickles, R.J.; Ye, H.; Yankaskas, J.R.; Vick, R.N.; Engelhardt, J.F.; Wilson, J.M.; Johnson, L.G.; Boucher, R.C. Inefficient gene transfer by adenovirus vector to cystic fibrosis airway epithelia of mice and humans. *Nature* **1994**, *371*, 802–806, doi:10.1038/371802a0.
- 95. Knowles, M.R.; Hohneker, K.W.; Zhou, Z.; Olsen, J.C.; Noah, T.L.; Hu, P.-C.; Leigh, M.W.; Engelhardt, J.F.; Edwards, L.J.; Jones, K.R.; et al. A Controlled Study of Adenoviral-Vector–Mediated Gene Transfer in the Nasal Epithelium of Patients with Cystic Fibrosis. *N. Engl. J. Med.* **1995**, *333*, 823–831, doi:10.1056/NEJM199509283331302.
- 96. Zabner, J.; Ramsey, B.W.; Meeker, D.P.; Aitken, M.L.; Balfour, R.P.; Gibson, R.L.; Launspach, J.; Moscicki, R.A.; Richards, S.M.; Standaert, T.A.; et al. Repeat administration of an adenovirus vector encoding cystic fibrosis transmembrane conductance regulator to the nasal epithelium of patients with cystic fibrosis. *J. Clin. Invest.* **1996**, *97*, 1504–1511, doi:10.1172/JCI118573.

- 97. Zabner, J.; Zeiher, B.G.; Friedman, E.; Welsh, M.J. Adenovirus-mediated gene transfer to ciliated airway epithelia requires prolonged incubation time. *J. Virol.* **1996**, *70*, 6994–7003.
- 98. Zabner, J.; Freimuth, P.; Puga, A.; Fabrega, A.; Welsh, M.J. Lack of high affinity fiber receptor activity explains the resistance of ciliated airway epithelia to adenovirus infection. *J. Clin. Invest.* **1997**, *100*, 1144–1149, doi:10.1172/JCI119625.
- 99. Pickles, R.J.; McCarty, D.; Matsui, H.; Hart, P.J.; Randell, S.H.; Boucher, R.C. Limited entry of adenovirus vectors into well-differentiated airway epithelium is responsible for inefficient gene transfer. *J. Virol.* **1998**, *72*, 6014–6023.
- 100. Chu, Q.; St. George, J.A.; Lukason, M.; Cheng, S.H.; Scheule, R.K.; Eastman, S.J. EGTA Enhancement of Adenovirus-Mediated Gene Transfer to Mouse Tracheal Epithelium in Vivo. *Hum. Gene Ther.* **2001**, *12*, 455–467, doi:10.1089/104303401300042348.
- 101. Pickles, R.J.; Barker, P.M.; Ye, H.; Boucher, R.C. Efficient Adenovirus-Mediated Gene Transfer to Basal but Not Columnar Cells of Cartilaginous Airway Epithelia. *Hum. Gene Ther.* **1996**, *7*, 921–931, doi:10.1089/hum.1996.7.8-921.
- 102. Gibson, J.S.; O'Neill, T.; Thackray, A.; Hannant, D.; Field, H.J. Serological responses of specific pathogen-free foals to equine herpesvirus-1: primary and secondary infection, and reactivation. *Vet. Microbiol.* 1992, 32, 199–214, doi:https://doi.org/10.1016/0378-1135(92)90145-J.
- 103. Hannant, D.; Jessett, D.M.; O'Neill, T.; Dolby, C.A.; Cook, R.F.; Mumford, J.A. Responses of ponies to equid herpesvirus-1 ISCOM vaccination and challenge with virus of the homologous strain. *Res. Vet. Sci.* **1993**, *54*, 299–305, doi:10.1016/0034-5288(93)90126-z.
- 104. Amorij, J.-P.; Hinrichs, W.L.J.; Frijlink, H.W.; Wilschut, J.C.; Huckriede, A. Needle-free influenza vaccination. *Lancet Infect. Dis.* **2010**, *10*, 699–711, doi:10.1016/S1473-3099(10)70157-2.
- 105. Lunn, D.P.; Soboll, G.; Schram, B.R.; Quass, J.; McGregor, M.W.; Drape, R.J.; Macklin, M.D.; McCabe, D.E.; Swain, W.F.; Olsen, C.W. Antibody responses to DNA vaccination of horses using the influenza virus hemagglutinin gene. *Vaccine* **1999**, *17*, 2245–2258, doi:https://doi.org/10.1016/S0264-410X(98)00496-4.
- 106. Nelson, K.M.; Schram, B.R.; McGregor, M.W.; Sheoran, A.S.; Olsen, C.W.; Lunn, D.P. Local and systemic isotype-specific antibody responses to equine influenza virus infection versus conventional vaccination. *Vaccine* **1998**, *16*, 1306–1313, doi:10.1016/s0264-410x(98)00009-7.
- 107. Wattrang, E.; Jessett, D.M.; Yates, P.; Fuxler, L.; Hannant, D. Experimental infection of ponies with equine influenza A2 (H3N8) virus strains of different pathogenicity elicits

- varying interferon and interleukin-6 responses. *Viral Immunol.* **2003**, *16*, 57–67, doi:10.1089/088282403763635456.
- 108. Oslund, K.L.; Baumgarth, N. Influenza-induced innate immunity: regulators of viral replication, respiratory tract pathology & adaptive immunity. *Future Virol.* **2011**, *6*, 951–962, doi:10.2217/fvl.11.63.
- 109. Forero, A.; Fenstermacher, K.; Wohlgemuth, N.; Nishida, A.; Carter, V.; Smith, E.A.; Peng, X.; Hayes, M.; Francis, D.; Treanor, J.; et al. Evaluation of the innate immune responses to influenza and live-attenuated influenza vaccine infection in primary differentiated human nasal epithelial cells. *Vaccine* **2017**, *35*, 6112–6121, doi:10.1016/j.vaccine.2017.09.058.
- 110. Fischer II, W.A.; Chason, K.D.; Brighton, M.; Jaspers, I. Live attenuated influenza vaccine strains elicit a greater innate immune response than antigenically-matched seasonal influenza viruses during infection of human nasal epithelial cell cultures. *Vaccine* **2014**, *32*, 1761–1767, doi:https://doi.org/10.1016/j.vaccine.2013.12.069.
- 111. Barría, M.I.; Garrido, J.L.; Stein, C.; Scher, E.; Ge, Y.; Engel, S.M.; Kraus, T.A.; Banach, D.; Moran, T.M. Localized mucosal response to intranasal live attenuated influenza vaccine in adults. *J. Infect. Dis.* **2013**, *207*, 115–124, doi:10.1093/infdis/jis641.
- 112. Matsukura, S.; Kokubu, F.; Noda, H.; Tokunaga, H.; Adachi, M. Expression of IL-6, IL-8, and RANTES on human bronchial epithelial cells, NCI-H292, induced by influenza virus A. *J. Allergy Clin. Immunol.* **1996**, *98*, 1080–1087, doi:10.1016/S0091-6749(96)80195-3.
- 113. Belyakov, I.M.; Ahlers, J.D. What role does the route of immunization play in the generation of protective immunity against mucosal pathogens? *J. Immunol.* **2009**, *183*, 6883–6892, doi:10.4049/jimmunol.0901466.
- 114. Lunn, D.P.; Hussey, S.; Sebring, R.; Rushlow, K.E.; Radecki, S. V; Whitaker-Dowling, P.; Youngner, J.S.; Chambers, T.M.; Holland, R.E.; Horohov, D.W. Safety, efficacy, and immunogenicity of a modified-live equine influenza virus vaccine in ponies after induction of exercise-induced immunosuppression. *J. Am. Vet. Med. Assoc.* **2001**, *218*, 900–906, doi:10.2460/javma.2001.218.900.
- 115. Chambers, T.M.; Holland, R.E.; Tudor, L.R.; Townsend, H.G.G.; Cook, A.; Bogdan, J.; Lunn, D.P.; Hussey, S.; Whitaker-Dowling, P.; Youngner, J.S.; et al. A new modified live equine influenza virus vaccine: phenotypic stability, restricted spread and efficacy against heterologous virus challenge. *Equine Vet. J.* **2001**, *33*, 630–636, doi:10.2746/042516401776249291.
- 116. Townsend, H.G.G.; Penner, S.J.; Watts, T.C.; Cook, A.; Bogdan, J.; Haines, D.M.; Griffin, S.; Chambers, T.; Holland, R.E.; Whitaker-Dowling, P.; et al. Efficacy of a coldadapted, intranasal, equine influenza vaccine: challenge trials. *Equine Vet. J.* **2001**, *33*, 637–643, doi:10.2746/042516401776249354.

- 117. Zarski, L.M.; Seong, K.K.; Lee, Y.; Holz, C.L.; Nelli, R.K.; Weber, P.S.D.; Soboll Hussey, G. Administration of recombinant adenovirus expressing inhibitory IR2 protein for control of equine herpesvirus 1 infection and disease. *Prep.* **2020**.
- 118. Livak, K.J.; Schmittgen, T.D. Analysis of Relative Gene Expression Data Using Real-Time Quantitative PCR and the 2–ΔΔCT Method. *Methods* **2001**, *25*, 402–408, doi:https://doi.org/10.1006/meth.2001.1262.
- 119. Keck, T.; Leiacker, R.; Heinrich, A.; Kuhnemann, S.; Rettinger, G. Humidity and temperature profile in the nasal cavity. *Rhinology* **2000**, *38*, 167–171.
- 120. Pecoraro, H.L.; Koch, D.; Soboll Hussey, G.; Bentsen, L.; Landolt, G.A. Comparison of innate immune responses in equine respiratory epithelial cells to modified-live equine influenza vaccine and related wild-type influenza virus. *J. Vet. Intern. Med.* **2014**, 28, 1346–1374, doi:10.1111/jvim.12375.
- 121. Hayden, F.G.; Fritz, R.; Lobo, M.C.; Alvord, W.; Strober, W.; Straus, S.E. Local and systemic cytokine responses during experimental human influenza A virus infection. Relation to symptom formation and host defense. *J. Clin. Invest.* **1998**, *101*, 643–649, doi:10.1172/JCI1355.
- 122. Sommereyns, C.; Paul, S.; Staeheli, P.; Michiels, T. IFN-lambda (IFN-lambda) is expressed in a tissue-dependent fashion and primarily acts on epithelial cells in vivo. *PLoS Pathog.* **2008**, *4*, e1000017–e1000017, doi:10.1371/journal.ppat.1000017.
- 123. Jewell, N.A.; Cline, T.; Mertz, S.E.; Smirnov, S. V; Flaño, E.; Schindler, C.; Grieves, J.L.; Durbin, R.K.; Kotenko, S. V; Durbin, J.E. Lambda interferon is the predominant interferon induced by influenza A virus infection in vivo. *J. Virol.* **2010**, *84*, 11515–11522, doi:10.1128/JVI.01703-09.
- 124. Schaller, M.; Hogaboam, C.M.; Lukacs, N.; Kunkel, S.L. Respiratory viral infections drive chemokine expression and exacerbate the asthmatic response. *J. Allergy Clin. Immunol.* **2006**, *118*, 294–295, doi:10.1016/j.jaci.2006.05.025.
- 125. Herold, S.; von Wulffen, W.; Steinmueller, M.; Pleschka, S.; Kuziel, W.A.; Mack, M.; Srivastava, M.; Seeger, W.; Maus, U.A.; Lohmeyer, J. Alveolar epithelial cells direct monocyte transepithelial migration upon influenza virus infection: impact of chemokines and adhesion molecules. *J. Immunol.* **2006**, *177*, 1817–1824, doi:10.4049/jimmunol.177.3.1817.
- 126. Ramos, I.; Fernandez-Sesma, A. Modulating the Innate Immune Response to Influenza A Virus: Potential Therapeutic Use of Anti-Inflammatory Drugs. *Front. Immunol.* **2015**, *6*, 361, doi:10.3389/fimmu.2015.00361.
- 127. Van Raemdonck, K.; Van den Steen, P.E.; Liekens, S.; Van Damme, J.; Struyf, S. CXCR3 ligands in disease and therapy. *Cytokine Growth Factor Rev.* **2015**, *26*, 311–327,

- doi:10.1016/j.cytogfr.2014.11.009.
- 128. Wang, J.; Nikrad, M.P.; Phang, T.; Gao, B.; Alford, T.; Ito, Y.; Edeen, K.; Travanty, E.A.; Kosmider, B.; Hartshorn, K.; et al. Innate immune response to influenza A virus in differentiated human alveolar type II cells. *Am. J. Respir. Cell Mol. Biol.* **2011**, *45*, 582–591, doi:10.1165/rcmb.2010-0108OC.
- 129. Salvi, S.; Holgate, S.T. Could the airway epithelium play an important role in mucosal immunoglobulin A production? *Clin. Exp. Allergy* **1999**, *29*, 1597–1605, doi:10.1046/j.1365-2222.1999.00644.x.
- 130. Pellett, P.; Roizman, B. Chapter 59. Herpesviridae. In *Fields Virology*; Knipe, D., Howley, P., Cohen, J., Griffin, D., Lamb, R., Martin, M., Racaniello, V., Roizman, B., Eds.; Lippincott, Williams & Wilkins: Philadelphia, PA, 2013; pp. 1803–1822.
- 131. Oladunni, F.S.; Horohov, D.W.; Chambers, T.M. EHV-1: A Constant Threat to the Horse Industry . *Front. Microbiol.* 2019, *10*, 2668.
- 132. Giessler, K.S.; Samoilowa, S.; Soboll Hussey, G.; Kiupel, M.; Matiasek, K.; Sledge, D.J.; Liesche, F.; Schlegel, J.; Fux, R.; Goehring, L.S. Viral load and cell tropism during early latent Equid Herpesvirus 1 infection differ over time in lymphoid and neural tissue samples from experimentally infected horses. *Front. Vet. Sci.* **2020**, *7*, doi:10.3389/fvets.2020.00621.
- 133. Marenzoni, M.L.; Stefanetti, V.; Danzetta, M.L.; Timoney, P.J. Gammaherpesvirus infections in equids: a review. *Vet. Med. (Auckland, N.Z.)* **2015**, *6*, 91–101, doi:10.2147/VMRR.S39473.
- 134. van Maanen, C. Equine herpesvirus 1 and 4 infections: an update. *Vet. Q.* **2002**, *24*, 58–78.
- 135. Gryspeerdt, A.C.; Vandekerckhove, A.P.; Garré, B.; Barbé, F.; Van de Walle, G.R.; Nauwynck, H.J. Differences in replication kinetics and cell tropism between neurovirulent and non-neurovirulent EHV1 strains during the acute phase of infection in horses. *Vet. Microbiol.* **2010**, *142*, 242–253, doi:10.1016/j.vetmic.2009.10.015.
- 136. Wilsterman, S.; Soboll-Hussey, G.; Lunn, D.P.; Ashton, L. V; Callan, R.J.; Hussey, S.B.; Rao, S.; Goehring, L.S. Equine herpesvirus-1 infected peripheral blood mononuclear cell subpopulations during viremia. *Vet. Microbiol.* **2011**, *149*, 40–47, doi:10.1016/j.vetmic.2010.10.004.
- 137. Scott, J.C.; Dutta, S.K.; Myrup, A.C. In vivo harboring of equine herpesvirus-1 in leukocyte populations and subpopulations and their quantitation from experimentally infected ponies. *Am. J. Vet. Res.* **1983**, *44*, 1344–1348.
- 138. van Der Meulen, K.M.; Nauwynck, H.J.; Buddaert, W.; Pensaert, M.B. Replication of

- equine herpesvirus type 1 in freshly isolated equine peripheral blood mononuclear cells and changes in susceptibility following mitogen stimulation. *J. Gen. Virol.* **2000**, 81, 21–25, doi:10.1099/0022-1317-81-1-21.
- 139. Shukla, G.C.; Singh, J.; Barik, S. MicroRNAs: Processing, maturation, target recognition and regulatory functions. *Mol. Cell. Pharmacol.* **2011**, *3*, 83–92.
- 140. Zheng, S.; Li, Y.; Zhang, Y.; Li, X.; Tang, H. MiR-101 regulates HSV-1 replication by targeting ATP5B. *Antiviral Res.* **2011**, *89*, 219–226, doi:10.1016/j.antiviral.2011.01.008.
- 141. Boss, I.W.; Renne, R. Viral miRNAs and immune evasion. *Biochim. Biophys. Acta* **2011**, *1809*, 708–714, doi:10.1016/j.bbagrm.2011.06.012.
- 142. Matsumura, T.; Kondo, T.; Sugita, S.; Damiani, A.M.; O'Callaghan, D.J.; Imagawa, H. An Equine Herpesvirus Type 1 Recombinant with a Deletion in the gE and gI Genes Is Avirulent in Young Horses. *Virology* **1998**, *242*, 68–79, doi:https://doi.org/10.1006/viro.1997.8984.
- 143. Shakya, A.K.; O'Callaghan, D.J.; Kim, S.K. Comparative Genomic Sequencing and Pathogenic Properties of Equine Herpesvirus 1 KyA and RacL11. *Front. Vet. Sci.* **2017**, *4*, 211, doi:10.3389/fvets.2017.00211.
- 144. Said, A.; Osterrieder, N. Equine herpesvirus type 1 (EHV-1) open reading frame 59 encodes an early protein that is localized to the cytosol and required for efficient virus growth. *Virology* **2014**, *449*, 263–269, doi:https://doi.org/10.1016/j.virol.2013.11.035.
- 145. Huang, R.; Hu, Z.; Cao, Y.; Li, H.; Zhang, H.; Su, W.; Xu, Y.; Liang, L.; Melgiri, N.D.; Jiang, L. MiR-652-3p inhibition enhances endothelial repair and reduces atherosclerosis by promoting Cyclin D2 expression. *EBioMedicine* **2019**, *40*, 685–694, doi:https://doi.org/10.1016/j.ebiom.2019.01.032.
- 146. Poudyal, D.; Herman, A.; Adelsberger, J.W.; Yang, J.; Hu, X.; Chen, Q.; Bosche, M.; Sherman, B.T.; Imamichi, T. A novel microRNA, hsa-miR-6852 differentially regulated by Interleukin-27 induces necrosis in cervical cancer cells by downregulating the FoxM1 expression. *Sci. Rep.* **2018**, *8*, 900, doi:10.1038/s41598-018-19259-4.
- 147. Mossman, K.L.; Ashkar, A.A. Herpesviruses and the innate immune response. *Viral Immunol.* **2005**, *18*, 267–281, doi:10.1089/vim.2005.18.267.
- 148. Ivashkiv, L.B.; Donlin, L.T. Regulation of type I interferon responses. *Nat. Rev. Immunol.* **2014**, *14*, 36–49, doi:10.1038/nri3581.
- 149. Kumari, P.; Narayanan, S.; Kumar, H. Herpesviruses: interfering innate immunity by targeting viral sensing and interferon pathways. *Rev. Med. Virol.* **2015**, 25, 187–201, doi:10.1002/rmv.1836.
- 150. Dupuis, S.; Jouanguy, E.; Al-Hajjar, S.; Fieschi, C.; Al-Mohsen, I.Z.; Al-Jumaah, S.;

- Yang, K.; Chapgier, A.; Eidenschenk, C.; Eid, P.; et al. Impaired response to interferon- $\alpha/\beta$  and lethal viral disease in human STAT1 deficiency. *Nat. Genet.* **2003**, *33*, 388–391, doi:10.1038/ng1097.
- 151. Bin, L.; Edwards, M.G.; Heiser, R.; Streib, J.; Richers, B.; Leung, D.Y.M. Identification Of Novel Gene Signatures In Atopic Dermatitis Complicated By Eczema Herpeticum. *J. Allergy Clin. Immunol.* **2014**, *133*, AB193, doi:10.1016/j.jaci.2013.12.690.
- 152. Oladunni, F.S.; Sarkar, S.; Reedy, S.; Balasuriya, U.B.R.; Horohov, D.W.; Chambers, T.M. Equid Herpesvirus 1 Targets the Sensitization and Induction Steps To Inhibit the Type I Interferon Response in Equine Endothelial Cells. *J. Virol.* **2019**, *93*, e01342-19, doi:10.1128/JVI.01342-19.
- 153. Sarkar, S.; Balasuriya, U.B.R.; Horohov, D.W.; Chambers, T.M. Equine herpesvirus-1 suppresses type-I interferon induction in equine endothelial cells. *Vet. Immunol. Immunopathol.* **2015**, *167*, 122–129, doi:10.1016/j.vetimm.2015.07.015.
- 154. Scherer, C.A.; Magness, C.L.; Steiger, K. V; Poitinger, N.D.; Caputo, C.M.; Miner, D.G.; Winokur, P.L.; Klinzman, D.; McKee, J.; Pilar, C.; et al. Distinct gene expression profiles in peripheral blood mononuclear cells from patients infected with vaccinia virus, yellow fever 17D virus, or upper respiratory infections. *Vaccine* **2007**, *25*, 6458–6473, doi:10.1016/j.vaccine.2007.06.035.
- 155. Schmid, S.; Mordstein, M.; Kochs, G.; García-Sastre, A.; Tenoever, B.R. Transcription factor redundancy ensures induction of the antiviral state. *J. Biol. Chem.* **2010**, 285, 42013–42022, doi:10.1074/jbc.M110.165936.
- 156. Groom, J.R.; Luster, A.D. CXCR3 ligands: redundant, collaborative and antagonistic functions. *Immunol. Cell Biol.* **2011**, *89*, 207–215, doi:10.1038/icb.2010.158.
- 157. Johnstone, S.; Barsova, J.; Campos, I.; Frampton, A.R. Equine herpesvirus type 1 modulates inflammatory host immune response genes in equine endothelial cells. *Vet. Microbiol.* **2016**, *192*, 52–59, doi:10.1016/j.vetmic.2016.06.012.
- 158. Proost, P.; Wuyts, A.; van Damme, J. Human monocyte chemotactic proteins-2 and -3: structural and functional comparison with MCP-1. *J. Leukoc. Biol.* **1996**, *59*, 67–74, doi:10.1002/jlb.59.1.67.
- 159. Sun, Y.; Iglesias, E.; Samri, A.; Kamkamidze, G.; Decoville, T.; Carcelain, G.; Autran, B. A systematic comparison of methods to measure HIV-1 specific CD8 T cells. *J. Immunol. Methods* **2003**, 272, 23–34, doi:10.1016/s0022-1759(02)00328-9.
- 160. Guidotti, L.G.; Chisari, F. V Noncytolytic control of viral infections by the innate and adaptive immune response. *Annu. Rev. Immunol.* **2001**, *19*, 65–91, doi:10.1146/annurev.immunol.19.1.65.

- 161. Paillot, R.; Ellis, S.A.; Daly, J.M.; Audonnet, J.C.; Minke, J.M.; Davis-Poynter, N.; Hannant, D.; Kydd, J.H. Characterisation of CTL and IFN-γ synthesis in ponies following vaccination with a NYVAC-based construct coding for EHV-1 immediate early gene, followed by challenge infection. *Vaccine* 2006, 24, 1490–1500, doi:https://doi.org/10.1016/j.vaccine.2005.10.019.
- 162. Paillot, R.; Daly, J.M.; Luce, R.; Montesso, F.; Davis-Poynter, N.; Hannant, D.; Kydd, J.H. Frequency and phenotype of EHV-1 specific, IFN-γ synthesising lymphocytes in ponies: The effects of age, pregnancy and infection. *Dev. Comp. Immunol.* **2007**, *31*, 202–214, doi:https://doi.org/10.1016/j.dci.2006.05.010.
- 163. Breathnach, C.C.; Soboll, G.; Suresh, M.; Lunn, D.P. Equine herpesvirus-1 infection induces IFN-gamma production by equine T lymphocyte subsets. *Vet. Immunol. Immunopathol.* **2005**, *103*, 207–215, doi:10.1016/j.vetimm.2004.09.024.
- 164. Favoreel, H.W.; Nauwynck, H.J.; Pensaert, M.B. Immunological hiding of herpesvirus-infected cells. *Arch. Virol.* **2000**, *145*, 1269–1290, doi:10.1007/s007050070090.
- 165. Carroll, M.C. The complement system in B cell regulation. *Mol. Immunol.* **2004**, *41*, 141–146, doi:10.1016/j.molimm.2004.03.017.
- 166. Wagner, C.; Hänsch, G.M. Receptors for complement C3 on T-lymphocytes: Relics of evolution or functional molecules? *Mol. Immunol.* **2006**, *43*, 22–30, doi:https://doi.org/10.1016/j.molimm.2005.06.027.
- 167. Wagner, C.; Ochmann, C.; Schoels, M.; Giese, T.; Stegmaier, S.; Richter, R.; Hug, F.; Hänsch, G.M. The complement receptor 1, CR1 (CD35), mediates inhibitory signals in human T-lymphocytes. *Mol. Immunol.* **2006**, *43*, 643–651, doi:https://doi.org/10.1016/j.molimm.2005.04.006.
- 168. Wilson, J.G.; Tedder, T.F.; Fearon, D.T. Characterization of human T lymphocytes that express the C3b receptor. *J. Immunol.* **1983**, *131*, 684 LP 689.
- 169. Werfel, T.; Kirchhoff, K.; Wittmann, M.; Begemann, G.; Kapp, A.; Heidenreich, F.; Götze, O.; Zwirner, J. Activated Human T Lymphocytes Express a Functional C3a Receptor. *J. Immunol.* **2000**, *165*, 6599 LP 6605, doi:10.4049/jimmunol.165.11.6599.
- 170. Oikonomopoulou, K.; Ricklin, D.; Ward, P.A.; Lambris, J.D. Interactions between coagulation and complement--their role in inflammation. *Semin. Immunopathol.* **2012**, *34*, 151–165, doi:10.1007/s00281-011-0280-x.
- 171. Davis, A.E. 3rd Biological effects of C1 inhibitor. *Drug News Perspect.* **2004**, *17*, 439–446, doi:10.1358/dnp.2004.17.7.863703.
- 172. Adams, R.L.C.; Bird, R.J. Review article: Coagulation cascade and therapeutics update: relevance to nephrology. Part 1: Overview of coagulation, thrombophilias and history of

- anticoagulants. *Nephrology (Carlton)*. **2009**, *14*, 462–470, doi:10.1111/j.1440-1797.2009.01128.x.
- 173. Sang, Y.; Miller, L.C.; Blecha, F. Macrophage Polarization in Virus-Host Interactions. *J. Clin. Cell. Immunol.* **2015**, *6*, 311, doi:10.4172/2155-9899.1000311.
- 174. Sutton, C.E.; Mielke, L.A.; Mills, K.H.G. IL-17-producing γδ T cells and innate lymphoid cells. *Eur. J. Immunol.* **2012**, *42*, 2221–2231, doi:10.1002/eji.201242569.
- 175. Lunn, D.P.; Holmes, M.A.; Gibson, J.; Field, H.J.; Kydd, J.H.; Duffus, W.P.H. Haematological changes and equine lymphocyte subpopulation kinetics during primary infection and attempted re-infection of specific pathogen free foals with EHV-1. *Equine Vet. J.* **1991**, *23*, 35–40, doi:10.1111/j.2042-3306.1991.tb04755.x.
- 176. McCulloch, J.; Williamson, S.A.; Powis, S.J.; Edington, N. The effect of EHV-1 infection upon circulating leucocyte populations in the natural equine host. *Vet. Microbiol.* **1993**, *37*, 147–161, doi:10.1016/0378-1135(93)90189-e.
- 177. Newman, A.M.; Steen, C.B.; Liu, C.L.; Gentles, A.J.; Chaudhuri, A.A.; Scherer, F.; Khodadoust, M.S.; Esfahani, M.S.; Luca, B.A.; Steiner, D.; et al. Determining cell type abundance and expression from bulk tissues with digital cytometry. *Nat. Biotechnol.* **2019**, *37*, 773–782, doi:10.1038/s41587-019-0114-2.
- 178. Cox, E.; Reddy, S.; Iofin, I.; Cohen, J.I. Varicella-Zoster Virus ORF57, Unlike Its Pseudorabies Virus UL3.5 Homolog, Is Dispensable for Viral Replication in Cell Culture. *Virology* **1998**, *250*, 205–209, doi:https://doi.org/10.1006/viro.1998.9349.
- 179. Dean, H.J.; Cheung, A.K. A 3' coterminal gene cluster in pseudorabies virus contains herpes simplex virus UL1, UL2, and UL3 gene homologs and a unique UL3.5 open reading frame. *J. Virol.* **1993**, *67*, 5955–5961.
- 180. Chaudhuri, V.; Sommer, M.; Rajamani, J.; Zerboni, L.; Arvin, A.M. Functions of Varicella-Zoster Virus ORF23 Capsid Protein in Viral Replication and the Pathogenesis of Skin Infection. *J. Virol.* **2008**, 82, 10231 LP 10246, doi:10.1128/JVI.01890-07.
- 181. Sun, Y.; Brown, S.M. The Open Reading Frames 1, 2, 71, and 75 Are Nonessential for the Replication of Equine Herpesvirus Type 1 in Vitro. *Virology* **1994**, *199*, 448–452, doi:https://doi.org/10.1006/viro.1994.1143.
- 182. Hussey, G.S.; Goehring, L.S.; Lunn, D.P.; Hussey, S.B.; Huang, T.; Osterrieder, N.; Powell, C.; Hand, J.; Holz, C.; Slater, J. Experimental infection with equine herpesvirus type 1 (EHV-1) induces chorioretinal lesions. *Vet. Res.* **2013**, *44*, 118, doi:10.1186/1297-9716-44-118.
- 183. Drummer, H.E.; Reubel, G.H.; Studdert, M.J. Equine gammaherpesvirus 2 (EHV2) is latent in B lymphocytes. *Arch. Virol.* **1996**, *141*, 495–504, doi:10.1007/BF01718313.

- 184. Mekuria, Z.H.; El-Hage, C.; Ficorilli, N.P.; Washington, E.A.; Gilkerson, J.R.; Hartley, C.A. Mapping B lymphocytes as major reservoirs of naturally occurring latent equine herpesvirus 5 infection. *J. Gen. Virol.* **2017**, *98*, 461–470, doi:10.1099/jgv.0.000668.
- 185. Zarski, L.M.; High, E.A.; Nelli, R.K.; Bolin, S.R.; Williams, K.J.; Hussey, G. Development and application of a quantitative PCR assay to study equine herpesvirus 5 invasion and replication in equine tissues in vitro and in vivo. *J. Virol. Methods* **2017**, *248*, doi:10.1016/j.jviromet.2017.04.015.
- 186. Bell, S.A.; Balasuriya, U.B.R.; Gardner, I.A.; Barry, P.A.; Wilson, W.D.; Ferraro, G.L.; MacLachlan, N.J. Temporal detection of equine herpesvirus infections of a cohort of mares and their foals. *Vet. Microbiol.* **2006**, *116*, 249–257, doi:10.1016/j.vetmic.2006.05.002.
- 187. Akkutay, A.Z.; Osterrieder, N.; Damiani, A.; Tischer, B.K.; Borchers, K.; Alkan, F. Prevalence of equine gammaherpesviruses on breeding farms in Turkey and development of a TaqMan MGB real-time PCR to detect equine herpesvirus 5 (EHV-5). *Arch. Virol.* **2014**, *159*, 2989–2995, doi:10.1007/s00705-014-2165-5.
- 188. Anders, S.; Pyl, P.T.; Huber, W. HTSeq—a Python framework to work with high-throughput sequencing data. *Bioinformatics* **2014**, *31*, 166–169, doi:10.1093/bioinformatics/btu638.
- 189. Li, H.; Handsaker, B.; Wysoker, A.; Fennell, T.; Ruan, J.; Homer, N.; Marth, G.; Abecasis, G.; Durbin, R.; Subgroup, 1000 Genome Project Data Processing The Sequence Alignment/Map format and SAMtools. *Bioinformatics* **2009**, *25*, 2078–2079, doi:10.1093/bioinformatics/btp352.
- 190. Pertea, M.; Kim, D.; Pertea, G.M.; Leek, J.T.; Salzberg, S.L. Transcript-level expression analysis of RNA-seq experiments with HISAT, StringTie and Ballgown. *Nat. Protoc.* **2016**, *11*, 1650, doi:10.1038/nprot.2016.095.
- 191. Andrews, S. FastQC: A quality control tool for high throughput sequence data Available online: http://www.bioinformatics.babraham.ac.uk/projects/fastqc/.
- 192. Martin, M. Cutadapt removes adapter sequences from high-throughput sequencing reads. *EMBnet.journal; Vol 17, No 1 Next Gener. Seq. Data Anal. 10.14806/ej.17.1.200* **2011**.
- 193. Friedländer, M.R.; Mackowiak, S.D.; Li, N.; Chen, W.; Rajewsky, N. miRDeep2 accurately identifies known and hundreds of novel microRNA genes in seven animal clades. *Nucleic Acids Res.* **2011**, *40*, 37–52, doi:10.1093/nar/gkr688.
- 194. Griffiths-Jones, S.; Saini, H.K.; van Dongen, S.; Enright, A.J. miRBase: tools for microRNA genomics. *Nucleic Acids Res.* **2007**, *36*, D154–D158, doi:10.1093/nar/gkm952.

- 195. Love, M.I.; Huber, W.; Anders, S. Moderated estimation of fold change and dispersion for RNA-seq data with DESeq2. *Genome Biol.* **2014**, *15*, 550, doi:10.1186/s13059-014-0550-8
- 196. Yu, G.; Wang, L.-G.; Han, Y.; He, Q.-Y. clusterProfiler: an R Package for Comparing Biological Themes Among Gene Clusters. *Omi. A J. Integr. Biol.* **2012**, *16*, 284–287, doi:10.1089/omi.2011.0118.
- 197. Carlson, M. org.Hs.eg.db: Genome wide annotation for Human 2019.
- 198. Supek, F.; Bošnjak, M.; Škunca, N.; Šmuc, T. REVIGO Summarizes and Visualizes Long Lists of Gene Ontology Terms. *PLoS One* **2011**, *6*, e21800.
- 199. Robinson, J.T.; Thorvaldsdóttir, H.; Winckler, W.; Guttman, M.; Lander, E.S.; Getz, G.; Mesirov, J.P. Integrative genomics viewer. *Nat. Biotechnol.* **2011**, 29, 24–26, doi:10.1038/nbt.1754.
- 200. Robinson, M.D.; McCarthy, D.J.; Smyth, G.K. edgeR: a Bioconductor package for differential expression analysis of digital gene expression data. *Bioinformatics* **2009**, *26*, 139–140, doi:10.1093/bioinformatics/btp616.
- 201. Van de Walle, G.R.; Goupil, R.; Wishon, C.; Damiani, A.; Perkins, G.A.; Osterrieder, N. A Single-Nucleotide Polymorphism in a Herpesvirus DNA Polymerase Is Sufficient to Cause Lethal Neurological Disease. *J. Infect. Dis.* **2009**, 200, 20–25, doi:10.1086/599316.
- 202. Pusterla, N.; Hussey, G.S. Equine Herpesvirus 1 Myeloencephalopathy. *Vet. Clin. North Am. Equine Pract.* **2014**, *30*, 489–506, doi:https://doi.org/10.1016/j.cveq.2014.08.006.
- 203. Hawkins, B.T.; Davis, T.P. The blood-brain barrier/neurovascular unit in health and disease. *Pharmacol. Rev.* **2005**, *57*, 173–185, doi:10.1124/pr.57.2.4.
- 204. Bazzoni, G.; Dejana, E. Endothelial Cell-to-Cell Junctions: Molecular Organization and Role in Vascular Homeostasis. *Physiol. Rev.* **2004**, *84*, 869–901, doi:10.1152/physrev.00035.2003.
- 205. Abbruscato, T.J.; Davis, T.P. Combination of Hypoxia/Aglycemia Compromises In Vitro Blood-Brain Barrier Integrity. *J. Pharmacol. Exp. Ther.* **1999**, 289, 668 LP 675.
- 206. Fischer, S.; Clauss, M.; Wiesnet, M.; Renz, D.; Schaper, W.; Karliczek, G.F. Hypoxia induces permeability in brain microvessel endothelial cells via VEGF and NO. *Am. J. Physiol. Physiol.* **1999**, 276, C812–C820, doi:10.1152/ajpcell.1999.276.4.C812.
- 207. Mark, K.S.; Davis, T.P. Cerebral microvascular changes in permeability and tight junctions induced by hypoxia-reoxygenation. *Am. J. Physiol. Circ. Physiol.* **2002**, 282, H1485–H1494, doi:10.1152/ajpheart.00645.2001.
- 208. Maxwell, L.K.; Bentz, B.G.; Gilliam, L.L.; Ritchey, J.W.; Pusterla, N.; Eberle, R.;

- Holbrook, T.C.; McFarlane, D.; Rezabek, G.B.; Meinkoth, J.; et al. Efficacy of the early administration of valacyclovir hydrochloride for the treatment of neuropathogenic equine herpesvirus type-1 infection in horses. *Am. J. Vet. Res.* **2017**, *78*, 1126–1139, doi:10.2460/ajvr.78.10.1126.
- 209. Aiello, A.; Farzaneh, F.; Candore, G.; Caruso, C.; Davinelli, S.; Gambino, C.M.; Ligotti, M.E.; Zareian, N.; Accardi, G. Immunosenescence and Its Hallmarks: How to Oppose Aging Strategically? A Review of Potential Options for Therapeutic Intervention. *Front. Immunol.* **2019**, *10*, 2247, doi:10.3389/fimmu.2019.02247.
- 210. Hansen, S.; Baptiste, K.E.; Fjeldborg, J.; Horohov, D.W. A review of the equine agerelated changes in the immune system: Comparisons between human and equine aging, with focus on lung-specific immune-aging. *Ageing Res. Rev.* **2015**, *20*, 11–23, doi:https://doi.org/10.1016/j.arr.2014.12.002.
- 211. Bolger, A.M.; Lohse, M.; Usadel, B. Trimmomatic: a flexible trimmer for Illumina sequence data. *Bioinformatics* **2014**, *30*, 2114–2120, doi:10.1093/bioinformatics/btu170.
- 212. Chen, Y.; McCarthy, D.; Ritchie, M.; Robinson, M.; Smyth, G. edgeR: differential analysis of sequence read count data. User's guide Available online: https://www.bioconductor.org/packages/release/bioc/vignettes/edgeR/inst/doc/edgeRUsers Guide.pdf.
- 213. Shaafi, S.; Sharifipour, E.; Rahmanifar, R.; Hejazi, S.; Andalib, S.; Nikanfar, M.; Baradarn, B.; Mehdizadeh, R. Interleukin-6, a reliable prognostic factor for ischemic stroke. *Iran. J. Neurol.* **2014**, *13*, 70–76.
- 214. Tanaka, T.; Narazaki, M.; Kishimoto, T. Immunotherapeutic implications of IL-6 blockade for cytokine storm. *Immunotherapy* **2016**, *8*, 959–970, doi:10.2217/imt-2016-0020.
- 215. Angel, P.; Karin, M. The role of Jun, Fos and the AP-1 complex in cell-proliferation and transformation. *Biochim. Biophys. Acta Rev. Cancer* **1991**, *1072*, 129–157, doi:https://doi.org/10.1016/0304-419X(91)90011-9.
- 216. Badr, Y.; Okada, A.; Abo-Sakaya, R.; Beshir, E.; Ohya, K.; Fukushi, H. Equine herpesvirus type 1 ORF51 encoding UL11 as an essential gene for replication in cultured cells. *Arch. Virol.* **2018**, *163*, 599–607, doi:10.1007/s00705-017-3650-4.
- 217. Schimmer, C.; Neubauer, A. The equine herpesvirus 1 UL11 gene product localizes to the trans-golgi network and is involved in cell-to-cell spread. *Virology* **2003**, *308*, 23–36, doi:https://doi.org/10.1016/S0042-6822(02)00060-0.
- 218. Meng, P.; Tang, X.; Jiang, X.; Tang, Q.; Bai, L.; Xia, Y.; Zou, Z.; Qin, X.; Cao, X.; Chen, C.; et al. Maternal exposure to traffic pollutant causes impairment of spermatogenesis and alterations of genome-wide mRNA and microRNA expression in F2 male mice. *Environ*.

- Toxicol. Pharmacol. 2018, 64, 1–10, doi:https://doi.org/10.1016/j.etap.2018.09.006.
- 219. Gui, Y.; Xu, Z.; Jin, T.; Zhang, L.; Chen, L.; Hong, B.; Xie, F.; Lv, W.; Hu, X. Using Extracellular Circulating microRNAs to Classify the Etiological Subtypes of Ischemic Stroke. *Transl. Stroke Res.* **2019**, *10*, 352–361, doi:10.1007/s12975-018-0659-2.
- 220. Pak, J.H.; Kim, I.K.; Kim, S.M.; Maeng, S.; Song, K.J.; Na, B.-K.; Kim, T.-S. Induction of cancer-related microRNA expression profiling using excretory-secretory products of Clonorchis sinensis. *Parasitol. Res.* **2014**, *113*, 4447–4455, doi:10.1007/s00436-014-4127-y.
- 221. Soliman, B.; Salem, A.; Ghazy, M.; Abu-Shahba, N.; El Hefnawi, M. Bioinformatics functional analysis of let-7a, miR-34a, and miR-199a/b reveals novel insights into immune system pathways and cancer hallmarks for hepatocellular carcinoma. *Tumour Biol. J. Int. Soc. Oncodevelopmental Biol. Med.* 2018, 40, 1010428318773675, doi:10.1177/1010428318773675.
- 222. Hermeking, H. The miR-34 family in cancer and apoptosis. *Cell Death Differ.* **2010**, *17*, 193–199, doi:10.1038/cdd.2009.56.
- 223. Wang, Y.; Huang, J.-W.; Castella, M.; Huntsman, D.G.; Taniguchi, T. p53 Is Positively Regulated by miR-542-3p. *Cancer Res.* **2014**, *74*, 3218 LP 3227, doi:10.1158/0008-5472.CAN-13-1706.
- 224. Bray, I.; Tivnan, A.; Bryan, K.; Foley, N.H.; Watters, K.M.; Tracey, L.; Davidoff, A.M.; Stallings, R.L. MicroRNA-542-5p as a novel tumor suppressor in neuroblastoma. *Cancer Lett.* **2011**, *303*, 56–64, doi:10.1016/j.canlet.2011.01.016.
- 225. Zhi, Y.; Xie, X.; Wang, R.; Wang, B.; Gu, W.; Ling, Y.; Dong, W.; Zhi, F.; Liu, Y. Serum level of miR-10-5p as a prognostic biomarker for acute myeloid leukemia. *Int. J. Hematol.* **2015**, *102*, 296–303, doi:10.1007/s12185-015-1829-6.
- 226. Ulivi, P.; Foschi, G.; Mengozzi, M.; Scarpi, E.; Silvestrini, R.; Amadori, D.; Zoli, W. Peripheral blood miR-328 expression as a potential biomarker for the early diagnosis of NSCLC. *Int. J. Mol. Sci.* **2013**, *14*, 10332–10342, doi:10.3390/ijms140510332.
- 227. Xu, X.T.; Xu, Q.; Tong, J.L.; Zhu, M.M.; Nie, F.; Chen, X.; Xiao, S.D.; Ran, Z.H. MicroRNA expression profiling identifies miR-328 regulates cancer stem cell-like SP cells in colorectal cancer. *Br. J. Cancer* **2012**, *106*, 1320–1330, doi:10.1038/bjc.2012.88.
- 228. Sha, H.-H.; Wang, D.-D.; Chen, D.; Liu, S.-W.; Wang, Z.; Yan, D.-L.; Dong, S.-C.; Feng, J.-F. MiR-138: A promising therapeutic target for cancer. *Tumour Biol. J. Int. Soc. Oncodevelopmental Biol. Med.* **2017**, *39*, 1010428317697575, doi:10.1177/1010428317697575.
- 229. Twenter, H.; Klohonatz, K.; Davis, K.; Bass, L.; Coleman, S.J.; Bouma, G.J.; Bruemmer,

- J.E. Transfer of MicroRNAs From Epididymal Epithelium to Equine Spermatozoa. *J. Equine Vet. Sci.* **2020**, 87, 102841, doi:https://doi.org/10.1016/j.jevs.2019.102841.
- 230. Bogedale, K.; Jagannathan, V.; Gerber, V.; Unger, L. Differentially expressed microRNAs, including a large microRNA cluster on chromosome 24, are associated with equine sarcoid and squamous cell carcinoma. *Vet. Comp. Oncol.* **2019**, *17*, 155–164, doi:10.1111/vco.12458.
- 231. Roos, J.; Enlund, E.; Funcke, J.-B.; Tews, D.; Holzmann, K.; Debatin, K.-M.; Wabitsch, M.; Fischer-Posovszky, P. miR-146a-mediated suppression of the inflammatory response in human adipocytes. *Sci. Rep.* **2016**, *6*, 38339, doi:10.1038/srep38339.
- 232. Pacholewska, A.; Mach, N.; Mata, X.; Vaiman, A.; Schibler, L.; Barrey, E.; Gerber, V. Novel equine tissue miRNAs and breed-related miRNA expressed in serum. *BMC Genomics* **2016**, *17*, 831, doi:10.1186/s12864-016-3168-2.
- 233. Stanisic, D.I.; Cutts, J.; Eriksson, E.; Fowkes, F.J.I.; Rosanas-Urgell, A.; Siba, P.; Laman, M.; Davis, T.M.E.; Manning, L.; Mueller, I.; et al. γδ T cells and CD14+ monocytes are predominant cellular sources of cytokines and chemokines associated with severe malaria. *J. Infect. Dis.* **2014**, *210*, 295–305, doi:10.1093/infdis/jiu083.
- 234. Smith, C.J.; Emsley, H.C.A.; Gavin, C.M.; Georgiou, R.F.; Vail, A.; Barberan, E.M.; del Zoppo, G.J.; Hallenbeck, J.M.; Rothwell, N.J.; Hopkins, S.J.; et al. Peak plasma interleukin-6 and other peripheral markers of inflammation in the first week of ischaemic stroke correlate with brain infarct volume, stroke severity and long-term outcome. *BMC Neurol.* **2004**, *4*, 2, doi:10.1186/1471-2377-4-2.
- 235. Nakase, T.; Yamazaki, T.; Ogura, N.; Suzuki, A.; Nagata, K. The impact of inflammation on the pathogenesis and prognosis of ischemic stroke. *J. Neurol. Sci.* **2008**, *271*, 104–109, doi:https://doi.org/10.1016/j.jns.2008.03.020.
- 236. Fassbender, K.; Rossol, S.; Kammer, T.; Daffertshofer, M.; Wirth, S.; Dollman, M.; Hennerici, M. Proinflammatory cytokines in serum of patients with acute cerebral ischemia: kinetics of secretion and relation to the extent of brain damage and outcome of disease. *J. Neurol. Sci.* **1994**, *122*, 135–139, doi:10.1016/0022-510X(94)90289-5.
- 237. Vila, N.; Castillo, J.; Dávalos, A.; Chamorro, Á. Proinflammatory cytokines and early neurological worsening in ischemic stroke. *Stroke* **2000**, *31*, 2325–2329, doi:10.1161/01.STR.31.10.2325.
- 238. Watson, C.; Whittaker, S.; Smith, N.; Vora, A.J.; Dumonde, D.C.; Brown, K.A. IL-6 acts on endothelial cells to preferentially increase their adherence for lymphocytes. *Clin. Exp. Immunol.* **1996**, *105*, 112–119, doi:10.1046/j.1365-2249.1996.d01-717.x.
- 239. Tang, Y.H.; Vital, S.; Russell, J.; Seifert, H.; Granger, D.N. Interleukin-6 mediates enhanced thrombus development in cerebral arterioles following a brief period of focal

- brain ischemia. Exp. Neurol. **2015**, 271, 351–357, doi:10.1016/j.expneurol.2015.06.004.
- 240. Basinska, K.; Marycz, K.; Śmieszek, A.; Nicpoń, J. The production and distribution of IL-6 and TNF-α in subcutaneous adipose tissue and their correlation with serum concentrations in Welsh ponies with equine metabolic syndrome. *J Vet Sci* **2015**, *16*, 113–120.
- 241. Coppelman, E.B. The use of biomarkers to determine the severity of osteoarthritis in the tarsus of an older horse population, University of Minnesota, 2017.
- 242. Zarski, L.M.; Weber, P.S.D.; Lee, Y.; Soboll Hussey, G. Transcriptomic profiling of equine and viral genes in peripheral blood mononuclear ceells in horses during equine herpesvirus 1 infection. *Prep.* **2020**.
- 243. Cevik, O.; Baykal, A.T.; Sener, A. Platelets Proteomic Profiles of Acute Ischemic Stroke Patients. *PLoS One* **2016**, *11*, e0158287, doi:10.1371/journal.pone.0158287.
- 244. Khaiboullina, S.F.; Morzunov, S.P.; St Jeor, S.C.; Rizvanov, A.A.; Lombardi, V.C. Hantavirus Infection Suppresses Thrombospondin-1 Expression in Cultured Endothelial Cells in a Strain-Specific Manner. *Front. Microbiol.* **2016**, *7*, 1077, doi:10.3389/fmicb.2016.01077.
- 245. Mar, C.; Tomás, S.; Mónica, M.; María, G.; Juan, A.; Florentino, N.; David, B.; Natalia, P. de la O.; Joaquín, S.; José, V.; et al. Serum Cellular Fibronectin and Matrix Metalloproteinase-9 as Screening Biomarkers for the Prediction of Parenchymal Hematoma After Thrombolytic Therapy in Acute Ischemic Stroke. Stroke 2007, 38, 1855–1859, doi:10.1161/STROKEAHA.106.481556.
- 246. Channappanavar, R.; Fehr, A.R.; Zheng, J.; Wohlford-Lenane, C.; Abrahante, J.E.; Mack, M.; Sompallae, R.; McCray Jr., P.B.; Meyerholz, D.K.; Perlman, S. IFN-I response timing relative to virus replication determines MERS coronavirus infection outcomes. *J. Clin. Invest.* **2019**, *129*, 3625–3639, doi:10.1172/JCI126363.
- 247. Channappanavar, R.; Fehr, A.R.; Vijay, R.; Mack, M.; Zhao, J.; Meyerholz, D.K.; Perlman, S. Dysregulated Type I Interferon and Inflammatory Monocyte-Macrophage Responses Cause Lethal Pneumonia in SARS-CoV-Infected Mice. *Cell Host Microbe* **2016**, *19*, 181–193, doi:10.1016/j.chom.2016.01.007.
- 248. Acharya, D.; Liu, G.; Gack, M.U. Dysregulation of type I interferon responses in COVID-19. *Nat. Rev. Immunol.* **2020**, *20*, 397–398, doi:10.1038/s41577-020-0346-x.
- 249. Pavulraj, S.; Kamel, M.; Stephanowitz, H.; Liu, F.; Plendl, J.; Osterrieder, N.; Azab, W. Equine Herpesvirus Type 1 Modulates Cytokine and Chemokine Profiles of Mononuclear Cells for Efficient Dissemination to Target Organs. *Viruses* **2020**, *12*, 999, doi:10.3390/v12090999.

- 250. Linton, P.J.; Dorshkind, K. Age-related changes in lymphocyte development and function. *Nat. Immunol.* **2004**, *5*, 133–139, doi:10.1038/ni1033.
- 251. Walford, R.L. THE IMMUNOLOGIC THEORY OF AGING. *Immunol. Rev.* **1969**, 2, 171, doi:10.1111/j.1600-065X.1969.tb00210.x.
- 252. Sikora, E.; Kamińska, B.; Radziszewska, E.; Kaczmarek, L. Loss of transcription factor AP-1 DNA binding activity during lymphocyte aging in vivo. *FEBS Lett.* **1992**, *312*, 179–182, doi:10.1016/0014-5793(92)80930-f.
- 253. Whisler, R.L.; Newhouse, Y.G.; Bagenstose, S.E. Age-related reductions in the activation of mitogen-activated protein kinases p44mapk/ERK1 and p42mapk/ERK2 in human T cells stimulated via ligation of the T cell receptor complex. *Cell. Immunol.* **1996**, *168*, 201–210, doi:10.1006/cimm.1996.0067.
- 254. Hutter, D.; Yo, Y.; Chen, W.; Liu, P.; Holbrook, N.J.; Roth, G.S.; Liu, Y. Age-related decline in Ras/ERK mitogen-activated protein kinase cascade is linked to a reduced association between Shc and EGF receptor. *J. Gerontol. A. Biol. Sci. Med. Sci.* **2000**, *55*, B125-34, doi:10.1093/gerona/55.3.b125.
- 255. Gorgas, G.; Butch, E.R.; Guan, K.-L.; Miller, R.A. Diminished activation of the MAP kinase pathway in CD3-stimulated T lymphocytes from old mice. *Mech. Ageing Dev.* **1997**, *94*, 71–83, doi:https://doi.org/10.1016/S0047-6374(96)01857-X.
- 256. Liu, B.; Carle, K.W.; Whisler, R.L. Reductions in the activation of ERK and JNK are associated with decreased IL-2 production in T cells from elderly humans stimulated by the TCR/CD3 complex and costimulatory signals. *Cell. Immunol.* **1997**, *182*, 79–88, doi:10.1006/cimm.1997.1226.
- 257. Douziech, N.; Seres, I.; Larbi, A.; Szikszay, E.; Roy, P.M.; Arcand, M.; Dupuis, G.; Fulop, T.J. Modulation of human lymphocyte proliferative response with aging. *Exp. Gerontol.* **2002**, *37*, 369–387, doi:10.1016/s0531-5565(01)00204-2.
- 258. Adams, A.A.; Breathnach, C.C.; Katepalli, M.P.; Kohler, K.; Horohov, D.W. Advanced age in horses affects divisional history of T cells and inflammatory cytokine production. *Mech. Ageing Dev.* **2008**, *129*, 656–664, doi:10.1016/j.mad.2008.09.004.
- 259. Horohov, D.W.; Kydd, J.H.; Hannant, D. The effect of aging on T cell responses in the horse. *Dev. Comp. Immunol.* **2002**, *26*, 121–128, doi:10.1016/S0145-305X(01)00027-1.
- 260. Katepalli, M.P.; Adams, A.A.; Lear, T.L.; Horohov, D.W. The effect of age and telomere length on immune function in the horse. *Dev. Comp. Immunol.* **2008**, *32*, 1409–1415, doi:10.1016/j.dci.2008.06.007.
- 261. Fulop, T.; Larbi, A.; Pawelec, G. Human T Cell Aging and the Impact of Persistent Viral Infections . *Front. Immunol.* 2013, *4*, 271.

- 262. Lanna, A.; Henson, S.M.; Escors, D.; Akbar, A.N. The kinase p38 activated by the metabolic regulator AMPK and scaffold TAB1 drives the senescence of human T cells. *Nat. Immunol.* **2014**, *15*, 965–972, doi:10.1038/ni.2981.
- 263. Gilden, D.; Nagel, M.A.; Cohrs, R.J. Varicella-zoster. *Handb. Clin. Neurol.* **2014**, *123*, 265–283, doi:10.1016/B978-0-444-53488-0.00012-2.
- 264. Goronzy, J.J.; Weyand, C.M. Understanding immunosenescence to improve responses to vaccines. *Nat. Immunol.* **2013**, *14*, 428–436, doi:10.1038/ni.2588.
- 265. Perkins, G.A.; Wagner, B. The development of equine immunity: Current knowledge on immunology in the young horse. *Equine Vet. J.* **2015**, *47*, 267–274, doi:10.1111/evj.12387.
- 266. Adams, D.H.; Rlloyd, A. Chemokines: leucocyte recruitment and activation cytokines. *Lancet* **1997**, *349*, 490–495, doi:https://doi.org/10.1016/S0140-6736(96)07524-1.
- 267. Mariani, E.; Pulsatelli, L.; Neri, S.; Dolzani, P.; Meneghetti, A.; Silvestri, T.; Ravaglia, G.; Forti, P.; Cattini, L.; Facchini, A. RANTES and MIP-1α production by T lymphocytes, monocytes and NK cells from nonagenarian subjects. *Exp. Gerontol.* **2002**, *37*, 219–226, doi:https://doi.org/10.1016/S0531-5565(01)00187-5.
- 268. Smith, K.C.; Mumford, J.A.; Lakhani, K. A comparison of equid herpesvirus-1 (EHV-1) vascular lesions in the early versus late pregnant equine uterus. *J. Comp. Pathol.* **1996**, *114*, 231–247, doi:https://doi.org/10.1016/S0021-9975(96)80045-4.
- 269. Cunningham, A.L.; Heineman, T.C.; Lal, H.; Godeaux, O.; Chlibek, R.; Hwang, S.-J.; McElhaney, J.E.; Vesikari, T.; Andrews, C.; Choi, W.S.; et al. Immune Responses to a Recombinant Glycoprotein E Herpes Zoster Vaccine in Adults Aged 50 Years or Older. *J. Infect. Dis.* **2018**, *217*, 1750–1760, doi:10.1093/infdis/jiy095.
- 270. Shingles (Herpes Zoster) Available online: https://www.cdc.gov/shingles/vaccination.html.
- 271. Detienne, S.; Welsby, I.; Collignon, C.; Wouters, S.; Coccia, M.; Delhaye, S.; Van Maele, L.; Thomas, S.; Swertvaegher, M.; Detavernier, A.; et al. Central Role of CD169(+) Lymph Node Resident Macrophages in the Adjuvanticity of the QS-21 Component of AS01. *Sci. Rep.* **2016**, *6*, 39475, doi:10.1038/srep39475.
- 272. Coccia, M.; Collignon, C.; Hervé, C.; Chalon, A.; Welsby, I.; Detienne, S.; van Helden, M.J.; Dutta, S.; Genito, C.J.; Waters, N.C.; et al. Cellular and molecular synergy in AS01-adjuvanted vaccines results in an early IFNγ response promoting vaccine immunogenicity. NPJ vaccines 2017, 2, 25, doi:10.1038/s41541-017-0027-3.
- 273. Didierlaurent, A.M.; Laupèze, B.; Di Pasquale, A.; Hergli, N.; Collignon, C.; Garçon, N. Adjuvant system AS01: helping to overcome the challenges of modern vaccines. *Expert*

- Rev. Vaccines **2017**, 16, 55–63, doi:10.1080/14760584.2016.1213632.
- 274. Ma, G.; Azab, W.; Osterrieder, N. Equine herpesviruses type 1 (EHV-1) and 4 (EHV-4)—Masters of co-evolution and a constant threat to equids and beyond. *Vet. Microbiol.* **2013**, *167*, 123–134, doi:https://doi.org/10.1016/j.vetmic.2013.06.018.
- 275. Young Go, Y.; Li, Y.; Chen, Z.; Han, M.; Yoo, D.; Fang, Y.; Balasuriya, U.B.R. Equine arteritis virus does not induce interferon production in equine endothelial cells: identification of nonstructural protein 1 as a main interferon antagonist. *Biomed Res. Int.* **2014**, 2014, 420658, doi:10.1155/2014/420658.
- 276. Thomas, P.D.; Campbell, M.J.; Kejariwal, A.; Mi, H.; Karlak, B.; Daverman, R.; Diemer, K.; Muruganujan, A.; Narechania, A. PANTHER: a library of protein families and subfamilies indexed by function. *Genome Res.* **2003**, *13*, 2129–2141, doi:10.1101/gr.772403.
- 277. Consortium, T.U. UniProt: a worldwide hub of protein knowledge. *Nucleic Acids Res.* **2018**, *47*, D506–D515, doi:10.1093/nar/gky1049.